

**Synthesis and Application of Functionalized *Bis*-Peptides
Through Hindered Amide Bond Formation**

By

Zachary Z. Brown

B.S. University of Wisconsin: Green Bay, 2004

Submitted to the Graduate Faculty of
Arts and Sciences in partial fulfillment
of the requirements for the degree of
Doctor of Philosophy

University of Pittsburgh

2010

UNIVERSITY OF PITTSBURGH
FACULTY OF ARTS AND SCIENCES

This dissertation was presented

by

Zachary Z. Brown

It was defended on

October 25th, 2010

and approved by

Toby Chapman, Associate Professor, Department of Chemistry

David Waldeck, Professor, Department of Chemistry

Dissertation Co-Advisor: Paul Floreancig, Associate Professor,
Department of Chemistry

Dissertation Co-Advisor: Christian Schafmeister, Associate Professor,
Department of Chemistry, Temple University

Copyright © by Zachary Z. Brown
2010

**Synthesis and Application of Functionalized *Bis*-Peptides
Through Hindered Amide Bond Formation**

Zachary Z. Brown, Ph.D.

University of Pittsburgh, 2010

This work presents significant advances towards installing chemical functionality within bis-peptide scaffolds, an important milestone towards designer, functional macromolecules for our group. First was the discovery of acyl-transfer coupling, a new synthetic route to assemble extremely hindered peptide bonds which were not previously accessible through conventional means. A novel amino-anhydride intermediate and five-membered ring acyl-transfer mechanism is postulated and multiple supporting pieces of evidence are presented. Applying this chemistry to the bis-amino acid building blocks developed in our group, the first functionalized *bis*-peptides were created which are oligomeric, diketopiperazine-based peptidomimetics. The first application for this new class of macromolecules was to mimic the bound conformation of the p53 α -helical domain to its binding partner hDM2. Further structure and function optimization and characterization of the compound's biological effects showed these *bis*-peptides to be potent inhibitors of this protein-protein interaction, be cell-permeable and elicit a surprising biological response with human liver cancer cells.

TABLE OF CONTENTS

1.0	INTRODUCTION	1
1.1	PROTEINS AS AN INSPIRATION FOR FUNCTIONAL MOLECULES	1
1.2	FOLDAMERS AS MIMICS OF PROTEIN STRUCTURE	3
1.3	CONTRIBUTION OF THIS WORK	6
2.0	ACYL-TRANSFER COUPLING OF HINDERED DIPEPTIDES	8
2.1	INTRODUCTION	9
2.2	RESULTS AND DISCUSSION	13
2.3	CONCLUSION	24
2.4	EXPERIMENTAL DETAILS	24
3.0	THE SYNTHESIS OF FUNCTIONALIZED <i>BIS</i> -PEPTIDES	34
3.1	INTRODUCTION	35
3.2	RESULTS AND DISCUSSION	37
3.3	CONCLUSION	54
3.4	EXPERIMENTAL DETAILS	54
4.0	<i>BIS</i> -PEPTIDES AS ALPHA-HELIX MIMICS	68
4.1	INTRODUCTION	69
4.2	RESULTS AND DISCUSSION	72
4.3	CONCLUSION	87
4.4	EXPERIMENTAL DETAILS	88
5.0	EXPANDING THE TOOLBOX OF FUNCTIONALIZED <i>BIS</i> -PEPTIDES	102
5.1	INTRODUCTION	103
5.2	RESULTS AND DISCUSSION	104
5.3	CONCLUSION	118

5.4	EXPERIMENTAL DETAILS	118
6.0	<i>BIS</i> -PEPTIDE MACROCYCLES VIA RESIN-BOUND CYCLIZATION	126
6.1	INTRODUCTION	127
6.2	RESULTS AND DISCUSSION	129
6.3	CONCLUSION.....	135
6.4	EXPERIMENTAL DETAILS	135
	APPENDIX	139
	BIBLIOGRAPHY.....	173

LIST OF TABLES

Table 2.1. Dipeptide Yields and Conditions	15
Table 3.1. Structures and of Functionalized Bis-Amino Acids	38
Table 4.1. Structures and Kd's of <i>Bis</i> -Peptides Exploring Functional Groups	78
Table 4.2. Structures and Kd's of <i>Bis</i> -Peptides Exploring Stereochemistry	79
Table 4.3. Structures and Kd's <i>Bis</i> -Peptides with an Additional Functional Group	81
Table 4.4. LC-MS Characterization of Bis-Peptides with Different Functional Groups.....	94
Table 4.5. LC-MS Characterization of <i>Bis</i> -Peptides for Diastereomer Scan	94
Table 4.6. LC-MS Characterization of <i>Bis</i> -Peptides for an Additional Functional Group.....	94
Table 4.7. Raw Values for Polarization of Oligomer 85	97
Table 4.8. Parameters Used for Polarization Plot of Oligomer 85	98
Table 4.9. Parameters Used for Polarization Plot of Figure 4.16	99
Table 6.1. Calculated and Found Masses for the Macrocycles.....	138
Table A.1. ¹ H and ¹³ C assignments for tetramer 69	150
Table A.2. ¹ H and ¹³ C assignments for tetramer 70	156
Table A.3. ¹ H and ¹³ C assignments for helix mimics 103	162

LIST OF FIGURES

Figure 1.1. Examples of Proteins for Protein-Protein Interactions and Catalysis	1
Figure 1.2. Peptides, Foldamers and Bis-Peptides.....	3
Figure 1.3. Alpha-Helix Peptidomimetics	5
Figure 1.4. From Hindered Amides to Peptidomimetics and Their Application.....	6
Figure 2.1. Structure of the Bioactive Peptides Cyclosporin and Alamethicin	9
Figure 2.2. Literature Precedence for Hindered Amide Synthesis	12
Figure 2.3. Hindered Amino Acids Used and Their Abbreviations	14
Figure 2.4. Chromatogram of Crude Dipeptide 9	16
Figure 2.5. ¹ H NMR Profile for Dipeptide 9	17
Figure 2.6. Synthesis and Characterization of Dipeptides for Racemization Experiment.....	18
Figure 2.7. Control Experiments for Hindered Amide Bond Formation	19
Figure 2.8. Competition Experiments to Highlight Neighboring Group Effect	20
Figure 2.9. Proposed Mechanism for Acyl Transfer Coupling.....	21
Figure 2.10. Examples of Other Amide-Forming Five-Membered Ring Acyl Transfers	22
Figure 2.11. Anhydride Trapping Experiment.....	23
Figure 2.12. Crude HPLC Trace of Dipeptide 9	26
Figure 2.13. Crude HPLC Trace of Dipeptide 10	27

Figure 2.14. Crude HPLC Trace of Dipeptide 16	28
Figure 2.15. Time Course for Dipeptides 9 and 10	29
Figure 2.16. Crude HPLC Trace of Dipeptide 12	29
Figure 2.17. Crude HPLC Trace of Dipeptides 12 and 23	30
Figure 2.18. HPLC Trace of Purified Compound 31	32
Figure 2.19. Crude HPLC Traces of Anhydride Trapping Experiments	33
Figure 3.1. Functionalized Bis-Peptides	34
Figure 3.2. Unfunctionalized and Functionalized Bis-Peptides and the Monomers Required.....	36
Figure 3.3. Failed Acylation Using Conventional Techniques.....	37
Figure 3.4. Synthesis of Symmetric Hexasubstituted Diketopiperazine 45	40
Figure 3.5. Proposed Mechanism of Activation of Functionalized Bis-Amino Acids	41
Figure 3.6. LC-MS Traces from Reaction to Form Asymmetric Diketopiperazine 49	43
Figure 3.7. Proposed Mechanism to Form Diketopiperzaine 49	44
Figure 3.8. Synthesis and Characterization of an Acyl Transfer Model System.....	46
Figure 3.9. Synthesis of Bis-Peptide Dimer 61	48
Figure 3.10. Competition Experiment of Prolinyl Acid vs. Amine	49
Figure 3.11. Synthesis of Functionalized Tetramer 69	50
Figure 3.12. Modeled Structure of Tetramer 69	52
Figure 3.13. Modeled Structure of Tetramer 70	53
Figure 3.14. Reductive Alkylation of Pro4 Amino Acid.....	55
Figure 3.15. HPLC Trace of Purified Dikeopiperazine sc1	59
Figure 3.16. HPLC Trace of Crude Dimer 67	62
Figure 3.17. HPLC Trace of Crude Trimer 68	63

Figure 3.18. HPLC Trace of Purified Tetramer 69	64
Figure 3.19. Solution Phase Synthesis of Tetramer 70	64
Figure 3.20. HPLC Trace of Crude Dimer sc2	65
Figure 3.21. HPLC Trace of Crude Trimer sc3	66
Figure 3.22. HPLC Trace of Purified Tetramer 70	67
Figure 4.1. Disrupting Protein-Protein Interactions with Bis-Peptides.....	69
Figure 4.2. Crystal Structure of the p53/hDM2 Interaction.....	70
Figure 4.3. Comparison of p53 Alpha-Helix and a Modeled Bis-Peptide Mimic.....	72
Figure 4.4. Structure of a Bis-Peptide Alpha-Helix Mimic.....	74
Figure 4.5. Solid-Phase Synthesis of Helix Mimic 84	76
Figure 4.6. Plot of Polarization vs. Log hDM2 Concentration for Bis-Peptide 84	80
Figure 4.7. Overlay of Bis-Peptides and p53 Alpha-Helix.....	80
Figure 4.8. Competition Experiment and Bis-Peptides 103 and 104	82
Figure 4.9. Fluorescence Microscopy Images of Cell Penetration of Bis-Peptide 85	84
Figure 4.10. Western Blot Analysis of Bis-Peptide 84 and Huh7 Cells.....	85
Figure 4.11 Western Blot Analysis of Huh7 And HepG2 Cells with Bis-Peptide 84	87
Figure 4.12. HPLC Trace of Purified Bis-Peptide 84	91
Figure 4.13. HPLC Trace of Purified Bis-Peptide 104	92
Figure 4.14. HPLC Trace of Purified Bis-Peptide 103	93
Figure 4.15. Plot of Polarization vs. Protein Concentration for Bis-Peptide 85	97
Figure 4.16. Plot of Polarization vs. Log Bis-Peptide 103 Concentration.....	98
Figure 4.17. Confocal Microscopy Image for Compound 85	100
Figure 5.1. Synthesis of Boc-protected Bis-Amino Acid.....	104

Figure 5.2. Comparison of Peptide and Bis-Peptide Solid-Phase Synthesis	106
Figure 5.3. Solid-Phase Synthesis of Bis-Peptide 122	108
Figure 5.4. LC-MS Analysis of Purified Bis-Peptide 122	109
Figure 5.5. Solid-Phase Synthesis of Bis-Peptide 126	111
Figure 5.6. Different Coupling Architectures of Pro4 Monomers.....	113
Figure 5.7. Fragments for the Tail to Tail Coupling.....	114
Figure 5.8. Synthesis of Bis-Peptide 128	115
Figure 5.9. Synthesis of the Tail to Tail Bis-Peptide 136	116
Figure 5.10. Modeled Structure of Bis-Peptide 136	117
Figure 6.1. Rendering of the Synthesized Macrocycles, Compounds 137-139	126
Figure 6.2. Beta-Cyclodextrin and cucurbit[7]uril	127
Figure 6.3. Solid-Phase Synthesis of Macrocycle 139	130
Figure 6.4. LC-MS Characterization of Purified Macrocycle 137	131
Figure 6.5. Structures of the Three Macrocycles, Compounds 137-139	132
Figure 6.6. Schematic of ANS Fluorescence in the Presence of Macrocycle 137	133
Figure A.1. ¹ H NMR (25mM in DMSO- <i>d</i> ₆) spectrum of dipeptide 9	140
Figure A.2. HMBC NMR (25mM in DMSO- <i>d</i> ₆) spectrum of dipeptide 9	141
Figure A.3. ¹ H NMR NMR (25mM in DMSO- <i>d</i> ₆) spectrum of dipeptide 16	142
Figure A.4. HMBC NMR (25mM in DMSO- <i>d</i> ₆) spectrum of dipeptide 16	143
Figure A.5. ¹ H NMR NMR (25mM in DMSO- <i>d</i> ₆) spectrum of dipeptide 10	144
Figure A.6. ¹ H NMR (500 MHz, DMSO- <i>d</i> ₆ , 365K) of Pro4(S,S)-benzyl functionalized 36	145
Figure A.7. ¹ H NMR (500 MHz, DMSO- <i>d</i> ₆ , 365K) of Pro4(S,S)-anisole functionalized 37	145
Figure A.8. ¹ H NMR (500 MHz, DMSO- <i>d</i> ₆ , 365K) of Pro4(S,S)-naphthyl functionalized 38 ..	146

Figure A.9. ^1H NMR (500 MHz, DMSO- d_6 , 365K) of Pro4(R,R)-isobutyl 40	146
Figure A.10. ^1H NMR (500 MHz, DMSO- d_6 , 365K) of Pro4(S,S)-Cbz-aminopropyl 41	147
Figure A.11. ^1H NMR (500 MHz, DMSO- d_6 , 365K) of Pro4(S,S)-benzyl carboxylate 42	147
Figure A.12. ^1H NMR (500 MHz, DMSO- d_6 , 298K) of Pro4(S,S)-Fmoc,OMe 66	148
Figure A.13. ^1H NMR (500 MHz, DMSO- d_6 , 365K) of Pro4(S,S)-Boc-amino acid 108	148
Figure A.14. ^1H NMR (500 MHz, DMSO- d_6 , 298K) of compound 62	149
Figure A.15. NMR key for the ^1H and ^{13}C assignments for tetramer 69	150
Figure A.16 Tetramer 69 ^1H : 10mM in DMSO.....	151
Figure A.17 Tetramer 69 COSY: 10mM in DMSO	152
Figure A.18 Tetramer 69 ROESY: 10mM in DMSO	153
Figure A.19 Tetramer 69 HMQC: 10mM in DMSO	154
Figure A.20 Tetramer 69 HMBC: 10mM in DMSO	155
Figure A.21. NMR key for the ^1H and ^{13}C assignments for tetramer 70	156
Figure A.22 Tetramer 70 ^1H : 10mM in DMSO.....	157
Figure A.23 Tetramer 70 COSY: 10mM in DMSO	158
Figure A.24 Tetramer 70 ROESY: 10mM in DMSO.....	159
Figure A.25 Tetramer 70 HMQC: 10mM in DMSO	160
Figure A.26 Tetramer 70 HMBC: 10mM in DMSO	161
Figure A.27. NMR key for the ^1H and ^{13}C assignments for helix mimic 103	162
Figure A.28 Helix Mimic 103 COSY: 10mM in DMSO.....	163
Figure A.29 Helix Mimic 103 HMQC: 10mM in DMSO	164
Figure A.30 Helix Mimic 103 HMBC: 10mM in DMSO	165
Figure A.31 Helix Mimic 103 ROESY: 10mM in DMSO.....	166

Figure A.32 Helix Mimic 84 COSY: 10mM in DMSO.....	167
Figure A.33 Helix Mimic 84 COSY: 10mM in DMSO.....	168
Figure A.34 Tail to Tail Oligomer 136 ¹ H: 10mM in DMSO	169
Figure A.35 Tail to Tail Oligomer 136 COSY: 10mM in DMSO	170
Figure A.36 Tail to Tail Oligomer 136 ROESY: 10mM in DMSO.....	171
Figure A.37 Tail to Tail Oligomer 136 HMBC: 10mM in DMSO.....	172

PREFACE

I would like to first and foremost thank Chris Schafmeister for his careful patience, mentoring and advice which will forever shape me as a scientist. All of the past and present Schafmeister group members have been instrumental in guiding and helping me. Of the past generation Greg Bird was a wonderful mentor who first showed me the way of the bis-peptides. My comrade Matt Parker is a fantastic chemist who I know will achieve great success in whatever he wants to do. I know without his advice and conversation, much of this chemistry may not have come to be. Jennifer Alleva is another colleague whose contributions cannot be measured, and I look forward to the future to see all of her amazing accomplishments. There was also the mentorship of Dr. Ron Starkey (UWGB), who was the first professor to truly believe in me. I will always be thankful for his guidance. Finally, I would like to thank my family for their unwavering love and support through this journey. Without all that they have given me, none of this would be possible.

And finally a quote from of my favorite stories, for the true inspiration for this science has been Mother Nature, the best chemist of all.

“These mysteries we thought only great Nature knew
Our expertise now dares to attempt it too!
Her way with living matter was to organize it
And we have learnt to crystallize it...”

-Goethe's *Faust, Part II*

List of Abbreviations

ACN	Acetonitrile
AcOH	Acetic acid
Aib	Aminoisobutyric acid
Boc	<i>tert</i> -Butoxycarbonyl
Boc ₂ O	Di- <i>tert</i> -butyl dicarbonate
Cbz	Carboxybenzyl
DIC	Diisopropylcarbodiimide
DCM	Dichloromethane
DIPEA	<i>N,N</i> -Diisopropylethylamine
DKP	Diketopiperazine
DMAP	4-Methyldiaminopyridine
DMF	<i>N,N</i> -Dimethylformamide
EtOAc	Ethyl acetate
Fmoc	9-Fluorenylmethoxycarbonyl
FP	Fluorescence polarization
HATU	<i>O</i> -(7-azabenzotriazol-1-yl)- <i>N,N,N',N'</i> -tetramethyluronium hexafluorophosphate
HFIP	Hexafluoroisopropanol
HMBC	Heteronuclear multiple bond correlation spectroscopy
HMQC	Heteronuclear multiple quantum coherence
HOAt	Hydroxyazabenzotriazole
HPLC	High performance liquid chromatography
LC-MS	Liquid chromatography with mass spectrometry
K _d	Dissociation constant
Melm	Methylimidazole
MeOH	Methyl alcohol
MS	Mass spectrometry
MSNT	1-(mesitylene-2-sulfonyl)-3-nitro-1,2,4-triazole
ROESY	Rotating frame Overhauser enhancement spectroscopy
TFA	Trifluoroacetic acid
THF	Tetrahydrofuran
TIPS	Triisopropylsilane

1.0 Introduction

1.1 Proteins as the Inspiration for Functional Macromolecules

Proteins are the fundamental nanomachines of life, catalyzing a myriad of reactions with exquisite efficiency and selectivity and performing fantastic feats of molecular recognition. In a simplistic sense, proteins achieve their remarkable properties by the precise positioning of chemical groups, both reactive and unreactive, in three dimensional space.¹ It is this complex orchestration of various chemical moieties that the proteomimetic community and our laboratory seeks to emulate in the hopes of creating designer, functionalized macromolecules that could be used for the purposes of catalysis or for molecular recognition.²

The design of macromolecules that approach the abilities of proteins would have enormous impact on the fields of chemistry and biology and so is a major research avenue of modern chemistry.³ Within the new frontiers of chemical biology, designer macromolecules could be used to disrupt protein-protein interactions, one of the most important techniques a cell uses to modulate signal transduction. These molecules could attempt to bridge the gap between small molecule drugs and biologics, to reach the approximately 80% of the human proteome which has been termed “undruggable”.⁴ These protein products either lack a deep hydrophobic pocket and so are not amenable to traditional medicinal chemistry or are intracellular targets

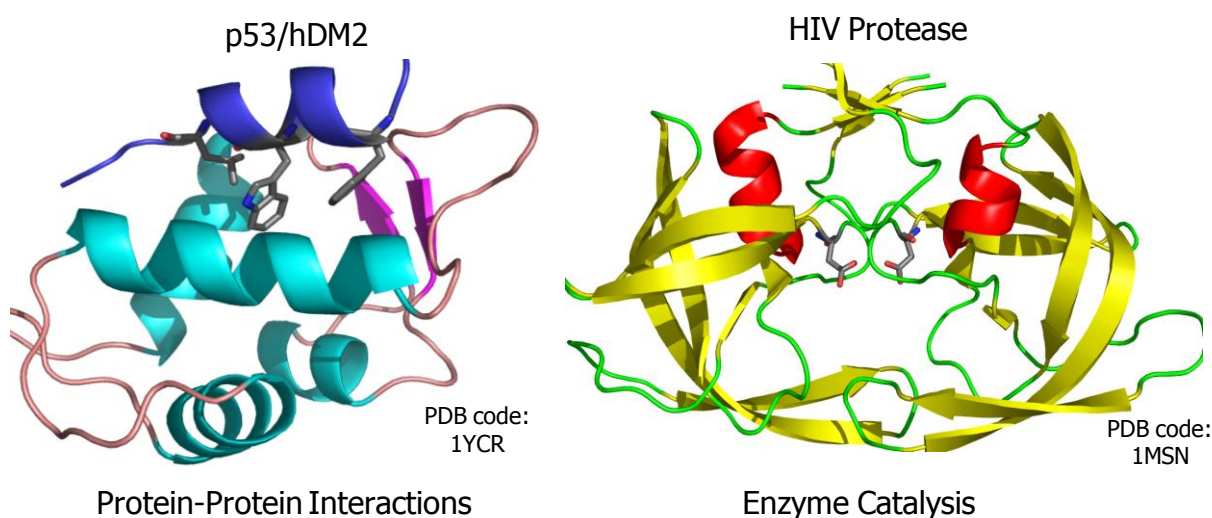


Figure 1.1. Two examples of how proteins align functional groups for desired biological means: protein-protein interactions (on the left hand side) and catalysis (on the right hand side). Images created with PyMol.⁵

and so biologics are not able to reach them. Industrially, designer molecules with enzyme-like catalytic abilities could be utilized to manufacture synthetic molecules, including applications in asymmetric synthesis. The applications of designer macromolecules for industrial synthesis or as biological agents are far reaching and could have a large impact on contemporary science.

Shown on the left in Figure 1.1 is an example of how proteins use these directed functional groups for the purposes of molecular recognition. This protein-protein interaction is the binding of p53 to hDM2, where nonpolar groups on one face of the p53 amphipathic helix are pointed toward a hydrophobic cleft on its binding partner, the hDM2 chaperone protein.⁶ This archetypal protein-protein interaction plays a pivotal role in the apoptosis pathway and illustrates how biochemical information can be mediated through the interaction of protein surfaces. By burying only a few hydrophobic residues of p53, hDM2 is able to maintain stable concentrations of p53 by constantly targeting it for degradation via the ubiquitination pathway. Via this mechanism, a cell is able to preserve the appropriate concentrations of p53 that is required for homeostasis.⁷ Upon detection of DNA damage, the hDM2 releases p53 to bind DNA and initiate either cell cycle arrest and repair of the genome or apoptosis of the cell. Thus, there is a significant interest in being able to therapeutically manipulate this protein-protein interaction as well as to develop a technology which could be used to selectively modulate other protein interactions.⁸

The right side of Figure 1.1 depicts reactive chemical groups, such as the two key aspartic acid residues of the active site of HIV protease, aligned at each other for catalytic purposes.⁹ In this instance, these reactive chemical functional groups are directed inward to the protein interior as well as toward each other to accelerate otherwise slow chemical reactions. Here the precisely orchestrated placement of two carboxylic acids is able to sever an amide bond, a thermodynamically favorable but kinetically slow transition. Therefore, through the precise placement of amino acid side chains, proteins are able to perform outstanding feats on the molecular level.¹⁰

Prior to the contribution outlined in this work, *bis*-peptides were shown to be highly structured and to be shape-persistent and shape-programmable backbone modules.² Thus, the structure element was well-developed by the previous members of the Schafmeister lab whose synthetic and structural studies helped to establish *bis*-peptides as a fascinating new class of shape-programmable oligomers. With the work detailed herein, both primary and secondary structure has been realized, a significant advance in *bis*-peptide technology. The chemistry to add functional groups to our monomers was optimized and imparts them with the diverse chemical properties just as side chains enrich amino acid monomers. Also beneficial is that

nearly any desired functional group may be appended to the monomer, as *bis*-amino acids are not limited by the use of proteogenic amino acids as nature is, and so an enormous variety of chemical groups may be used. Novel chemistry was then developed to use these functionalized monomers and connect them together through highly substituted diketopiperazine linkages.^{11,12} This organization of functional groups in various three-dimensional arrays amounts to secondary structure, how local segments amino acid units are arrayed adjacent to one another. Therefore, it is appropriate that the first application of these functionalized *bis*-peptides was to mimic α -helices, the most common protein secondary structure. These helix mimics were shown to disrupt the p53/hDM2 protein-protein interaction as well as be cell permeable and elicit an exciting biological response *in vivo*.

1.2 Foldamers as Mimics of Protein Structure

As discussed earlier, proteins fold into their functional conformations by a variety of forces, including hydrophobic interactions, the formation of intramolecular hydrogen bonds and van der

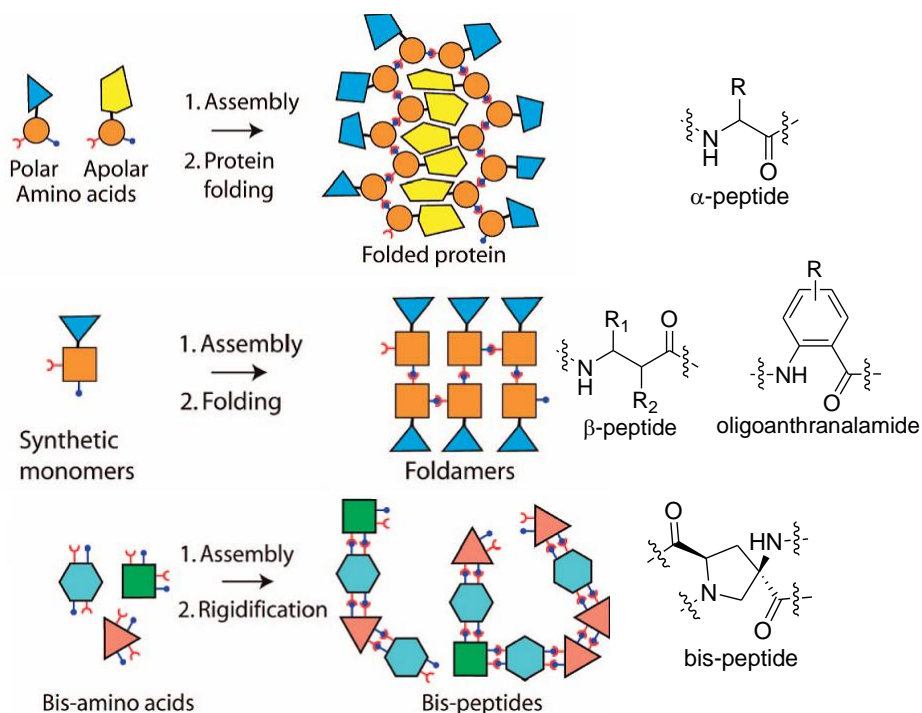


Figure 1.2. How monomers are assembled and yield unique three dimensional macromolecules: on the top is the assembly and folding of α -amino acids into native proteins. In the middle is the concept of foldamers, where synthetic monomers fold into predictable shapes that could potentially be used to replicate protein structure. Finally there are *bis*-peptides, where the issue or predicting a macromolecule folding pattern has been circumvented by using monomers that connect with two amide bonds, thus rigidifying the structure.

Waals forces.¹ This idea is illustrated in the top portion of Figure 1.2, where primarily nonpolar amino acids are buried in the core of the protein away from bulk water and polar amino acids are more often found on the exterior. This gives the fully folded native state of the protein and allows it to perform its biochemical role. However, this folding process is poorly understood, and although much progress has been made, it remains a “Holy Grail” of bioinformatics to predict a protein’s folded three dimensional structure from only its primary sequence.¹³

Foldamers are a significant synthetic advance towards functional macromolecules which do not have some of the major drawbacks of oligomers of α -amino acids, such as the protein folding problem. Moore defines a foldamer as “any oligomer that folds into a conformationally ordered state in solution, the structures of which are stabilized by a collection of noncovalent interactions between nonadjacent monomer units.”¹⁴ Thus, the monomers must have intrinsic conformational preferences which, in addition to hydrophobic and other noncovalent interactions, can translate into secondary structures. A schematic of foldamers and a few examples are shown in the middle portion of Figure 1.2 and include β -peptides³ and oligoanthranalamides.¹⁵ Many more example of foldamers have appeared in the literature in the last 20 years including γ -peptides,¹⁶ peptoids,¹⁷ terphenyls¹⁸ and others.^{14,19} Much success has been achieved in the mimicry of helical architectures and diverse chemical functionality may be positioned by these systems for many different applications.²⁰ However, foldamers have been unable to replicate more diverse protein secondary structure and even higher order structures, although progress continues to be made with β -peptides and α,β -hybrid systems.²¹ This requires understanding of the subtle noncovalent interactions and remains a formidable challenge to the design of macromolecules which can fold back onto themselves in a manner similar to proteins. These systems also have the inherent difficulty is that they may be only marginally stable structures, with only a weak free energy of folding.^{14,20} Thus, only one or a few modest substitutions (which would be necessary to explore structure-function relationships of designer macromolecules) may cause the foldamer’s well-defined structure to be lost.

Stabilization of helical secondary structure may also be achieved by a secondary covalent linkage; two examples of α -helix mimics are hydrogen bond surrogates²² and stapled peptides²³ and the helical structures and are shown in Figure 1.3. Hydrogen bond surrogates replace one of the backbone hydrogen bonds with an alkene cross-link to template helix

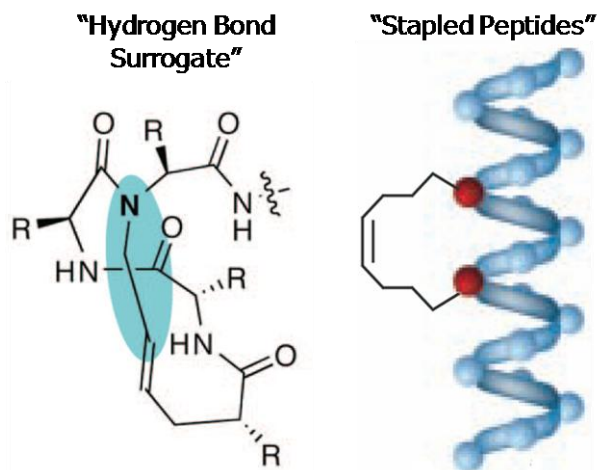


Figure 1.3. Two examples of peptidomimetics which utilize covalent linkages to stabilize secondary structure. Reproduced from ref 7,8.

formation, placing an olefinic cross-link where one of the hydrogen bonds would be. Stapled peptides also use a metathesized linker but here connect side chains of the amino acids which will reside on the same helical face, again templating helical structure. These systems have found great success in stabilizing the helical fold they were designed for. However, this is not a general solution to the design of proteomimetic systems as only a single type of secondary structure is achieved.

In our group we have developed a different approach to shape programmable oligomers.² We have created a toolbox of cyclic monomers which create spiro-ladder oligomers by the formation of two amide bonds between each monomer. The resulting *bis*-peptides have well-defined three dimensional structures based on the conformational preferences of the rings and the stereochemistry of the constituent monomers. Much work has been performed in demonstrating *bis*-peptides are have designer shapes by elegant synthetic and structural work by members of the Schafmeister group and their collaborators. Although there was rich structural diversity available to the *bis*-peptide chemist, the lack of chemical functionality within the oligomer was a major impediment towards the full realization of the potential of *bis*-peptides.

1.3 Contribution of this Work

This work details studies on the installment of chemical functionality within a *bis*-peptide scaffold, solving the significant synthetic impediment to creating these hindered amide bonds and applying these new peptidomimetics towards mimicking the bound conformation of a helical peptide. This flow of ideas is illustrated in Figure 1.4 and encompasses the findings of Chapters 2-5 in how novel chemistry allowed the creation of new macromolecules which were shown to have potent and selective *in vivo* activity. Chapter 2 introduces our acyl-transfer chemistry to create hindered tertiary amides, a contribution towards solving a longstanding problem in peptide synthesis. This acyl-transfer coupling is then applied to our *bis*-peptides in Chapter 3,

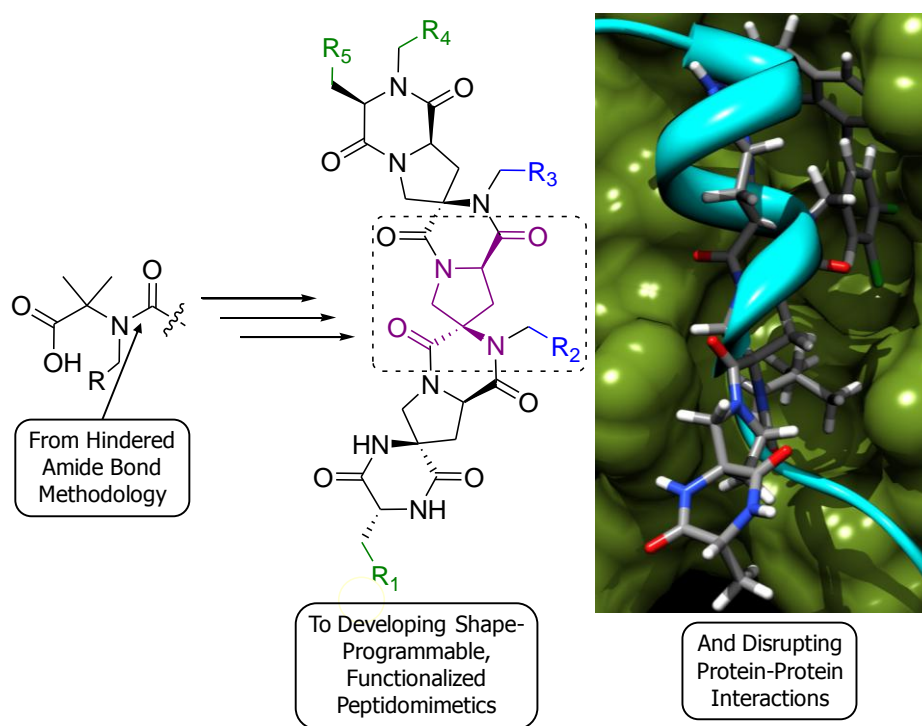


Figure 1.4. The contribution of this work highlighting the creation of hindered amide bonds, the subsequent assembly into functionalized peptidomimetics and finally applying these molecules to disrupt a protein-protein interaction.

where symmetric and asymmetric hexasubstituted diketopiperazines as well as the first functionalized *bis*-peptides are synthesized and characterized. Organizing multiple functional groups and building secondary structure, including the disruption of a protein-protein interaction is outlined in Chapter 4. These *bis*-peptide oligomers were also shown to be cell-permeable and active *in vivo*. Chapter 5 details the development of the solid-phase assembly of functionalized *bis*-peptides as well as other advances of *bis*-peptide methodology. Finally, Chapter 6 is the

synthesis of a series of macrocycles using unfunctionalized *bis*-amino acids that have variable sizes to show the creation of structured, hydrophobic cavities with tunable sizes.

Chapter 2
Exploiting an Inherent Neighboring Group Effect of α -Amino Acids
To Synthesize Extremely Hindered Dipeptides

Chapter 2 details our methodology of acyl-transfer coupling of α -amino acids to assemble extremely hindered dipeptides, a novel amide bond forming reaction that we discovered. Highlights of this strategy include an operationally simple and mild procedure for peptide bond formation which utilizes commercially available materials. This chapter includes the synthesis, structural characterization and mechanistic insights using a variety of sterically hindered amino acids.

Acyl-transfer coupling has become a cornerstone for most of the chemistry detailed in this thesis and is now the foundation of *bis*-peptide technology. Therefore, this reaction mechanism will be referenced multiple times through the course of this work.

A portion of this chapter is published as:
Zachary Z. Brown and Christian E. Schafmeister
J. Am. Chem. Soc., **2008**, 130 (44), 14382

2.1 Introduction

Peptides are found throughout biology where they perform an enormous variety of biological tasks, and are now being used more extensively in biotechnological applications.²⁴ Although a small number of examples exist of native peptides being used as medicinal agents (for example, Fuzeon²⁵), the vast majority are non-ribosomal peptides that use peptide modification to bolster therapeutic potential.²⁶ These can be from a natural origin, such as peptide secondary metabolites, or from synthetic design, such as stapled-peptide technology introduced in Chapter 1. The rich pharmacological potential of peptides is derived from their primary structure (the constituent amino acids) which controls their bound conformation, and thus a peptide's biological function. Therefore, increasing the number of peptide modifications which can alter a peptide's structure and function would be of great interest to a medicinal chemist. The two most common forms of peptide modification are *N*-alkylation of the peptide bond and disubstitution of the alpha carbon (*C*-alkylation), both of which confer numerous therapeutic benefits to the peptide of interest.²⁷

Proteogenic peptides suffer several drawbacks in their use as medicinal agents, all of which may be augmented by peptide modification. First, they are rapidly degraded *in vivo* by

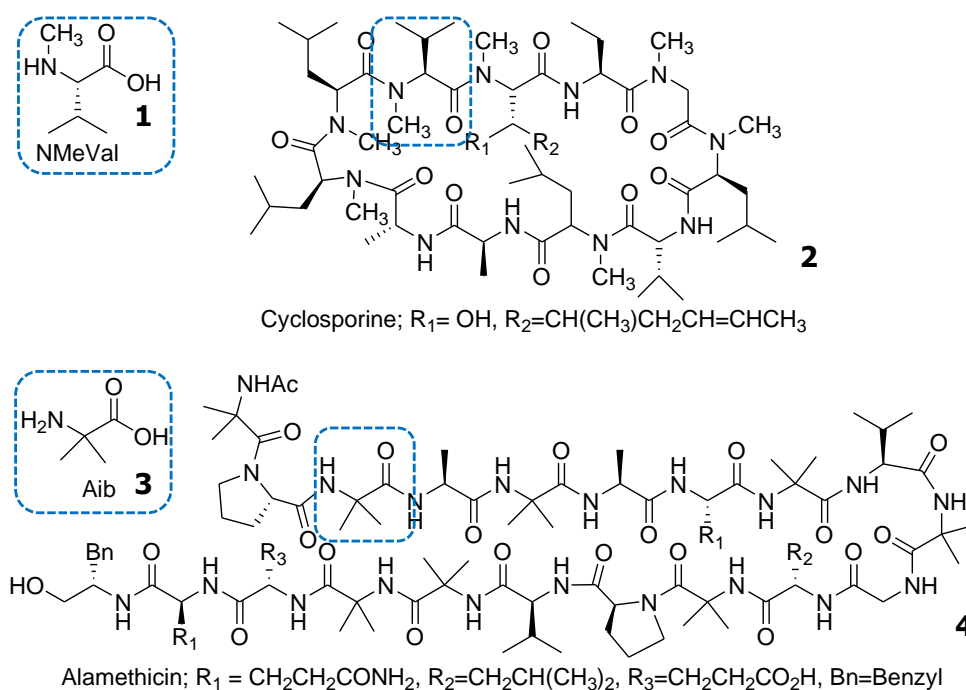


Figure 2.1. The structures of the bioactive, hindered peptides Cyclosporin 2 and Alamethicin 4 with examples of sterically hindered peptides highlighted.

proteases and so have a severely limited residence time in blood plasma. Many smaller peptides also exhibit little secondary structure when excised from the parent protein and so show weak activity because of the entropic penalty to form the bioactive conformation. Finally, peptides are generally not permeable to the cellular membrane because of their highly polar nature and extensive hydration of the amide backbone.²⁸

N-alkylation of the peptide bond, with a representative *N*-methyl amino acid (NMe-Valine **1**) highlighted in peptide **2** in Figure **2.1**, is a common backbone substitution and plays a key role in the bioactivity of many peptide secondary metabolites. *N*-methylation of the amide can confer proteolytic resistance, increase lipophilicity and improve bioavailability by reducing the number of hydrogen bond donors, and produce novel conformational biases by altering the hydrogen-bonding patterns of the peptide.²⁹ One example of a pharmaceutically relevant molecule which contains *N*-methyl peptide bonds is Cyclosporine,³⁰ peptide **2**, shown in Figure **2.1**. Cyclosporine is a macrocyclic peptide of eleven amino acids and is in current medicinal use as an immune system suppressant. Numerous hindered amide bonds are present in this non-ribosomal peptide and help to give this macrocycle its unique biological function. By methylating several of the amide bonds and diminishing the ability of the macrocycle to hydrogen bond with bulk solvent, the peptide is able to cross the lipid bilayer and elicit an intracellular response.

C-alkylation is another important structural modification and can induce secondary structure formation and confer biological activity to even short peptides, which are normally unstructured in solution. The disubstitution of a residue significantly increases the steric bulk about the α -carbon and can induce the formation of either 3-10 helices or β -turns.²⁷ From a synthetic standpoint, substitution of this position will also eliminate the concern of racemization during peptide assembly and so can be a valuable alteration for some peptides. Peptaibols are one example of biologically active peptides which contain numerous disubstituted amino acids and hindered tertiary amides. Here the presence of multiple aminoisobutyric acid (Aib, compound **3**) residues induces helix formation and gives the molecule therapeutic potential by aggregating within the lipid bilayer. Shown in Figure **2.1** is a representative member of the Peptaibol family, Alamethicin, compound **4**, which is a peptide antibiotic, forming voltage-dependent ion channels.³¹

To date, there has been very little study on the effects of juxtaposing these two peptide modifications, presumably because their synthesis was not achievable using known peptide coupling methodology (see below). The severe steric hindrance and the resulting restriction of conformational space about this peptide should impart significant conformational biases. Moretto *et al* found that the incorporation of a *N*-methyl-aminoisobutyric acid (NMe-Aib)

promoted the formation of β -bends in a dipeptidyl unit,³² although the global effects on a larger peptide which contained this unit could not be studied because the synthesis could not be achieved. Therefore, methodology which allows access to these hindered amide bonds could provide an entry into studying peptides containing these *N*-alkyl- α,α -disubstituted amino acids.

With the central importance the peptide bond has in the role of protein structure and medicinal chemistry, its synthesis and characterization is one of the most developed areas of organic chemistry. Indeed, the first dipeptide was synthesized by Emil Fischer in 1912³³ and new developments continue to appear in the literature.³⁴ Conventional peptide synthesis utilizes an amine protecting group on the residue to be activated and an ester protecting group on the residue to be acylated. This allows for chemoselective amide bond formation followed by deprotection and subsequent chain extension. The most common and convenient amine protecting groups are based on the carbamate group, and include the carboxybenzyl group (Cbz), the *tert*-butyl carbamate group (Boc) and the 9-fluorenylmethylenecarboxyl group (Fmoc).³⁵ Their orthogonality, ease of removal using mild conditions, and commercial availability of proteogenic and unnatural amino acids with urethane-based protecting groups are just some of the reasons why their use has become so commonplace. When performing solution phase couplings a carboxylate protecting group is conventionally employed in the form of an ester. This is commonly a methyl ester, although other orthogonal groups are commercially available (for example, benzyl or *t*-butyl esters) for different assembly strategies.

In peptide chemistry, steric hindrance of the coupling partners plays a critical role which dictates the ease of the reaction. Owing to continual advances in the field, the coupling of proteogenic amino acids in either solution or solid-phase is now relatively straightforward. Numerous coupling agents exist and are all based on the premise of the creation of a more active leaving group of the carboxylic acid and condensing this with the amine nucleophile. Examples of activated groups include acyl halides, acyl azides, acylimidazoles, anhydrides, esters and other highly activated leaving groups³⁴ and can be formed in a separate activation process or *in situ* depending on the method employed. There have been many excellent reviews of amide bond forming reactions and it remains a rich area of research in contemporary organic chemistry.³⁶ Even the coupling of proteogenic amino acids with more hindered systems, for example when one partner contains either *N*- or *C*-alkylation, can be accomplished if one of the more powerful methods mentioned above is employed. Both Cyclosporin **2** and Alamethicin **4**, the synthetically challenging peptides shown above in Figure 2.1, have succumbed to total syntheses and remain benchmarks for new methodologies.^{30,37} One of the few remaining challenges is the creation of amide bonds where both the amine and carboxyl components are

sterically hindered³⁸ (for example, *N*-methyl-valine **1** and α -amino-isobutyric acid **3**). The reduced nucleophilicity of the amino component translates into slower reactivity and the occurrence of side reactions, for example premature Fmoc deprotection or racemization of the activated residue. The hindrance of the carboxylate may also compound this problem and further slow down the desired coupling reaction, again allowing side reactions to take place.

One of the most powerful means of electrophilic activation of a carboxylic acid is the formation of an acid chloride. However, this strategy suffers from being “over activated” and is prone to side reactions and so is not compatible with urethane-based amine protecting groups. On the other hand, acid fluorides represent a compromise of enhanced reactivity with few side reactions; they are even applicable in the coupling of some sterically hindered systems.³⁹ But as shown in Figure 2.2, neither acid chlorides nor acid fluorides have sufficient reactivity when both the electrophile and nucleophile are extremely sterically hindered. Here Fmoc-Aib-OH is activated as either the acid chloride or the acid fluoride, and, in the presence of either DIPEA or

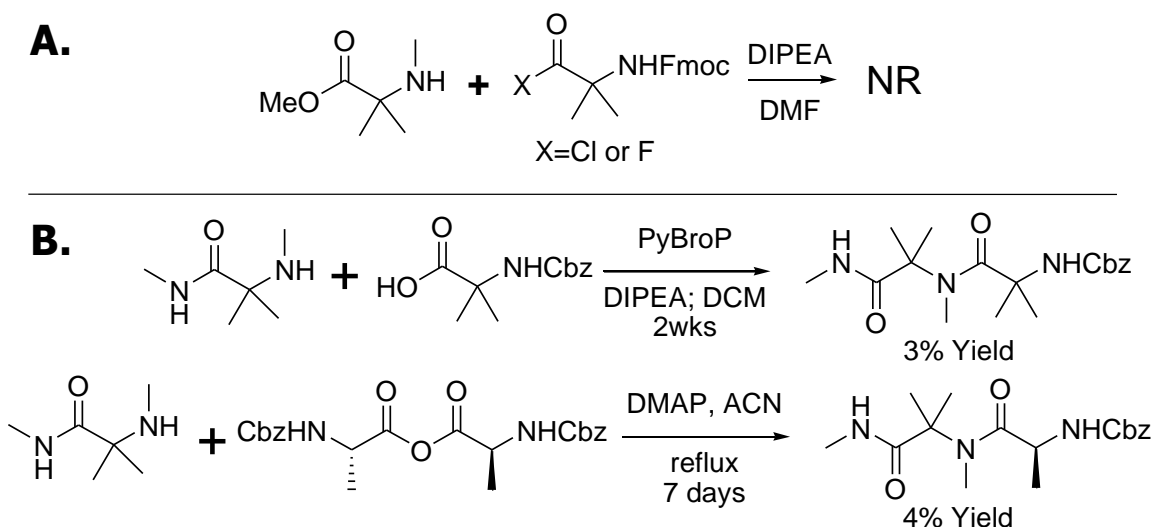


Figure 2.2. The only literature examples of the coupling of extremely hindered peptides. **A.**) Negative control experiments showing conventional techniques are not applicable. Reprod. from ref. 38. **B.**) Hindered dipeptide synthesis, Reprod. from ref. 32.

a silylating agent (*N,O*-Bis(trimethylsilyl)acetamide, BSA), no dipeptide formation was observed and included significant side reactions. This lead Carpino to state:³⁸ “*With hindrance of this magnitude the practical limit for urethane-based amino acid couplings appear to have been reached.*” It is only with the use of a tosyl-derived protecting group and acid chlorides that any dipeptidyl product can be observed. Unfortunately, the use of tosyl protecting groups has limited utility owing to the difficulty in deprotection and problems implementing the chemistry in modern peptide synthesis protocols. Peptide bond chemistry must be both robust in tolerance and simple to execute owing to the repetitive nature of the target systems.

To the best of our knowledge, the only other literature example to target these hindered peptide bonds using carbamate protecting groups is shown in Figure 2.2.B.³² Here again both the nucleophilic and the electrophilic partners of the coupling reaction are extremely hindered and powerful activation means are necessary, although very poor yields are obtained. The first example in Figure 2.2.B employs PyBrop (bromotripyrrolidinophosphonium hexafluorophosphate) which has been shown to be effective in the coupling of both Aib residues and *N*-methylated amino acids.⁴¹ However, even this acylating agent is only able to provide a 3% yield of dipeptidyl product after an extended period of time. Another example from that paper, using the symmetric anhydride of alanine in the presence of the nucleophilic catalyst DMAP, produces only 4% of the desired dipeptide after a seven day reflux in acetonitrile. Of particular note in this system is that even the coupling of a proteogenic amino acid such as alanine can be nearly impossible when faced with such severe steric hindrance of the nucleophilic component. Thus, there is scant literature precedence for the coupling of *N*-alkyl- α,α -disubstituted amino acids and any methodology which could form these tertiary amide bonds would be a substantial contribution to this area.

2.2 Results and Discussion

Dipeptide synthesis. The Fmoc-protected amino acid fluorides were synthesized in excellent yields with minor changes to a published procedure using diethylaminosulfur trifluoride (DAST), a reagent used to synthesize acid fluorides directly from carboxylic acids.⁴² Briefly, the Fmoc-amino acid is suspended in DCM, followed by the addition of a few drops of DMF until complete dissolution of the material. Next, a slight excess of DAST (1.2 equivalents) is added in a single portion and allowed to react at room temperature for approximately one hour. An aqueous wash removes all byproducts and excess DAST, followed by drying over sodium sulfate and evaporation of the solvent *in vacuo*. The resulting semisolid or crystalline solid acid fluorides were used without further purification and are bench stable. An esterification test was performed prior to the use of each acid fluoride by dissolving the material in methanol with 10% DIPEA and subjecting an aliquot to LC-MS analysis. Under these conditions any acid fluoride would be quantitatively converted to the methyl ester, and if less than 95% of the methyl ester was found the material was not used and a fresh batch was prepared.

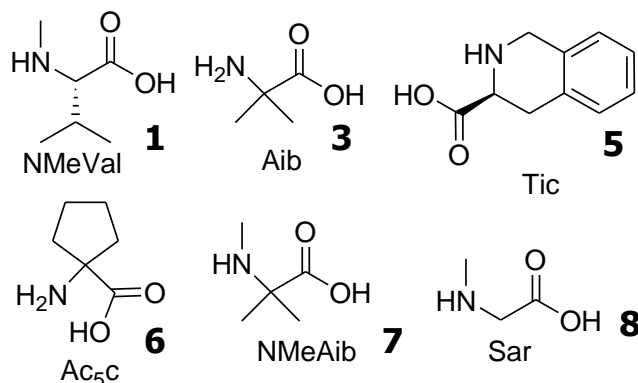
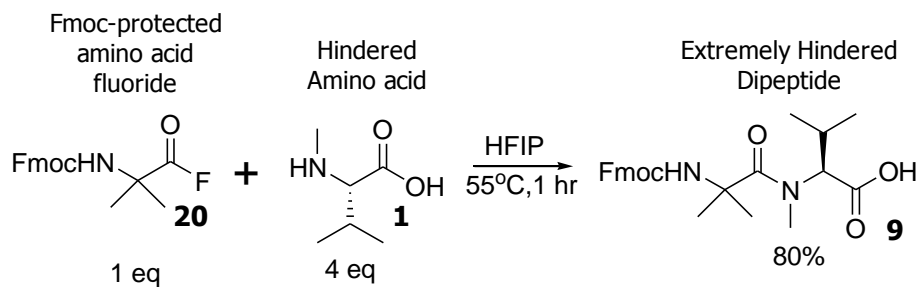


Figure 2.3. The hindered amino acids and their abbreviations used in this study. Abbreviations: NMeVal: (S)-N-Methyl-Valine, Aib: α -amino-isobutyric acid, Tic: (L)-1,2,3,4-Tetrahydroisoquinoline-3-carboxylic acid, NMeAib: N-Methyl- α -amino-isobutyric acid, Ac₅C: 1-amino-cyclopentanecarboxylic acid, Sar: Sarcosine (N-Methyl-Glycine).

The unprotected amino acids used in these trials are shown in Figure 2.3 and represent a variety of commercially available, hindered amino acids that are present in both natural and nonnatural peptides. All are either N-alkyl (NMeVal 1, Tic 5, and Sar 8), α,α -disubstituted (Aib 3 and Ac₅C 6) or both (NMeAib 7). Hexafluoroisopropanol (HFIP) was chosen as a solvent because of it consistently solubilized the unprotected amino acids, compounds which are insoluble in organic solvents. First, four equivalents of the raw amino acid was dissolved in HFIP to a concentration of 0.2M and allowed to prewarm in an oven at 55°C for 15 minutes. This allowed the solution to come to the reaction temperature prior to the addition of all components as well as aid in complete dissolution of the amino acid at these concentrations. Next, the preformed Fmoc-amino acid fluoride (for example, compound 20, one equivalent) was added and the solution placed in a conventional oven set at 55°C and allowed to react for the time shown in Table 2.1. An aliquot of the reaction was then dissolved in ACN/H₂O and analyzed via LC-MS. This straightforward process of using the preformed acid fluorides under baseless conditions in the presence of an excess of amino acid is a mild and simple procedure that is compatible with many protecting group configurations.



Compound	Dipeptide ^a	Yield	Conditions ^b
9	Fmoc-Aib-(S)-NMeVal-OH	80%	1hr
10	Fmoc-Aib-(S)-Tic-OH	86%	1hr
11	Fmoc-Aib-NMeAib-OH	60%	1hr
12	Fmoc-(S)-NMeVal-(S)-NMeVal-OH	78%	5min
13	Fmoc-(S)-NMeVal-(S)-Tic-OH	80%	5min
14	Fmoc-(S)-NMeVal-NMeAib-OH	68%	5min
15	Fmoc-(S)-NMeVal-Sar-OH	78%	5min
16	Fmoc-Ac5c-(S)-NMeVal-OH	74%	45min
17	Fmoc-Ac5c-(S)-Tic-OH	79%	45min
18	Fmoc-Ac5c-NMeAib-OH	60%	45min
19	Fmoc-Ac5c-Sar-OH	78%	45min

Table 2.1. Yield and conditions for the synthesis of hindered dipeptides. ^aSee Figure for abbreviations of the amino acids. ^bConditions: 1eq Fmoc acid fluoride, 4eq amino acid, 0.2M HFIP (concentration of amino acid), 55°C, Specified time.

Shown in Figure 2.4 is the HPLC chromatogram of the reaction mixture between Fmoc-Aib-F and (S)-NMeVal-OH (compound 9, Table 2.1), with the most prominent peak (80% by area) having a mass consistent with the dipeptide. The peak labeled “A” has a mass of the hydrolyzed acid fluoride, Fmoc-Aib-OH and the peak labeled “B” has a mass of the solvolyzed acid fluoride, Fmoc-Aib-OCH(CF₃)₂. Although the reaction is not quantitative, the byproducts may be separated by chromatography, with the potential to regenerate the Fmoc-amino acid from the corresponding hexafluoroisopropyl ester via hydrolysis. This general procedure was used to synthesize the other entries in Table 2.1, resulting in good to excellent yields of some extremely hindered dipeptidyl systems in moderate reaction times using conventional heating.

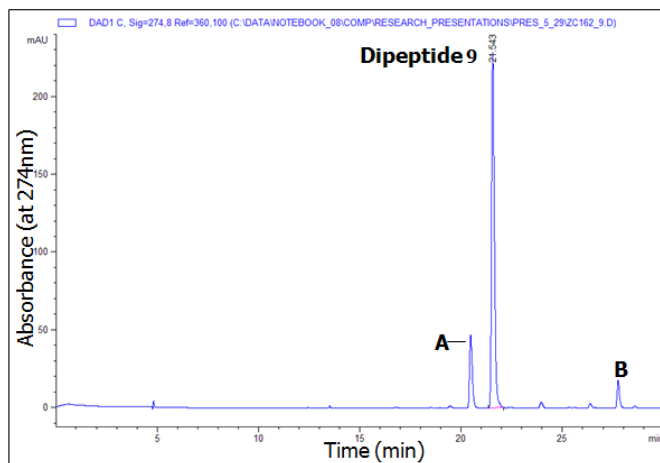


Figure 2.4. HPLC chromatogram (5%-95% H₂O/ACN w/0.1% FA) of the crude reaction of Fmoc-Aib-F with (S)-NMeVal-OH. The peak marked “A” has a mass consistent with Fmoc-Aib-OH, the peak marked “Dipeptide 9” has the mass of Fmoc-Aib-NMeVal-OH (compound **9**, Table 2.1), and “B” has the mass of Fmoc-Aib-OCH(CF₃)₂. Unlabeled peaks did not have identifiable masses.

Characterization of the dipeptides. All entries in Table 2.1 were analyzed by HPLC with low-resolution mass spectral analysis and showed masses consistent with that of the dipeptidyl products. The yield of each species was given in Table 2.1 was calculated via the chromatographic area of each peak at 274nm. The Fmoc group will absorb at this wavelength and so both dipeptidyl product as well as any side reaction of the Fmoc-acid fluoride was apparent. Compounds **9**, **10** and **16** were chosen for further analysis to verify the structure of the dipeptidyl products. These entries were subjected to high-resolution mass spectrometry (HRMS) and showed the expected masses of the Fmoc-protected dipeptides. In addition, two entries (**9** and **16**) had their structures confirmed by the heteronuclear NMR experiment HMBC (See Appendix, Figures A.2 and A.4). In particular, heteronuclear correlations were used to confirm the existence of the tertiary amide. In the example of dipeptide **9**, correlations could be seen from the protons of the *N*-methyl group to both the carbonyl carbon of Aib as well as the α -carbon of the NMeVal residue. Also, the two methyl groups of Aib have different chemical shifts indicating that they are diastereotopic as a consequence of their coupling to a chiral residue, the (S)-NMeVal. Prior to the coupling to the chiral residue, these enantiotopic methyl groups would have the same chemical shift.

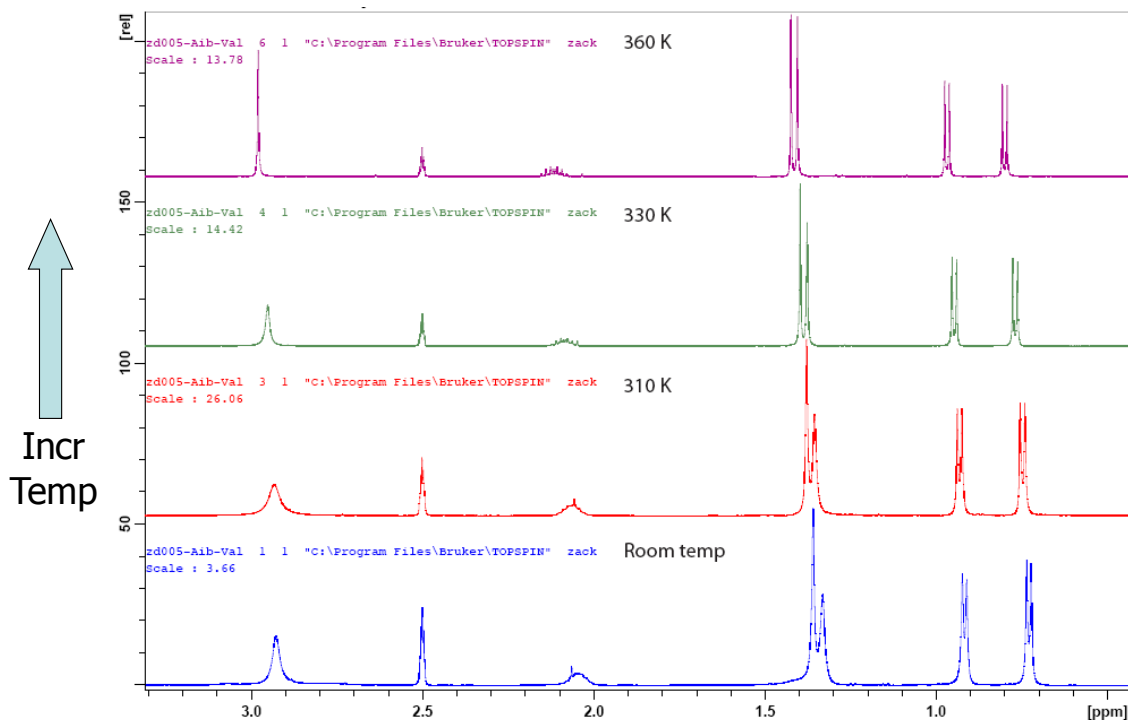
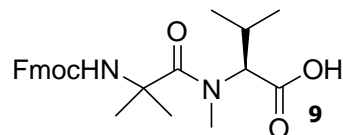


Figure 2.5 . Temperature coalescence profile of the dipeptide Fmoc-Aib-(S)-NMe-Val-OH, dipeptide **9** of Table 2.1.

Also consistent with the presence of the tertiary amide bond is the evidence of rotamers in the ^1H NMR at room temperature. For example, there is significant line broadening for a few of the signals at room temperature which become sharp at 360K. Fmoc-Aib-(S)-NMe-Val-OH, compound **9** of Table 2.1, is the hindered dipeptide whose ^1H spectra in $\text{DMSO}-d_6$ is given as a function of temperature in Figure 2.5. The *N*-methyl peak at approximately 2.9 ppm demonstrates this principle well, with a broad peak shape at room temperature (blue curve). As the temperature is increased to 330K, the peak begins to sharpen to the distinctive sharp methyl it should be. Finally, at 360K, complete coalescence is achieved and the spectrum shows no evidence of rotamer contamination. Other signals also show this: the resonance of the β -methine peak at 2.05 ppm of the NMe-Val residue has virtually no fine structure at room temperature but adopts the expected multiplet signal at elevated temperatures. Therefore, multiple pieces of independent evidence support the existence of the newly formed hindered tertiary amide across the dipeptide.

Racemization investigation. Of paramount importance in peptide chemistry is the preservation of optical integrity of each residue during the synthesis. Racemization of either stereocenter in the assembled dipeptide would lead to difficulties in purification. The loss of stereochemical purity of an amino acid is normally associated with oxazolone formation of the residue which is activated, which significantly increases the acidity of the α -proton.³⁶ The choice of both the α -amine protecting group and the activation strategy here is critical to suppressing this and other side reactions. As mentioned previously, carbamate protecting groups are preferred in this situation because of their resistance to oxazolone formation and this is one of the reasons their derivatives have been adopted as the standard protecting group in peptide chemistry. Acid fluorides have also been shown to be resistant to oxazolone formation providing all of the desired benefits of a highly active acylating species while preserving the stereochemical purity of the system.³⁹

HPLC was used to investigate the possibility of racemization in the synthesis of these hindered amide bonds. Although traditional RP-HPLC cannot resolve enantiomers without employing a specialized column with a chiral stationary phase, it can resolve diastereomers. In accordance with this principle, compound **12** in Table 2.1 was chosen for further study. The HPLC chromatogram of the dipeptidyl product of Fmoc-(S)-NMeVal-F **21** and (S)-NMeVal-OH **1** shows a single sharp peak at 24 minutes during a 40 minute chromatographic run of 0 to 100% H₂O/ACN (See Figure 2.6.B, red trace). Compare this to the coupling of Fmoc-(S)-NMeVal-F **21** and a racemic mixture of NMeVal-OH **22**, shown in Figure 2.6.A; this produces two

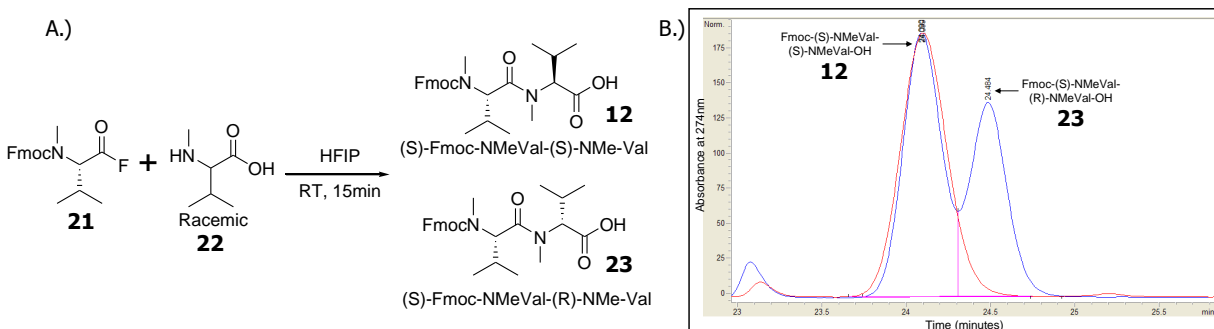


Figure 2.6. A.) Synthetic scheme for the racemization trials of Fmoc-NMeVal-F **21** with racemic NMeVal-OH **22** yielding two diastereomeric products **12** and **23**. B.) Overlay of the crude chromatograms of the racemization trials: the trace in red in the coupling of Fmoc-(S)-NMeVal-F with (S)-NMeVal-OH (compound **12**, Table 2.1), while the trace in blue is the product from the coupling of Fmoc-(S)-NMeVal-F **21** and (S,R)-NMeVal-OH **22**; the corresponding peaks for each dipeptide are annotated.

diastereomeric dipeptides **12** and **23** which resolve using the chromatographic conditions detailed above. With this result, stereochemical integrity (>90%) must be preserved in both

chiral centers through the dipeptide synthesis. Should significant racemization take place at the residue which is activated (Fmoc-(S)-NMeVal-F **21**), it would produce a certain amount of the diastereomeric dipeptide Fmoc-(R)-NMeVal-(S)-NMeVal-OH (not shown). This species would have the same retention time as its enantiomer, Fmoc-(S)-NMeVal-(R)-NMeVal-OH **23**, which resolves in a chromatographic run from the desired product, Fmoc-(S)-NMeVal-(S)-NMeVal-OH **12** as shown in Figure 2.6.B. Although less likely, if epimerization took place on the nucleophilic amino acid, the dipeptide Fmoc-(S)-NMeVal-(R)-NMeVal-OH **23** would also be evident from LC-MS. Therefore, this result provides evidence that this reaction is a racemization-free method of amino acid coupling.

Mechanistic investigations. To further understand the novel reactivity observed in this study, several experiments were performed to probe the mechanism. First, a number of conventional peptide coupling strategies were employed to highlight the difficult nature of the couplings and prove that traditional strategies had insufficient reactivity. This involves using the amino methyl ester **25** (commercially available as the HCl salt) as the nucleophilic residue and activating the carboxylic acid of an Fmoc-protected amino acid (here Fmoc-Aib-OH, compound **24**) using various reagents. Here only the direct acylation pathway is possible and so provides a unique control to highlight the neighboring group effect of α -amino acids. The two residues are normally used stoichiometrically to avoid unwanted side reactions, such as premature Fmoc removal from the excess amine present if more than one equivalent of nucleophile is employed. (In the traditionally used DMF solvent system, there is a competition between the amine acylation and deblocking the Fmoc group. Normally the rate of acylation is much faster, but with

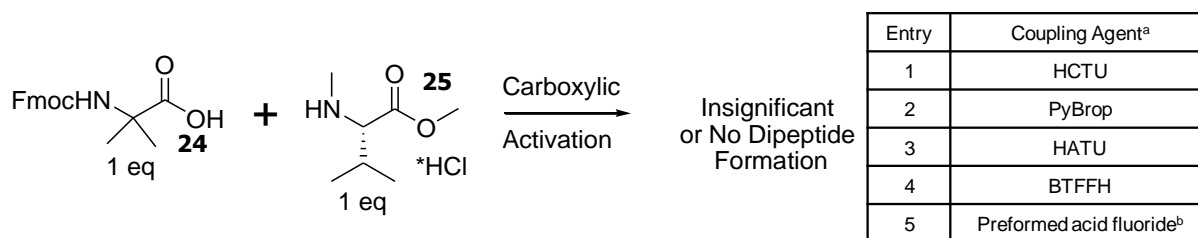


Figure 2.7. Control experiments showing that conventional peptide coupling agents have insufficient reactivity to produce peptide product in these hindered systems. ^aAll reactions performed in DMF using standard conditions. ^bPreformed acid fluorides synthesized using DAST as described in the text.

hindered systems it may become problematic.)⁴⁰ The coupling agents used here are among the most powerful available for the modern peptide chemist:³⁶ HCTU (O-(6-Chlorobenzotriazol-1-yl)-N,N,N',N'-8-tetramethyluronium hexafluorophosphate), HATU (O-(7-Azabenzotriazol-1-yl)-N,N,N',N'-tetramethyluronium hexafluorophosphate), PyBrop, BTFFH ((Fluoro-N,N,N',N'-

bis(tetramethylene)formamidinium hexafluorophosphate, an *in situ* acid fluoride forming reagent) as well as the preformed acid fluorides used in the above acylation trials. One equivalent of Fmoc-Aib-OH **24** (or the preformed acid fluoride), one equivalent of (S)-NMeVal-OMe*HCl **25** and one equivalent of activating agent (if applicable) were combined in DMF with the appropriate amount of DIPEA (3 equivalents of DIPEA for entries **1-4** and 2 equivalents for entry **5** in Figure 2.7) and allowed to react overnight. Only insignificant amounts (i.e. <5%) were found by LC-MS analysis of the crude reaction mixtures for each of the activation trials, including substantial amounts of premature Fmoc removal and other side reactions which were not readily identifiable by LC-MS. Thus, direct acylation of the amine does not occur to any useful degree and the difficulty of forming these hindered dipeptides in a straightforward manner is obvious.

Next, a competition experiment was performed to test the hypothesis that a neighboring group effect is involved in the dipeptide forming reactions. Competition experiments can be used to judge the relative nucleophilicity between two species while subjecting them to the same conditions. By placing both in the same reaction vessel and allowing them to compete for the same electrophile, a direct comparison between the two nucleophiles may be accomplished. Shown in Figure 2.8 is the schematic for the competition experiment: one equivalent of Fmoc-Aib-F **20** is combined with four equivalents of an amino acid, (S)-NMeVal-OH **1** and four equivalents of an amino methyl ester, (S)-NMeVal-OMe*HCl **25** and subjected to the standard

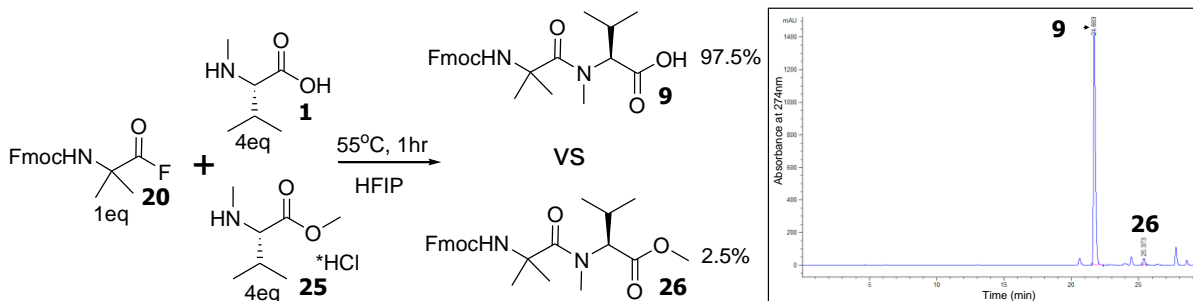


Figure 2.8. Competition experiments highlight the apparent neighboring group effect of the α -carboxylic acid to affect efficient acylation. Here the acid fluoride **20** is combined with 4 equivalents of (S)-NMeVal-OH **1** and 4 equivalents of (S)-NMeVal-OMe*HCl **25** and allowed to react under the standard acylation conditions. Also shown is the HPLC chromatogram shows the dipeptidyl acid **9** is 97.5% of the dipeptide product while the methyl ester **26** is only 2.5% of product.

conditions of the dipeptide formation of this study (0.2M HFIP, 55°C for one hour). If there is no neighboring group effect in these acylations, roughly equal amounts of the dipeptidyl acid and dipeptidyl methyl ester would be expected since the nucleophilicity of the amines would be approximately the same. However, if one of the tertiary amide products is formed to a greater

extent than the other, a neighboring group effect may be taking place to enhance the reactivity of one nucleophile relative to the other. The HPLC chromatogram of the reaction mixture is shown in Figure 2.8, with 97.5% of the dipeptidyl product being that of the carboxylic acid **9** while only 2.5% is that of the methyl ester **26**. Therefore, there is significant neighboring group participation to produce such a substantial amount of dipeptide acid as compared to the dipeptide ester.

Examination of the yields and conditions in Table 2.1 gives some insight into the nature of the reaction. As can be seen, the steric hindrance of the electrophile is the major factor in determining the amount of time needed for completion of the reaction (time course data for compounds **9** and **10** in Table 2.1 are given in the Experimental Details). For example, while reactions with α,α -disubstituted acid fluorides (compounds **9-11** and **16-19**) require a on the order of 45 minutes to complete, the reactions involving Fmoc-(S)-NMeVal-F **21** as the electrophile are complete within 5 minutes. Also, only minor changes in yield of the dipeptides are found when dramatically changing the steric hindrance of the nucleophilic amino acid. Compare compounds **12** and **15** of Table 2.1: the addition of the isopropyl group of NMeVal (dipeptide **12**) gives an identical yield (78%) to that of the reaction with sarcosine (dipeptide **15**), which only has a methylene at the α -carbon. Only a modest reduction in yield is found when the

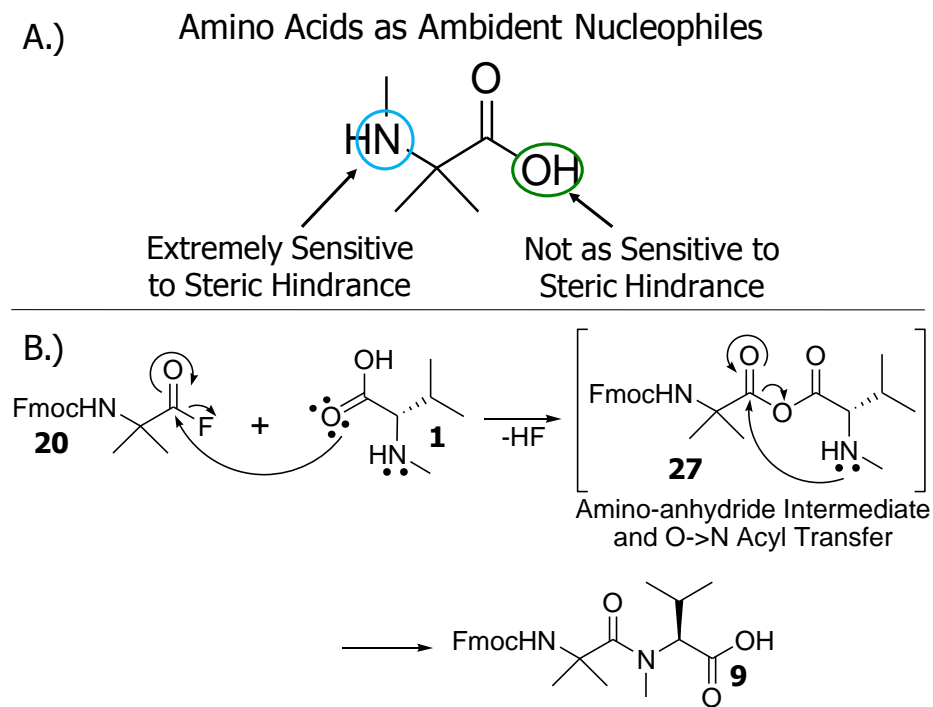


Figure 2.9. A.) Schematic to show how the carboxylic acid may be the nucleophile where the steric hindrance of the amine precludes direct acylation. B.) Proposed acyl transfer mechanism in the synthesis of hindered dipeptides. First the carboxylate of the amino acid attacks to form the amino anhydride intermediate, followed by O→N acyl transfer to form the tertiary amide.

nucleophile is changed to NMeAib (68%, compound **14**), showing that the steric crowding of the amine has only a minor effect on the yield of dipeptidyl product. This is in stark contrast to conventional peptide coupling strategies where the hindrance of the amine is directly responsible for slowed couplings and the occurrence of side reactions.

The proposed reaction mechanism for this reaction is shown in Figure 2.9.B (this mechanism uses the reaction to form dipeptide **9**, Table 2.1). Because the severe steric hindrance of the secondary amine prevents it from directly attacking the acid fluoride, the carboxylate may be acting as the nucleophile since it may not be as sensitive to the encumbered nature of the peptide. This would lead to the formation of an amino-anhydride

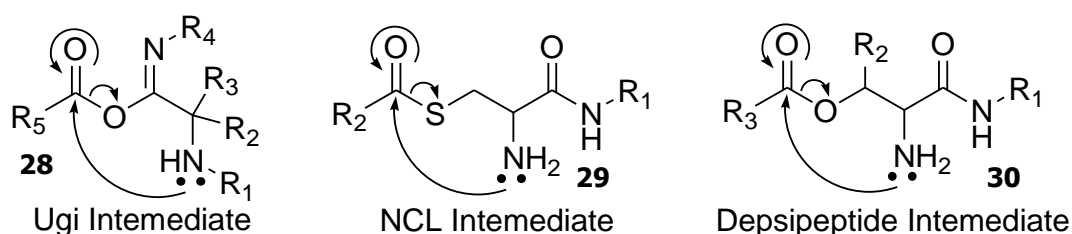


Figure 2.10. Examples of other five-membered ring rearrangements used to create amide bonds: the remote Mumm rearrangement⁴³ **28** of the Ugi reaction, thioester mediated acyl transfer **29** from Native Chemical Ligation (NCL)⁴⁴, and ester mediated acyl transfer **30** used in the depsipeptide technique.⁴⁵

intermediate **27** which could rearrange through a five-membered ring transition state yielding the tertiary amide. This “O->N” acyl transfer has been known to form amide bonds through similar reaction mechanisms such as those depicted in Figure 2.10: the “remote” Mumm rearrangement⁴³ of the Ugi reaction (intermediate **28**) and the “depsipeptide technique” of peptide synthesis⁴⁵ (intermediate **30**), as well as the “S->N” acyl transfer which has been utilized in Native Chemical Ligation (NCL)⁴⁴ (intermediate **29**). Thus, similar reaction mechanisms have been reported in the literature, but, to the best of our knowledge, no one has ever reported the five-membered ring “O->N” acyl transfer from an amino-anhydride intermediate to form an amide bond.

To provide evidence as to whether anhydrides might be involved in the reaction mechanism, a trapping experiment was designed and is shown in Figure 2.11. A tertiary amino acid, *N*-(2-methylnaphthylene)-sarcosine **31**, was synthesized with a distinctive UV-chromophore, a naphthyl group, to allow quantitation via HPLC area. Here, the carboxylate of this amino acid would still be able to attack the acid fluoride to form an anhydride, but would be unable to undergo the acyl transfer to the tertiary amide. Since the reaction is run in HFIP, the addition of 10% DIPEA would quench the reaction by solvolyzing any reactive species, whether

it would be remaining acid fluoride or an anhydride species. Solvolysis of the mixed amino-anhydride **32** could occur at either hindered acyl group: attack at the acyl group of *N*-(2-methylnaphthylene)-sarcosine would give ester **34** whereas attack at the other acyl group of the anhydride intermediate would yield ester **33**. It is the transfer of reactivity to the acyl unit of the sarcosine derivative (to yield compound **34**) that would be a hallmark of anhydride formation and provide evidence for the proposed mechanism. Thus, we would have activated the acyl group of the tertiary amino acid towards nucleophilic attack which presumably could have happened only through the postulated anhydride formation (intermediate **32**) with the Fmoc-protected acid fluoride.

The reaction between Fmoc-Aib-F **20** (1eq) and *N*-(2-methylnaphthylene)-sarcosine **31** (4eq) was performed using the standard conditions of the dipeptide reaction, withdrawing an aliquot of the reaction mixture at various time points. This aliquot was quenched with 10% DIPEA and allowed to sit on the bench top for at least 20 minutes to allow complete solvolysis of

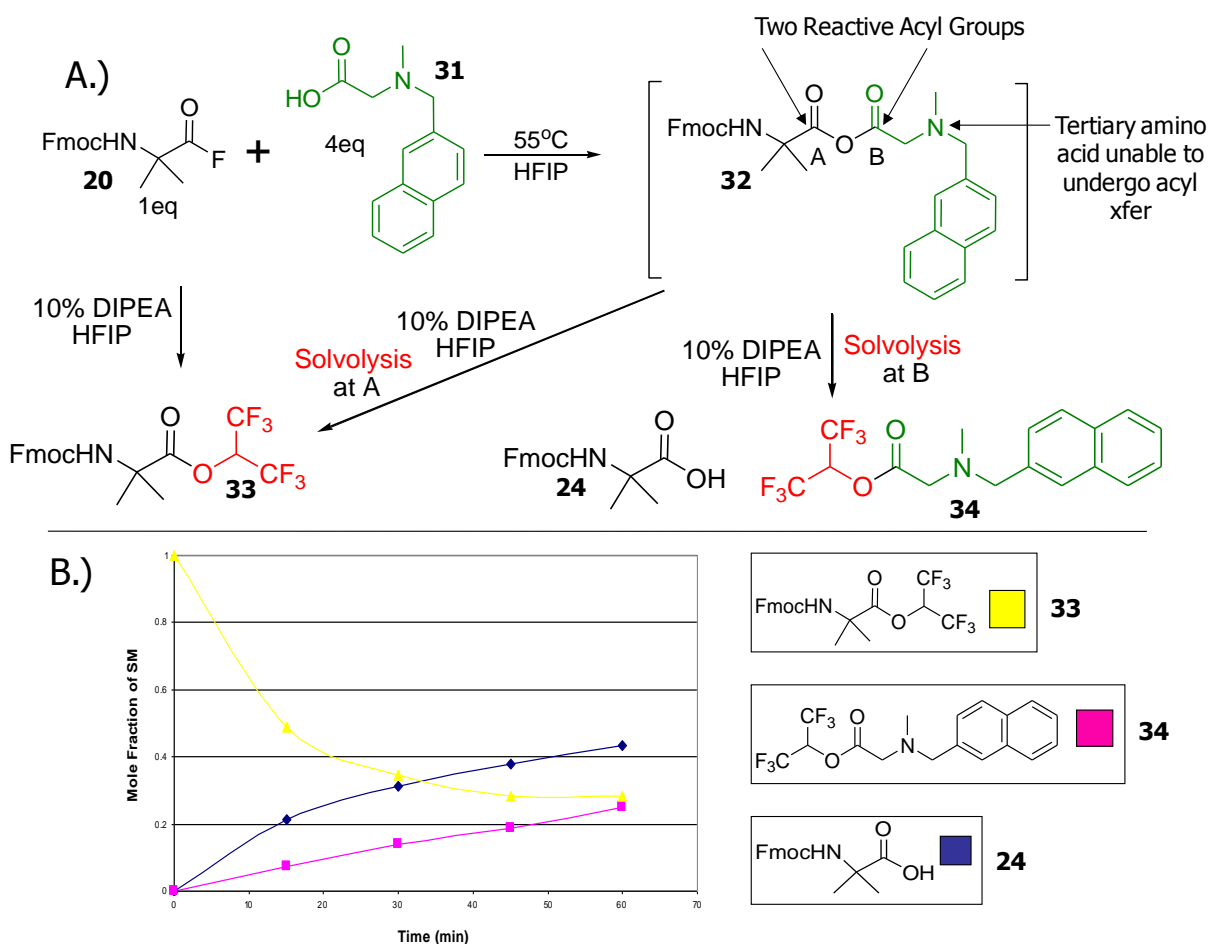


Figure 2.11. Schematic of the anhydride trapping experiment: Fmoc-Aib-F is reacted with a tertiary amino acid. Unable to undergo the acyl transfer, the addition of base solvolyzes any reactive species, be it acid fluoride or anhydride. **B.)** Plot of mole fraction of each species as a function of time.

any reactive species followed by analysis by LC-MS. The HPLC areas of the products are then converted to mole fractions of each species using previously determined calibration curves of the naphthyl chromophores and dividing that by the initial concentration of Fmoc-Aib-F **20**. The result is the time course of the mole fraction of each of the esterified products and is shown in Figure **2.11.B**. If the hypothesized anhydride mechanism is operating in this reaction, we should see a steady decrease in the amount of Fmoc-Aib-OCH(CF₃)₂ **33** (from the solvolyzed Fmoc-Aib-F) as more anhydride is formed, with a steady increase of both the *N*-(2-methylnaphthylene)-Sar-OCH(CF₃)₂ **34** and the Fmoc-Aib-OH **24** as the anhydride forms and is solvolyzed at this position of the mixed anhydride. These trends are exactly what is observed in the time course data, with the amount of ester **34** steadily increasing as the amino-anhydride is formed and solvolyzed at the acyl position of the sarcosine derivative. Through the time course of the experiment, about 8% of the total sarcosine is converted to the corresponding hexafluoroisopropyl ester **34**, showing that significant amounts of anhydride are forming in the time scale of the reaction. Since the only way the acyl group of the *N*-(2-methylnaphthylene)-sarcosine could be activated is through the formation of the mixed anhydride, the evolution of the solvolyzed species on the time scale of the reaction is powerful evidence that the proposed mechanism is operating in this reaction.

2.3 Conclusions

A synthetic scheme for the assembly of extremely hindered dipeptides has been presented. This mild, operationally simple strategy uses commercially available materials. This has been achieved by exploiting a neighboring group effect of unprotected α -amino acids in a highly polar solvent, hexafluoroisopropanol (HFIP). Good to excellent yields have been obtained for some dipeptidyl products which were not synthetically accessible before and the procedure has also been shown to be racemization-free. A novel amino-anhydride rearrangement was postulated for this and evidence for this mechanism was presented.

2.4 Experimental Details

General Methods. HFIP (1,1,1,3,3,3-Hexafluoro-2-propanol), DAST, Dichloromethane (DCM), anhydrous Dimethylformamide (DMF), anhydrous Methanol (MeOH) and redistilled Diisopropylethylamine (DIPEA) were obtained from Sigma-Aldrich and used without purification. All Fmoc-amino acids and unprotected amino acids were obtained from either Novabiochem or

Bachem. All other chemicals were purchased from Sigma-Aldrich and used without purification. HPLC-MS analysis was performed on a Hewlett-Packard Series 1200 with a Waters Xterra MS C18 column (3.5 μ m packing, 4.6 mm x 100mm) with a solvent system of H₂O/acetonitrile with 0.1% formic acid at a flow rate of 0.8mL/min. NMR experiments were performed on a Bruker 500MHz NMR with chemical shifts (δ) reported relative to DMSO-*d*₆ residual solvent peaks. Analysis of 2D NMR data was performed using Sparky 3, T. D. Goddard and D. G. Kneller, University of California, San Francisco. Preparatory Scale HPLC purification was performed on a Varian Prostar Prep HPLC with a Waters Xterra column (5 μ m packing, 19 mm x 100mm) with a solvent system of H₂O/acetonitrile with 0.1% formic acid at a flow rate of 18 mL/min. HRMS analysis was performed by either the University of Pittsburgh (Waters LC/Q-ToF) or Ohio State University (ToF/ES).

General procedure for acid fluoride formation. Fmoc protected amino acid fluorides were synthesized with the reagent DAST by the method of Carpino. In a polypropylene tube, the Fmoc-amino acid (0.92 mmole) was suspended in 4mL anhydrous dichloromethane and a few drops of DMF were added to give complete dissolution. Then 145 μ L (1.1 mmole) of DAST was added in a single portion. After 1 hr, the mixture was washed with ice water, the organic layer was dried over sodium sulfate, filtered through a cotton plug and the solvent was removed *in vacuo*. An esterification test was performed to assure quantitative acid fluoride formation by dissolving 5 mg of Fmoc-amino acid fluoride in 0.3 mL of anhydrous Methanol with 10% DIPEA and allowed to react for 15 min at room temperature. An aliquot was then removed and analyzed by HPLC-MS showing less than 2% of residual Fmoc-amino acid present.

General procedure for dipeptide synthesis. In a typical experiment the Fmoc amino acid fluoride (0.3 mmole, 1eq) was weighed into a polypropylene tube. The amino acid (1.2 mmole, 4eq) was dissolved in HFIP (6 mL) to a concentration of 0.2M. For reactions run at 55°C, the amino acid solution was placed in the oven for 15 minutes to allow the solution to come to temperature. The amino acid solution was then added to the Fmoc-acid fluoride and the vessel placed in an oven for the specified amount of time. An aliquot was then removed, dissolved in H₂O/acetonitrile with 0.1% formic acid and the results analyzed by HPLC-MS.

Fmoc-Aib-(S)-NMeVal-OH (dipeptide **9**):

Fmoc-Aib-F **20** was synthesized via the general procedure for acid fluoride formation, and the dipeptide was synthesized by the general procedure for dipeptide synthesis. (S)-NMeVal-OH **1** (106mg, 808 μ mole, 4 eq) was dissolved in HFIP (4.03mL, concentration of 0.2 M) in a polypropylene tube. Fmoc-Aib-F (66 mg, 202 μ mole) was then added and the reaction placed in a conventional oven held at 55°C. After 1hr, an aliquot of the reaction mixture was removed, dissolved in H₂O/acetonitrile with 0.1% formic acid and the results analyzed by HPLC-MS. The crude yield (80%) is estimated from HPLC area integration, monitoring at 274nm. HPLC-MS analysis (see Figure **2.12**): calcd for Fmoc-Aib-(S)-NMeVal-OH **9** + H⁺: 439.2, found 439.2. The product was purified by RP purification. Anal. Calcd for C₂₅H₃₀N₂O₅Na: 461.2052 (difference 3.5 ppm), Found: 461.2036. ¹H NMR (500 MHz, DMSO-*d*₆ with 1% trifluoroacetic acid), δ 7.88 (d, *J* = 7.6 Hz, 2H), 7.79 (s, 1H, -NH), 7.69 (d, *J* = 7.4 Hz, 2H), 7.41 (t, *J* = 7.6 Hz, 2H), 7.32 (m, 2H), 4.47 (d, *J* = 9.6 Hz, 1H, -CHCH(CH₃,CH₃)), 4.32 (m, 2H), 4.19 (t, *J* = 6.5 Hz, 1H), 2.93 (s, 3H, -N(CH₃)), 2.05 (m, 1H, -CHCH(CH₃)₂), 1.36 (s, 3H, -C(CH₃,CH₃)), 1.33 (s, 3H, -C(CH₃,CH₃)), 0.92 (d, *J* = 6.5 Hz, 3H, -CHCH(CH₃,CH₃)), 0.73 (d, *J* = 6.8 Hz, 3H, -CHCH(CH₃,CH₃)); ¹³C NMR (from HMQC and HMBC, 500 MHz, DMSO-*d*₆ with 1% trifluoroacetic acid), δ 172.5, 172.0, 154.2, 143.6 (2C), 140.6 (2C), 127.4 (2C), 126.7 (2C), 125.1 (2C), 120.1 (2C), 64.7, 63.3, 56.2, 46.5, 32.1, 26.2, 25.5 (2C), 19.8, 18.8

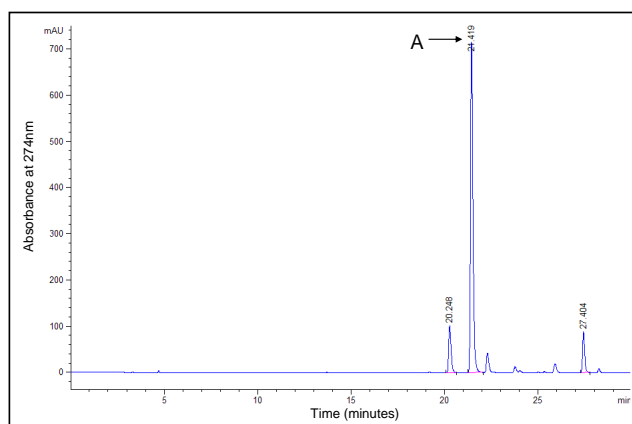


Figure **2.12**. Crude HPLC trace of the reaction of Fmoc-Aib-F with (S)-NMeVal-OH to give dipeptide **9**, monitoring at a wavelength of 274nm with a gradient of 5-95% ACN/H₂O with 0.1% formic acid over 30 minutes. The peak marked “A” has a m/z = 439.2 (calcd for Fmoc-Aib-NMeVal-OH **9** + H⁺: 439.2).

Fmoc-Aib-(S)-Tic-OH (compound 10)

Fmoc-Aib-F was synthesized via the general procedure for acid fluoride formation, and the dipeptide was synthesized by the general procedure for dipeptide synthesis. H-Tic-OH **5** (88 mg, 497 μ mole, 4 eq) was dissolved in HFIP (2.49 mL, concentration of 0.2 M) in a polypropylene tube. Fmoc-Aib-F (41 mg, 124 μ mole, 1eq) was then added and the reaction placed in a conventional oven held at 55°C. After 1hr, an aliquot of the reaction mixture was removed, dissolved in H₂O/acetonitrile with 0.1% formic acid and the results analyzed by HPLC-MS (See Figure 2.13). The crude yield (86%) is estimated from HPLC area integration, monitoring at 274nm. HPLC-MS analysis: calcd for Fmoc-Aib-Tic-OH **10** + H⁺: 485.2, found 485.2. The product was purified by RP purification. Anal. Calcd for C₂₉H₂₈N₂O₅Na: 507.1896, Found: 507.1875 (diff 4.1 ppm). ¹H NMR consistent with two rotamers, including multiple signal overlap.

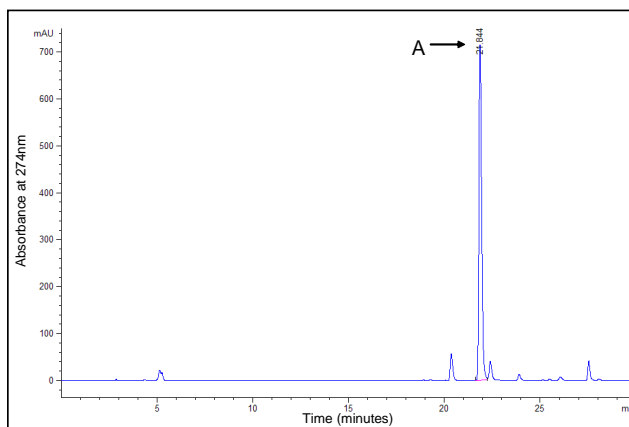


Figure 2.13. Crude HPLC trace of the reaction of Fmoc-Aib-F with H-Tic-OH to give dipeptide **10**, monitoring at a wavelength of 274nm with a gradient of 5-95% ACN/H₂O with 0.1% formic acid over 30 minutes. The peak marked “A” has a m/z = 485.2 (calcd for Fmoc-Aib-Tic-OH **10** + H⁺: 485.2).

Fmoc-Ac₅c-(S)-NMe-Val-OH (compound 16)

Fmoc-Ac₅c-F was synthesized via the general procedure for acid fluoride formation, and the dipeptide was synthesized by the general procedure for dipeptide synthesis. (S)-NMeVal-OH **1** (86 mg, 657 μ mole, 4 eq) was dissolved in HFIP (3.29 mL, concentration of 0.2 M) in a polypropylene tube. Fmoc-Ac₅c-F (58 mg, 164 μ mole, 1eq) was then added and the reaction placed in a conventional oven held at 55°C. After 45 min, an aliquot of the reaction mixture was removed, dissolved in H₂O/acetonitrile with 0.1% formic acid and the results analyzed by HPLC-

MS. The crude yield (74%) is estimated from HPLC area integration, monitoring at 274nm (See Figure 2.14). HPLC-MS analysis calced for Fmoc-Ac5c-(S)-NMe-Val-OH **16** + H⁺: 465.2, found 465.2. The product was purified by RP purification. Anal Calced for C₂₇H₃₂N₂O₅Na: 487.2209, Found: 487.2177 (diff 6.5 ppm). ¹H NMR (500 MHz, DMSO-*d*₆ with 1% trifluoroacetic acid), δ

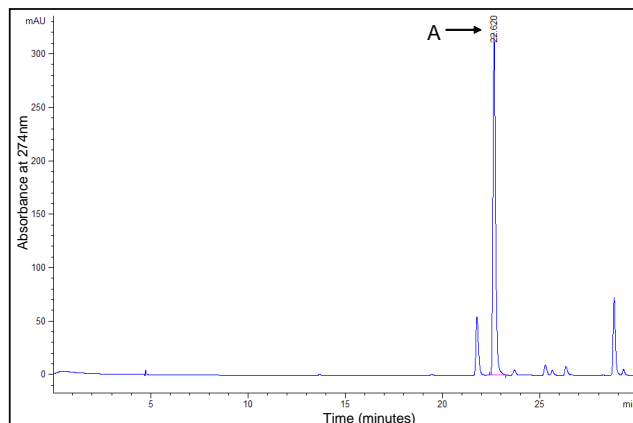


Figure 2.14. Crude HPLC trace of the reaction of Fmoc-Ac₅c-F with (S)-NMe-Val-OH to give dipeptide **16**, monitoring at a wavelength of 274nm with a gradient of 5-95% ACN/H₂O with 0.1% formic acid over 30 minutes. The peak marked “A” has a m/z = 465.2 (calced for Fmoc-Ac₅c-(S)-NMe-Val-OH **16** + H⁺: 465.2).

7.87 (d, *J* = 7.6 Hz, 2H), 7.84 (s, 1H, -NH, overlap with δ 7.87), 7.67 (m, 2H), 7.41 (t, *J* = 7.4 Hz, 2H), 7.32 (t, *J* = 7.4 Hz, 2H), 4.39 (d, *J* = 10.2 Hz, 1H, -CHCH(CH₃,CH₃)), 4.32 (m, 1H), 4.25 (m, 1H), 4.19 (m, 1H), 2.93 (s, 3H, -N(CH₃)), 2.23 (m, 1H), 2.04 (m, 1H, -CHCH(CH₃)₂), 1.96 (m, 2H), 1.87 (m, 1H), 1.55 (m, 4H), 0.90 (d, *J* = 6.3 Hz, 3H, -CHCH(CH₃,CH₃)), 0.67 (d, *J* = 6.3 Hz, 3H, -CHCH(CH₃,CH₃)); ¹³C NMR (from HMQC and HMBC, 500 MHz, DMSO-*d*₆ with 1%trifluoroacetic acid), δ 172.3, 172.1, 153.9, 143.7 (2C), 140.4 (2C), 127.4 (2C), 126.7 (2C), 124.9 (2C), 120.0 (2C), 65.9, 64.7, 62.9, 46.7, 39.6, 35.9, 35.8, 32.3, 26.2, 23.7, 19.8, 18.8

Time Course Data. Time course data was undertaken to verify the time scale of the reaction. Dipeptides **9** and **10** were synthesized according to the procedures here in the Experimental Details. At the appropriate time points, an aliquot of the reaction mixture was withdrawn, dissolved in H₂O/acetonitrile with 0.1% formic acid and the results analyzed by LC-MS. The results are shown in Figure 2.15.

Racemization Trials. To assess potential racemization at either stereocenter of the resulting dipeptide, a diastereomeric mixture was synthesized with Fmoc-(S)-NMeVal and either (S)-NMeVal-OH or a racemic mixture of (S)-NMeVal-OH and (R)-NMeVal-OH.

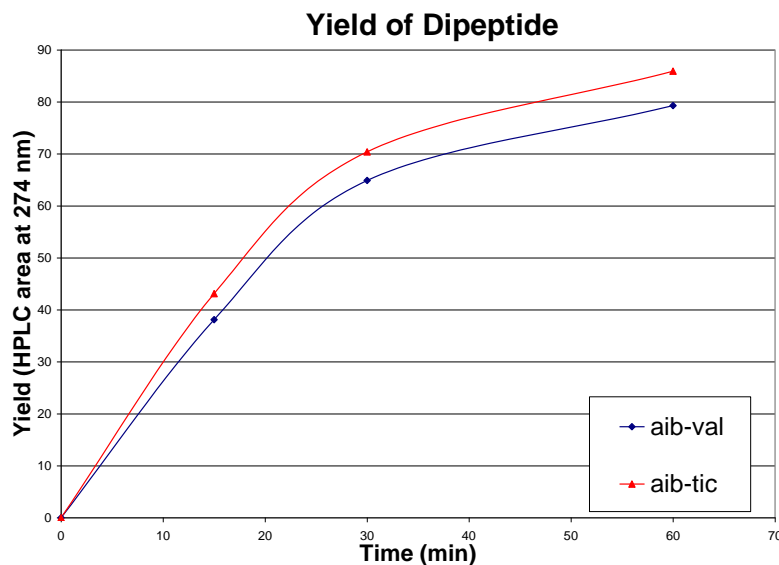


Figure 2.15. Time course data for the formation of dipeptides Fmoc-Aib-(S)-NMeVal-OH (dipeptide **9**, marked “aib-val”) and Fmoc-Aib-(S)-Tic-OH (dipeptide **10**, marked “aib-tic”). The yield is shown as the integrated area of each chromatogram at 274 nm.

Fmoc-(S)-NMeVal-F was synthesized via the general procedure for acid fluoride formation, and the dipeptide was synthesized by the general procedure for dipeptide synthesis. (S)-NMeVal-OH **1** (27 mg, 207 μ mole, 4 eq) was dissolved in HFIP (1.03 mL, concentration of 0.2 M) in a polypropylene tube. Fmoc-(S)-NMeVal-F **21** (25 mg, 52 μ mole, 1eq) was then added and the reaction placed in a conventional oven held at 55°C. After 5 min, an aliquot of the reaction mixture was removed, dissolved in H₂O/acetonitrile with 0.1% formic acid and the results analyzed by LC-MS (See Figure 2.16).

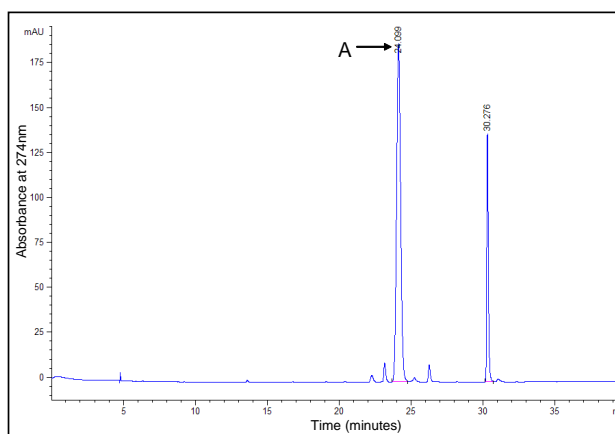


Figure 2.16. Crude HPLC trace of the reaction of Fmoc-(S)-NMeVal-F with H-(S)-NMeVal-OH to give dipeptide **12**, monitoring at a wavelength of 274nm with a gradient of 5-95% ACN/H₂O with 0.1% formic acid over 40 minutes. The peak marked “A” has a m/z = 467.2 (calcd for Fmoc-(S)-NMeVal-(S)-NMeVal-OH **12** + H⁺: 467.2).

Fmoc-(S)-NMeVal-F was synthesized via the general procedure for acid fluoride formation, and the dipeptide was synthesized by the general procedure for dipeptide synthesis. H-(S,R)-NMeVal-OH **22** (22 mg, 166 μ mole, 4 eq) was dissolved in HFIP (0.83 mL, concentration of 0.2 M) in a polypropylene tube. Fmoc-(S)-NMeVal-F (20 mg, 41 μ mole, 1eq) was then added and the reaction placed in a conventional oven held at 55°C. After 5 min, an aliquot of the reaction mixture was removed, dissolved in H₂O/acetonitrile with 0.1% formic acid and the results analyzed by LC-MS (See Figure 2.17).

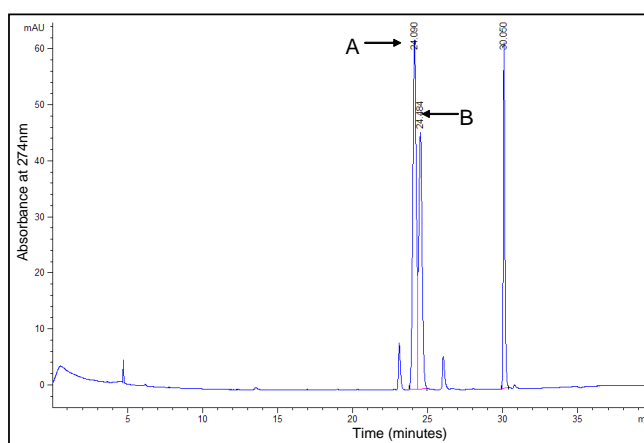


Figure 2.17.. Crude HPLC trace of the reaction of Fmoc-(S)-NMeVal-F with (S,R)-NMeVal-OH to give dipeptides **12** and **23**, monitoring at a wavelength of 274nm with a gradient of 5-95% ACN/H₂O with 0.1% formic acid over 40 minutes. Both peaks marked “A” and “B” have a m/z = 467.2 (calcd for Fmoc-(S)-NMeVal-(S)-NMeVal-OH + H⁺: 467.2), indicating that the diastereomeric dipeptides resolve in the present chromatography conditions.

Control Acylations. A number of conventional carboxylic activating agents were also tried for control acylations using a methyl ester protected amino acid. In a typical experiment, 32 mg (99 μ mole, 1eq), 1eq activating agent, and 18 mg of (S)-NMeVal-OMe*HCl **25** (99 μ mole, 1eq) were dissolved in 493 μ L of DMF (concentration of reagents 0.2M) in a polypropylene tube. After complete dissolution of all materials, the appropriate amount of DIPEA was added (3 equivalents of DIPEA for entries **1-4** and 2 equivalents for entry **5** in Figure 2.7). The reaction was stirred overnight at room temperature after which an aliquot of the reaction mixture was removed, dissolved in H₂O/acetonitrile with 0.1% formic acid and the results analyzed by HPLC-MS. No significant amount of dipeptide (<5%) was seen for any of the reactions. Significant amounts of premature deblocking of the Fmoc group occurred for most acylation trials as

evidenced by the appearance of a dibenzofulvene peak in HPLC-MS analysis as well as other side reactions not readily identifiable by LC-MS analysis.

Competition Experiments: To test the hypothesis that a neighboring group effect is involved in the dipeptide formation reaction we carried out a competition experiment in which we combined NMeVal-OH **1** and NMeVal-OMe.HCl **25** in one pot as potential coupling partners with Fmoc-Aib-F. The relative amounts of the two possible dipeptide products: Fmoc-Aib-NMeVal-OH **9** and Fmoc-Aib-NMeVal-OMe **26** were quantified and identified by HPLC-MS. If no neighboring group effect is involved then we would expect roughly equal amounts of the two dipeptide products.

Fmoc-Aib-F was synthesized via the general procedure for acid fluoride formation, and the dipeptide was synthesized by the general procedure for dipeptide synthesis. H-(S)-NMeVal-OH (53 mg, 404 μ mole, 4 eq) and H-(S)-NMeVal-OMe*HCl (73mg, 404 μ mole, 4eq) was dissolved in HFIP (2.02 mL, concentration of 0.2 M) in a polypropylene tube. Fmoc-Aib-F (33 mg, 101 μ mole, 1eq) was then added and the reaction placed in a conventional oven held at 55°C. After 60 min, an aliquot of the reaction mixture was removed, dissolved in H₂O/acetonitrile with 0.1% formic acid and the results analyzed by LC-MS. The LC-MS results showed a ratio of Fmoc-Aib-NMeVal-OH **9** to Fmoc-Aib-NMeVal-OMe **26** of 97.5:2.5, consistent with a significant neighboring group effect.

Anhydride Trapping Experiment:

***N*-Naphthyl-Sarcosine-OH (compound 31).** Sarcosine-OtBu*HCl (150 mg, 830 μ mole, 1eq) and 2-(Bromomethyl)-naphthalene (830 μ mole, 183 mg, 1eq) were placed in a 25 mL round bottom flask and the vessel was charged with 8 mL of tetrahydrofuran. DIPEA (290 μ L, 1.6 mmole, 2 eq) was then added and the reaction left to stir overnight. The crude product was concentrated *in vacuo* and used without further purification. The residue was dissolved 5 mL DCM, an equal volume of trifluoroacetic acid was added, and the reaction was allowed to stir at room temperature for 2 hrs. The product was then purified by RP purification and lyophilized from the ACN/H₂O with 0.1% formic acid solvent mixture. HPLC-MS analysis (See Figure **2.18**) for the product found $m/z = 230.0$ (calcd for *N*-Naphthyl-Sarcosine-OH **31** + H⁺ = 230.1). ¹H NMR (500 MHz, DMSO-*d*₆ with 1% trifluoroacetic acid), δ 8.07 (bs, 1H), 8.02 (d, 1H), 7.97 (m, 2H), 7.64 (dd, 1H), 7.6 (m, 2H), 4.52 (bs, 2H), 4.13 (s, 2H), 2.83 (s, 3H). ¹³C NMR (500 MHz, DMSO-*d*₆

with 1% trifluoroacetic acid), δ 167.8, 133.8, 133.1, 131.7, 129.0, 128.6, 128.5, 128.1, 127.6, 127.4, 127.1, 59.8, 55.1, 41.0.

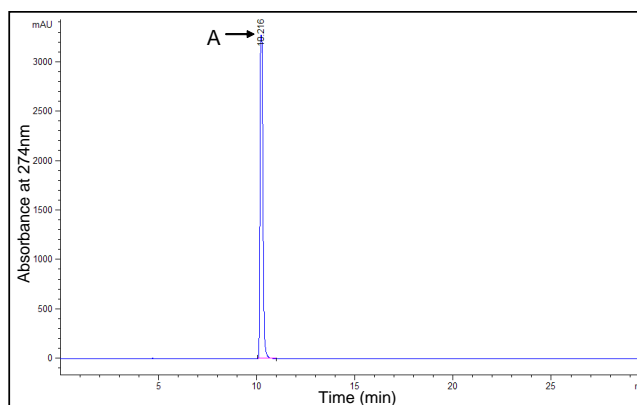


Figure 2.18. HPLC trace of the purified product *N*-naphthyl-Sarcosine-OH **31**, monitoring at a wavelength of 274 nm with a gradient of 5-95% ACN/H₂O with 0.1% formic acid over 30 minutes. The peak marked “A” has a *m/z* = 230.0 (calcd for *N*-naphthyl-Sarcosine-OH **31** + H⁺: 230.1).

To investigate the hypothesis that a transient amino anhydride is formed during the reaction, *N*-Naphthyl-Sarcosine-OH **31** was combined with Fmoc-Aib-F **20**. The carboxylate of the amino acid **31** can still attack the acid fluoride **20** forming the anhydride **32**, but this intermediate would not be able to undergo the hypothesized acyl transfer necessary for amidation. Quenching this reaction with 10% DIPEA would lead to solvolysis of any active acylating species (either acid fluoride or anhydride), and anhydride solvolysis could occur at either acyl group to give two different hexafluoroisopropyl esters.

Fmoc-Aib-F was synthesized via the general procedure for acid fluoride formation, and the trapping experiment was performed using the general procedure for dipeptide synthesis. *N*-naphthyl-Sarcosine-OH **31** (30 mg, 131 μ mole, 1 eq) was dissolved in 670 μ L of HFIP (conc of 200mM) and Fmoc-Aib-F **20** (11 mg, 34 μ mole, 1 eq) was added. At 15 minute intervals, an aliquot of the reaction was withdrawn, quenched with 10% DIPEA, and allowed to stand for at least 20 minutes at room temperature. 75% ACN/H₂O with 0.1% formic acid was then added and the mixture analyzed by LC-MS (See Figure 2.19).

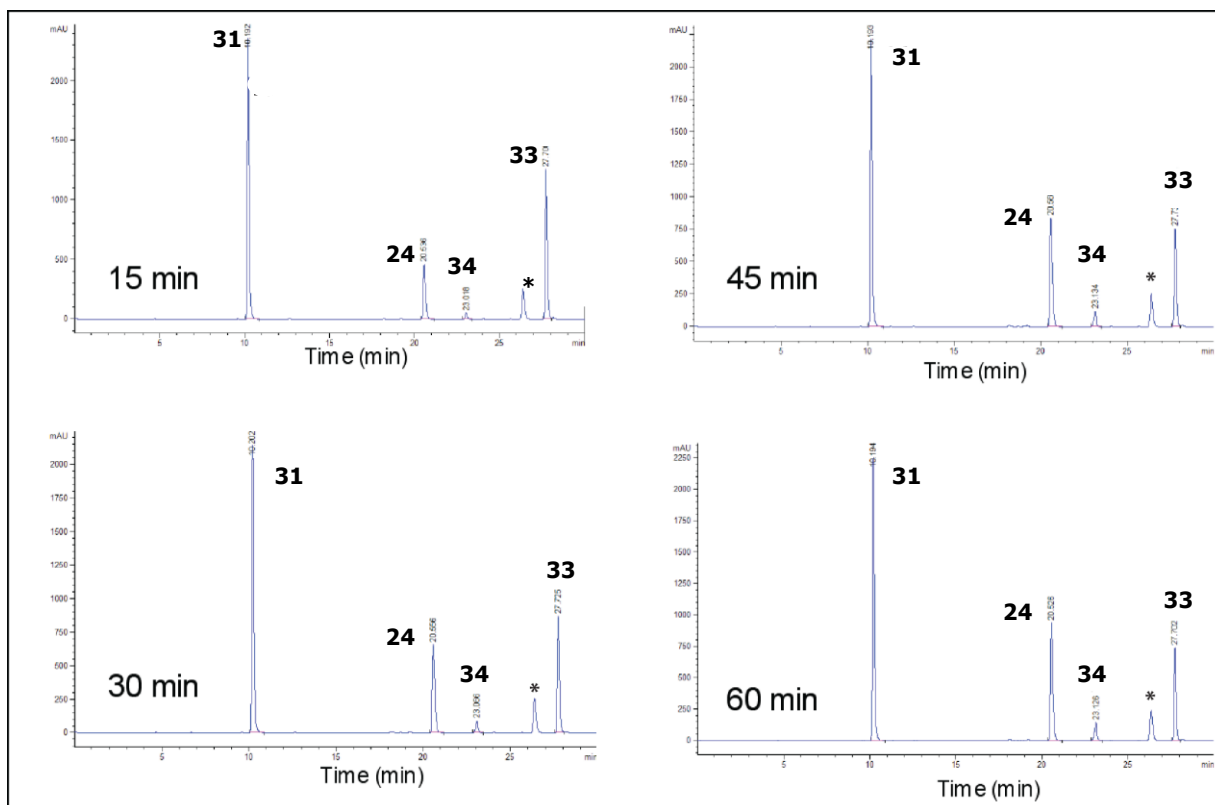


Figure **2.19**. HPLC trace of the crude products of the time course experiments with Fmoc-Aib-F **20** and *N*-naphthyl-Sarcosine-OH **31**, monitoring at a wavelength of 274 nm with a gradient of 5-95% ACN/H₂O with 0.1% formic acid over 30 minutes. The peaks labeled **24**, **34** and **33** have *m/z* values consistent with those compound numbers: compound **24** *m/z* = 326.1 (calc. for Fmoc-Aib-OH + H⁺ = 326.1); the peak marked **34** has a *m/z* = 380.1 (calc. for *N*-naphthyl-Sarcosine-OCH(CF₃)₂ + H⁺: 380.1); the peak marked **33** has a *m/z* = 498.0 (calc. for Fmoc-Aib- OCH(CF₃)₂ + Na⁺ = 498.1); the peak marked **31** has a retention time and UV/VIS spectrum consistent with compound **31** but for this run we did extend the mass-spectrometry window down to the mass of **31**; the peak marked “*” had no mass spectrum but the UV/VIS spectrum and retention time is consistent with dibenzofulvene (Fmoc deprotection).

To rule out the possibility that *N*-Naphthyl-Sarcosine-OCH(CF₃)₂ **34** is due to background transesterification in HFIP under the dipeptide reaction conditions, a control reaction with only the *N*-naphthyl-Sarcosine-OH **31** dissolved in HFIP was carried out. *N*-naphthyl-Sarcosine-OH (10 mg, 44 μmole) was dissolved in 220 μL of HFIP and placed in an oven at 55°C for one hour. No esterification product was found by LC-MS of the solution.

Chapter 3

The Synthesis of Functionalized Bis-Peptides

This chapter details the novel chemistry developed to create highly hindered tertiary amides from *bis*-amino acids, including mechanistic insights and the synthesis of the first fully functionalized *bis*-peptide scaffolds. The synthetic strategy is a radical departure from the conventional *bis*-peptide synthesis, and highlights the fascinating reactivity that can be explored with a versatile system such as *bis*-amino acids. This chapter includes the synthesis of hexasubstituted diketopiperazines, the activation and coupling of the unprotected, hindered amino acids to form functionalized *pro4* oligomers such as those shown in Figure 3.1 as well as mechanistic hypotheses and investigations.

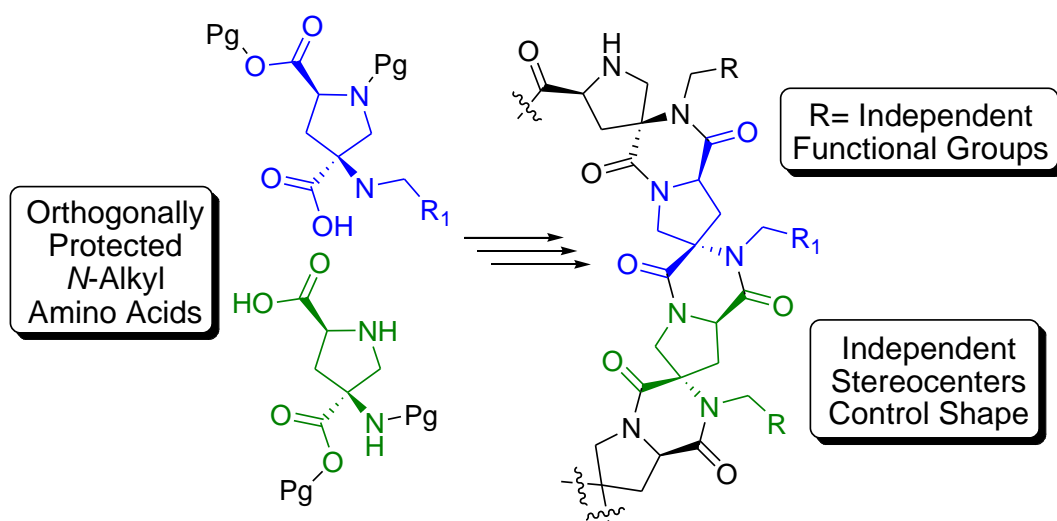


Figure 3.1. Schematic of a functionalized *bis*-peptide comprised of *pro4* monomers. Each functional group and stereocenter in the oligomer may be independently controlled. Assembly is accomplished by the coupling of multiple orthogonally protected, functionalized *bis*-amino acids through a novel activation strategy.

A portion of this chapter is published as:

Zachary Z. Brown and Christian E. Schafmeister

Org. Lett., 2010, 12 (7), p.1436

3.1 Introduction

Proteins are the functional macromolecules of life and depend critically on the ability to position multiple functional groups in well-defined constellations. These elegant assemblies of side chains are organized to accomplish incredible feats of molecular recognition and catalysis. Nature uses the amino acid as the basic monomer of proteins: secondary and tertiary structure positions the diverse chemical functionality of the amino acid side chains through the complex process of protein folding.¹ It is this ability, to precisely position multiple functional groups in space, which is a central goal of the proteomimetic community and our lab. The unique attribute of *pro4* oligomers is that they are shape programmable with a universe of different shapes accessible by combining different building blocks and so can provide the scaffolding to append these chemical groups by rational design.

As referenced in the introductory remarks, foldamers have risen to a prominent place in modern organic chemistry both as a tool to understand how folding architectures work as well as an instrument for molecular biology.²⁰ These macromolecules are able to fold into well-defined, usually helical conformations which allows the design and construction of proteomimetic systems through a variety of noncovalent interactions. The challenge for these approaches will be to solve the problem of designing oligomers that can mimic arbitrary peptide architectures and form higher order assemblies with tertiary structures. Some progress has been made with systems such as β -peptides and mixed α/β -peptides but the requisite rational design element is still lacking.²¹

Bis-peptides, however, form stable, rigid structures in solution that are more amenable to rational design because their shapes are controlled by changing the sequence of constituent monomers. This represents a distinct advantage over foldamers, where the conformation of the macromolecule must be deduced and may only be of a few limited architectures. Also, many foldamer systems have only a modest free energy of folding, therefore seemingly small mutations of one or a few residues may cause the entire macromolecule to unfold.¹⁹ This can be a significant impediment in the design and implementation of functionalized macromolecules if they have only a limited tolerance of substitution. Numerous structural studies of *bis*-peptides have confirmed they are shape-persistent and shape-programmable systems and that the computational design is quite accurate in predicting the solution-phase structures.² Their solution phase conformations should be independent of the appended functionality and so represent a promising platform to explore the design of functional macromolecules.

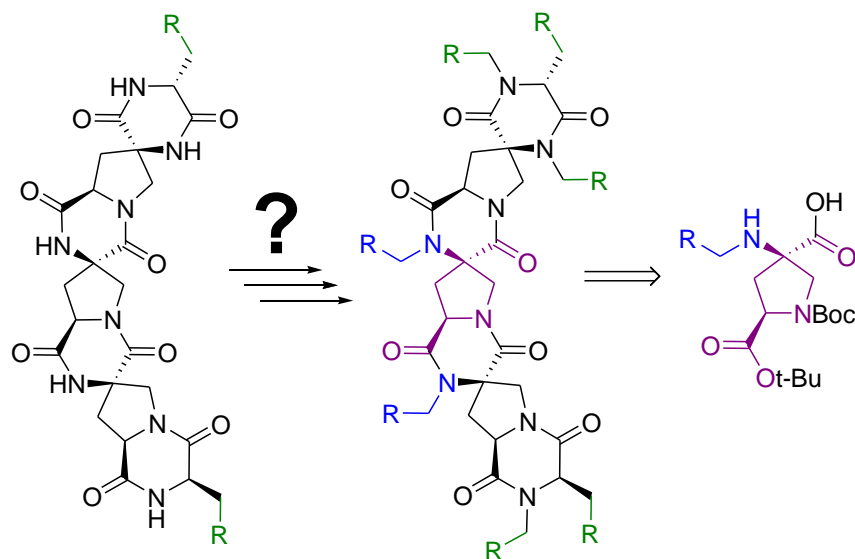


Figure 3.2. The functionalization of *bis*-peptide scaffolds enriches their utility and allows many more applications. However, this does impose significant synthetic problems to create them from the functionalized monomers, which are *N*-alkyl- α,α -disubstituted amino acids.

Prior to the contribution outlined in this chapter, our *bis*-peptide oligomers only had functionalizable positions at the termini of the oligomer through amino acids coupled to the ends of the *bis*-peptide, such as the oligomer shown on the left in Figure 3.2. This secondary amide within the oligomer is an ideal location to install new functionality, since the primary amine (prior to acylation) is the position most easily functionalized during monomer synthesis (see Figure 3.2). However, as discussed in Chapter 2 this newly formed secondary amine is an extremely poor nucleophile which prevents direct acylation.⁴⁰ Shown in Figure 3.3 is an solid-phase example of the difficulty faced with the direct acylation of *N*-alkyl- α,α -disubstituted amino ester. With a *pro4* monomer on the resin, the primary amine is functionalized with a suitable electrophile, such as benzyl bromide. Standard acylation conditions with an incoming *pro4* monomer in fivefold excess, activated as the -OAt ester, produces no coupling product after characterizing the cleavage product of the resin. Even using acetic anhydride with the standard acetyl capping conditions produces none of the desired tertiary amide product. Thus, this newly formed secondary amine adjacent to a quaternary carbon is an extremely hindered nucleophile and presents a formidable challenge in the synthesis of functionalized *bis*-peptides. Also, paralleling conventional peptide chemistry, we wish to create oligomers of the functionalized *bis*-amino acids by sequential coupling of the monomers. With this in mind, the assembly chemistry must be robust, reliable and scalable to allow successful iterations to build up the larger oligomers.

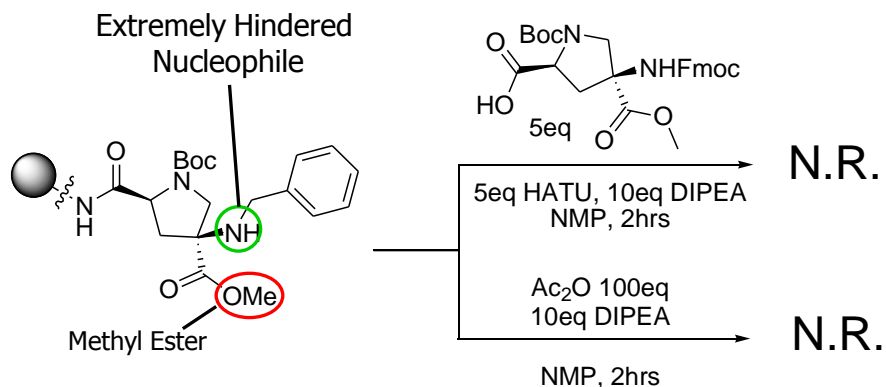


Figure 3.3. The acylation of an *N*-alkyl- α,α -disubstituted amino ester using conventional techniques is nearly impossible (N.R. means No Reaction).

This chapter details a solution to this synthetic challenge through a novel activation strategy and application of the acyl-transfer reaction introduced in the Chapter 2. This chemistry is applied to the construction of highly hindered amides and substituted diketopiperazines and some mechanistic explorations, including the first fully functionalized *bis*-peptide oligomers.

3.2 Results and Discussion

Functionalization of the *pro4* monomers. The conventional *pro4* monomer synthesis has been published and is a reliable and a robust synthesis, with the key transformation being a Bucherer-Bergs reaction to form two diastereomeric hydantoins.² This diastereomeric pair is then separated by flash chromatography and hydrolyzed to the corresponding *pro4* amino acid **35**, the starting material for the reductive alkylation reaction shown in Table 3.1. At this point in the synthesis, all of the functional groups of the monomer are set; all that remains is protecting group chemistry, which is four steps to the usual protecting group motif. This amino acid intermediate is an ideal location to install chemical functionality on the primary amine, although a new chemistry had to be devised to fully utilize this intermediate.

Two of the most common methods of transforming a primary amine into a secondary amine are halide displacement and reductive alkylation.⁴⁶ Halide displacement, with an electrophile such as benzyl bromide, was used in the above solid-phase example to install a benzyl group on the amino ester. Although halide displacement is notoriously difficult to stop at the secondary amine stage, using an excess of electrophile (10 equivalents, 55°C, overnight) in the above example usually amounted to only 10-20% of tertiary amine (as judged by LC-MS after cleavage from the resin) presumably because of the steric hindrance of the α,α -disubstituted amino ester. The major issue of halide displacement if used on the amino acid is

the potential of esterification of the α -carboxylic acid; the acid would need to be suitably protected as an ester derivative before subjecting the amino ester to an alkylation reaction of an aryl halide. In contrast, reductive alkylation using an aldehyde or ketone with a mild reducing agent would tolerate all existing functional groups on the *bis*-amino acid without the prerequisite monomer protecting group manipulation.⁴⁷ Also, a wide variety of aldehydes are commercially available and almost all types of chemical functionality could be readily installed. This strategy also has the benefit of not introducing any new stereocenters if an aldehyde is employed since upon reduction a methylene group is formed. Thus, we chose reductive alkylation with an aldehyde and a mild reducing agent as the method of choice to functionalize the primary amine

Compound	Aldehyde	Product	Yield
36			62%
37			68%
38			52%
39			84%
40			80%
41			59%
42			55%

Table 3.1. The functionalization of *pro4* monomers using reductive alkylation, showing the variety of aldehydes used to install diverse functionality. Yields given are recovered yields after RP purification and lyophilization. Stereochemistry is not shown here because a variety of stereochemistries were used and when a specific monomer is used the stereochemistry is given in the text.

of *bis*-amino acids.

The reductive alkylation of the *pro4 bis*-amino acid is straightforward and produced good yields with a variety of aldehydes, including hindered aliphatic and aromatic aldehydes. All aldehydes are commercially available except for the glyoxylate derivative used to produce compound **42**, Table **3.1** which was synthesized from a straightforward cleavage of the tartrate using periodic acid.⁴⁸ The set of functionalized monomers synthesized for this study are shown in Table **3.1**; all reactions use a similar set of conditions (MeOH, RT, 1.3 equivalents of sodium cyanoborohydride (NaCNBH₃)), with the only variable being the time necessary for quantitative conversion. Aromatic aldehydes (compounds **36-39**, Table **3.1**) were allowed to react overnight whereas aliphatic or unconjugated aldehydes (entries **40-42**, Table **3.1**) require only 1-2 hrs for complete conversion to the secondary amine. The functionalized monomers were then RP purified from H₂O/ACN and then lyophilized before use. The crude product was first loaded onto Celite and then purified using an ISCO purification system with an appropriately sized C18 column. The fractions containing the pure product were then combined and lyophilized prior to their incorporation into oligomers.

Synthesis of symmetric diketopiperazines. Exploratory solution phase experiments with the functionalized *bis*-amino acids began with the synthesis of symmetric, hexasubstituted diketopiperazines and are detailed in Figure **3.4**. Although these symmetric molecules are less interesting in terms of the creation of asymmetric oligomers, there is still limited literature precedence for their synthesis.⁴⁹ As shown in Figure **3.4**, the functionalized *bis*-amino acid, *pro4(2R,4R)* here with a methoxybenzyl group (monomer **37**, Table **3.1**), is dissolved in a 2:1 DCM/DMF mixture and the baseless activating conditions of DIC/HOAT are used.⁵¹ In these initial experiments, only 0.5 equivalents of activating agent were used to determine if any amide bond product could be formed. After one hour at room temperature, the LC-MS trace reveals starting material **37** (~20%), the final symmetric diketopiperazine product (compound **44**, ~60%) and a product with a mass spectrum consistent with a single dehydration reaction between two *bis*-amino acids (compound **43**, ~20%). A second addition of 0.5 equivalents of DIC/HOAT converts all remaining starting material and the intermediate product into that of the final symmetric diketopiperazine **44**. Treatment of the reaction mixture with HBr provides global deprotection to amino acid **45** within 30 minutes, which was then RP purified. The ¹H NMR spectrum of diketopiperazine product **45** (500MHz, 25mM in DMSO-*d*₆) shows all signals of the molecule, but, owing to the C_{2v} symmetry axis through the molecule, each signal represents double the number of protons.

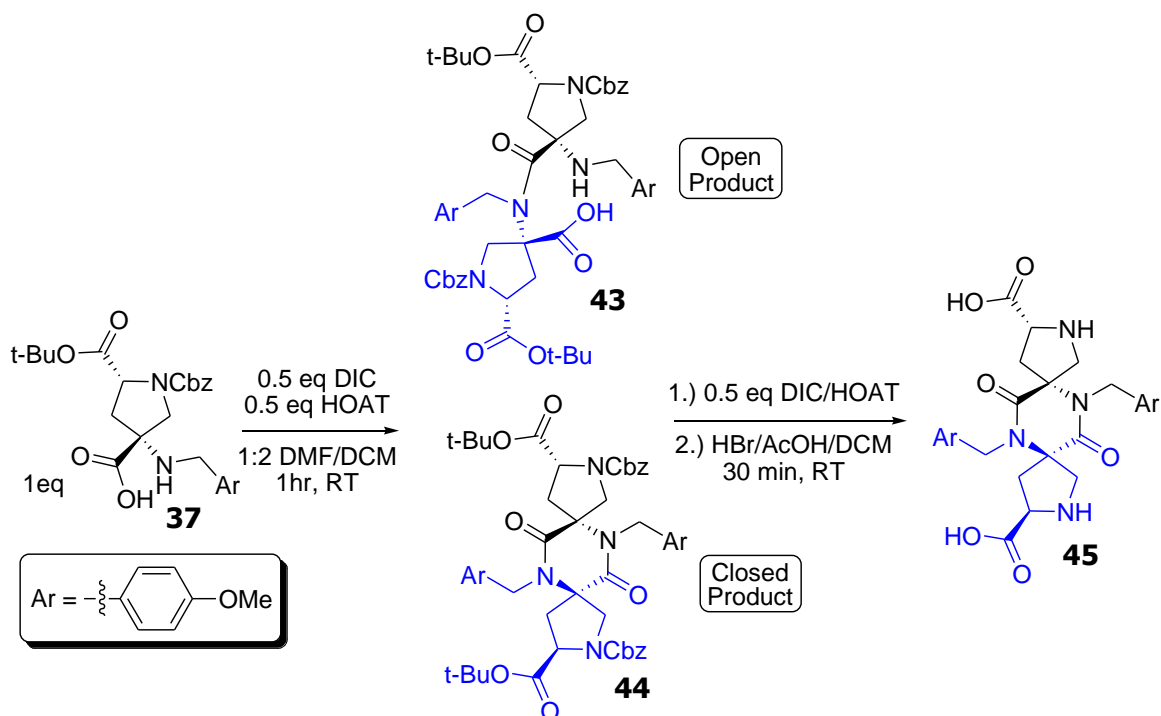


Figure 3.4. The synthesis of symmetric, hexasubstituted diketopiperazines with a functionalized *bis*-amino acid **37**. LC-MS of the initial crude reaction shows starting material, the diketopiperazine product **44** (labeled “Closed Prod”), and an intermediate with a mass spectrum consistent with a single amide product **43** (labeled “Open Prod”) by. Upon the addition of another aliquot of DIC/HOAT, the starting material and intermediate “Open Prod” vanish, coalescing into a single peak of the “Closed Prod” **44**. Treatment with HBr then gives the deprotected diketopiperazine **45**.

This represents an advance because there are few good ways to synthesize such highly substituted diketopiperazines, and they are considered privileged pharmacological scaffolds.⁴⁹ This result was also very encouraging in that it demonstrated amide bond formation between two extremely hindered, *N*-alkyl- α,α -disubstituted amino acids. However, the production of the symmetric diketopiperazine is not the final goal and so methods needed to be developed to create asymmetric diketopiperazines and ultimately functionalized *bis*-peptides.

The steric hindrance of the *N*-alkyl- α,α -disubstituted amino acids suggested an elegant and efficient manner with which to activate and couple the *bis*-amino acids. We hypothesized that if the carboxylic acid could be quantitatively activated as its -OAt ester such as **47**, the steric hindrance of the secondary amine would preclude the molecule from spontaneous self-reaction to form the symmetric diketopiperazine such as **44**. Said another way, the extreme steric environment of the secondary amine would prevent the active monomer from spontaneous dimerization even though a competent electrophile was present in the solution.

However, to the best of our knowledge no literature precedent existed for the direct activation and coupling of hindered, unprotected amino acids such as those found in Table 3.1.

Synthesis of asymmetric diketopiperazines. To achieve the synthesis of asymmetric diketopiperazines, we exploited the severe steric hindrance of the secondary amine. We formed amino-OAt ester **47** by adding one equivalent of DIC to hindered amino acid **40** in the presence of six equivalents of HOAt. (*pro4* derivative **40** has a *N*-Boc group, see Chapter 5 for a discussion of protecting groups). Any amount less than six equivalents and substantial amounts of the corresponding symmetric diketopiperazine was seen. The excess HOAt traps the *O*-acyl isourea **46** in near quantitative amounts.

A schematic of the hypothesized mechanism is detailed in Figure 3.5, and begins with the activation of *pro4*(2*R*,4*R*) monomer **40** with DIC to yield the *O*-acylisourea **46**, an extremely reactive electrophile. This is the critical step, since multiple nucleophiles may now attack this intermediate. If HOAt would attack it would yield the amino-OAt ester, the desired activated species **47**. However, unreacted amino acid may also attack either of the two electrophilic intermediates (either compound **46** or **47**) and would lead to one of two reaction products seen above in the synthesis of symmetric diketopiperazines. Therefore, the two activation rates must

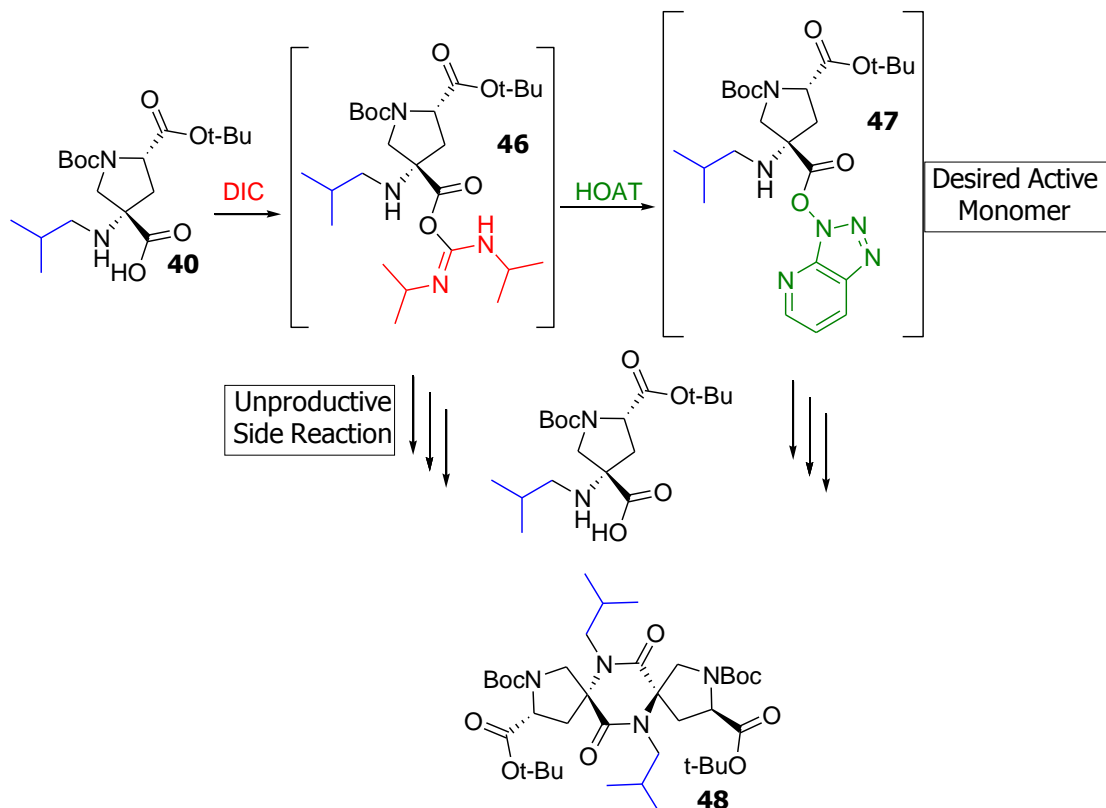


Figure 3.5.. Proposed mechanism for the activation of the *pro4* monomer and the dimerization side reaction that needed to be suppressed.

be accelerated: the activation of the carboxylic acid with DIC (to form **46**) and the subsequent esterification with HOAt (to form **47**). Increasing these two rates would simultaneously suppress the unproductive pathway of homodimerization by quickly removing the nucleophilic amino acid **40**, the starting material. The rate of carbodiimide activation has been shown to be dependent on the solvent polarity for the activation of Cbz-Aib-OH, and is much faster in nonpolar solvents (dichloromethane, $t_{1/2} = 2\text{min}$), versus polar solvents (DMF, $t_{1/2} = 27\text{min}$).⁵⁰ Although most unprotected amino acids would have limited solubility in organic solvents, our functionalized *pro4* monomers are soluble in DCM:DMF mixtures. A 2:1 DCM:DMF mixture was found to be optimal to balance the factors of low dielectric constant to accelerate the *O*-acylisourea formation and a protic solvent to help solvate the amino acid. The pathway of subsequent HOAT activation was found to require an excess of HOAT present, with six equivalents being sufficient and less than six leading to substantial amounts of homodimerization. Other activation procedures were also investigated, but any protocol involving an exogenous base, such as a tertiary amine, lead to quantitative homodimerization. For example, using the standard conditions for HATU activation (stoichiometric HATU with respect to carboxylic acid and 2 equivalents of DIPEA), the symmetric diketopiperazine was formed quantitatively. This is presumably because deprotonation of the carboxylic acid forms the more nucleophilic carboxylate. Therefore, the baseless conditions of DIC/HOAT were used throughout the assembly of functionalized *bis*-peptides. Currently these conditions of DIC/HOAT in the DCM/DMF solvent mixture are the only identified protocol to give complete direct activation of a hindered amino acid such as **40**.

This protocol, subjecting functionalized *pro4* amino acids such as those in Table **3.1** with 1 equivalent DIC, 6 equivalent HOAT for 1.5 hours at room temperature ensures near quantitative activation of the carboxylic acid to the –OAt ester as judged by LC-MS. Quantitative activation may be determined with a chromophoric functionalized *pro4* derivative, such as compound **38** in Table **3.1**. To establish the amount of activated monomer, the hindered amino acid is subjected to the activation conditions detailed above and a small aliquot is withdrawn. A nucleophile, for example benzylamine, is then added in excess (>10 equivalents) and allowed to react for at least 30 minutes to quench the active acylating species. LC-MS is used to judge the relative amount of *pro4* amino acid **38** (from failed activation) versus the amount of benzylamine adduct. If the amount was ever less than 95%, the material was not used in the synthesis and a fresh batch prepared and assayed prior to coupling.

Once a competent activation protocol for the amino-OAt ester was established, the first synthesis that was undertaken was to make asymmetric, hexasubstituted diketopiperazines. First, an isobutyl functionalized *pro4(2S,4S)* (compound **40**, Table 3.1) was activated to give amino-OAt ester **51** followed by the addition of a pyrenyl-functionalized *pro4(2S,4S)* monomer (compound **39** in Table 3.1) along with two equivalents of DIPEA. After 1.5 hours, an aliquot of the reaction was withdrawn and LC-MS analysis (Figure 3.6) revealed multiple distinct species. At just over 22 minutes, the *pro4(2S,4S)* pyrene-functionalized amino acid **39** was seen and

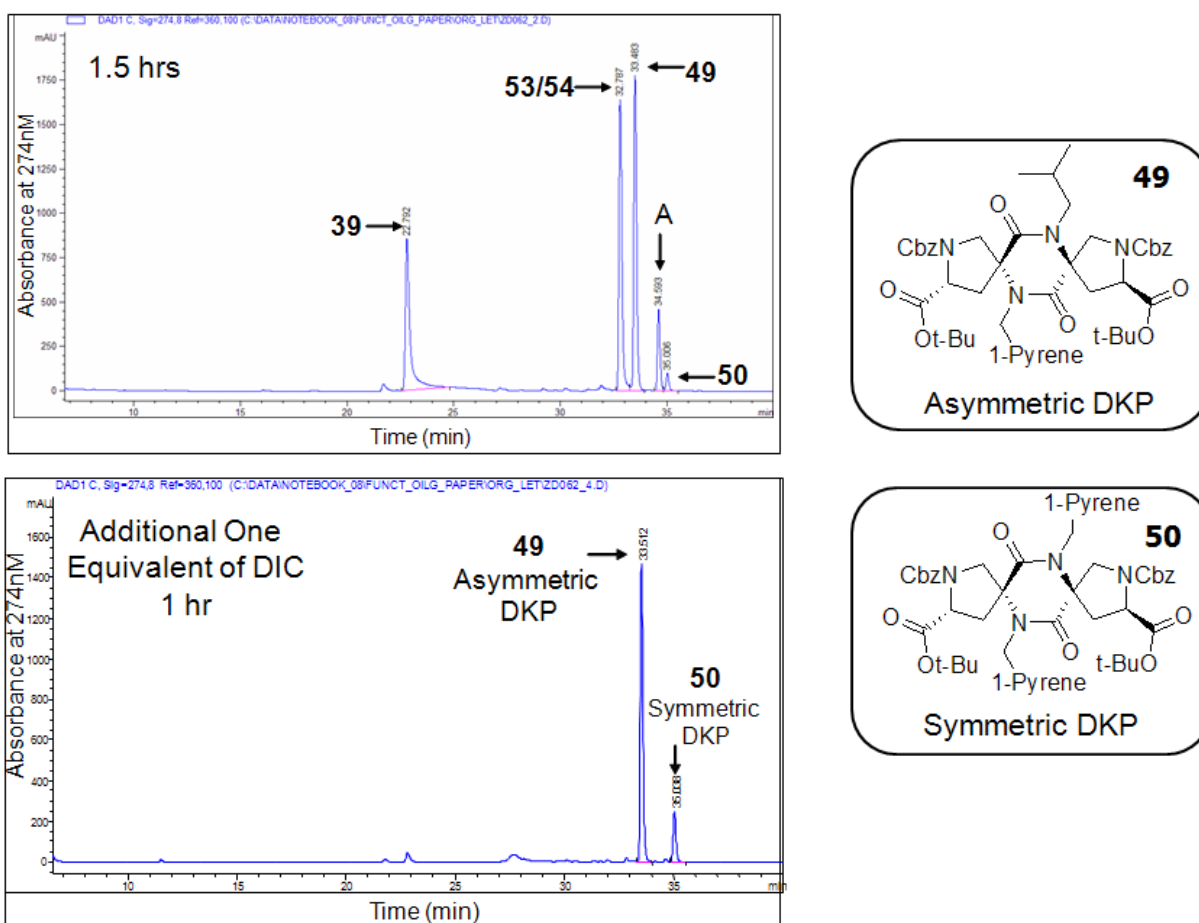


Figure 3.6.. LC-MS traces of the reactions to form asymmetric, hexasubstituted diketopiperazine **49**.

indicated the reaction was incomplete (the other amino acid starting material, compound **40**, Table 3.1 would not have UV absorbance and so would not be present in a chromatogram monitoring at a wavelength of 274nm). Also in the LC-MS analysis were both the open and closed forms of the desired asymmetric DKP, marked **53/54** and **49** respectively (See also Figure 3.7 for compound identifications). Interestingly though, there were also two other open

and closed DKP's (marked peaks "A" and **50**): those corresponding to both the open and closed forms of the symmetric DKP of the pyrenyl-functionalized *pro4* amino acids. Upon the addition of a further portion of DIC, all peaks converge to only the asymmetric and the symmetric DKP with an over 80% yield (HPLC yield) of asymmetric DKP relative to either of the amino acids starting materials.

The poor nucleophilicity of the secondary amine, as evidenced by the quantitative activation to the amino-OAt ester in the first place, precludes any direct acylation pathways of the system. The proposed mechanism is shown in Figure 3.7 and involves the attack of the incoming carboxylate of monomer **39** (in the deprotonated, and thus more nucleophilic form,

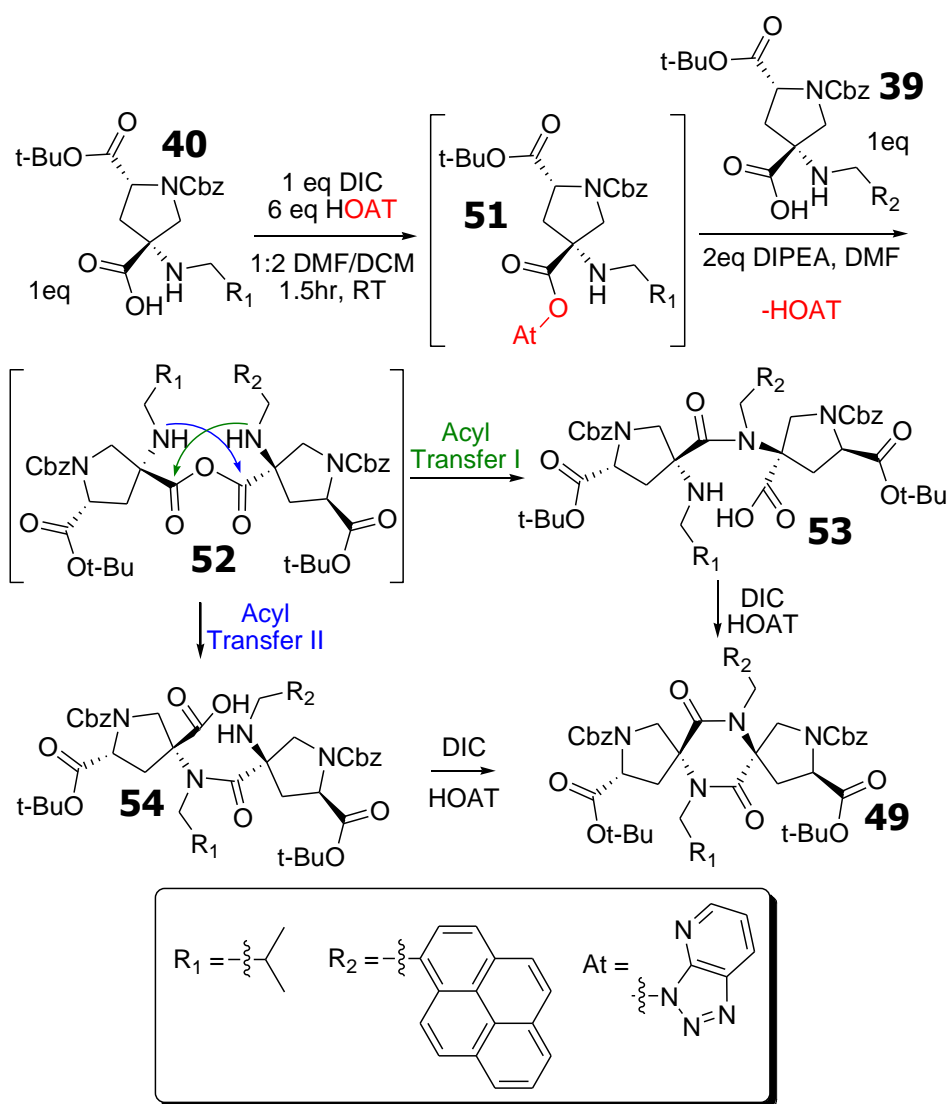


Figure 3.7. Synthesis of the asymmetric, hexasubstituted diketopiperazine **49** via the active ester **51**. The proposed mechanism involves the mixed amino-anhydride **52** as the critical step.

because of the addition of DIPEA) to attack the activated species **51** to form mixed anhydride **52**. This critical intermediate, mixed anhydride **52**, is now capable of undergoing two distinct acyl transfers to form two regioisomeric single amide products **53** and **54**. (Only one peak with a mass consistent with the single amide product is seen in the chromatogram, although the two peaks might not resolve. Thus, it is not clear if only one product is formed or if it's just that the two products do not resolve.) Upon the addition of a further one equivalent of DIC, both single amide products converge to the same asymmetric diketopiperazine **49**. The symmetric DKP **50**, comprised of two pyrenyl-functionalized *pro4*'s, presumably came from interception of the mixed anhydride **52** by either an additional pyrenyl-functionalized *pro4* or even a molecule of HOAT. This observation implies that the mixed anhydride has a finite (although possibly short) lifetime, and that the attack of an additional nucleophile is on a similar time scale as the acyl transfer. This hypothesis would require additional control experiments to test but still serves to highlight some of the remaining questions as to what the full scope of the acyl-transfer mechanism is. Perhaps the most important point here is that, as seen in the dipeptidyl study in the previous chapter, this transference of electrophilicity to an adjacent acyl group is a hallmark that anhydrides are formed through the course of the reaction and the proposed mechanism is consistent with the observed product.

The ^1H NMR (500MHz, 25mM in DMSO- d_6) shows separate signals for each of the *pro4* monomer protons of the asymmetric diketopiperazine **49**, consistent with desymmetrization of the system introduced by having two unique functional groups on the diketopiperazine even though the stereocenters have the same absolute configuration. For example, the two alpha protons of the building blocks can now be seen as separate signals at about 4.5ppm in the ^1H NMR spectrum.

Mechanistic investigations. We decided to probe this hypothesized mechanism of an amino-anhydride intermediate even further. An α -carboxylic acid seems to be required for efficient acylation of the hindered amine, since, as the above activation protocol shows, the amine itself is too hindered to undergo direct acylation. What about the isolated carboxylate itself, is it a competent nucleophile to attack an active ester to form the anhydride intermediate and undergo the requisite acyl transfer? Anhydrides have long been a postulated intermediate during various carboxylic acid activation protocols,³⁴ but our hypothesized acyl-transfer is a new mechanism and so requires further study.

The further experiment to study the nucleophilicity of the carboxylic acid and subsequent acyl transfer is shown in Figure 3.8. An isobutyl functionalized *pro4*(2*S*,4*S*) amino acid (compound **40**, Table 3.1) was activated as the OAt ester using the above protocol, and an Fmoc-protected amino acid, here bromo-phenylalanine (compound **55**) was added stoichiometrically with two equivalents of DIPEA. Therefore, there is only one electrophilic site, the OAt activated *pro4* monomer, and only one nucleophilic site, the carboxylate of Fmoc-bromo-phenylalanine. After reacting at room temperature for three hours, an aliquot of the reaction was removed and analyzed by LC-MS. The chromatogram in Figure 3.8 reveals only two prominent peaks with the absorbance profile of the Fmoc group. The peak at 25 minutes

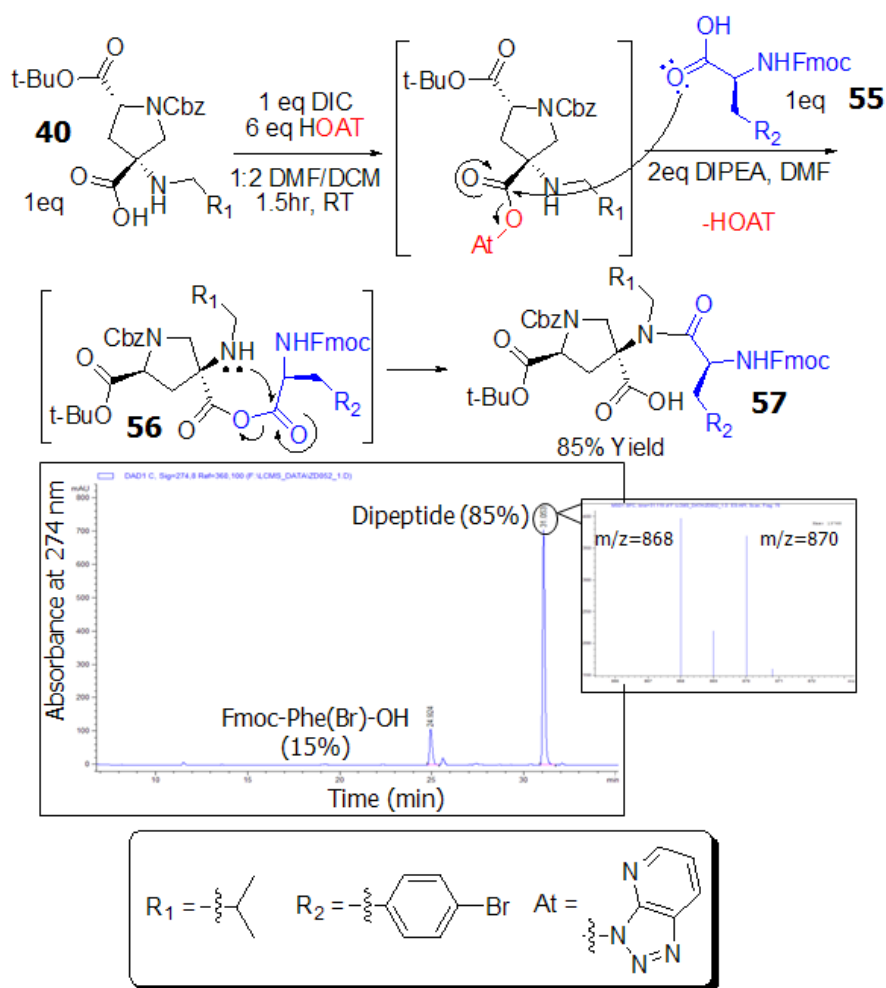


Figure 3.8. Synthesis and characterization of an acyl transfer model system: activation of a functionalized *bis*-amino acid monomer, followed by the addition of an Fmoc-protected amino acid, where the carboxylate is the only nucleophile of the system. The RP-HPLC of the crude reaction is shown, including the mass spectrum as an inset showing the expected isotope abundance of the brominated product.

(~15% of product, HPLC yield) has a mass spectrum consistent with the phenylalanine starting material (compound **55**), while the peak at 31 minutes (~85% of product, HPLC yield) has a mass spectrum consistent with the dipeptide (compound **57**), including the conspicuous isotopic abundance of bromine (the M and M+2 mass peaks have nearly identical abundance) as seen in the inset of Figure **3.8**. This is consistent with the hypothesis that the carboxylate may be the nucleophile in our reactions and the mechanism operates as shown in Figure **3.8**. First, the carboxylate attacks the activated acyl group, expelling the -OAt group to form the intermediate amino-anhydride **56**. Rearrangement of the amino-anhydride occurs by attack of the secondary amine to the distal carbonyl of the anhydride through a five-membered ring transition state, followed by the expulsion of the carboxylate from the tetrahedral intermediate to collapse to the desired tertiary amide **57**. Therefore, this experiment provides evidence consistent with the hypothesis that the carboxylic acid is a competent nucleophile and that subsequent acyl transfer is taking place.

Functionalized *pro4* oligomers. With the employment of orthogonal protecting groups, this activation procedure provides an oligomerization strategy to functionalized *bis*-peptide scaffolds to allow larger scaffolds to be constructed. As shown in Figure **3.9**, a *pro4*(2*S*,4*S*) monomer functionalized with a naphthyl group (compound **38**, Table **3.1**) is activated using the above DIC/HOAT strategy. An orthogonally protected *pro4*(2*R*,4*R*) (compound **58**, here with two base labile groups, the Fmoc and the ODmab) with the prolinyl amino acid portion exposed was then added with DIPEA and allowed to react for one hour at room temperature. LC-MS analysis of the reaction mixture showed two unresolved peaks at nearly 33 minutes during a 40 minute chromatographic run. The mass spectrum of each of these peaks is consistent with one (compounds **59** and **60**) and two dehydration products (compound **61**) between the two *bis*-amino acids. Compounds **59** and **60** represent the two possible amide bonds which could have formed although it is not clear which one it is. Subsequent addition of another aliquot of DIC converts all of the unclosed material into the final diketopiperazine product **61**. Since both monomers are used stoichiometrically, a nearly quantitative crude yield was obtained as judged by LC-MS in the second chromatogram in Figure **3.9**.

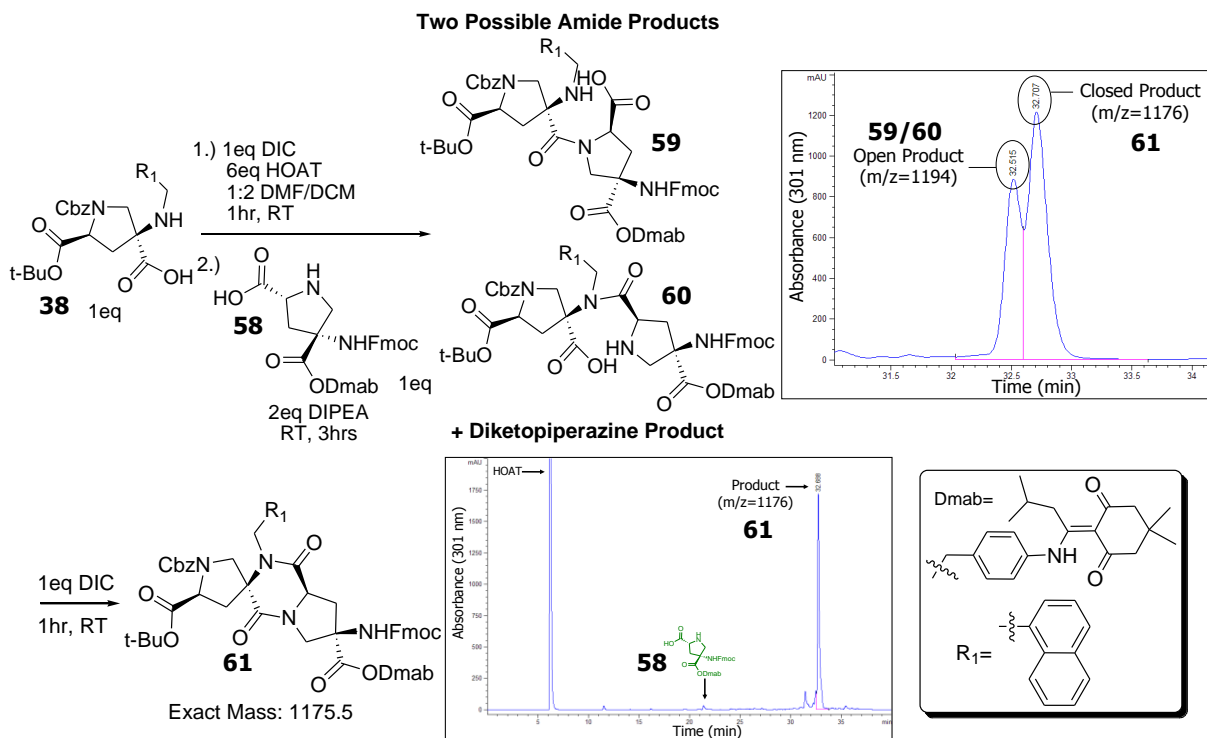


Figure 3.9. Synthesis of a *bis*-amino acid dimer **61** with orthogonal protecting groups on the termini. Here the first chromatogram shown is the LC-MS of the initial crude reaction; upon the addition of another equivalent of DIC, nearly all of the material is converted to the desired pentasubstituted diketopiperazine **61** as shown in the second LC-MS trace.

Contrary to the previous examples of the synthesis of hexasubstituted diketopiperazines, the synthesis of the dimer involves the use of the prolinyl amino acid portion of monomer **58**. Even though this is still a secondary amine, it is much more nucleophilic as compared to the more hindered secondary amines of compounds **36-42** because it is constrained within a five-membered ring. Therefore, the mechanism of acyl transfer might not be operating and so further experiments were undertaken to investigate this.

A competition experiment was designed which would isolate the amine and carboxylic acid nucleophiles of monomers such as **58** to judge their relative nucleophilicities while still subjecting them to the same reaction conditions. As shown in Figure 3.10, proline methyl ester **63** would serve as a representative for the pyrrolidine nitrogen while an *N*-naphthylmethyl-proline **62** would represent the carboxylic acid nucleophile. To aid in the characterization of the competition experiment, compound **38**, Table 3.1, was used so that both the activated *pro4*(2*S*,4*S*) monomer and one of the nucleophiles (compound **62**) had a naphthyl group. Thus one product, compound **65**, resulted from the direct acylation of the proline methyl ester **63** and the activated *pro4* and includes one naphthyl group. The other product, compound **64**, resulted

from the *N*-alkyl-proline carboxylate of compound **62** attacking the amino-OAt building block to form a mixed anhydride followed by acyl transfer; this product contains two naphthyl groups and so would have twice the extinction coefficient as compared to compound **65**. Both the amine and the carboxylate nucleophiles (each at a five-fold excess) along with DIPEA were added to

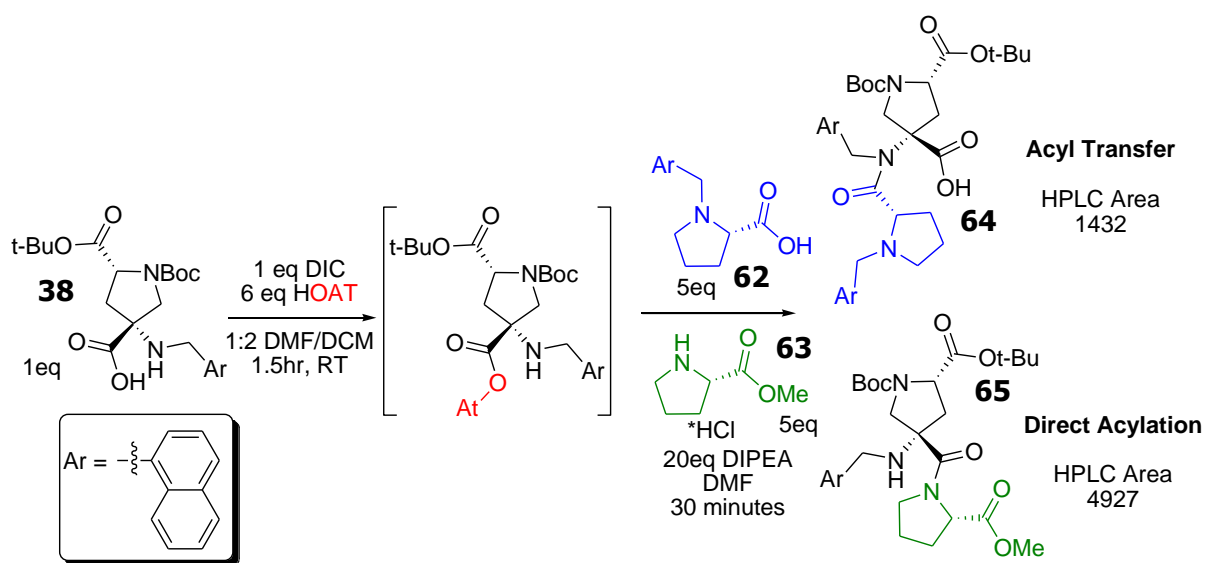


Figure 3.10. Schematic of the competition experiment to assess the relative nucleophilicity of the pyrrolidine nitrogen versus that of the carboxylic acid of proline. The integrated areas from the chromatogram of the crude competition experiment are shown next to the respective products.

the activated *pro4* derivative and allowed to react for 30 minutes after which time an aliquot of the reaction was subjected to LC-MS analysis. The products of both nucleophiles are found in the reaction and the integrated HPLC areas are shown in Figure 3.10 next to the respective products. Assuming that compound **64** has an extinction coefficient twice that of direct acylation product **65** (because has two naphthyl groups while has only one), the product ratio will be: (Area **65**)/(Area **64**/2), or product **65**:product **64** = 6.9. Here we can see that even though the prolinyl secondary amine is more nucleophilic, the carboxylate is still competitive and acyl transfer is a feasible mechanism in this circumstance.

We extended the approach outlined above to synthesize two oligomers of *bis*-amino acids, using a variety of functionalized building blocks, to show that the chemistry is applicable to larger structures containing more building blocks. The synthesis of the first tetramer is outlined in Figure 3.11 and begins with a *pro4*(2*S*,4*S*) building block (compound **66**) with the quaternary amino acid side protected with a Fmoc group and a methyl ester and the prolinyl amino acid side exposed. The next functionalized monomer, here one equivalent of *pro4*(2*S*,4*S*) with a benzyl group (compound **36**, Table 3.1), is activated with the DIC/excess HOAT protocol

outlined above and then added to compound **66**. After a sufficient reaction time, usually allowed to proceed overnight, an additional aliquot of DIC was added to fully convert any remaining material with only a single amide bond into that of the diketopiperazine product. This second amidolysis reaction proceeded within a few hours at room temperature as judged by LC-MS. An acidic, aqueous wash then removed much of the HOAT as well as the DIPEA present, followed by deprotection of the next amino acid portion. The deprotection was found to proceed smoothly with HBr/AcOH in DCM,³⁵ and the product was RP-purified and lyophilized to give dimer **67**

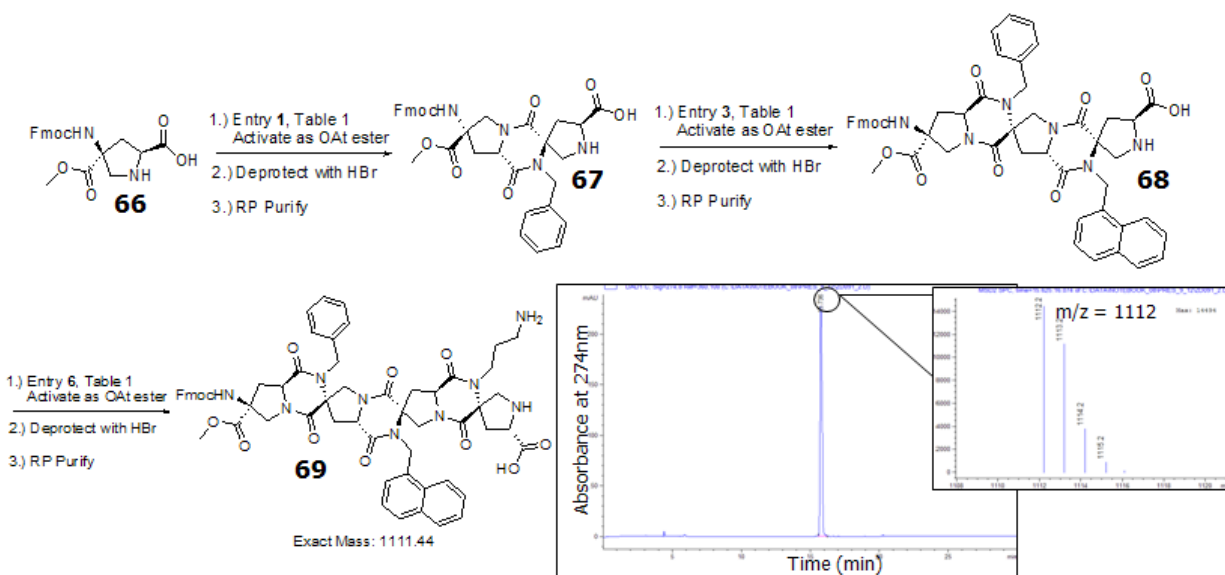


Figure 3.11. Synthesis of functionalized tetramer **69** bearing the phenyl, naphthyl and propyl amine side chains. The chromatogram with the corresponding mass spectrum is shown.

(68% recovered yield). This protocol of coupling by activation of the quaternary carboxylic acid of the incoming building block, reaction with the exposed amino acid portion of the growing oligomer, and finally deprotection with HBr and RP-purification was then repeated. After the benzyl functionalized *pro4(2S,4S)* monomer (compound **36**, Table 3.1), then a naphthyl functionalized *pro4(2S,4S)* (compound **38**, Table 3.1, giving trimer **68**, in 77% recovered yield), and finally a *pro4(2S,4S)* with a Cbz-protected propyl amine (compound **41**, Table 3.1). All monomers were used stoichiometrically, demonstrating that this coupling procedure is an efficient assembly strategy. The final deprotection with HBr affords the amino acid of the building block as well as deprotects the propyl amine of the final side chain to give the completed tetramer in a 59% recovered yield after RP purification. The chromatogram of the purified tetramer **69** is shown in Figure 3.11.

A second tetramer was also synthesized using three different functional groups and diastereomeric building blocks within the scaffold. The synthesis parallels that of the preceding functionalized tetramer, with the same protocol of activation, acylation, deprotection and purification being repeated three times. The first monomer is again a *pro4(2S,4S)* with the quaternary amino acid protected with an Fmoc and a methyl ester (compound **66**). Next, a *pro4(2R,4R)* with an isobutyl group (compound **40**, Table **3.1**) is coupled (68% recovered yield) followed by a *pro4(2R,4R)* with an anisole group (compound **37**, Table **3.1**) with a 65% recovered yield. Finally, a *pro4(2S,4S)* building block with a benzyl protected carboxylate (compound **42**, Table **3.1**) is coupled and subsequently deprotected to produce tetramer **70** shown in Figure **3.13** (recovered yield 52%).

The new synthetic strategy developed here has several advantages over our previous approach to assembling *bis*-peptides.² First, we can introduce chemical functionality to the primary amine of the building block late in the monomer synthesis using reductive alkylation: mixing stoichiometric amounts of the amino acid with aldehyde in the presence of a mild reducing agent yields the alkylated amine with recovered yields of 60%-80% after RP purification. Also, this monomer strategy avoid the use of the conventional protecting group scheme with our monomers and in doing so shortens the synthetic route of our building blocks from ten steps to six, a valuable savings of both time and resources because of the amounts of building blocks we produce. Finally, at least for the synthetic scheme for functionalized oligomers shown here, is that the rigidification step which closed the diketopiperazines, is now combined with the acylation step to yield the completed oligomer when assembly is finished. Prior to this, *bis*-peptide oligomers were assembled on solid support and at the end of the synthesis all diketopiperazines were closed in one step; we often encountered problems including sluggish reactions and epimerization because of strongly basic conditions. Primarily though, the installation of chemical functionality within each monomer of an oligomer is the realization of a long-standing goal of our research group.

Characterization of the oligomers. To verify the structure of the tetramers, a series of NMR experiments were performed to assign nearly all of the ¹H and ¹³C signals. These include a ¹H spectrum, COSY, and ROESY as well as the heteronuclear experiments HMQC and HMBC. Also, a stochastic search using the molecular mechanics package MOE was performed (Amber 94 force field) to identify low energy conformers which qualitatively fit the ROESY data. (In computational searches, as well as the renderings in Figures **3.12** and **3.13**, an acetate group was used in place of the Fmoc group to simplify the structure.)

The first tetramer, compound **69** (shown in Figure 3.12) is a homochiral oligomer (composed of all *pro4(2S,4S)* monomers) and has a benzyl, naphthyl and an aliphatic amine as the functional groups. These groups were chosen to represent the proteogenic side chains of phenylalanine, tryptophan (with the naphthyl group being an unreactive isostere of an indole ring), and the primary amine of ornithine. Shown in Figure 3.12 is one of the three lowest energy conformers from the stochastic search (using the computational package MOE⁵¹) and was the best fit for the ROESY data for the orientation of the functional groups. As can be seen from the structure, the functional groups pack against the rigid scaffold as can be determined by ROESY correlations. For example, one of the diastereotopic methylene hydrogens of the benzyl group show a ROESY correlation to one of the delta protons of the building block as shown in Figure 3.12, inset A. An analogous ROESY correlation is also evident from one of the diastereotopic hydrogens of the methylene of the naphthyl group to a delta proton of the scaffold as shown in Figure 3.12, inset B. Thus, the functional groups pack against the scaffold in a relatively

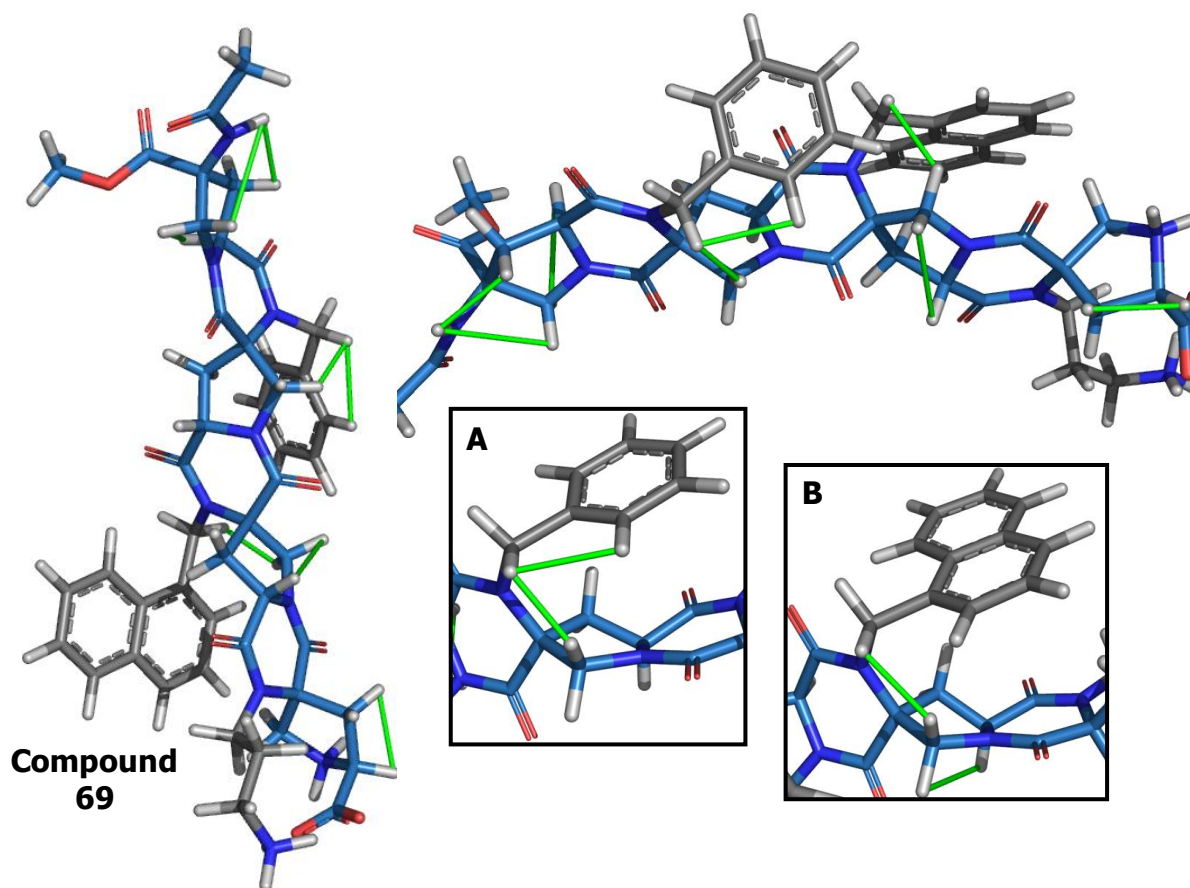


Figure 3.12. Lowest energy structure of tetramer from calculations with select ROESY cross-peaks shown in green.

restricted fashion as modeling would suggest from such a sterically crowded environment. Also of note is the correlation of an Amber 94⁵² derived structure (a very simple molecular mechanics potential that can minimize a structure of this complexity in seconds on a normal desktop computer) which is consistent with the ROESY cross-peak analysis. In the structure of tetramer **69** the stereochemistry of the component monomers arranges the three functional groups in a left-handed helical arrangement and they superimpose well on the side-chains of residues i , $i+3$ and $i+6$ of a model α -helical peptide (structure not shown). The distance between each successive pairs of functionalized amide nitrogens is about 5.6 angstroms. Thus this new methodology is a robust approach towards functional macromolecules and alignment of multiple functional groups.

The second tetramer (compound **70**), depicted in Figure 3.13, is the heterochiral oligomer with three other functional groups. The isobutyl group represents the aliphatic side chain of the amino acid leucine, the anisole group is a protected version of the side chain of tyrosine, and the carboxylate is representative of aspartic acid. Again, a stochastic search was performed (using an acetate cap in place of the Fmoc protecting group) using the Amber 94

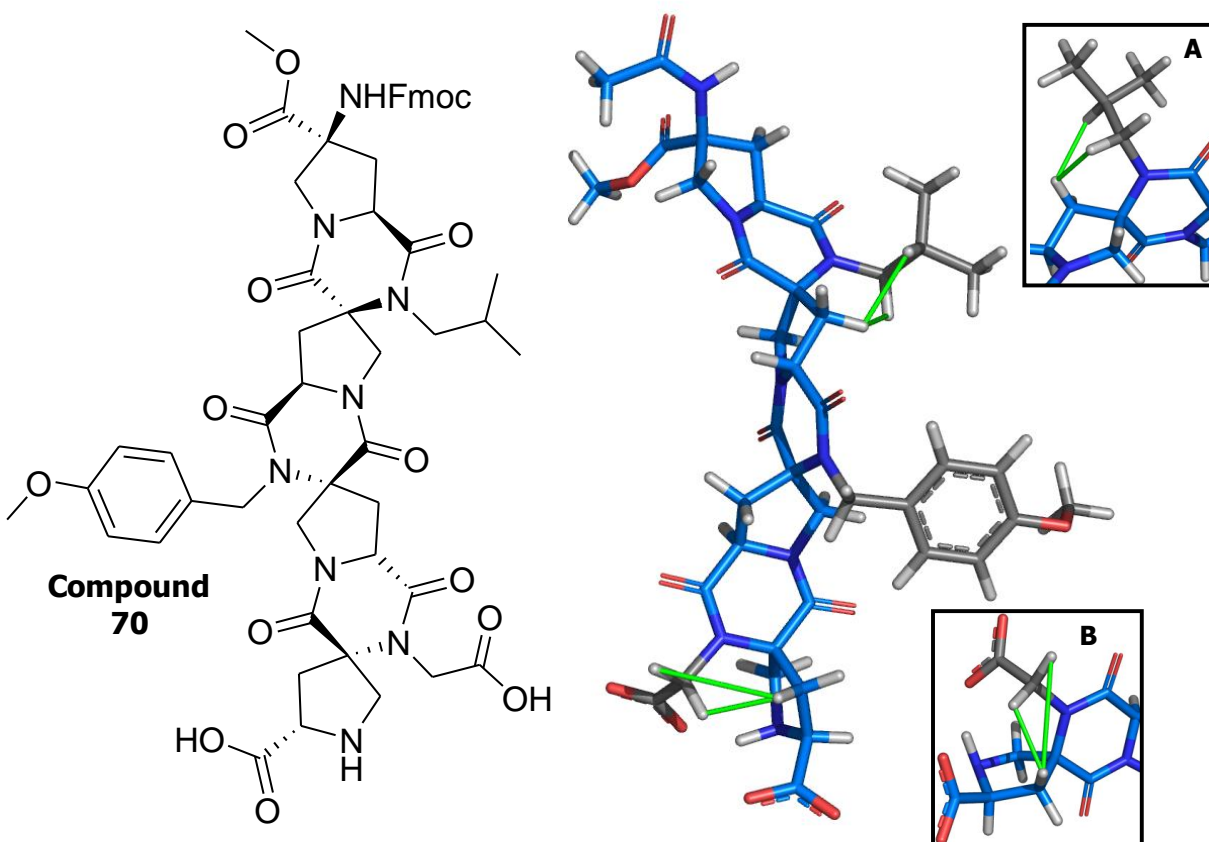


Figure 3.13. Lowest energy structure of the heterochiral tetramer which contains the isobutyl, methoxybenzyl and the methylcarboxylate functionality. ROESY correlations are shown in green.

force field as implemented in MOE and both the two- and three-dimensional structures is shown in Figure 3.13. In this tetramer, ROESY correlations are seen from the isobutyl group (one of the diastereotopic hydrogens of the methylene carbon and the hydrogen of the methine carbon) to one of the beta protons of the preceding pyrrolidine ring. In the structure of tetramer **70** the functional groups are arranged in a right-handed helical arrangement that superimpose well on the side-chains of residues i , $i+4$, $i+8$. A distance of 5 angstroms between each successive pair of functionalized amide nitrogens is found. This additional presentation of functional groups shows the precision control of being able to subtly change their arrangement as well as being able to incorporate a wide variety of groups using reductive alkylation chemistry and the monomer assembly presented here.

3.3 Conclusion

In conclusion, a new activation protocol of the *pro4* amino acid was developed which exploits the steric hindrance of the functionalized secondary amine. The strategy was utilized for the synthesis of both symmetric and asymmetric hexasubstituted diketopiperazines and extended to a new solution-phase synthesis of functionalized *bis*-peptides. This chapter also detailed mechanistic analysis experiments, including isolation of the carboxylate nucleophile and showing that by itself it underwent the acyl transfer, as well as a competition experiment which directly compared the nucleophilicity of the amine and the carboxylic acid of an amino acid in a model system. Two examples of functionalized tetramers were synthesized with a variety of *pro4* building blocks and chemical functionality. These scaffolds were then characterized by various NMR techniques to verify the connectivity and begin studying this new class of macromolecules.

3.4 Experimental Details

General Methods. Anhydrous dichloromethane (DCM), anhydrous dimethylformamide (DMF), anhydrous methanol (MeOH), HBr (33% in glacial AcOH) and redistilled diisopropylethylamine (DIPEA) were obtained from Sigma-Aldrich and used without purification. Pd/C was obtained from Strem Chemicals. All amino acids were obtained from either Novabiochem or Bachem. HOAT was obtained from Genscript. All other reagents were obtained from Sigma-Aldrich and used without further purification.

HPLC-MS analysis was performed on a Hewlett-Packard Series 1200 with a Waters Xterra MS C18 column (3.5 μ m packing, 4.6 mm x 150mm) with a solvent system of H₂O/acetonitrile with 0.1% formic acid at a flow rate of 0.8mL/min. NMR experiments were performed on a Bruker Advance 500mHz NMR; NMR chemical shifts (δ) reported relative to DMSO-*d*₆ residual solvent peaks unless otherwise noted. When possible, rotamers were resolved by performing the analysis at 365K. Assignment of 2D NMR data was performed using Sparky 3, T. D. Goddard and D. G. Kneller, University of California, San Francisco.

RP-purification was performed on an ISCO (Teledyne, Inc.) automated flash chromatography system with a RediSep R_f-12gm RP column or on a Varian Prostar Prep HPLC with a Waters Xterra column (5 μ m packing, 19 mm x 100mm) with a solvent system of H₂O/acetonitrile with 0.1% formic acid at a flow rate of 18 mL/min. HRMS analysis was performed by Ohio State University Proteomics Research Facility (ToF/ES).

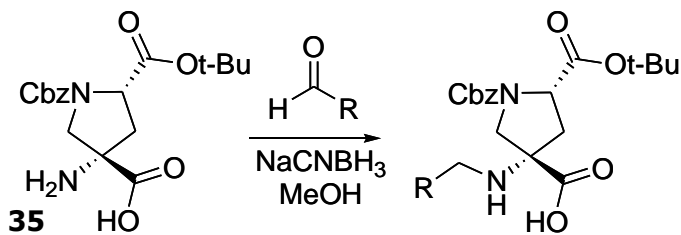


Figure 3.14. The reductive alkylation of the *pro4* amino acid **35**. The structures of the products are shown in Table 3.1.

General Procedure for the Reductive Alkylation of the *Pro4* monomers. The starting material, the *pro4* amino acid (compound **35** or *ent-35*), was synthesized according to a published procedure.² In a representative reaction of the reductive alkylation, *pro4* amino acid **35**, compound **35** or *ent-35*, (300mg, 824 μ mole) was dissolved in methanol (5mL, concentration of 165mM) and the aldehyde (824 μ mole) was added in a single portion. The solution was stirred at room temperature for 30 minutes and then NaCNBH₃ (52mg, 824 μ mole) was added in a single portion as a solid¹. The reaction was allowed to proceed for the specified amount of time at room temperature at which time the product was loaded onto Celite by removal of the solvent *in vacuo* and RP-purified with a gradient of 30-100% H₂O/ACN with 0.1% formic acid. The desired fractions were pooled and lyophilized.

***Pro4*(S,S)-benzyl functionalized (Compound **36**, Table 3.1).** The reaction was performed via the general procedure of the reductive alkylation with *pro4*(2S,4S) amino acid, compound **35**, (300mg, 824 μ mole) and benzaldehyde (84 μ L, 824 μ mole) and the reaction allowed to proceed

overnight. The product was obtained as a white solid (232mg, yield 62%). LCMS analysis (5-95% H₂O/ACN with 0.1% formic acid): t_r= 17.02min; calced for compound **36** +H⁺: 455.2; found: 455.0; ¹H NMR (500 MHz, DMSO-*d*₆, 365K), δ= 7.35 (m, 9H), 7.24 (m, 1H), 5.09 (s, 2H), 4.28 (m, 1H), 3.90 (d, 1H, *J*=11Hz), 3.68 (dd, 2H, *J*=12.6Hz, 13.6Hz), 3.44 (d, 1H, *J*=11Hz), 2.72 (m, 1H), 2.09 (m, 1H), 1.35 (s, 9H). ¹³C NMR (from HMBC, 500 MHz, DMSO-*d*₆, 365K), δ 173.3, 169.7, 153.0, 139.3 (2C), 136.1, 136.0 (2C), 127.2 (2C), 126.6 (2C), 126.4, 126.1 (2C), 79.9, 66.6, 63.4, 58.3, 53.9, 47.8, 37.9, 27.0 (3C).

Pro4(R,R)-anisoле functionalized (Compound 37, Table 3.1). The reaction was performed via the general procedure of the reductive alkylation with *pro4*(2R,4R) amino acid, compound **ent-35**, (300mg, 824μmole) and anisaldehyde (100μL, 824μmole) and the reaction allowed to proceed overnight. The product was obtained as a white solid (272mg, yield 68%). LC-MS analysis (5-95% H₂O/ACN with 0.1% formic acid): t_r= 17.3min; calced for Entry **37** +H⁺: 485.2; found: 485.1; ¹H NMR (500 MHz, DMSO-*d*₆, 365K), δ= 7.33 (m, 5H), 7.22 (d, 1H, *J*=8.4Hz), 6.85 (d, 1H, *J*=8.4Hz), 5.07 (m, 2H), 4.31 (m, 1H), 3.75 (s, 3H), 3.69 (m, 3H, signal overlap), 3.60 (m, 1H), 2.44 (m, 1H), 2.28 (m, 1H), 1.38 (s, 9H). ¹³C NMR (from HMBC, 500 MHz, DMSO-*d*₆, 365K), δ 172.1, 170.0, 157.8, 153.2, 136.2, 131.7 (2C), 128.2 (4C), 126.7 (2C), 113.1 (2C), 80.2, 66.7, 65.5, 58.5, 53.5, 46.7, 39.7, 37.5, 26.9 (3C).

Pro4(S,S)-naphthyl functionalized (Compound 38, Table 3.1). The reaction was performed via the general procedure of the reductive alkylation with *pro4*(2S,4S) amino acid, compound **35**, (300mg, 824μmole) and 1-naphthylaldehyde (112μL, 824μmole) and the reaction allowed to proceed overnight. The product was obtained as a white solid (216mg, yield 52%). LC-MS analysis (5-95% H₂O/ACN with 0.1% formic acid): t_r= 19.55min; calced for Entry **38** +H⁺: 505.2; found: 505.0; ¹H NMR (500 MHz, DMSO-*d*₆, 365K), δ= 8.2 (d, 1H, *J*=8.4Hz), 7.89 (m, 1H), 7.79 (d, 1H, *J*=7.9Hz), 7.51 (m, 3H), 7.42 (m, 1H), 7.35 (m, 5H), 5.08 (s, 2H), 4.30 (m, 1H), 4.12 (m, 1H), 4.06 (d, 1H, *J*= 10.4Hz), 3.46 (d, 1H, *J*=10.4Hz), 2.78 (m, 1H), 2.07 (m, 1H), 1.31 (s, 9H). ¹³C NMR (from HMBC, 500 MHz, DMSO-*d*₆), δ 174.5, 170.0, 153.1, 137.1, 136.2, 135.3, 132.8, 130.8, 130.5 (2C), 130.2 (2C), 127.4(2C), 126.6, 125.5 (2C), 125.2, 123.7, 123.1, 79.9, 65.4, 60.6, 45.6, 39.6, 38.3, 27.1 (3C).

Pro4(R,R)-isobutyl functionalized (Compound 40, Table 3.1). The reaction was performed via the general procedure of the reductive alkylation with *pro4*(2R,4R) amino acid, compound

ent-35, (300mg, 824 μ mole) and isobutyraldehyde (75 μ L, 824 μ mole) and the reaction allowed to proceed for two hours. The product was obtained as a white solid (277mg, yield 80%). LCMS analysis (5-95% H₂O/ACN with 0.1% formic acid): t_r= 16.35min; calcd for Entry **40** +H⁺: 421.2; found: 421.0; ¹H NMR (500 MHz, DMSO-*d*₆, 365K), δ = 7.35 (m, 5H), 5.09 (s, 2H), 4.25 (m, 1H), 3.91 (d, 1H, *J*=10.4Hz), 3.48 (d, 1H, *J*=10.4Hz), 2.66 (m, 1H), 2.36 (m, 1H), 2.26 (m, 1H), 1.99 (m, 1H), 1.65 (m, 1H), 1.38 (s, 9H), 0.88 (m, 6H). ¹³C NMR (from HMBC, 500 MHz, DMSO-*d*₆, 365K), δ 173.1, 169.7, 152.9, 135.9, 127.1, 126.5 (4C), 80.0, 66.4, 58.5, 53.7, 51.6, 43.8, 39.5, 27.3, 27.0 (3C), 19.5 (2C).

Pro4(S,S)-Cbz-aminopropyl functionalized (Compound 41, Table 3.1). The reaction was performed via the general procedure of the reductive alkylation with *pro4*(2S,4S) amino acid, compound **35**, (300mg, 824 μ mole) and 3-[(Benzyloxycarbonyl)amino]propionaldehyde (171mg, 824 μ mole) and the reaction allowed to proceed for two hours. The product was obtained as a white solid (270mg, yield 59%). LCMS analysis (5-95% H₂O/ACN with 0.1% formic acid): t_r= 17.85min; calcd for Entry **41**+H⁺: 556.3; found: 556.2; ¹H NMR (500 MHz, DMSO-*d*₆, 365K), δ = 7.34 (m, 10H), 5.07 (s, 2H), 5.03 (s, 2H), 4.24 (m, 1H), 3.92 (d, 1H, *J*=10.6Hz), 3.34 (d, 1H, *J*=10.6Hz), 3.07 (m, 2H), 2.64 (m, 1H), 2.54 (m, 2H, overlap with DMSO), 1.57 (m, 2H), 1.38 (s, 9H). ¹³C NMR (from HMBC, 500 MHz, DMSO-*d*₆, 365K), δ 173.1, 169.8, 155.4, 152.9, 136.8 (2C), 135.9 (2C), 127.0 (8C), 79.9, 66.4, 65.5, 64.6, 58.5, 53.8, 41.5, 39.7, 38.1, 37.3, 29.6 (3C).

Pro4(S,S)-Benzyl carboxylate functionalized (Compound 42, Table 3.1). Benzyl glyoxylate was synthesized via cleavage of dibenzyl tartrate with periodic acid³ and used without further purification or characterization. The reductive alkylation was performed via the general procedure of the reductive alkylation with *pro4*(2S,4S) amino acid, compound **35**, (300mg, 824 μ mole) and benzyl glyoxylate (440mg, 2.47mmole) and the reaction allowed to proceed overnight. The product was obtained as a white solid (232mg, yield 55%). LCMS analysis (5-95% H₂O/ACN with 0.1% formic acid): t_r= 21.06min; calcd for Entry **42** +H⁺: 513.2; found: 513.2; ¹H NMR (500 MHz, DMSO-*d*₆, 365K), δ = 7.35 (m, 10H), 5.14 (s, 2H), 5.08 (bs, 2H), 4.26 (m, 1H), 3.91 (d, 1H, *J*=11.0Hz), 3.38 (d, 1H, *J*=11.0Hz), 2.64 (dd, 1H, *J*=8.7,4.4Hz), 2.04 (dd, 1H, *J*=7.9,5.6Hz), 1.35 (s, 9H). ¹³C NMR (from HMBC, 500 MHz, DMSO-*d*₆, 365K), δ 173.2, 170.2, 169.6, 152.9, 136.2, 135.3, 127.8 (2C), 127.1 (2C), 127.0 (3C), 126.6 (3C), 79.9, 65.6, 65.1, 58.3, 53.9, 45.6, 39.6, 37.4, 27.0 (3C).

Pro4(R,R)-Pyrenyl functionalized (Compound 39, Table 3.1). The reaction was performed via the general procedure of the reductive alkylation with *pro4*(R,R) amino acid, compound **ent-35**, (220mg, 604 μ mole) and 1-pyrenecarboxaldehyde (139mg, 604 μ mole) and the reaction allowed to proceed overnight. The product was obtained as a yellow solid (290mg, yield 84%). LCMS analysis (5-95% H₂O/ACN with 0.1% formic acid): t_r = 22.8min; calcd for Entry **39** +H⁺: 579.2; found: 579.0. This product was not characterized further and was used in the synthesis of hexasubstituted diketopiperazine **49**.

General Procedure for Bis-amino Acid Coupling. The bis-amino acid to be activated (1eq) and HOAT (6eq) were dissolved in 1:2 DMF/DCM (concentration of 55mM), DIC (1eq) was then added and the activation was allowed to proceed for 1.5 hours. The nucleophilic bis-amino acid (1eq) was dissolved in DMF (concentration of 200mM), DIPEA (2eq) was added and the solution combined with the activated amino acid. The reaction was allowed to proceed at room temperature for between 5 and 16 hours, at which time an additional aliquot of DIC (1eq) was added and reaction allowed to stir again for at least 1 hour. The reaction mixture was then diluted with 3x the amount of DCM and the crude mixture was washed twice with 10% aqueous HCl. The reaction mixture was dried over sodium sulfate, and the solvent was removed *in vacuo*.

General Procedure for HBr deprotection of Cbz and tert-butyl ester groups. The crude, protected material was dissolved in DCM (approx. 1mL/50mg product) and an equal volume of HBr (33% in AcOH) was added and the deprotection was allowed to proceed for 30 minutes. The solvent was removed *in vacuo*, resuspended and the solvent removed under reduced pressure with DCM twice to remove excess HBr, and then purified via reverse-phase chromatography.

Synthesis of Hexasubstituted Diketopiperazine (Compound 49). *Pro4*(R,R)-isobutyl functionalized (Compound **40**, Table **3.1**, 45mg, 110 μ mole) was dissolved in 1:2 DMF/DCM (2mL, conc. of 55mM) with HOAT (90mg, 660 μ mole) with stirring in a 15mL polypropylene tube. Diisopropylcarbodiimide (17 μ L, 110 μ mole) was then added and the activation was allowed to proceed for 1.5 hours at room temperature to produce compound. *Pro4*(R,R)-pyrenyl functionalized (Compound **39**, Table **3.1**, 64mg, 110 μ mole) was dissolved in DMF (0.5mL, conc. of 200mM) and DIPEA (38 μ L, 220 μ mole) was added; this solution was then combined with activated compound **40** from above and allowed to react for 1.5 hours at room temperature. LC-

MS analysis (5-95% H₂O/ACN with 0.1% formic acid) was performed on the reaction mixture. At this point, one additional aliquot of DIC was added and the reaction was allowed to proceed for an hour. An aliquot of the reaction was removed, dissolved in ACN with 0.1% formic acid and subjected to LC-MS analysis (5-95% H₂O/ACN with 0.1% formic acid, 40 minute run): t_r = 33.7min; calcd for compound **49** +Na⁺: 985.4; found: 985.3. DCM (8mL) was added and the reaction mixture was washed twice with 2mL of 10% aqueous HCl. The organic layer was dried over sodium sulfate and concentrated *in vacuo*. The residue was then suspended in 3mL of DCM and 3mL of 33% HBr in AcOH was added and the deprotection was allowed to proceed for 30 minutes. The reaction mixture was then concentrated *in vacuo*, the residue was suspended in ACN with 0.5% formic acid, purified by preparatory HPLC, and the desired fractions pooled and lyophilized to yield the deprotected hexasubstituted diketopiperazine **sc1** (45mg, 70% yield). Final product characterization: LC-MS analysis, see figure **3.15** (5-95% H₂O/ACN with 0.1% formic acid). Diketopiperazine **sc1**: t_r = 13.1min., calcd. for product(**sc1**)+H⁺ = 583.2; found: 583.2. ¹H NMR (500 MHz, DMSO-*d*₆), δ = 8.35 (m, 3H), 8.32 (m, 1H), 8.26 (d, 1H, J = 7.9Hz), 8.17 (m, 2H), 8.10 (t, 1H, J = 7.7, 15.3Hz), 7.88 (d, 1H, J = 7.9Hz), 5.65 (d, 1H, J = 17.8Hz), 5.41 (d, 1H, J = 17.8Hz), 4.52 (m, 1H), 4.44 (m, 1H), 3.83 (t, 2H, J = 13.5, 26.9Hz), 3.68 (d, 1H, J = 13.1Hz), 3.45 (m, 2H), 3.32 (m, 1H), 2.94 (m, 1H), 2.90 (m, 1H), 2.81 (t, 1H, J = 12.9, 26.3Hz), 2.58 (t, 1H, J = 13.0, 26.2Hz), 2.23 (m, 1H), 0.99 (d, 6H, J = 6.8Hz). ¹³C NMR (from HMBC, 500 MHz, DMSO-*d*₆), δ = 168.3 (2C), 167.3 (2C), 129.9 (3C), 129.3 (2C), 128.4 (2C), 126.7 (2C), 126.1 (2C), 125.3 (2C), 124.5, 123.2, 121.3 (2C), 67.3, 57.9 (2C), 50.3 (2C), 49.6, 44.8, 37.7, 37.5, 26.3, 26.0, 20.0 (2C).

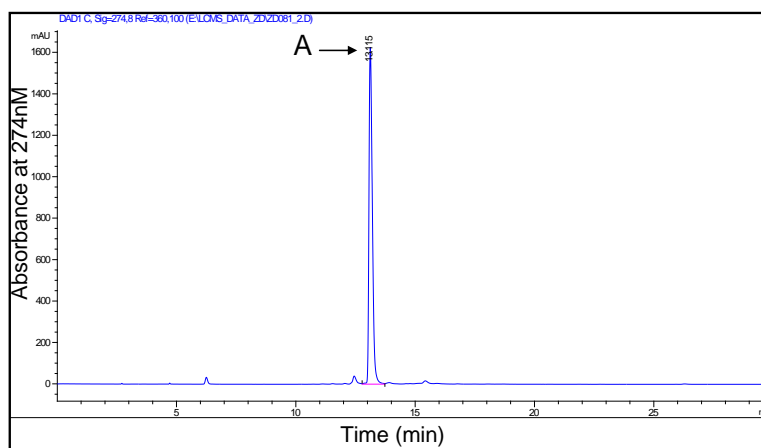


Figure **3.15**. HPLC trace of purified diketopiperazine **sc1**, monitoring at a wavelength of 274nm with a gradient of 5-95% ACN/H₂O with 0.1% formic acid over 30 minutes. The peak marked "A" has a m/z = 583.2 (calcd for compound **sc1** + H⁺: 583.2).

***N*-(2-methylenenaphthylene)-proline methyl ester (sc4).** To a 100mL round bottom flask was added proline-methyl ester(*HCl) (500mg, 1.4mmole), 2eq of diisopropylethylamine (478 μ L), 2-(Bromomethyl)naphthalene (303mg, 1.4mmole) and dichloromethane (14mL, conc of 100mM). The reaction was allowed to proceed overnight with stirring. LCMS analysis (5-95% H₂O/ACN with 0.1% formic acid): t_r = 9.14min; calcd for Entry sc6+H⁺: 270.1; found: 270.2. The product was not characterized and taken to the next reaction.

***N*-(2-methylenenaphthylene)-proline (sc5).** *N*-(2-methylenenaphthylene)-proline methyl ester, sc4, (375mg, 1.4mmole) was placed in a round bottom flask and dissolved in 14mL of THF. 2M KOH (4.2mL) was added with vigorous stirring. The reaction was allowed to proceed for 3hours at room temperature at which time the reaction mixture was transferred to separatory funnel and 50mL of diethyl ether was added. The aqueous layer was isolated and neutralized with a dropwise addition of 2M HCl. The product was then filtered through a Buchner funnel and dried overnight under vacuum at 50°C to yield a pale yellow solid (327mg, 92% yield). LCMS analysis (5-100% H₂O/ACN with 0.1% formic acid, 40min run): t_r = 10.6min; calcd for Entry **sc5**+H⁺: 256.1; found: 256.2. ¹H NMR (500 MHz, DMSO-*d*₆), δ = 8.10 (s, 1H), 7.97 (m, 3H), 7.68 (m, 1H), 7.58 (m, 2H), 4.70 (d, 1H, J=12.8Hz), 4.55 (d, 1H, J=12.8Hz), 4.49 (m, 1H), 3.50 (m, 1H), 3.37 (m, 1H), 2.47 (m, 1H, overlap with DMSO), 2.06 (m, 2H), 1.90 (m, 1H). ¹³C NMR (500 MHz, DMSO-*d*₆), δ 169.0, 132.5 (2C), 129.9, 127.5, 127.0 (2C), 126.4 (2C), 125.9 (2C), 64.7, 56.8, 53.9, 27.3, 21.3.

Competition Experiments. To address the question of nucleophilicity of the secondary amine versus that of the carboxylic acid, a competition experiment was performed (see Figure **3.10**). Pro4(S,S)-naphthyl, compound **38**, (1eq, 23mg, 49 μ mole) was activated as the amino-OAt ester as described in the "General Procedure for Bis-Amino Acid Coupling". *N*-(2-methylenenaphthylene)-proline, **sc5**, (5eq, 63mg, 245 μ mole) and proline methyl ester(*HCl) (5eq, 40mg, 245 μ mole) were dissolved in DMF (1.2mL, conc. of 200mM) and 20eq of diisopropylethylamine (171 μ L) added. This solution was then transferred to the activated amino ester solution and the reaction stirred at room temperature for 30 minutes. An aliquot of the reaction mixture was then removed, dissolved in H₂O/ACN with 0.1% formic acid and subjected to LC-MS analysis (5-100% H₂O/ACN with 0.1% formic acid, 40min run). The product of direct acylation of proline methyl ester, compound **65** in Figure **3.10**, had an HPLC area of 4927, while the acyl transfer product, compound **64** in Figure **3.10**, had an HPLC area of 1432. Assuming

that **64** has an extinction coefficient twice that of **65** (because **64** has two naphthyl groups while **65** has only one), the product ratio will be: (Area **65**)/(Area **64**/2), or **65:64** = 6.9.

Pro4(S,S)-Fmoc,OMe (compound **66**, 488 μ mole, 200mg) was prepared from the previously published monomer.² The Boc group was removed with 1:1 TFA/DCM for 30 minutes and the solvent was removed *in vacuo* and dried overnight under high vacuum. The product was obtained as a brown solid (184mg, yield 92%). LCMS analysis (5-95% H₂O/ACN with 0.1% formic acid): t_r = 14.3min; calcd for compound **66** +H⁺: 411.1; found: 411.0; ¹H NMR (500 MHz, DMSO-*d*₆, See Supplemental Figure 16), δ = 8.37 (s, 1H), 7.89 (d, 2H, J =7.52Hz), 7.70 (d, 2H, J =7.17Hz), 7.42 (t, 2H, J =7.38Hz), 7.34 (t, 2H, J =7.38Hz), 4.50 (t, 1H, J =8.29Hz), 4.41 (m, 1H), 4.32 (m, 1H), 4.23 (t, 1H, J =6.58Hz), 3.80 (m, 1H), 3.68 (s, 3H), 3.62 (m, 1H), 2.71 (m, 1H), 2.55 (m, 1H). ¹³C NMR (from HMBC, 500 MHz, DMSO-*d*₆, See Supplemental Figure), δ \square 170.4, 168.5, 155.2, 142.8 (2C), 140.1 (2C), 126.9 (2C), 126.3 (2C), 124.3 (2C), 119.4 (2C), 65.0, 62.5, 57.0, 52.3, 45.8, 39.1, 35.9.

Synthesis of Functionalized Dimer (compound 67). *Pro4(S,S)*-benzyl functionalized (compound **36**, Table 3.1, 66mg, 146 μ mole) was dissolved in 1:2 DMF/DCM (2.7mL, conc. of 55mM) with HOAT (120mg, 876 μ mole) with stirring in a 15mL polypropylene tube. Diisopropylcarbodiimide (23 μ L, 146 μ mole) was then added and the activation was allowed to proceed for 1.5 hours at room temperature to produce activated **36**. *Pro4(S,S)*-Fmoc,OMe (compound **66**, 146 μ mole, 60mg) was dissolved in DMF (730 μ L, conc. of 200mM) and DIPEA (51mL, 292 μ mole) was added. This solution was then combined with the amino-OAt ester (activated compound **36**) and the reaction was allowed to proceed overnight. An additional aliquot of diisopropylcarbodiimide (23 μ L, 146mole) was added and the reaction was allowed to stir for 1 hour at room temperature. DCM (10mL) was added and the reaction mixture was washed twice with 3mL of 10% aqueous HCl. The organic layer was dried over sodium sulfate and concentrated *in vacuo*. The residue was then suspended in 3mL of DCM and 3mL of 33% HBr in AcOH was added and the deprotection was allowed to proceed for 30 minutes. An aliquot of the reaction was removed, dissolved in ACN with 0.5% formic acid and subjected to LC-MS analysis (5-95% H₂O/ACN with 0.1% formic acid, 30 minute run, see Supplemental Figure 3.16): t_r = 17.9min; calcd for compound **67** +H⁺: 639.2; found: 639.0. The reaction mixture was then loaded onto Celite by removal of the solvent *in vacuo*. The product was

purified by RP purification, the desired fractions pooled and lyophilized to yield dimer **67** (64mg, 68% yield)

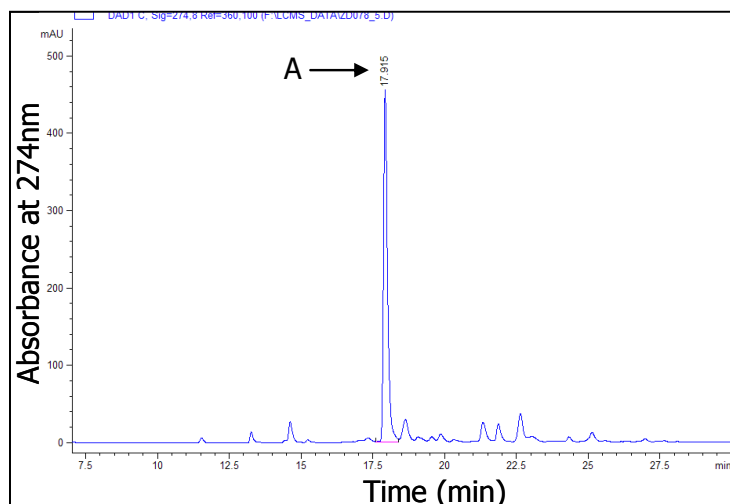


Figure 3.16. HPLC trace of crude reaction mixture of dimer **67**, monitoring at a wavelength of 274nm with a gradient of 5-95% ACN/H₂O with 0.1% formic acid over 30 minutes. The peak marked “A” has a $m/z = 639.2$ (calcd for dimer **67** + H⁺: 639.0). Only a portion of the chromatogram (from 7-30 minutes) is shown: from 0-7 minutes the only peak is that of HOAT at 6 minutes. Unlabeled peaks did not have identifiable masses

Synthesis of Functionalized Trimer (compound 68). *Pro4(S,S)*-naphthyl functionalized (compound **38**, Table 3.1, 51mg, 101 μ mole) was dissolved in 1:2 DMF/DCM (1.8mL, conc. of 55mM) with HOAT (82mg, 606 μ mole) with stirring in a 15mL polypropylene tube. Diisopropylcarbodiimide (17 μ L, 101 μ mole) was then added and the activation was allowed to proceed for 1.5 hours at room temperature to produce activated compound **38**. Functionalized dimer (compound **67**, 100 μ mole, 64mg) was dissolved in DMF (502 μ L, conc. of 200mM) and DIPEA (35 μ L, 200 μ mole) was added. This solution was then combined with the amino-OAt ester (activated compound **38**) and the reaction was allowed to proceed overnight. An additional aliquot of diisopropylcarbodiimide (17 μ L, 101 μ mole) was added and the reaction was allowed to stir for 1 hour at room temperature. DCM (10mL) was added and the reaction mixture was washed twice with 3mL of 10% aqueous HCl. The organic layer was dried over sodium sulfate and concentrated *in vacuo*. The residue was then suspended in 3mL of DCM and 3mL of 33% HBr in AcOH was added and the deprotection was allowed to proceed for 30 minutes. An aliquot of the reaction was removed, dissolved in ACN with 0.5% formic acid and subjected to LC-MS analysis (5-95% H₂O/ACN with 0.1% formic acid, 40 minute run, see Figure 3.17): $t_r = 20.1$ min; calcd for compound **68** + H⁺: 917.3; found: 917.2. The reaction mixture was then

loaded onto Celite by removal of the solvent *in vacuo*. The product was purified by RP purification, the desired fractions pooled and lyophilized to yield trimer **68** (70mg, 77% yield).

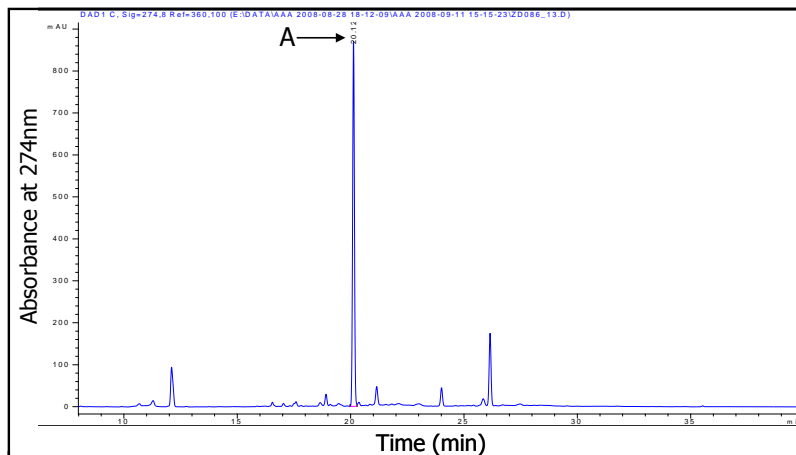


Figure 3.17. HPLC trace of crude reaction mixture of trimer **68**, monitoring at a wavelength of 274nm with a gradient of 5-95% ACN/H₂O with 0.1% formic acid over 40 minutes. The peak marked “A” has a $m/z = 917.2$ (calcd for trimer **38** + H⁺: 917.3). Only a portion of the chromatogram (from 7-30 minutes) is shown: from 0-7 minutes the only peak is that of HOAT at 6 minutes. Unlabeled peaks did not have identifiable masses.

Synthesis of Functionalized Tetramer (compound 69). *Pro4(S,S)*-Cbz-aminopropyl (compound **41**, Table 3.1, 42mg, 76 μ mole) was dissolved in 1:2 DMF/DCM (1.4mL, conc. of 55mM) with HOAT (63mg, 456 μ mole) with stirring in a 15mL polypropylene tube. Diisopropylcarbodiimide (13 μ L, 76 μ mole) was then added and the activation was allowed to proceed for 1.5 hours at room temperature to produce activated compound **41**. Functionalized trimer (compound **68**, 76 μ mole, 70mg) was dissolved in DMF (380 μ L, conc. of 200mM) and DIPEA (26 μ L, 152 μ mole) was added. This solution was then combined with the amino-OAt ester (activated compound **41**) and the reaction was allowed to proceed overnight. An additional aliquot of diisopropylcarbodiimide (13 μ L, 76 μ mole) was added and the reaction was allowed to stir for 1 hour at room temperature. DCM (8mL) was added and the reaction mixture was washed twice with 2.5mL of 10% aqueous HCl. The organic layer was dried over sodium sulfate and concentrated *in vacuo*. The residue was then suspended in 2.5mL of DCM and 2.5mL of 33% HBr in AcOH was added and the deprotection was allowed to proceed for 30 minutes. The reaction mixture was then loaded onto Celite by removal of the solvent *in vacuo*. The product was purified by RP purification, the desired fractions pooled and lyophilized to yield tetramer (**69**): (25mg, 59% yield). Final product characterization: LC-MS analysis; see Figure 3.18 (5-95% H₂O/ACN with 0.1% formic acid). Tetramer (**69**): $t_r=15.74$ min., calcd. for product(**69**)+H⁺=

1112.4; found: 1112.2. Anal. Calcd for $C_{61}H_{61}N_9O_{12}$: 1112.4518, Found: 1112.4545 (difference 2.4ppm). See Appendix for NMR characterization.

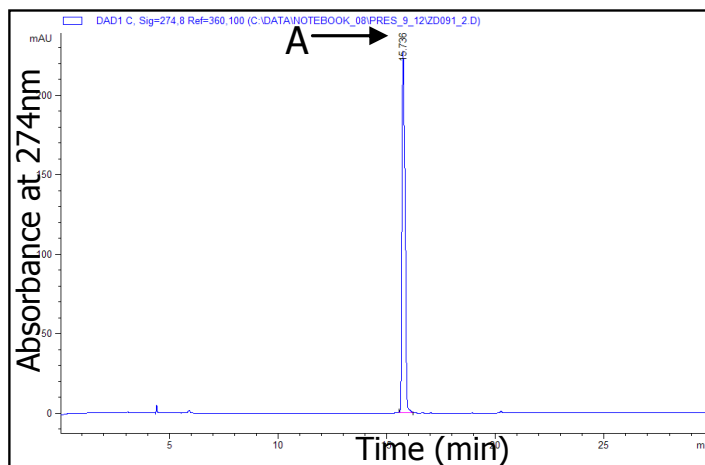


Figure 3.18. Purified HPLC trace of tetramer **69**, monitoring at a wavelength of 274nm with a gradient of 5-95% ACN/H₂O with 0.1% formic acid over 30 minutes. The peak marked “A” has a m/z = 1112.2 (calcd for tetramer **69** + H⁺: 1112.4).

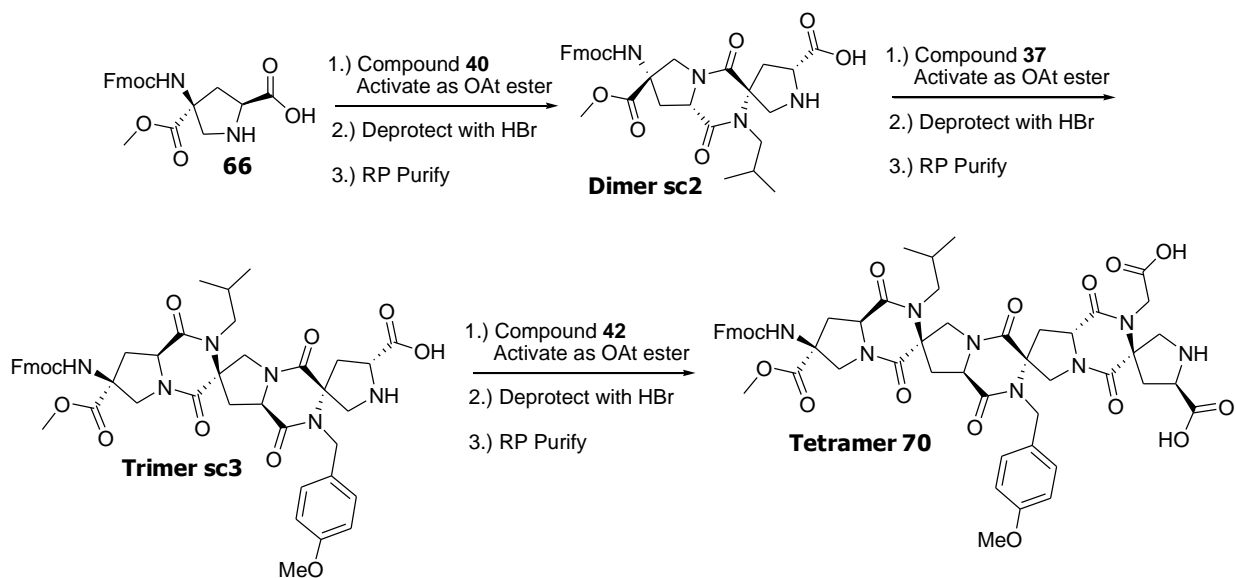


Figure 3.19. The solution phase synthesis of tetramer **70**.

Synthesis of Functionalized Dimer (sc2). *Pro4(R,R)*-isobutyl functionalized (compound **40**, Table 3.1, 51mg, 122 μ mole) was dissolved in 1:2 DMF/DCM (2.2mL, conc. of 55mM) with

HOAT (100mg, 732 μ mole) with stirring in a 15mL polypropylene tube. Diisopropylcarbodiimide (19 μ L, 122 μ mole) was then added and the activation was allowed to proceed for 1.5 hours at room temperature to produce compound. *Pro4(S,S)*-Fmoc,OMe (compound **66**, 122 μ mole, 50mg) was dissolved in DMF (610 μ L, conc. of 200mM) and DIPEA (43 μ L, 244 μ mole) was added. This solution was then combined with the amino-OAt ester (compound **40**) and the reaction was allowed to proceed overnight. An additional aliquot of diisopropylcarbodiimide (19 μ L, 122 μ mole) was added and the reaction was allowed to stir for 1 hour at room temperature. DCM (10mL) was added and the reaction mixture was washed twice with 3mL of 10% aqueous HCl. The organic layer was dried over sodium sulfate and concentrated *in vacuo*. The residue was then suspended in 3mL of DCM and 3mL of 33% HBr in AcOH was added and the deprotection was allowed to proceed for 30 minutes. An aliquot of the reaction was removed, dissolved in ACN with 0.5% formic acid and subjected to LC-MS analysis (5-95% H₂O/ACN with 0.1% formic acid, 40 minute run, see Figure **3.20**): t_r = 16.5min; calcd for

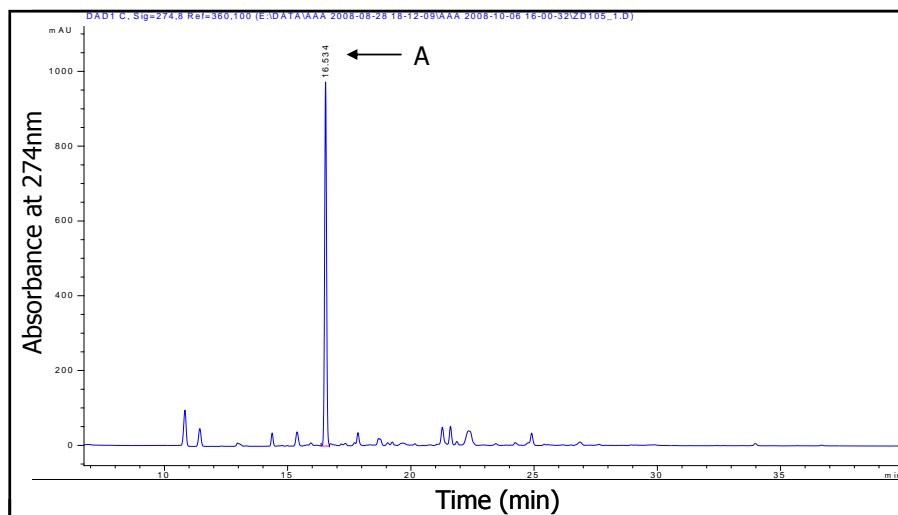


Figure **3.20**. HPLC trace of crude reaction mixture of dimer **sc2**, monitoring at a wavelength of 274nm with a gradient of 5-95% ACN/H₂O with 0.1% formic acid over 40 minutes. The peak marked “A” has a m/z = 605.2 (calcd for trimer **sc2** + H⁺: 605.3). Only a portion of the chromatogram (from 7-30 minutes) is shown: from 0-7 minutes the only peak is that of HOAT at 6 minutes. Unlabeled peaks did not have identifiable masses.

compound **sc2**+H⁺: 605.3; found: 605.2. The reaction mixture was then loaded onto Celite by removal of the solvent *in vacuo*. The product was purified by RP purification, the desired fractions pooled and lyophilized to yield dimer **sc2** (52mg, 68% yield).

Synthesis of Functionalized Trimer (sc3). Pro4(R,R)-anisole functionalized (compound **37**, Table 1, 42mg, 87 μ mole) was dissolved in 1:2 DMF/DCM (1.6mL, conc. of 55mM) with HOAT (72mg, 522 μ mole) with stirring in a 15mL polypropylene tube. Diisopropylcarbodiimide (14 μ L, 87 μ mole) was then added and the activation was allowed to proceed for 1.5 hours at room temperature to produce activated compound **37**. Functionalized dimer (compound **sc2**, 87 μ mole, 53mg) was dissolved in DMF (435 μ L, conc. of 200mM) and DIPEA (30 μ L, 176 μ mole)

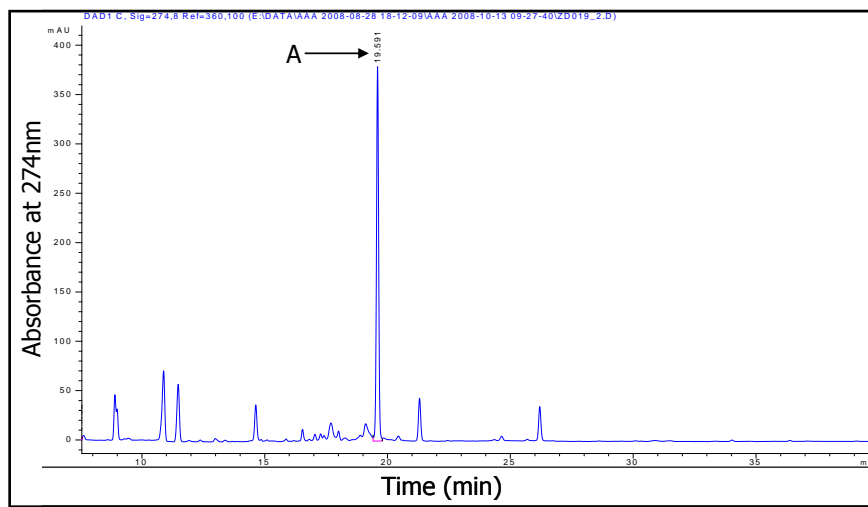


Figure 3.21. HPLC trace of crude reaction mixture of trimer **sc3**, monitoring at a wavelength of 274nm with a gradient of 5-95% ACN/H₂O with 0.1% formic acid over 40 minutes. The peak marked “A” has a m/z = 863.3 (calcd for trimer **sc3** + H⁺: 863.4). Only a portion of the chromatogram (from 7-30 minutes) is shown: from 0-7 minutes the only peak is that of HOAT at 6 minutes. Unlabeled peaks did not have identifiable masses.

was added. This solution was then combined with the amino-OAt ester (compound **37**) and the reaction was allowed to proceed overnight. An additional aliquot of diisopropylcarbodiimide (14 μ L, 87 μ mole) was added and the reaction was allowed to stir for 1 hour at room temperature. DCM (10mL) was added and the reaction mixture was washed twice with 3mL of 10% aqueous HCl. The organic layer was dried over sodium sulfate and concentrated *in vacuo*. The residue was then suspended in 3mL of DCM and 3mL of 33% HBr in AcOH was added and the deprotection was allowed to proceed for 30 minutes. An aliquot of the reaction was removed, dissolved in ACN with 0.5% formic acid and subjected to LC-MS analysis (5-95% H₂O/ACN with 0.1% formic acid, 40 minute run, see Figure 3.21): t_r= 16.5min; calcd for compound **sc3** +H⁺: 863.4; found: 863.3. The reaction mixture was then loaded onto Celite by removal of the solvent *in vacuo*. The product was purified by RP purification, the desired fractions pooled and lyophilized to yield trimer **sc3** (49mg, 65% yield).

Synthesis of Functionalized Tetramer (compound 70). *Pro4(S,S)*-benzyl carboxylate (compound **42**, Table 3.1, 29mg, 57 μ mole) was dissolved in 1:2 DMF/DCM (1.0mL, conc. of 55mM) with HOAT (47mg, 342 μ mole) with stirring in a 15mL polypropylene tube. Diisopropylcarbodiimide (9 μ L, 57 μ mole) was then added and the activation was allowed to proceed for 1.5 hours at room temperature to produce activated compound **42**. Functionalized trimer (compound **sc3**, 57 μ mole, 49mg) was dissolved in DMF (285 μ L, conc. of 200mM) and DIPEA (20 μ L, 114 μ mole) was added. This solution was then combined with the amino-OAt ester (compound **42**) and the reaction was allowed to proceed overnight. An additional aliquot of diisopropylcarbodiimide (9 μ L, 57 μ mole) was added and the reaction was allowed to stir for 1 hour at room temperature. DCM (8mL) was added and the reaction mixture was washed twice with 2mL of 10% aqueous HCl. The organic layer was dried over sodium sulfate and concentrated *in vacuo*. The residue was then suspended in 3mL of DCM and 3mL of 33% HBr in AcOH was added and the deprotection was allowed to proceed for 30 minutes. The reaction mixture was then loaded onto Celite by removal of the solvent *in vacuo*. The product was purified by RP purification, the desired fractions pooled and lyophilized to yield tetramer **70** (31mg, 52% yield). Final product characterization: LC-MS analysis, See Figure 3.22, (5-95% H₂O/ACN with 0.1% formic acid). Tetramer (**70**): $t_r=20.98$ min., calced. for product(**70**)+H⁺= 1058.4; found: 1058.7. Anal. Calced for C₅₄H₅₈N₈O₁₅: 1059.4100, Found: 1059.4137 (difference 3.5ppm). See Appendix for NMR characterization.

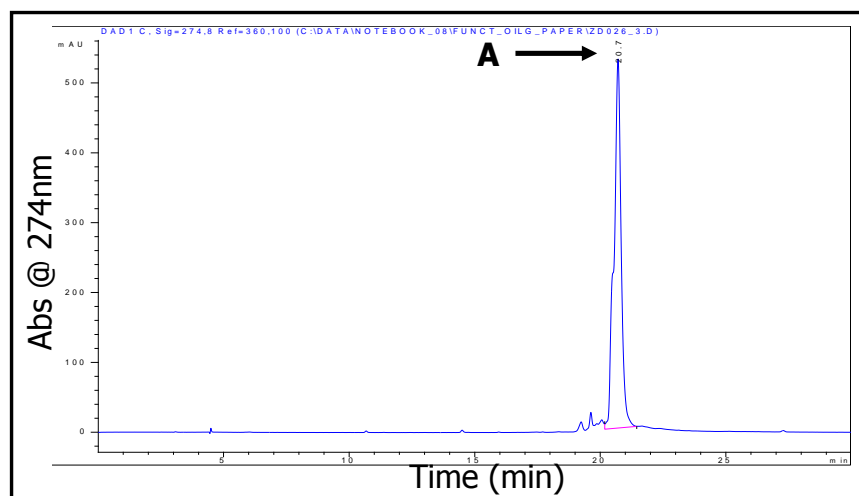


Figure 3.22. Purified HPLC trace of tetramer **70**, monitoring at a wavelength of 274nm with a gradient of 5-95% ACN/H₂O with 0.1% formic acid over 30 minutes. The peak marked “A” has a $m/z = 1058.7$ (calced for tetramer **69** + H⁺: 1058.4).

Chapter 4

***Bis*-Peptide as α -Helix Mimics**

In Chapter 2 the acyl transfer chemistry was introduced as a novel means of constructing hindered tertiary amides. Using this chemistry as detailed in Chapter 3, functionalized *bis*-peptide oligomers, which consist of two hindered tertiary amides between each monomer, were finally realized. In Chapter 4, these functionalized *bis*-peptides are applied to disrupt the protein-protein interaction of the p53/hDM2 system. More specifically, the *bis*-peptides were found to be competent inhibitors of the p53/hDM2 interaction, they are cell-permeable and have shown dose-dependent, *in vitro* activity with human liver cancer cells. The activity of the *bis*-peptide was surprising in that it suppresses p53 levels rather than activating p53. The *bis*-peptide displays two competing functions: it stabilizes hDM2 which causes the degradation of p53 and competes with p53 to bind hDM2 which should activate p53. However, biochemical experiments indicate that the suppression of p53 is more prevalent which could prove to be a valuable therapeutic application of this *bis*-peptide.

Acknowledgments: The solid-phase synthesis of the *bis*-peptide oligomers was accomplished with the assistance of Jennifer Alleva, former undergraduate in the Schafmeister Lab. Kavitha Akula and Marcus Jackson (both are graduate students in the Schafmeister Lab) expressed and purified the hDM2 protein and assisted with a few of the FP assays. Alla Arzumanyan (Feitelson Lab, Temple University) did all of the cell culture work, including the fluorescence microscopy and the Western blot analysis.

4.1 Introduction

Protein-protein interactions mediate intra- and inter-cellular communication whereby information is transmitted via macromolecular complexes of proteins. Large, amphiphilic and often disparate areas of protein surface are buried to induce an effect in the binding partner.⁵³ Although traditionally considered a difficult task for small molecule therapeutics because of the lack of discreet hydrophobic pockets, foldamers have recently been examined as scaffolds capable of spanning a large surface area to interact with a few key residues.⁴ This illustrates the concept of “hot spots”, the idea that, although large amounts of surface area are buried in protein-protein interactions, only a few functional groups of particular amino acids may contribute a substantial amount of the binding free energy.⁵⁴ Thus, mimicry of the three-dimensional arrangement of these residues on a non-natural scaffold may allow for the synthesis of molecules which are capable of participating in these binding events and eliciting a biological response.⁷ In these systems, the scaffold serves to position the chemical functionality and does not contribute directly to the binding interaction. Here *bis*-peptides could serve as a new peptidomimetic capable of positioning the appropriate functional groups that interact with the protein partner and illicit a desired biological response. The premise is simple and is shown in Figure 4.1: the hot spots of an important protein-protein interaction are taken from the literature, identified by

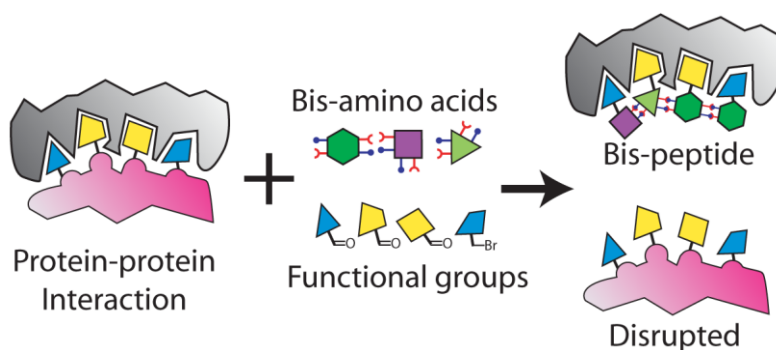


Figure 4.1. The concept of disrupting protein-protein interactions using *bis*-peptides.

mutational analysis or structural studies. *Bis*-peptides, with proteogenic or non-proteogenic appended functional groups, may be rapidly designed, synthesized and assayed for binding and disruption of this interaction. Given the ability of *bis*-peptides to display a variety of functional groups and their ability to control the presentation of the functional groups by incorporating other building blocks into the oligomer, an enormous number of potential inhibitors may be created. The application of *bis*-peptides to protein-protein interactions is a particularly worthwhile venture

and the results presented here show that *bis*-peptides are well suited as proteomimetic therapeutics.

The transcription factor p53 has been called the “guardian of the genome” because of its role in the maintenance of genetic integrity in times of cellular stress.⁶ The cytoplasmic and nuclear concentrations of this protein are tightly controlled through a regulatory feedback loop with its chaperone protein hDM2 during homeostasis. Upon the detection of DNA damage or other irregularities, p53 can attempt to repair the genomic damage through mechanisms such as cell cycle arrest and the activation of DNA repair enzymes.⁵⁵ p53 even has the capability of initiating the apoptotic cycle if the damage is deemed too excessive to repair. Therefore, mutations in these proteins and abnormalities in the functioning of this pathway are intrinsic in many forms of cancer and so there is extensive interest in being able to mimic this amphipathic helix of the N-terminus of p53 and displace the p53 protein from its chaperone protein hDM2. A therapeutic agent which could bind hDM2 would free p53 and protect it from cellular destruction. This would allow p53 to continue its genomic guardianship, increasing cytoplasmic p53 levels and hopefully initiating apoptosis in cancerous cells. The therapeutic potential of this strategy has been realized and compounds are currently in various stages of development as cancer

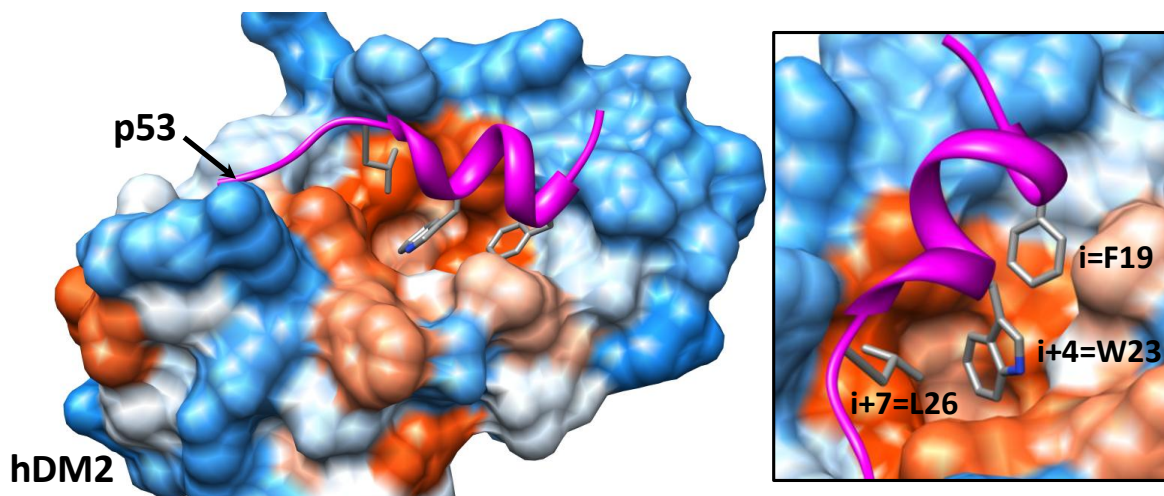


Figure 4.2. The p53/hDM2 protein/protein interaction with the key interacting residues of the helical transactivation domain highlighted. PDB Code: 1YCR.⁶ Image created with Chimera.

treatments.⁵⁶

On the other hand, p53 suppression represents a valuable new therapeutic avenue to protect normal (noncancerous) cells from p53 dependent apoptosis during cancer treatment.⁵⁷ Genotoxic stress, such as the conventional cancer treatments of chemo- and radiotherapy, will induce apoptosis in normal cells as a side effect during treatment to kill the cancerous cells. An

agent which could prevent the undesired apoptosis of healthy cells during these treatments would be especially valuable as these side effects can be quite toxic. Only one notable compound class, the pifithrin series of molecules, has been identified which can suppress p53 and prevent healthy cells from undergoing programmed cell death as a consequence of genotoxic stress.⁵⁸ However, the mechanism of action is still unknown and debate continues in the literature as conflicting reports of the therapeutic value of pifithrins have been presented. Therefore, a compound which could suppress the p53 apoptotic cycle in normal cells would be a valuable treatment option for suppressing the side effects of cancer therapy.

Aside from these therapeutic applications, the p53/MDM2 system represents a fascinating case study in the use of helical scaffolds to disrupt protein-protein interactions. hDM2 is a E3 ubiquitin ligase that binds to an α -helical transactivation domain of p53, ubiquitinates it which accelerates its cellular degradation.⁸ This α -helix projects the i (F19), $i+4$ (W23), and $i+7$ (L26) on one helical face to be buried in a deep hydrophobic cleft of hDM2⁶ (a rendering of the crystal structure is shown in Figure 4.2). Here three hydrophobic side chains of the amphipathic α -helix of p53 point deep into the hDM2 pocket with little other interaction from the helical peptide and provide most of the free energy of binding for the interaction as determined from mutational studies.⁷

The p53/hDM2 protein-protein interaction has been targeted by many types of therapeutic agents, including small molecules,⁵⁹ macrocyclic peptides,⁶⁰ mini-proteins⁶¹ and foldamers.⁷ Small molecule examples include the Nutlin series of compounds as well as a spirooxindole-based family of compounds which are both potent and selective for p53/hDM2 disruption.⁵⁹ Examples of foldamers which have targeted this interaction include peptoids, β -peptides, and the terphenyl scaffolds.⁷ Foldamers and other oligomeric based scaffolds have also targeted this system because of the possibility they could address some of the therapeutic drawbacks of peptides. For example, foldamers would be expected to show enhanced proteolytic stability and perhaps exhibit cellular penetration. Success within the p53/hDM2 system would then provide encouragement that the foldamer technology could be applied to other helical epitopes of protein-protein interactions. Finally, α -peptide based systems have also been used to target the p53/hDM2 interaction.⁶² These include a macrocyclic, β -turn based peptide⁶⁰ which presented the helical epitope as well as a mini-protein⁶¹ system found by Schepartz which included a α -helical domain which could be reengineered to present other side chains.

One drawback with the use of peptides, foldamers and other macromolecular systems larger than small molecules is the difficulty with cellular penetration.⁴ In order for a potential

intracellular therapeutic to be viable, it must be able to cross the cell membrane. Unfortunately, this can be a major impediment as the lipid bilayer surrounding a cell is a highly nonpolar environment and is designed to sequester the cell from foreign agents, particularly small molecules. This also has the effect of preventing the desired therapeutics from entering the cytoplasm and making pharmaceutical science significantly more challenging as these various properties are addressed.

Therefore, disruption of the p53/hDM2 system represents a judicious choice as an introduction into the realm of protein-protein interactions for *bis*-peptides. All aspects of *bis*-peptides as potential therapeutic agents could be tested, such as binding to a protein target, cellular penetration, and finally *in vitro* activity.

4.2 Results and Discussion

Bis-peptide design. Preliminary computer modeling was used to assess whether *bis*-peptides could approximate the presentation of three residues residing on the same face of a α -helix.

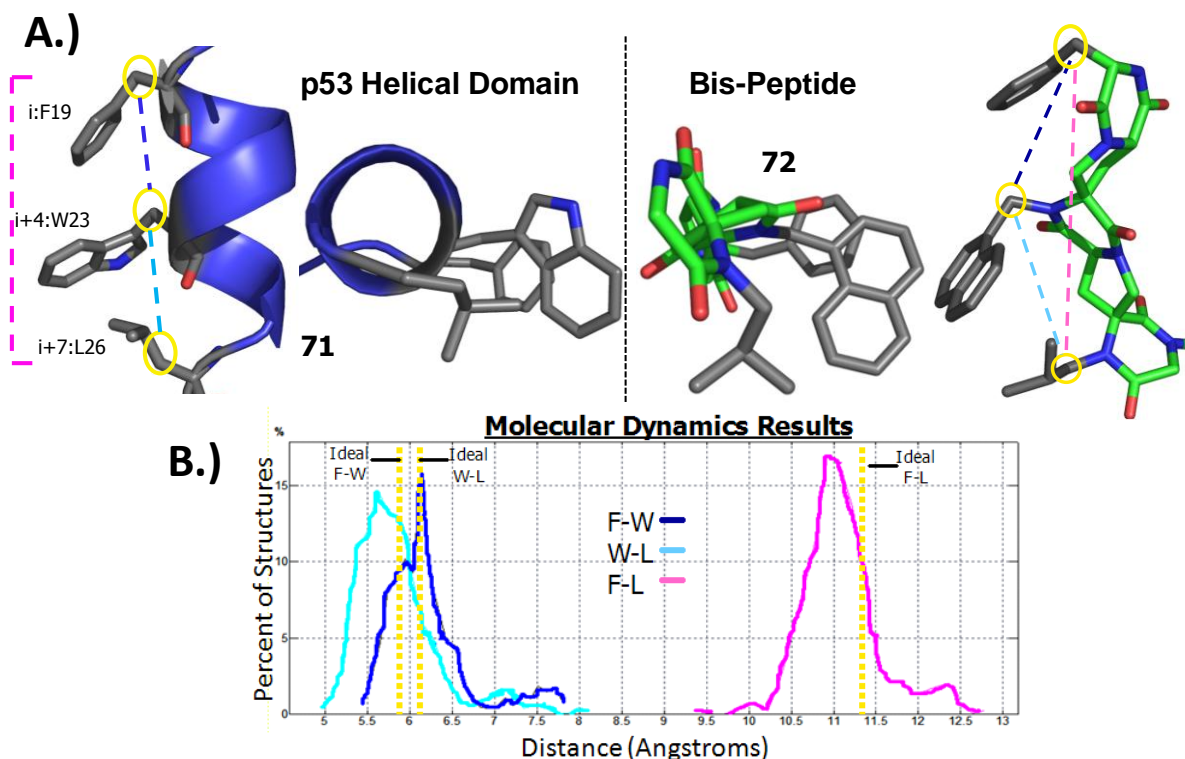


Figure 4.3. **A.)** Comparison of the structures of the p53 transactivation domain **71** (from PDB code: 1YCR⁶), including the geometrical distances measured for comparison to a bis-peptide **72** designed to mimic that display. **B.)** Results of a 100-psec molecular dynamics simulation (Amber 94, implemented in MOE⁵¹), showing the comparison between the color-coded distances shown in Part **A** and those measured during the molecular dynamics run.

This highlights one of the most beneficial properties of *bis*-peptide oligomers: they are highly amenable to computational design because the polycyclic nature of the scaffold severely restricts the conformational freedom of the oligomer. A multitude of structural data has been amassed with the unfunctionalized scaffolds showing that *bis*-peptides are both shape-persistent and shape-programmable structures.² To a first approximation, molecular mechanics (specifically the Amber series of potentials, which have been parameterized for oligopeptides and proteins⁵²) has proven to be a viable level of theory to investigate *bis*-peptides. This allows rapid geometry optimizations and structural searching with only a desktop computer, and the initial molecular designs for the *bis*-peptide α -helix mimics employed this level of computational theory.

Shown in Figure 4.3.A is the p53 helical transactivation domain, compound **71**, with the three binding side chains displayed, that of Phe19, Trp23 and Leu26. As can be seen, the groups are projected towards one helical face as each residue lies one adjacent turn away. The other model shown is that of a *bis*-peptide with all *pro4*(2S,4S) monomers, compound **72**, which displays the same groups (with a naphthyl group as an isostere of the indole ring). The two views of the structures show that the side chains are oriented in very similar fashions toward a particular face. A 100 picosecond molecular dynamics simulation employing the Amber94 force field (using the computational suite MOE⁵¹) was also performed to examine the behavior of the scaffold. One geometric measure that could show if the *bis*-peptide holds the side chains in the appropriate orientation would be the distance measured between the β -carbons of the α -helix side chains. The distances on the native peptide as well as the *bis*-peptide structure are highlighted in Figure 4.3.A and are indicated by the color coded dashed lines. As measured in the crystal structure in helix **71**, the F19-W23 distance is 5.9 angstroms, the W23-L26 distance is 6.1 angstroms and the F19-L26 distance is 11.4 angstroms. Throughout the molecular dynamics simulation, snapshots of the structure were taken and analyzed for these geometric distances. For each scaffold distance, a distribution is found that does contain the ideal crystal structure distance and so the *bis*-peptide appears to be able to approximate the helical presentation well and the data is shown in Figure 4.3.B. As shown in Figure 4.3.B, the distances measured from the crystal structure for the three functional groups (yellow dashed lines) are preserved during the course of the dynamics simulation (the distances found from the simulation are the cyan, blue and magenta curves). However, computational modeling (especially with a molecular mechanics potential such as Amber94⁵²) is only an approximation which can serve as a guide as to which molecules to pursue. In this project, it provides evidence that the initially

selected bis-peptide oligomer **72** (a homochiral *pro4*(2*S*,4*S*) scaffold) may present the side chains appropriately to serve as an α -helix mimic.

Solid-phase synthesis of the bis-peptide helix mimics. The previous chapter detailed the solution phase assembly of functionalized bis-peptides with the novel amino acid activation strategy. To facilitate the rapid synthesis and assay of the helix mimics this chemistry was transferred to solid phase while retaining the same basic principles of acyl-transfer coupling. A complete discussion of the solid-phase chemistry is beyond the scope of this chapter and is thoroughly detailed in Chapter 5.

Figure 4.4 shows the target *bis*-peptide **73** that modeling suggested was a good candidate for a p53 helix mimic. It consists of one unfunctionalized *pro4* monomer **75** to link it to the HMBA resin through an ester bond, then two functionalized *pro4* monomers **76** and **77** provide the isobutyl and the naphthyl group and finally an amino acid **78** brings in the benzyl side chain of phenylalanine. The final amino acid, here lysine derivative **74**, allowed cyclorelease of the material from the resin and served as a synthetic handle to attach a fluorophore for the fluorescence polarization described below.

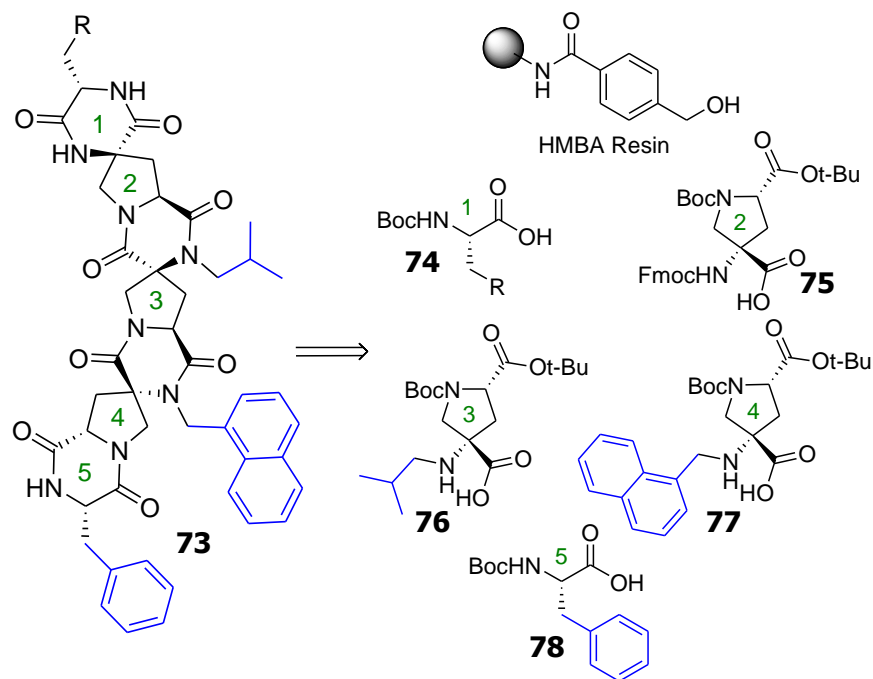


Figure 4.4. The structure of the first α -helix mimicking bis-peptide and the monomers required to construct it on solid-phase using the HMBA resin.

The solid-phase synthesis of the *bis*-peptide helix mimics followed the general procedure for the solid-phase synthesis using the HMBA linker which is presented in detail in Chapter 5. A representative synthesis is outlined here and all of the *bis*-peptide helix mimics follow a similar

protocol. Briefly, the hydroxymethylbenzamide (HMBA) resin was coupled with the Fmoc-protected *pro4* derivative **75** using the standard esterification coupling of MSNT/Melm⁶³ followed by removal of the Boc and *t*-butyl protecting groups with TFA treatment. The subsequent *pro4* monomers **40** and **79** were activated via DIC/HOAT method developed to couple the functionalized *bis*-amino acids outline in Chapter 3. For those that were coupled with a Boc protecting group on the pyrrolidine nitrogen, this protecting group was removed with TFA treatment. For the functionalized *pro4* monomers which used with the Cbz group instead this was removed using 33% HBr/AcOH in DCM on the resin which also removed the *tert*-butyl ester protecting group. (See Chapter 5 for a discussion of the protecting group manipulations of the monomer.) A Boc-protected amino acid, homophenylalanine **80** in Figure 4.5, was then coupled to cap the oligomer and bring in the final functional group as an amino acid side chain to produce resin-bound oligomer **81**. The Fmoc group on the first *pro4* monomer was then removed using 20% piperidine in DMF and the final residue, an orthogonal lysine derivative **82**, was coupled to the first *pro4* monomer. The ϵ -amine was exposed via treatment with piperidine and the resin was reacted with fluorescein isothiocyanate overnight to give the fluoresceinated oligomer **83**. The final Boc group was removed and the material subjected to basic conditions to initiate cyclorelease of the fully rigidified oligomer **84**. Typically overnight cleavage was performed although 4-5 hours at room temperature was found to be sufficient for most oligomers. A representative chromatogram of the crude cleavage is shown in Figure 4.5 and shows excellent purity of compound **84** with the exception of a small amount of HOAT that elutes at 6 minutes. The *bis*-peptide helix mimic elutes at about 21.5 minutes and the mass spectrum of this peak is consistent with oligomer and gave the distinctive isotopic pattern of a molecule that has two chlorine atoms (see inset of Figure 4.5). The *bis*-peptide was then purified via preparative HPLC and lyophilized. Prior to a binding assay, the lyophilized *bis*-peptide was resuspended in aqueous buffer (0.1M PBS, pH=7.2) and the concentration was measured using the UV absorbance at 493nm using an extinction coefficient of 83,000.⁶⁴

This modular synthesis is highly amenable to incorporating a variety of functional groups at the designated positions merely by substituting other building blocks in the solid phase construction of the oligomer. This included the use of both *pro4* monomers bearing different functional groups as well as other stereochemistries to allow the examination of both the identity and spatial presentation of the side chains. All of the oligomers in this chapter were synthesized in an analogous fashion using the scheme presented in Figure 4.5 on the HMBA resin. The *bis*-peptides synthesized for the competition experiments (compounds **103** and **104**) did not have a fluorophore and so a glutamic acid was used at this position. This was accomplished by

substitution of a glutamic acid derivative for lysine derivative **82**, followed by deprotection of the amino acid and cyclorelease of the material.

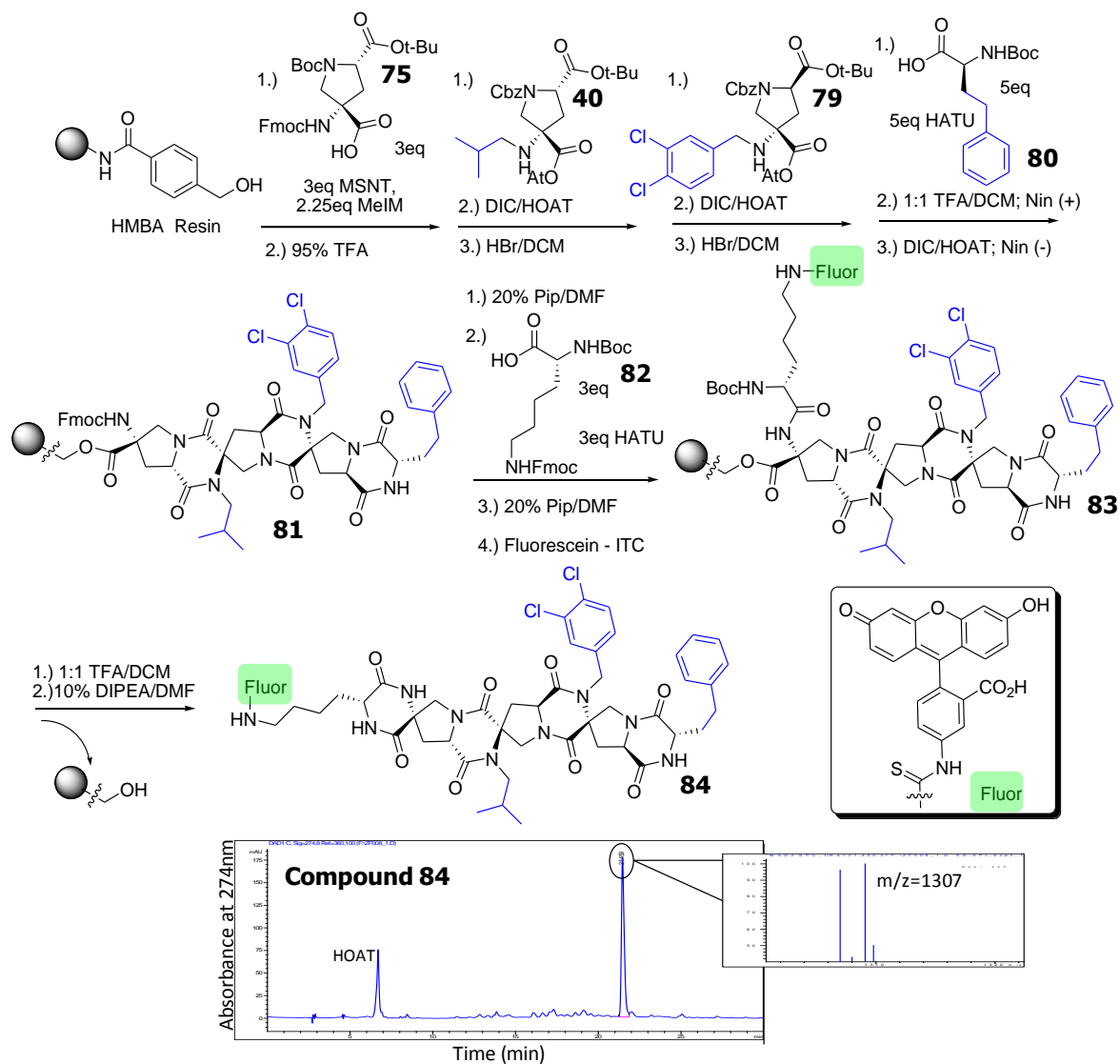


Figure 4.5. Solid phase synthesis of the complete *bis*-peptide helix mimic **84**. Also shown is the LC-MS trace (5-95% H_2O/ACN over 30 minutes) with the mass spectrum as an inset. Exact mass of **Compound 84** + H^+ = 1307.4, Found: 1307.1. The peak at 6 minutes has a retention time and UV profile consistent with HOAT and is marked on the chromatogram.

The installation of an additional functional group on the amine of the homophenylalanine was also accomplished on the solid-phase intermediate to explore the effect of binding affinity as a function of substitution at this position (See Table 4.3, compounds **100-102**). After acylation with the Boc-protected homophenylalanine residue, the Boc group was removed with TFA. At this stage, the amine was subjected to reductive alkylation conditions, with 5 equivalents of

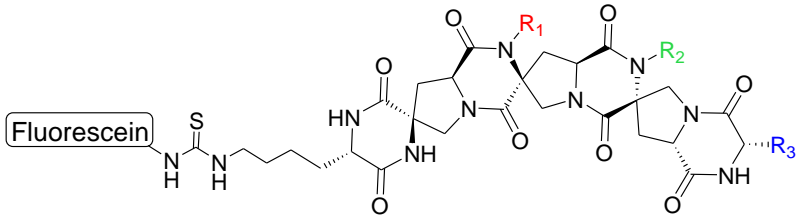
aldehyde, 5 equivalents of sodium cyanoborohydride in 1:1 MeOH/DMF mixture overnight.⁴⁷ Diketopiperazine closure then proceeded normally and the rest of the synthesis was identical to the previous synthetic scheme (Figure 4.5) to complete the respective oligomer.

The assay which was chosen to characterize binding of the *bis*-peptide to the target hDM2 protein is a fluorescence polarization assay.^{7,65} This direct binding experiment relies on the principle that a fluorescent tracer covalently attached to a ligand (small molecule or peptide) freely tumbles in solution at a certain rate. Excitation of the fluorophore with plane polarized light means that after a certain time period the fluorescent light that is emitted will exhibit low polarization (the molecule will tumble rapidly and the subsequent emission will be from a randomized orientation). However, if the ligand binds to a much larger molecular entity, for example a protein, the rate of molecular tumbling will decrease and incident plane polarized excitatory light will exhibit high polarization. This extremely sensitive assay is a standard high throughput assay used by the pharmaceutical industry because it is amenable to large scale screening and can provide information about the compound directly binding to the biomolecule of interest.⁶⁶ It also consumes a small amount of ligand although does require expressed and purified protein to bind to (sometimes large amounts, depending upon the dissociation constants that are measured). The assay can be conducted in a 96-well (or more) plate format, and consists of small concentrations of fluorescent tracer (here 10nM *bis*-peptide) and then increasing amounts of purified hDM2 protein (typical ranges from ~1nM up to 50 μ M). The plot of the logarithm of protein concentration versus the measured polarization will give the characteristic sigmoidal curve of a binding isotherm (see Figure 4.11). Commercially available software was then used to extract a dissociation constant from the dataset.⁷⁵ In this assay format, the native peptide (^Fp53) had a K_d of 615nM, in close agreement with published values.⁶⁷ This positive control shows that the assay is functioning properly, with the protein being functional as well as the binding assay working correctly.

The initial screen of *bis*-peptides attempted to find the appropriate functional groups to mimic the side chains of leucine, tryptophan and phenylalanine of the p53 helix. This first series of scaffolds was the initially the all (S,S) diastereomeric scaffold, the stereochemistry which was computationally modeled in oligomer 72. To our delight, the first *bis*-peptide synthesized, compound in Table 4.1, with the isobutyl, 2-naphthyl and a benzyl group bound with the modest yet measurable K_d of 46 μ M. This was extremely encouraging given that a low micromolar binding affinity is considered to be a lead compound. In other words, having a measurable K_d allows the chemist to make discreet changes to the molecule and ascertain the effects of binding, either positive or negative. This first result validated our hypothesis of rational design of

these oligomers since only a molecular mechanics potential was used and the oligomer had a measurable binding constant. This initial result also allowed us to hypothesize the *bis*-peptide backbone does not interfere with the binding: the scaffold could have directly interfered with the protein though a steric or electrostatic clash abolishing the binding interaction, but this seemed not to be the case.

Additional molecules were then synthesized with different functional groups (still all with the same homochiral, all *S*, stereochemistry) and assayed to find the best side chains for the hDM2 cleft. This again highlights the versatility of the *bis*-peptide approach, with many different functional groups being able to be incorporated into the scaffold because they are simply brought in as aldehydes in the last step of the synthesis. The naphthyl regioisomer compound **85** improved the binding almost 3-fold, but then incorporation of an additional methylene group by using the homologs of the functional groups (compounds **87** and **88**) proved to diminish the binding to barely being measurable. The use of the chloro-indole moiety in derivative **89** slightly improved the binding, although it was clear that other functional groups needed to be explored. Schepartz and co-workers found that the β -peptide scaffolds that utilized a dichlorobenzyl group in this position significantly improved the binding of their system and so the same was attempted here.⁶⁸ Compounds **90-93** all employ the dichlorobenzyl group as the aromatic side

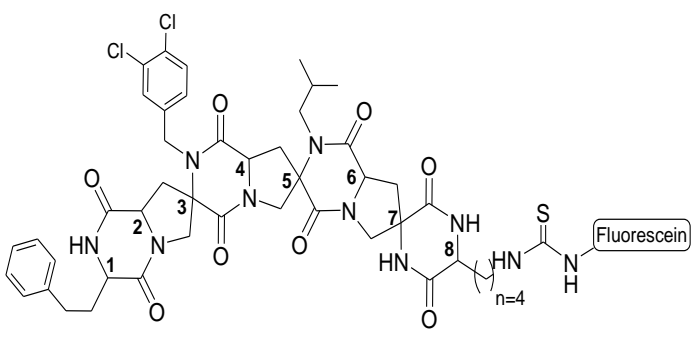


Compound	R ₁	R ₂	R ₃	K _d (μM)	Compound	R ₁	R ₂	R ₃	K _d (μM)
85				46.0	90				6.3
86				16.0	91				21.2
87				>50	92				6.5
88				>50	93				5.9
89				14.3					

Table 4.1. Structures and dissociation constants (given in μM) of the functional group scan of the *bis*-peptide oligomers.

chain and show improved binding as compared to any other aromatic functional group used. Through the course of optimizing the binding of the functional groups, an 8-fold improvement in binding was achieved (from a 46 μ M lead compound to a 5.9 μ M oligomer with the dichlorobenzyl group). Although encouraging, tighter binding scaffolds still needed to be discovered to facilitate biological experimentation.

With tighter binding side chains now identified, optimization of the scaffold's stereochemistry was then initiated. This highlights a completely novel attribute of the *bis*-peptide peptidomimetics: by changing the stereogenic centers of the oligomer the presentation of the functional group can be altered and tuned. The computer package CANDO² was used to iterate through possible combinations of building blocks and each of their associated conformers. Hits were defined as *bis*-peptides which could position the functional groups similarly to the p53 crystal structure. Shown in Table 4.2 is the stereochemistry and resulting K_d 's of a six of the 256 total possible diastereomers chosen from the CANDO search. Compounds **94** to **84** (as shown in Table 4.2) showed almost a 60-fold decrease in K_d from, an exceptional increase in binding affinity from only small differences in functional group presentation. Especially noteworthy are examples such as the comparison of compounds **98** and **84** which are epimers, and that the configuration of a single stereocenter can make a four-fold change in binding. Comparison of another epimeric pair, compounds **96** and **97**, shows essentially no change in binding. This highlights how these subtle functional group presentations can be very sensitive. Shown in



Compound	Stereocenter								K_d (μ M)
	1	2	3	4	5	6	7	8	
94	R	S	R	S	S	S	S	S	22.3
95	S	R	S	S	S	S	S	S	6.7
96	R	R	R	S	S	S	S	R	4.8
97	R	S	R	S	S	S	S	R	4.6
98	S	S	S	S	S	S	S	R	1.6
84	S	R	S	S	S	S	S	R	0.4

Table 4.2. Structural key to the stereochemical designation and the table of K_d values (shown in μ M) for the diastereomeric series of *bis*-peptides.

Figure 4.7 is the overlay of compound **97-84** (colored by elements) and the p53 α -helix (colored blue for clarity). The three scaffolds present the binding side chains in roughly the same fashion, with only subtle differences. These examples illustrate how subtle structural changes which can

be achieved with *bis*-peptide technology can have significant contributions on the measured binding affinity.

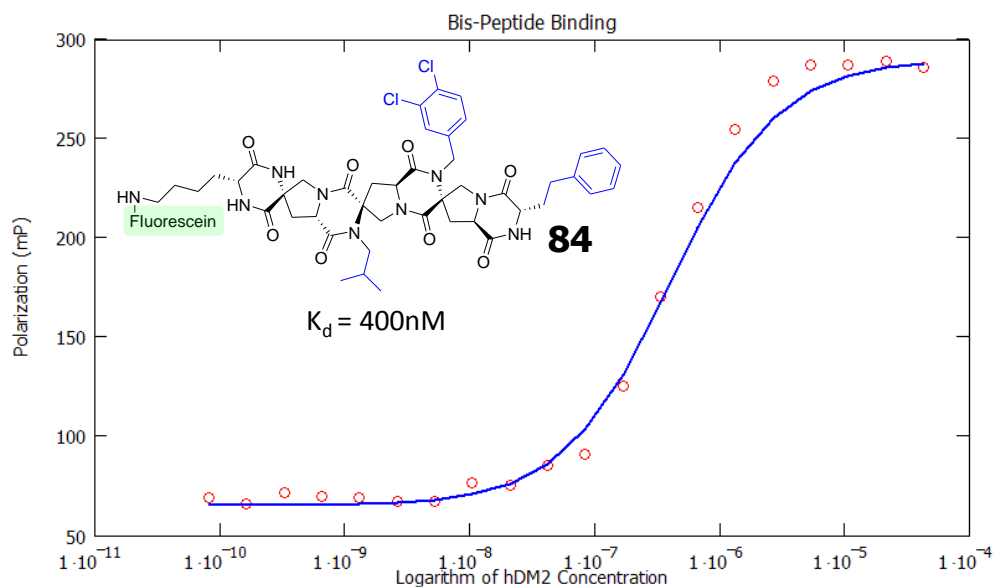


Figure 4.6. Plot of the polarization (in mP units) of compound **84** versus the logarithm of protein concentration. The measured polarization values are depicted as red circles with an ideal binding curve in blue.

Diastereomer **84** in Table 4.2 exhibits the highest binding affinity of a *bis*-peptide to the hDM2 system to date, with a K_d of 400nM. The direct binding data for this potent inhibitor is shown in Figure 4.6 along with the structure of bis-peptide **84**. This ~115-fold improvement in

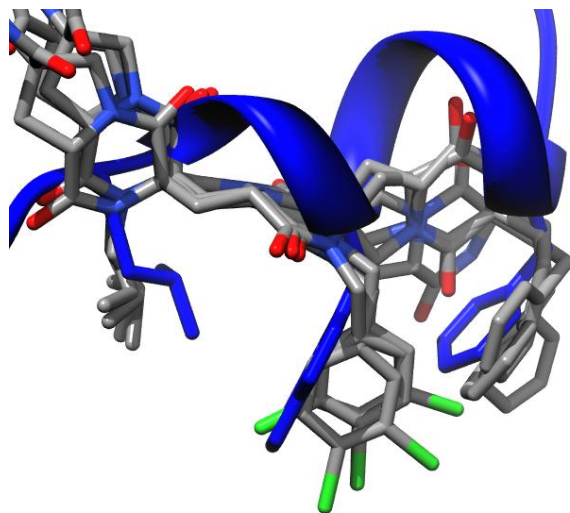


Figure 4.7. Overlay of p53 peptide (colored blue) and 3 *bis*-peptide scaffolds, compounds **97**, **98** and **84** from Table 4.2. Hydrogens were omitted for clarity. Image created with Chimera.⁶⁹

binding from the original oligomer within the span of about 20 molecules is very encouraging, validating our hypothesis of rational design coupled with the rapid synthesis and assay of the oligomers.

It was hypothesized that an additional functional group at the terminus of the oligomer might be able to contribute to the binding of the oligomer via additional hydrophobic interactions with the hDM2 protein. This approach highlights another benefit of the *bis*-peptide methodology: the oligomers can be extended and further functional groups may be appended in an attempt to further interact with a protein target. The first oligomer that was synthesized to explore this effect was a derivative of compound **98**, Table **4.2** which substituted a benzyl group at this position (compound **100**, Table **4.3**). This produced an almost two-fold improvement versus the secondary amide at this position and so provided evidence that perhaps other groups could also enhance binding. Next, the tightest binding *bis*-peptide identified, oligomer **84**, Table **4.2** ($K_d = 400\text{nM}$), was chosen to see if the affinity could be improved. One aromatic (a methoxybenzyl derivative, compound **102**, Table **4.3**) as well as one aliphatic (an isobutyl derivative, compound **101**, Table **4.3**) were synthesized and assayed for their respective contributions. However, both compounds slightly diminished binding towards hDM2 with this diastereomer. Although somewhat disappointing, derivations such as these in conjunction with the diastereomeric series could provide valuable insight if they were able to be coupled with structural data, such as an X-ray crystal structure. Efforts are currently underway in the Schafmeister group to acquire a diffraction quality co-crystal of a *bis*-peptide with hDM2. If successful, this data set and others will be invaluable towards further rational design of an even more potent inhibitor of the system.

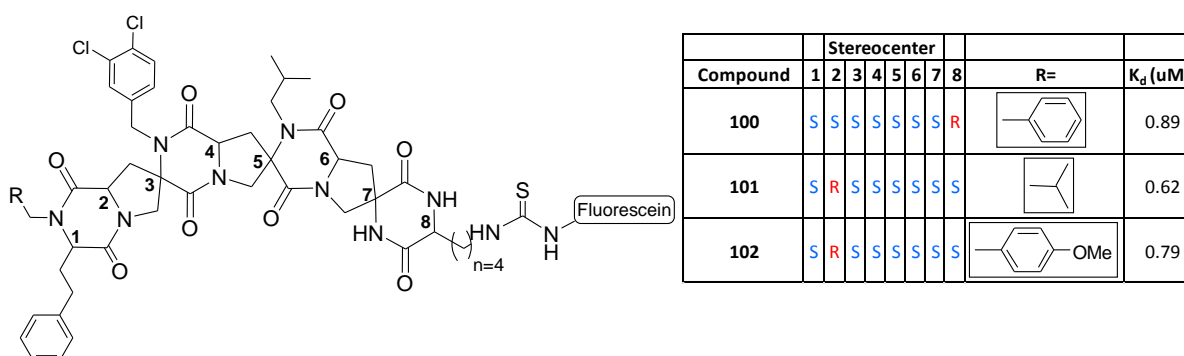


Table **4.3**. Structures and dissociation constants (K_d 's are given in μM) of *bis*-peptides that have an additional functional group on the homophenylalanine residue.

To confirm that the *bis*-peptide was binding to the hydrophobic cleft of hDM2 where the native p53 α -helix would bind, a competition experiment was undertaken.⁶⁶ This is necessary because the readout from a direct binding fluorescence polarization assay is only the dissociation constant of the macromolecular complex, not what site the ligand might be binding to. If the ligand were complexing to a completely separate part of the protein this would be less interesting since our rational design approach would have failed. To rule out this possibility, a fluorescently labeled native p53 peptide is used and a helix mimic *bis*-peptide (without the fluorescent label, also known as a “cold” ligand, one that does not have a fluorescent label) is titrated in. As shown in Figure 4.8, prior to the addition the fluorescently labeled native peptide occupies the binding site and gives a high fluorescence polarization signal because the macromolecular complex tumbles slowly in solution. As a competitive, non-fluorescent binder (here the *bis*-peptide) is titrated in it displaces the peptide and the resulting fluorescence polarization signal exhibits lower polarization since the p53 peptide now tumbles more freely in solution. This provides evidence that the *bis*-peptide occupies the same binding pocket of the peptide. A derivative of compound **85**, Table 4.1 was synthesized that had a (L)-glutamic acid in

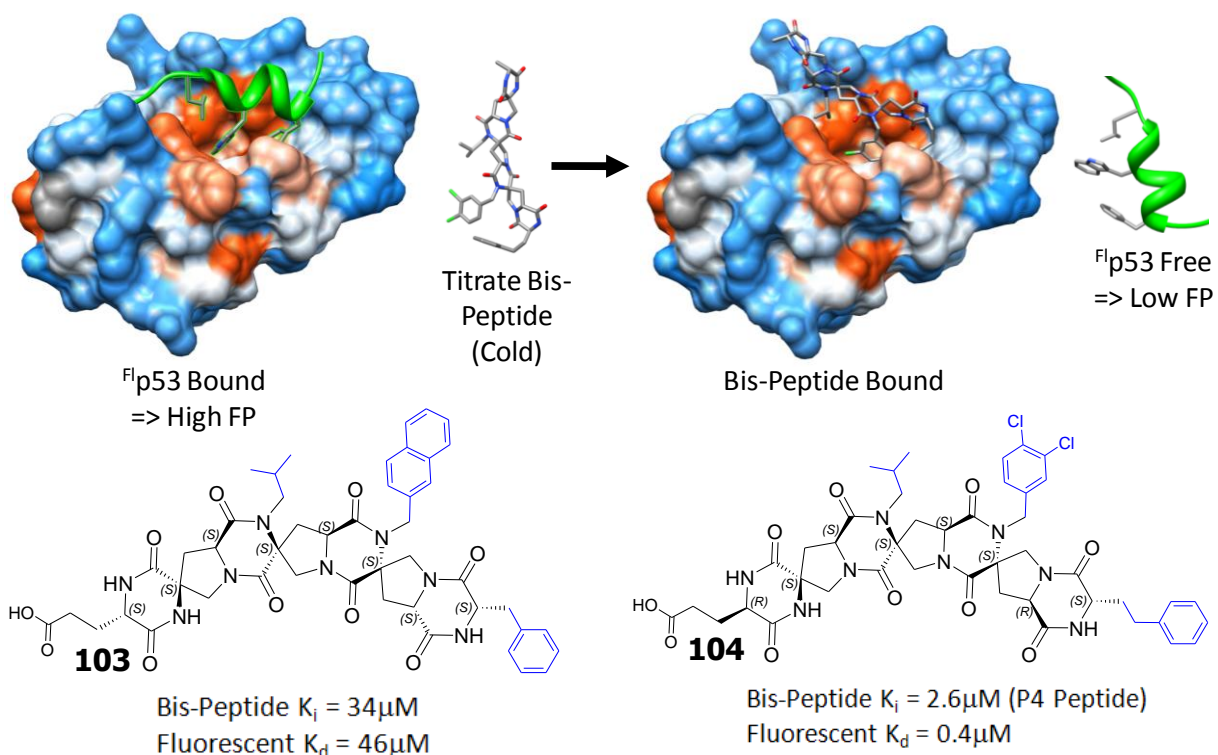


Figure 4.8. Schematic of a competition experiment and the structures and inhibition constants of the *bis*-peptides (**103** and **104**) designed for the competition experiments.

place of the (L)-lysine that had the fluorescently-labeled side chain to give competition oligomer **103**. Titrating increasing amounts of oligomer **103** in the presence of 2 μ M hDM2 and 10nM fluorescently F p53 gave a sigmoidal curve with decreasing fluorescence polarization as more *bis*-peptide was added that had a calculated inhibition constant of 34 μ M. Therefore, a fluorescently labeled p53 peptide was competed off the protein by increasing amounts of the *bis*-peptide.

To confirm these results, another peptide which bound to hDM2 with a published low nanomolar affinity was synthesized and used as an additional positive control in the binding assays. This peptide, called the F p4 peptide, gave a K_d of 4.0nM under the same assay conditions and corresponds well to a literature value of 5.4nM.⁷⁰ This peptide was used in an additional competition experiment with compound, a derivative of the tightest binding scaffold, diastereomer **84** in Table **4.2**. Again the fluorescently labeled (D)-lysine was replaced with a (D)-glutamic acid residue to give oligomer **104** and subjected to conditions similar to the other competition experiment. Here the *bis*-peptide gave an apparent K_i of 2.6 μ M. These independent results suggest that the *bis*-peptides were binding exactly as they were designed to, within the p53 cleft of the hDM2 protein since it is competing for the F p53 binding site.

Another important concern when validating a potential protein antagonist is that of selectivity: compounds must show affinity for the target protein as well as a substantially reduced affinity for any other proteins.⁶⁴ If there was significant binding to other proteins, undesired biological responses could be elicited along with the desired response. This is an unacceptable side reaction and so must be addressed.

hDMX is a closely related homolog of hDM2, and even though it binds p53, hDMX is unable to induce p53 degradation.⁷⁰ It is known that the p53 binding cleft is similar to that of hDM2, although a few structural changes are present and so there is a difference in binding affinity. This provides an opportunity of testing how selective a compound is versus other similar proteins. There is only one example of a lead compound which has been generated to have hDMX potency (disruption of the p53/hDMX interaction with an EC_{50} =2.3 μ M) and its potency for hDM2 is less.⁷¹ However, all other examples of small molecules which bind hDM2 have significantly weaker binding than for hDMX.⁷²

For the purposes of this *bis*-peptide project, the hDM2/hDMX systems present an opportunity to establish if the oligomers are selective for two structurally similar proteins. Two compounds with high affinity for hDM2 were selected to assess their affinities for hDMX. Compound **97**, Table **4.2**, had a 4.6 μ M K_d for hDM2, while for hDMX it only had a K_d of 24 μ M, an almost 6-fold difference. An even greater contrast was seen with compound **84**, Table **4.2**;

with hDM2 there was a measured K_d of $0.4\mu\text{M}$, whereas with hDMX a K_d of $19.2\mu\text{M}$ was found. This was a 48-fold difference, a substantial divergence in the affinity of this relatively strong binder to the homolog of hDM2. These results establish that the *bis*-peptides selected have a more modest affinity to the hDMX system, and so can be selective for structurally similar proteins.

The *bis*-peptide α -helix mimics have been shown to be potent and selective for the hDM2 protein. However, this does not necessarily mean that the oligomer would be a viable therapeutic since the compound must still show activity within the cell, and this has its own associated challenges. As referenced in the introduction to this chapter, cellular penetration can be very problematic to address. Larger, more polar macromolecules such as peptides are usually not cell-permeable and so this can be a serious limitation to their use as therapeutics.⁷ In a standard cell-permeability assay, Verdine and coworkers found that a derivative of the native peptide, $^{\text{Fl}}$ p53, was not cell-permeable.⁶⁷ However, by manipulating the charge on a

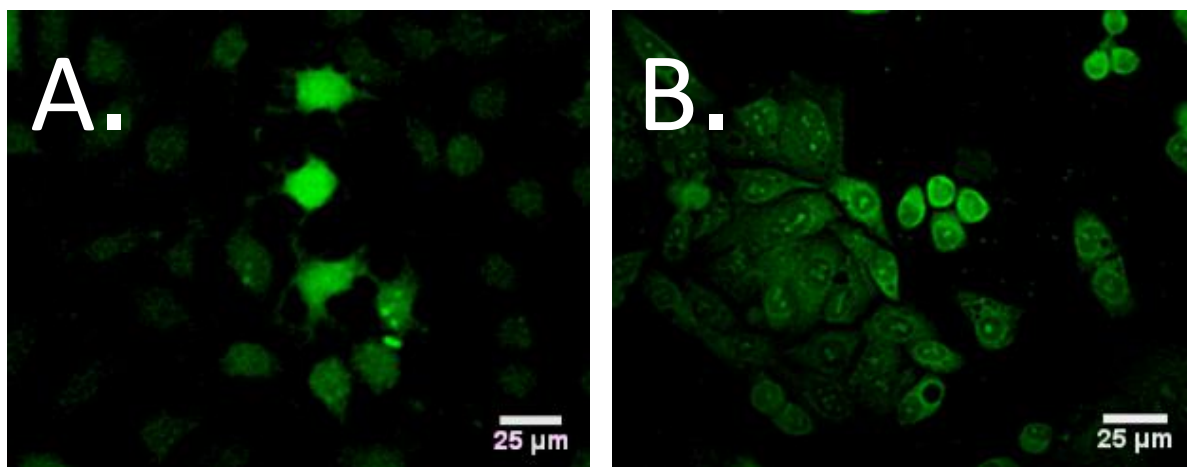


Figure 4.9. A.) Fluorescence microscope images of bis-peptide **85** treatment with A.) Huh7 cells ($2\mu\text{M}$ bis-peptide) and B.) HepG2 cells ($2\mu\text{M}$ *bis*-peptide). These images show internalization of the bis-peptide after 5 hours of treatment. (Uptake was seen in both cell lines after only one hour of treatment.⁷⁴)

stapled peptide derivative from anionic to cationic they were able to show some measure of cellular penetration.

Initial experiments used two different human cell lines to assess whether the *bis*-peptides would prove to be cell-permeable and target the protein of interest. The first cell line, HepG2, expresses wild-type p53 while the second cell line, Huh7, expresses mutant p53.⁷³ Preliminary experiments were undertaken to see if a representative bis-peptide would be cell-permeable. The two cell lines (HepG2 and Huh7) were treated with $2\mu\text{M}$ of bis-peptide **85**,

which bound hMDM2 with a $K_d=46\mu\text{M}$. After five hours of incubation, the cells were analyzed with fluorescence microscopy to determine if any bis-peptide had been internalized within the cell. Because a fluorescein molecule was covalently attached to the *bis*-peptide, it could easily be visualized within the cell. Shown in Figure 4.9 are fluorescent microscopy images of fixed Huh7 cells (Figure 4.9.A, bis-peptide 85 concentration was $2\mu\text{M}$) and fixed HepG2 cells (Figure 4.9.B, bis-peptide 85 concentration was $0.5\mu\text{M}$). The uptake of the *bis*-peptide is apparent, with many cells within the image view fluorescently glowing with the distinctive color of fluorescein. (A fluorescein control failed to produce any fluorescence in either cell line which demonstrates that the bis-peptide must be the cell penetrating element.) Confocal images (see Experimental Details, Figure 4.17) show that the bis-peptide 85 is internalized in the cell, not just contained within the lipid bilayer. Also evident from the fluorescent microscopy images is that the bis-peptide is distributed throughout the cytoplasm and was even found in the nucleus. These results showed that the bis-peptide 85 was taken up by the cell and was dispersed throughout the cell. This was very encouraging since the oligomer is rather large (MW=1274 Daltons) and so we were unsure if the oligomer would even cross the cell membrane.⁴

With the knowledge that *bis*-peptide 85 was cell permeable, we set about to determine if

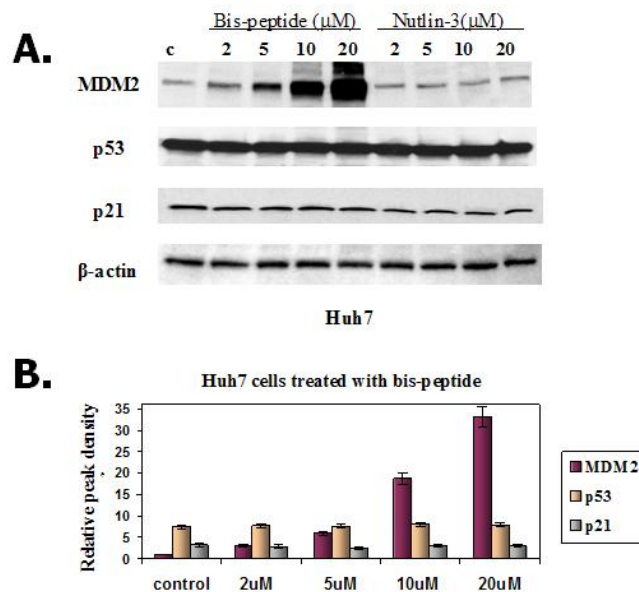


Figure 4.10. A.) Western blot analysis of Huh7 treated with 2, 5, 10 and $20\mu\text{M}$ *bis*-peptide 84 and 2, 5, 10 and $20\mu\text{M}$ Nutlin-3. B.) Histogram of the band intensities from the Western blot analysis shown in Part 4.10.A of the *bis*-peptide 84 treated Huh7 cells.

bis-peptide helix mimic **84** ($K_d=400\text{nM}$) could elicit a biological response *in vivo* with the protein target of interest (p53/hDM2). Again, both cell lines (Huh7 and HepG2) were treated with 2, 5, 10 and $20\mu\text{M}$ *bis*-peptide for 24 hours, after which time the cells were lysed and the protein was harvested and subjected to Western blot analysis to quantify the amounts of the key proteins hDM2 and p53. In addition to the target protein system p53/hDM2, p21 levels were also measured because p21 expression levels are regulated by p53 and so provide a downstream readout of p53 activity.⁶² We also used a positive control which is a potent small-molecule inhibitor of the p53/hDM2 interaction, Nutlin-3, which has been used by others as a tool to investigate the p53/hDM2 interaction since it is a low nanomolar inhibitor.⁷³ Here Nutlin-3 would bind to hDM2 and prevent p53 from binding and being degraded and so act as a p53 activator.

Shown in Figure **4.10** are the results of the Western blot analysis of Huh7 cells (human liver cancer cells with mutant p53) treated with increasing concentrations of *bis*-peptide **84**. As apparent from the histogram in **4.10.B**, the hDM2 protein levels are increased by approximately 33-fold, a very large increase in terms of protein levels. Since this cell line has mutant p53, the increasing levels of hDM2 do not affect the subsequent p53 or p21 levels. In accordance with this idea, neither the levels of p53 nor p21 change by a significant amount (see histograms of Figure **4.10.B**).

To see such a massive increase in hDM2 levels (~33-fold) within the Huh7 cells, there are only two possibilities. Either the protein is being stabilized as hypothesized above, or the transcription of hDM2 is being initiated by *bis*-peptide **84** in a dose-dependent manner and so more protein is being manufactured by the Huh7 cell. To test the transcription activation hypothesis, PCR analysis was used to monitor the RNA levels of the hDM2 during real-time and end-point analysis. Both of these RNA quantification techniques showed no effect on the RNA as *bis*-peptide levels increase. This suggests that the *bis*-peptide is not initiating transcription of hDM2 but stabilizing the protein towards degradation.

In contrast to the Huh7 cell line, HepG2 cells have wild-type p53 and so have an intact p53/hDM2 signaling pathway. Here the negative regulatory feedback loop of p53/hDM2 will mean that p53 levels are kept relatively constant during homeostasis because hDM2 continually targets p53 for proteasomal degradation via ubiquitination.⁵⁶ hDM2 is also a gene whose transcription is activated by p53, so suppression of p53 would result in low levels of hDM2 in due to feedback. However, if a therapeutic agent was to bind to hDM2 and stabilize this protein, hDM2 would continue to be able to degrade p53 with these heightened levels of hDM2 available. The native regulatory feedback loop would then be perturbed, with a competition between p53 degradation and stabilization. In the presence of the *bis*-peptide, the stabilization

of hDM2 and thus p53 suppression is the dominant pathway for the system. This would have the effect of suppressing the apoptotic signaling and protecting the cell from induced p53-dependent cell death. This is in contrast with a hDM2 binder, such as Nutlin-3, which should bind to hDM2 but only free p53 to induce apoptosis.

Examination of the Western blot analysis of Figure 4.11 for HepG2 cells (human liver cancer cells with wild-type p53) shows data that is consistent with the hDM2 stabilization hypothesis. First, the hDM2 levels remain low through the dosing regime, which could be consistent with the p53 suppression as outlined above. Even more convincing though is the

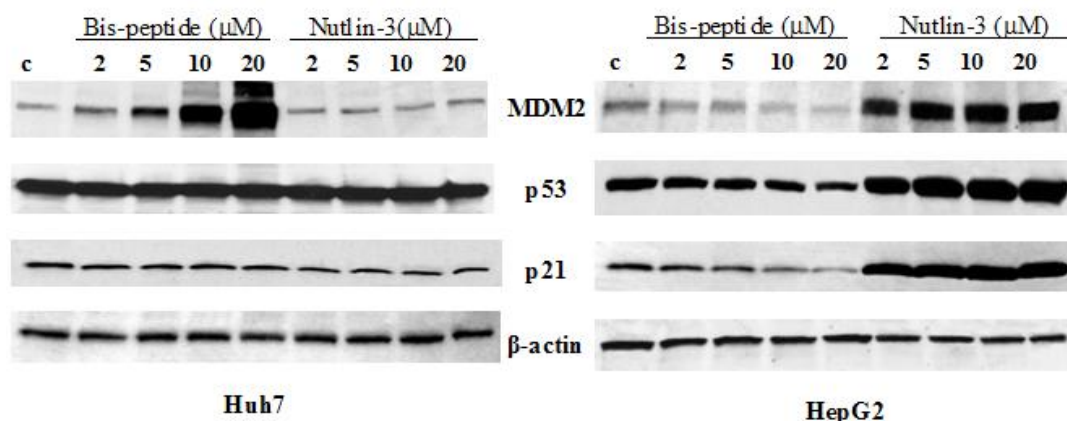


Figure 4.11. Western blot analysis of Huh7 cells as compared to HepG2 cells in a dose-dependent manner for both *bis*-peptide 84 and Nutlin-3.

decrease in both p53 and p21 levels in a dose-dependent manner with higher concentrations of *bis*-peptide 84. This data could be explained by the p53 suppression via hDM2 stabilization mechanism. This is in contrast to the findings for Nutlin-3, the low nanomolar-binder of hDM2 which increases the p53 levels in HepG2 cells as can be seen in the Western blot on the right of Figure 4.11. Since Nutlin-3 does not stabilize hDM2, p53 levels are increased.

4.3 Conclusion

This chapter detailed the first application of functionalized *bis*-peptides: creating α -helix mimics and disrupting the important protein-protein interaction of the p53/hDM2 system. Molecular modeling was performed and a scaffold was designed to mimic the presentation of three functional groups of the p53 helix; subsequent solid-phase synthesis of this compound showed it was a low micromolar binder. Optimization of both the functional groups and the

presentation of the group (by optimizing the stereochemistry of the scaffold) resulted in finding a potent inhibitor, oligomer **84**, ($K_d=400\text{nM}$) through fluorescence polarization assays. A competition experiment also helped to establish the *bis*-peptide was binding in the p53 cleft of hDM2, and an assay with hDMX showed *bis*-peptides to have moderate selectivity for a structurally similar protein.

Finally, *in vitro* studies showed cell-permeability of two *bis*-peptides, and one compound showed activity by stabilizing the hDM2 protein, a promising new therapeutic effect to may help to suppress p53-dependent apoptosis. Western blot analyses of hDM2, p53 and p21 as well as measurement of RNA levels are consistent with hDM2 stabilization and subsequent p53 suppression. Therefore, p53-dependent apoptosis may also be suppressed by this *bis*-peptide. This p53 suppression by hDM2 stabilization has tremendous therapeutic potential in chemotherapy and other forms of cancer treatment where p53-dependent apoptosis causes much of the secondary damage to healthy cells as a consequence of cancer treatment. Efforts to more fully elucidate the biochemical mechanism of *bis*-peptide **84** and the effects on the p53/hDM2 system are ongoing in our lab to realize the full potential of this discovery. This work has established functionalized *bis*-peptides as a new class of peptidomimetics and this research avenue will hopefully prove fruitful in the future to target other protein-protein interactions.

4.4 Experimental Details

General Procedure for the Preparation of Functionalized Building Blocks. The functionalized *pro4* derivatives were prepared from the corresponding *pro4* amino acids using the method of reductive alkylation as described in Chapter 3 and their syntheses and characterization are presented there except as noted below. The building blocks were reverse-phase purified and the desired fractions pooled and lyophilized and used in the activation procedure as described below.

***Pro4(2R,4S)*-Dichlorobenzyl (Compound **sc1**).** The reaction was performed via the general procedure of the reductive alkylation with *pro4(2S,4S)* amino acid, compound, (450mg, 1.36mmole) and dichlorobenzaldehyde (237mg, 1.36mmole) and the reaction allowed to proceed overnight. The product was obtained as a white solid (500mg, yield 75%). LCMS analysis (5-95% H₂O/ACN with 0.1% formic acid): $t_r= 20.1\text{min}$; calced for compound **sc1**+H⁺:

489.1; found: 489.3; ^1H NMR (500 MHz, $\text{DMSO-}d_6$, 365K), δ = 7.58 (s, 1H), 7.50 (d, 1H, $J=8.3\text{Hz}$), 7.30 (d, 1H, $J=8.3\text{Hz}$), 4.16 (m, 1H), 3.85 (d, 1H, $J=10.9\text{Hz}$), 3.67 (dd, 2H, $J=17.3\text{Hz}$, 14.1Hz), 3.48 (m, 1H), 3.32 (d, 1H, $J=10.9\text{Hz}$), 2.67 (m, 1H), 2.01 (m, 1H), 1.41 (s, 9H), 1.39 (s, 9H). ^{13}C NMR (from HMBC, 500 MHz, $\text{DMSO-}d_6$, 365K), δ 173.5, 173.3, 170.0, 141.1, 129.9, 129.1, 128.5, 127.6, 127.4, 79.7, 78.4, 66.2, 58.3, 55.4, 53.7, 37.9, 27.4 (3C), 27.2 (3C).

General Procedure for Removal of Boc and *t*-Butyl Groups. The Boc and *t*-Butyl ester protecting groups were simultaneously cleaved from the resin bound oligomer by treatment with 95% trifluoroacetic acid (TFA) with 5% triisopropylsilane (TIS) used as a scavenger. The deprotection was allowed to proceed for one hour, washing the resin 5x with DCM, and then the deprotection was repeated for an hour. The resin was then washed 5x with DCM, 5x with DMF, and neutralized with 5% DIPEA in DMF.

General Procedure for Removal of Cbz and *t*-Butyl Groups. The Cbz and *t*-Butyl ester protecting groups were simultaneously cleaved from the resin bound oligomer by treatment with 1:1 33% HBr/AcOH in DCM. The deprotection was allowed to proceed for 30 minutes, washing the resin 5x with DCM, and then the deprotection was repeated for 30 minutes. The resin was then washed 5x with DCM, 5x with DMF, and neutralized with 5% DIPEA in DMF.

General Procedure for Bis-Amino Acid Activation and Coupling. The *bis*-amino acid to be activated (3eq relative to resin loading) was suspended in a 1:2 mixture of DMF:DCM (conc. of 50mM) followed by HOAT (6eq relative to amino acid). With stirring, the diisopropylcarbodiimide (DIC, 1eq relative to amino acid) was then added and the activation allowed to proceed for 1.5 hours at room temperature. The resin was then suspended in a minimal amount of DMF (~200 μL), and DIPEA (2eq relative to resin loading) was added. The preactivated amino-OAt ester was then added in a single portion and allowed to react for the specified amount of time. The resin was then washed 3x with DCM and then 3x with DMF. The resin was then treated with an additional aliquot of DIC (5eq relative to resin loading) and HOAT (5eq relative to resin loading) in a 1:2 DCM:DMF mixture and allowed to react for 1hour to convert any of the single amide product into the corresponding diketopiperazine.

General Procedure for Removal of Fmoc Group. Fmoc deprotection was conducted by treatment of the resin with 20% piperidine in DMF for 5minutes, washing the resin 5x with DMF, treatment with 20% piperidine in DMF for 15minutes, and finally washing the resin 5x with DMF.

Solid Phase Synthesis of *Bis*-Peptide Helix Mimics. The solid-phase synthesis of fluoresceinated *bis*-peptide **84** (compound, $K_d=400\text{nM}$) and the competition experiment *bis*-peptide (compound **104**, $K_i=2.6\mu\text{M}$, competing with the P4 peptide) are detailed below as representative examples. All other syntheses of *bis*-peptide helix mimics follow a similar format using the corresponding building blocks. The LC-MS characterization for all oligomers is shown in the Tables **4.4-4.6**. Recovered yields, after RP purification, were usually 20%-40%.

Solid Phase Synthesis of Oligomer 81. 75mg of HMBA-AM resin (1.1mmole/gm resin loading, 83 μmole) was charged to an 8mL solid phase reactor and agitated using a magnetic stir bar and thoroughly washed with DCM. The first *bis*-amino acid, compound **75**, (247 μmole , 137mg), MSNT (1-(2-Mesitylenesulfonyl)-3-nitro-1H-1,2,4-triazole⁶³, 247 μmole , 73mg) and *N*-methylimidazole (186 μmole , 15 μL) were dissolved in 1.2mL of DCM (anhydrous), added to the resin, and allowed to react for 2 hours. The *bis*-amino acid was then deprotected with 1.5mL of 95% TFA using the “General Procedure for Removal of Boc and *t*-Butyl Groups”. The first *bis*-amino acid, compound **40** (247 μmole , 104mg), was activated and coupled for 3 hours using the “General Procedure for *Bis*-Amino Acid Activation and Coupling” followed by deprotection using the “General Procedure for Removal of Cbz and *t*-Butyl Groups”. The next *bis*-amino acid, compound **79** (247 μmole , 129mg), was activated and coupled for 3 hours using the “General Procedure for *Bis*-Amino Acid Activation and Coupling” followed by deprotection using the “General Procedure for Removal of Cbz and *t*-Butyl Groups”. Boc-(L)-HomoPhe-OH, compound **80** (413 μmole , 115mg) and HATU (413 μmole , 157mg) were combined in DMF (2.1mL, conc. of 200mM); DIPEA (825 μmole , 144 μL) was added and the reaction mixture allowed to sit for 10 minutes. The preactivated species was then added to the resin and allowed to react for one hour, followed by thorough washing of the resin with 5x DMF, and then 5x with DCM. The Boc group was then removed with 1.5mL of 1:1 TFA in DCM for 20 minutes, followed by washing of the resin with 5x DCM and repeating the Boc deprotection treatment. The resin was then washed 5x with DCM, 5x with DMF, and neutralized with 5% DIPEA in DMF. A ninhydrin test was positive, which indicated the presence of a primary amine. The resin was then treated with an additional aliquot of DIC (5eq relative to resin loading) and HOAT (5eq relative to resin loading) in a 1:2 DCM:DMF mixture and allowed to react for 1hour. A subsequent ninhydrin test was negative, which indicated the diketopiperazine had been closed and the secondary amide

had been formed. The resin was then washed 5x with DCM and 5x with DMF. The Fmoc group was removed using the “General Procedure for Removal of Fmoc Group”.

Solid Phase Synthesis of Fluoresceinated Bis-Peptide (Compound **84, $K_d=400\text{nM}$).** Boc-(D)-Lys(Fmoc)-OH, compound **82** (413 μmole , 193mg) and HATU (413 μmole , 157mg) were

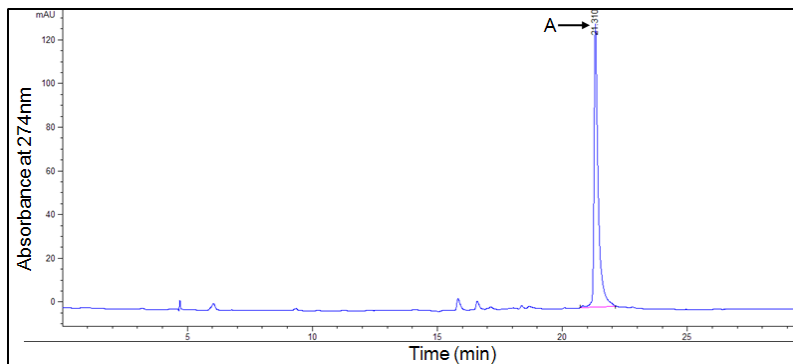


Figure 4.12. HPLC trace of purified bis-peptide **84**, monitoring at a wavelength of 274nm with a gradient of 5-95% ACN/H₂O with 0.1% formic acid over 30 minutes. The peak marked “A” has a m/z = 1307.2 (calcd for oligomer **84** + H⁺: 1307.4).

combined in DMF (2.1mL, conc. of 200mM); DIPEA (825 μmole , 144 μL) was added and the reaction mixture allowed to sit for 10 minutes. The preactivated species was then added to the resin and allowed to react for 1hour, followed by thorough washing of the resin with 5x DMF, and then 5x with DCM. The Fmoc group was then removed from the lysine side chain using the “General Procedure for Removal of Fmoc Group”. The fluorescein label was then attached using fluorescein 6-isothiocyanate (247 μmole , 96mg) in DMF (2.1mL, conc. of 200mM) with DIPEA (247 μmole , 43 μL) overnight followed with thorough washing of the resin with DMF and then DCM. The Boc group was then removed with 1.5mL of 1:1 TFA in DCM for 20 minutes, followed by washing of the resin with 5x DCM and repeating the Boc deprotection treatment. The oligomer was then cleaved from the resin with 10% DIPEA in DMF (total of 1.5mL of solution) overnight at room temperature. LC-MS analysis, See Figure 4.5 for crude LC-MS trace (5-95% H₂O/ACN with 0.1% formic acid) for oligomer (**84**): $t_r=21.3\text{min.}$, calcd. for product(**84**)+H⁺= 1307.4; found: 1307.2. The crude product was then RP purified (see Figure 4.12) and lyophilized. Anal. Calcd for C₆₆H₆₄Cl₂N₁₀O₁₃S+Na⁺: 1329.3650, Found: 1329.3607 (difference 3.2ppm). See Appendix for NMR characterization.

Solid Phase Synthesis of Bis-Peptide (Oligomer **104, $K_i=2.6\mu\text{M}$).** The solid phase synthesis was continued from that of oligomer **81** above using 50mg of resin. The Fmoc group was

removed using the “General Procedure for Removal of Fmoc Group”. Boc-(D)-Glu(OtBu)-OH, (413 μ mole, 125mg) and HATU (413 μ mole, 157mg) were combined in DMF (2.1mL, conc. of 200mM); DIPEA (825 μ mole, 144 μ L) was added and the reaction mixture allowed to sit for 10minutes. The preactivated species was then added to the resin and allowed to react for 1hour, followed by thorough washing of the resin with 5x DMF, and then 5x with DCM. The resin was then deprotected with 1.5mL of 95% TFA using the “General Procedure for Removal of Boc and t-Butyl Groups”. The resin was thoroughly washed with DCM and DMF, followed by treatment of the resin with 30% diethylamine in ACN for 2hours at room temperature. LC-MS analysis, (5-95% H₂O/ACN with 0.1% formic acid). Oligomer (**104**): t_r =18.6min., calcd. for product(**104**)+H⁺= 919.3; found: 919.2. The solvent was then removed *in vacuo*, the residue suspended in H₂O/ACN with 0.1% formic acid, RP-HPLC purified (see Figure 4.13), and the desired fractions pooled and lyophilized. Anal. Calcd for C₄₄H₄₈Cl₂N₈O₁₀+Na⁺: 941.2768, Found: 941.2729 (difference 4.1ppm). See Appendix for NMR characterization.

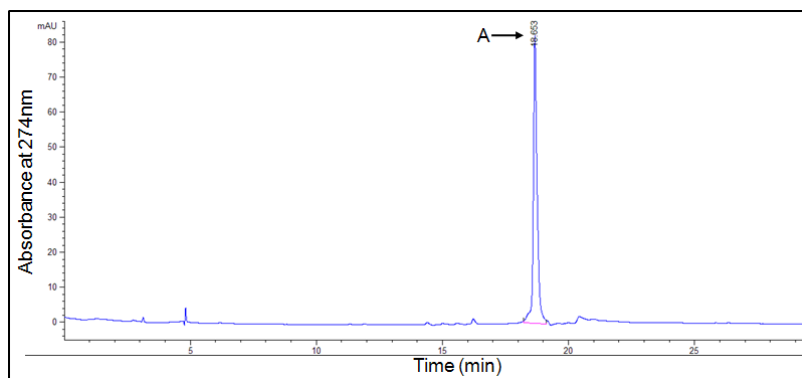


Figure 4.13. HPLC trace of purified bis-peptide **104** (K_i =2.6 μ M), monitoring at a wavelength of 274nm with a gradient of 5-95% ACN/H₂O with 0.1% formic acid over 30 minutes. The peak marked “A” has a m/z = 919.2 (calcd for bis-peptide **104** + H⁺: 919.3).

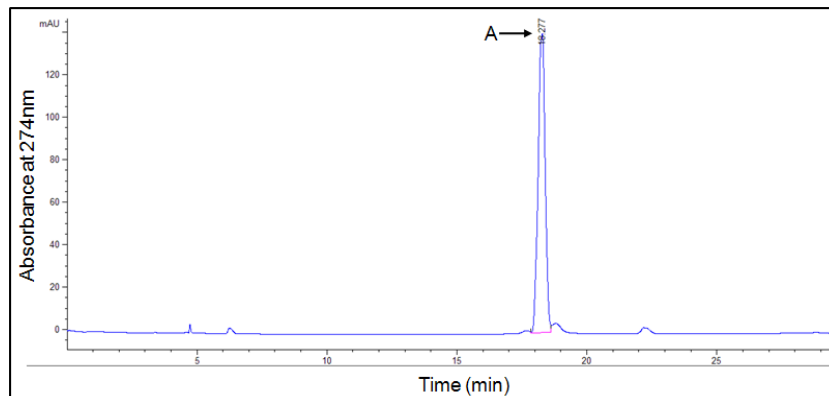


Figure 4.14. HPLC trace of purified bis-peptide **103** ($K_i=34\mu\text{M}$), monitoring at a wavelength of 274nm with a gradient of 5-95% ACN/H₂O with 0.1% formic acid over 30 minutes. The peak marked “A” has a $m/z = 887.3$ (calcd for bis-peptide **103** + H⁺: 887.4).

Competition Experiment Bis-Peptide, Oligomer 103 ($K_i=34\mu\text{M}$). The solid phase synthesis of oligomer **103** parallels that of oligomer **104** above. The crude material was RP-HPLC purified, and the desired fractions pooled and lyophilized. LC-MS analysis, See Figure 4.14 (5-95% H₂O/ACN with 0.1% formic acid). Oligomer (**103**): $t_r=18.3\text{min.}$, calcd. for product(**103**)+H⁺= 887.4; found: 887.3.

Compound	Retention Time (min)	Expected Mass + H ⁺	Found Mass
85	20.4	1275.4	1275.3
86	20.7	1275.4	1275.2
87	20.8	1289.5	1289.2
88	22.1	1317.5	1317.1
89	19.8	1298.4	1298.1
90	21.3	1307.4	1307.1
91	21.4	1319.4	1319.2
92	21.2	1357.4	1357.2
93	22.3	1335.4	1335.2

Table 4.4. LC-MS characterization data for the *bis*-peptides **85-93** which explored the use of different functional groups on hDM2 binding.

Compound	Retention Time (min)	Expected Mass + H ⁺	Found Mass
94	21.3	1307.4	1307.2
95	21.4	1307.4	1307.3
96	21.2	1307.4	1307.1
97	21.2	1307.4	1307.6
98	21.3	1307.4	1307.8
84	21.3	1307.4	1307.2

Table 4.5. LC-MS characterization data for the *bis*-peptides **94-98** and **84** which explored the effect of just stereochemistry on hDM2 binding.

Compound	Retention Time (min)	Expected Mass + H ⁺	Found Mass
100	24.6	1397.4	1397.2
101	23.7	1363.4	1363.0
102	24.1	1427.4	1426.9

Table 4.6. LC-MS characterization data for the *bis*-peptides **100-102** which explored the effect of an additional functional group on hDM2 binding.

Acknowledgment: The protein expression was performed by Kavitha Akula and Marcus Jackson of the Schafmeister group. They also assisted with a few of the fluorescence polarization assays. For their help I am extremely grateful.

HDM2 Protein Expression. A fusion protein consisting of residues 1-140 (the plasmid was a generous gift from the lab of Neil Zondlo, University of Delaware) was prepared by over-expression.⁶⁴ Plasmids were used to transform chemically competent E-coli BL21 Cells (Novagen), and a single colony was used to inoculate 2x4 ml LB media culture tubes containing 0.1 mg/ml ampicillin, at 37°C overnight. These overnight cultures were used to inoculate a 1 L culture of TB media containing 0.1mg/ml ampicillin. The culture was incubated at 37°C with shaking at 250 rpm until the optical density at 600 nm reached to 0.9 absorbance units. Protein over expression was then induced by the addition of 20% isopropyl β-D-thiogalactoside (IPTG) to 0.4 mM final concentration. The culture was then grown for additional 5 hours at 30°C. Then cells were harvested at 4°C by centrifugation at 4500 rpm for 20 min. The cell pellet was

resuspended in chilled 1x Binding Buffer (0.5M NaCl, 20mM Tris-HCl, 5mM imidazole, pH 7.9), frozen and stored at -80°C until protein purification.

Protein Purification. The frozen cell pellet was thawed at 4°C and lysed by sonication for 2 minutes with 10 sec on and 20 sec off. Cell debris was pelleted by centrifugation for 30min at 15000 g, 4°C and the supernatant was filtered through a 0.2µm syringe filter. A column was prepared using 2mL Novagen His-Bind suspended resin and resin was washed with 3 vol DI water. The flow rate maintained was not more than 0.5 ml/min throughout the purification. The resin was charged with 5 vol 1x Charge Buffer (50mM NiSO₄) and then equilibrated with 3 vol 1x Binding Buffer (5mM imidazole). After loading the column with prepared extract, the resin was washed with 10 vol 1x Binding Buffer and then with 6 vol 1x Wash Buffer (10mM imidazole). Protein was then eluted with 6 vol 1x Elution Buffer (1M imidazole). The eluate was captured in fractions of 0.5 ml. Fractions were assayed with coomassie blue and desired fractions were combined and dialyzed using spectra/por 6 Dialysis Membranes of 10,000 MWCO (Spectrum Laboratories) in PBS (pH 7.4, 5mM EDTA and 0.5 mM DTT) for overnight. The resulting protein was characterized by SDS-PAGE (4-20% gradient gel) for purity analysis and concentrations were measured by UV analysis. Experimental protein yields were about 1.7mg from 1L culture. Fresh protein was used immediately for protein binding experiments.

Synthesis of ^{Fl}p53 Control Peptide (sc1). A control peptide corresponding to residues 14-29 of the p53 protein was synthesized on an Apex 396 multiple peptide synthesizer (aapptec, Louisville, KY). Rink Amide-AM resin, HATU activation and 30 minute, double couplings were used for all residues. A β-Ala was installed on the N-terminus followed by fluorescein labeling by exposure of the peptidyl resin to 5eq of FITC and 5eq of DIPEA overnight. The primary sequence of the peptide was: Fluorescein-β-Ala-L-S-Q-E-T-F-S-D-L-W-K-L-L-P-E-N-NH₂. The product was cleaved from the resin by treatment with 2mL of 95% TFA/2.5% H₂O/2.5% TIS for 2 hours followed by concentration of the cleavage solution with a rotovap. The residue was then suspended in H₂O/ACN and the crude material RP-HPLC purified, and the desired fractions pooled and lyophilized. LC-MS analysis, (5-95% H₂O/ACN with 0.1% formic acid). p53^{Fl} Peptide (sc1): t_r=15.7min., calcd. for peptide(sc1)+H⁺= 2379.1; found: 2379.7.

Synthesis of p4 Control Peptide (sc2). A control peptide called P4 which was identified from phage display as a very tight inhibitor of hDM2⁷⁰ was synthesized by the Temple University Solid-Phase Peptide Synthesis Facility on an CEM Liberty peptide synthesizer (CEM Corp,

Matthews, NC). A β -Ala was installed on the N-terminus followed by fluorescein labeling by exposure of the peptidyl resin to 5eq of FITC and 5eq of DIPEA overnight. The primary sequence of the peptide was: Fluorescein- β -Ala-L-T-F-E-H-Y-W-A-Q-L-T-S-OH. The product was cleaved from the resin by treatment with 2mL of 95% TFA/2.5% H_2O /2.5%TIS for 2 hours followed by concentration of the cleavage solution with a rotovap. The residue was then suspended in H_2O /ACN and the crude material RP-HPLC purified, and the desired fractions pooled and lyophilized. LC-MS analysis, (5-95% H_2O /ACN with 0.1% formic acid). P4^{Fl} Peptide (**sc2**): $t_r=15.1$ min., calcd. for peptide(**sc2**)+ H^+ = 1955.8; found: 1955.7.

Fluorescence Polarization Experiments. Binding experiments were performed in a black 96-well Costar plate and used an Analyst GT plate reader (Molecular Devices, Sunnyvale, CA). The binding buffer used for all experiments was PBS (pH 7.4) with 5mM EDTA and 0.5 mM DTT. All plates were read using the fluorescein excitation filter of 485nm and the emission filter of 530nm.

Direct Binding Fluorescence Polarization Experiments. Fluorescence polarization experiments were undertaken to assess the ability of bis-peptide oligomers to bind hDM2, a protein with hydrophobic cleft which binds the p53 N-terminal helical domain. Fluoresceinated oligomers (conc. of 10nM) was incubated for 30minutes at room temperature with sequential dilutions of hDM2 protein (final conc. 85 μ M to 0.33 μ M, See Figure 4.6) followed by recording of the polarization data. The data was processed using the Graphpad Prism program⁷⁵ using a one-site, specific binding model. See Figures 4.15 and Tables 4.7 and 4.8 for the data.

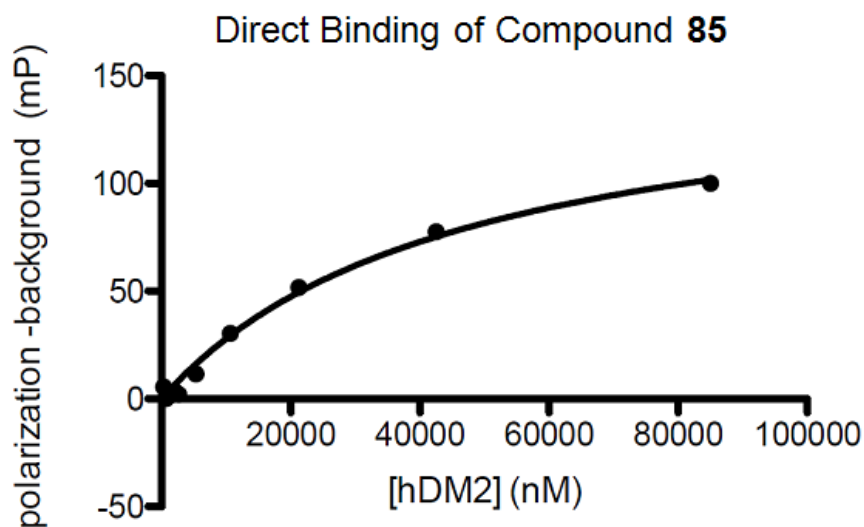


Figure 4.15. Plot of hDM2 concentration (in nM) versus background adjusted polarization (in millipolarization units) for oligomer 85.

		X	A		
		X Title	Data Set-A		
	⊗	X	A:Y1	A:Y2	A:Y3
1	Title	85000.0000	214.70	221.98	228.80
2	Title	42500.0000	190.57	184.78	180.95
3	Title	21250.0000	140.60	140.36	149.49
4	Title	10625.0000	111.68	103.58	111.51
5	Title	5312.5000	76.59	80.38	78.10
6	Title	2656.2500	64.39	59.31	65.05
7	Title	1328.1250	63.64	50.24	72.36
8	Title	664.0625	56.24	67.69	54.35
9	Title	332.0313	70.56	74.64	60.28

Table 4.7. Table of raw values used for the plot in Figure 4.15; X values are hDM2 concentration (in nM) and Y values are polarization (in millipolarization units) for oligomer 85; data from three independent trials is shown as Y1, Y2 and Y3.

		Direct binding compound 25
		A
Nonlin fit		Data Set-A
1	One site -- Specific binding	
2	Best-fit values	
3	Bmax	156.8
4	Kd	46009
5	Std. Error	
6	Bmax	10.45
7	Kd	6192
8	95% Confidence Intervals	
9	Bmax	135.3 to 178.3
10	Kd	33254 to 58763
11	Goodness of Fit	
12	Degrees of Freedom	25
13	R square	0.9819
14	Absolute Sum of Squares	604.3
15	Sy.x	4.916
16	Number of points	
17	Analyzed	27

Table 4.8. Parameters used for the non-linear fit for plot in Figure 4.15.

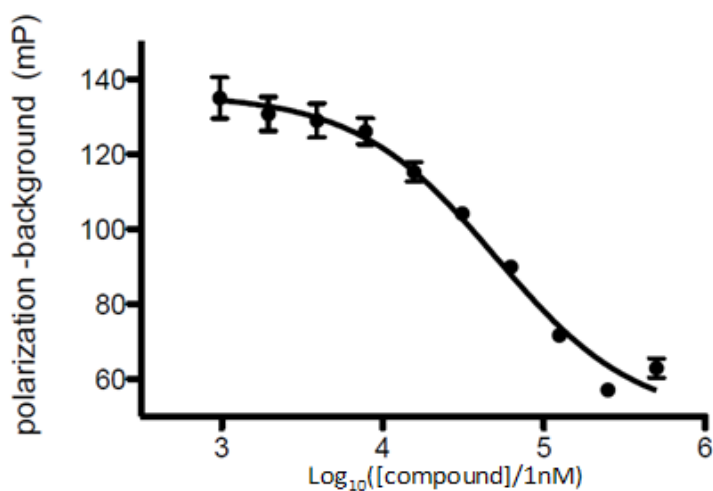


Figure 4.16. Plot of log oligomer **103** concentration versus background adjusted polarization (in millipolarization units) as a measure of the ability of compound **103** to displace fluoresceinated p53 peptide.

Competition Fluorescence Polarization Experiments. To assess the ability of oligomer **103** to displace fluoresceinated p53 peptide from hDM2, competition experiments were undertaken. hDM2 (2 μ M) and p53 control peptide (10nM) were incubated at room temperature for 30minutes in binding buffer, followed by the addition of serial dilutions of oligomer **103** (final conc. 500 μ M to 0.975 μ M). The binding experiments were incubated for a further 30 minute time period, followed by recording of the polarization data. See Figure **4.16**, and Supplemental Table **4.9**.

Nonlin fit		Competition experiment compound_23
		A
		Data Set-A
1	One site - Fit Ki	
2	Best-fit values	
3	logKi	4.696
4	HotNM	= 10.00
5	HotKdNM	= 614.1
6	Bottom	48.96
7	Top	136.0
8	Ki	49633
9	Std. Error	
10	logKi	0.07651
11	Bottom	3.809
12	Top	2.176
13	95% Confidence Intervals	
14	logKi	4.539 to 4.853
15	Bottom	41.14 to 56.77
16	Top	131.5 to 140.4
17	Ki	34576 to 71247
18	Goodness of Fit	
19	Degrees of Freedom	27
20	R square	0.9626
21	Absolute Sum of Squares	925.5
22	Sy.x	5.855
23	Constraints	
24	HotNM	HotNM = 10.00
25	HotKdNM	HotKdNM = 614.1
26	Number of points	
27	Analyzed	30

Table **4.9**. Parameters used for the non-linear fit for plot in Figure **4.16**.

Acknowledgment: Cell Culture, Fluorescence Microscopy, and Western blot analysis were performed by Alla Arzumanyan of the Feitselson Lab, Temple University. RNA experiments were performed by R. Arzumanyan. Alla also produced a few of the figures in this chapter. For their contributions I am extremely grateful.

Cell Culture and Treatment. HepG2 (expressing wild-type p53) and Huh7 (expressing mutant p53) cell lines were purchased from the American Type Culture Collection (ATCC) and cultured as monolayers in Dulbecco's modified Eagle's medium (DMEM) (Invitrogen) supplemented with 100 mM nonessential amino acid solution, 100 mM sodium pyruvate, 100 U/mL penicillin, 100 µg/mL streptomycin, and 10% heat inactivated fetal bovine serum (FBS) (all from Hyclone). Cells were maintained at 37°C and 5% CO₂. Nutlin-3 (Sigma) was dissolved in 0.01% DMSO (Sigma). This concentration of DMSO did not affect cell phenotype. Both nutlin-3 and *bis*-peptide were added into the medium at 2µM, 5µM, 10µM and 20µM for 24 hours.

Fluorescent and Confocal Microscopy. Fluorescent and confocal microscopy was assayed with live and fixed cells. Cells were grown on glass chambers and fixed with ice-cold 95:5 ethanol/acetic acid for 10 minutes at -20°C. Sections were washed with PBS and mounted in Vectashield aqueous mounting medium with DAPI (Vector laboratories). Fluorescent specimens were analyzed using an ECLIPSE Ti microscope (Nikon), lenses with hardened

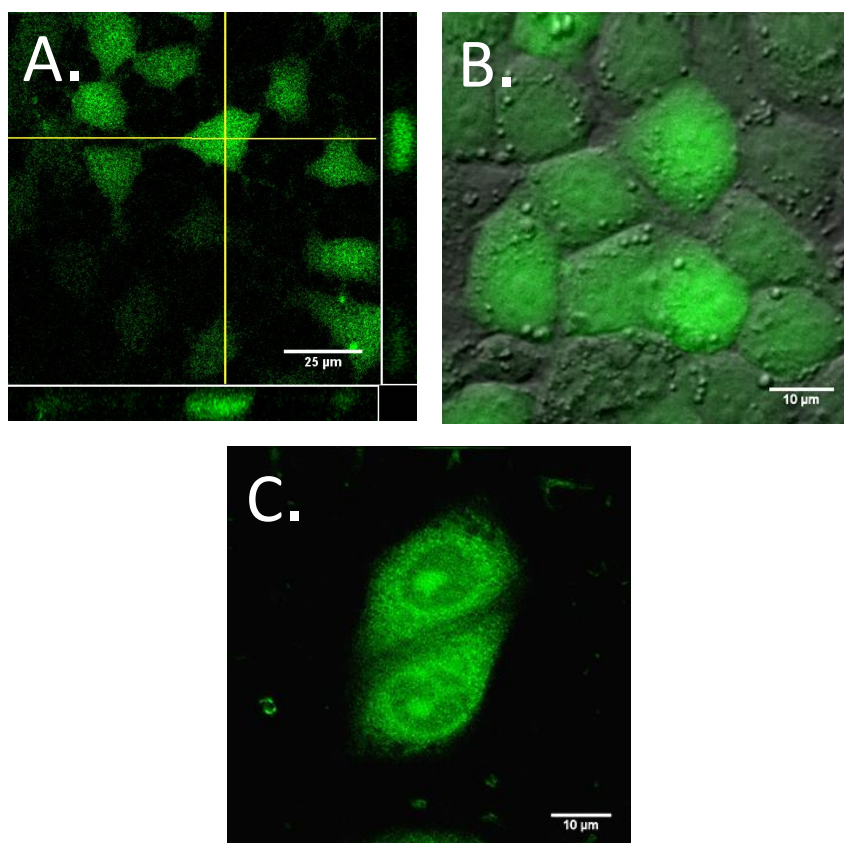


Figure 4.17. Detection of bis-peptide in live Huh7 (A, B) and HepG2 (C) cells by confocal microscopy. Image A is the section of cells with green fluorescence within the cell (red arrows). Bis-peptide is found in both cytoplasmic and nuclear compartments (C).

filters (Nikon), and a Nikon DS-Fi1 camera, which was operated by NIS Elements computer software (Nikon). Confocal microscopy was performed with a Leica SP-1 microscope, with illumination at 488 and 543 nm and spectral detection.

Western Blotting. For protein extraction cells were lysed in cell lysis buffer (Cell Signaling) with protease inhibitor cocktail for 20 minutes on ice. Protein extracts (50 µg) were separated by SDS-PAGE electrophoresis, transferred to nitrocellulose membranes (Schleicher & Schuell), and incubated overnight with primary antibodies to p53, MDM2, p21, and β-actin (all from Santa Cruz Biotechnology). The blots were developed using ECL plus detection system (Amersham Biosciences) and exposed to Kodak imaging films (Kodak BioMax).

RNA Extraction, Reverse Transcription and PCR Analysis. Total RNA was extracted using High Pure RNA Isolation Kit (Roche Applied Science) according to enclosed instructions. cDNA was prepared using RETROscript Reverse Transcription Kit (Ambion). Mdm2 primers (Ensembl gene database: Mdm2, ENSG00000135679) were 5'-GGTGCTGTAACACCTCACA-3' (f) 5'-TTTTTGTGCACCAACAGACTTT-3'(rev). These primers recognize cDNAs of all Mdm2 isoforms with p53 binding sequence [1] and generate 102 bp amplicon. β-actin primers for 243 bp PCR transcript (Ensemble gene: Actb, ENSRNOG00000034254) were 5'-TACCACTGGCATTGTGATGG-3' (forward) and 5'-GGGCAACATAGCACAGCTTC-3' (reverse). Primers were designed using Primer3Plus Web Interface. cDNA was amplified using FastStart SYBR Green Master Kit (Roche Applied Science). Real-time quantitative PCR was performed using Stratagene Mx 3005P QPCR system. PCR samples were amplified in 40 cycles; each cycle consisted of 60 sec of denaturation at 95°C, 60 sec of annealing at 60°C, and 60 sec of elongation at 72°C. Mathematical model described by Pfaffl [2] and MxPro software (Stratagene) were used to process PCR data. End-point PCR reactions were assayed with PCR Master Mix (Promega). Samples were amplified in 34 cycles; each cycle consisted of 30 sec of denaturation at 95°C, 30 sec of annealing at 60°C, and 30 sec of elongation at 72°C. After 34 cycles, samples were subjected to final elongation for 5 minutes at 72°C. Amplification products were separated by 2% agarose gel electrophoresis, and images of DNA bands were visualized by ethidium bromide staining.

Chapter 5

Expanding the Toolbox of Functionalized *Bis*-Peptides

Presented in this chapter are experiments that explore and expand the ability to create *bis*-peptide oligomers. Changing the Cbz group to the Boc protecting group allowed the use of Boc peptide synthesis protocols and added another dimension of protecting group orthogonality.³⁵ Another significant advance was the implementation of functionalized *bis*-peptide assembly onto solid-phase which allowed more synthetic versatility and a greater number of molecules to be synthesized and was a key element in enabling *bis*-peptide α -helix-mimics presented in Chapter 4. A more thorough discussion of transferring *bis*-peptide synthesis from the solution phase assembly of Chapter 3 is presented. Also introduced here is work that demonstrates that bis-amino acids can be coupled in the reverse direction to achieve different oligomeric architectures.

Acknowledgments: The solid-phase synthesis of the bis-peptide oligomers was accomplished with the assistance of Jennifer Alleva, former undergraduate in the Schafmeister Lab.

5.1 Introduction

One of the exciting aspects of *bis*-peptide technology is to be able to use a small repertoire of synthetic steps to create molecules with an enormous amount of structural diversity.² Hopefully a few scaffolds will then be able to position the functional groups in the desired fashion to have the designed function. Using software designed by the Schafmeister group, we are able to computationally screen potential *bis*-peptide scaffolds *in silico* to determine if they have the appropriate structure we are seeking for a particular application. The greater number of structural motifs that can be accessed the greater chance of being able to find a structure to match the one desired. Therefore, any synthetic methodology which can increase the amount of synthetically accessible *bis*-peptide targets would be a contribution toward the larger effort of functional macromolecules for various applications.

Solid-phase synthesis has risen to a prominent place in modern organic chemistry as a means of producing compounds with high purity and in an efficient manner. The premise of solid-phase is that the molecule is attached to an insoluble polymeric support, such as a polystyrene resin, and reagents and building blocks are flowed through it to build up the molecule.⁷⁶ An excess of reagents may be employed to drive the reactions to completion in a timely manner. This technique is especially amenable to repetitive, oligomeric type chemistries such as peptide synthesis, where the molecule is produced via recurring steps of acylation and deprotection. In chapter 3 a solution phase protocol was outlined using the novel DIC/HOAT activation strategy developed for hindered amino acids. Here we combine this technique with solid-phase synthesis to construct highly functionalized *pro4* oligomers on solid support. This allows rapid synthesis of the oligomers as well as simple means to achieve diverse structures by splitting the resin beads into different portions at various stages of the syntheses and coupling different building blocks. In this manner, both the functional groups of the monomers and the building blocks themselves may be screened for interesting properties as shown in Chapter 4 with the synthesis and assay of the α -helix mimics.

This chapter outlines a few procedures to access a greater number of functionalized *bis*-peptide architectures. Aside from the ability to create *bis*-peptides more rapidly using solid-phase synthesis, the idea of reversing the direction of coupling the *bis*-amino acids is shown. Since *pro4* (and all other *bis*-amino acids) consist of two orthogonally protected amino acids, there exists the ability to connect these amino acids in various fashions depending on the chosen protecting groups. In Chapter 3, the hexa- and the penta-substituted diketopiperazines are examples of how the different amino acids can be connected; this chapter introduces the

final possible permutation of the tetra-substituted diketopiperazine. This “tail to tail” coupling (according to the vernacular used in our lab) couples the prolinyl amino acids together and points two functional groups at each other, a potentially valuable motif that may find use in the future (see Figure 5.6).

5.2 Results and Discussion

Synthesis of the Boc amino acid. In the solution-phase synthesis of the *pro4* oligomers shown in chapter 3, the Cbz group was employed as the pyrrolidine nitrogen protecting group. Upon moving the chemistry to solid-phase, a more convenient masking group was employed since the Cbz group requires either strong acid (for example 33% HBr/AcOH) or hydrogenolysis for removal. Using the Boc group frees up a dimension of protecting group orthogonality to the oligomer. Since the *t*-butyl ester would still have to be removed via TFA, if a Boc group were to be used instead of the Cbz the amino acid would be subjected to the relatively mild treatment of TFA rather than the harsher HBr formerly employed.³⁵ Thus, Cbz/benzyl protecting groups could

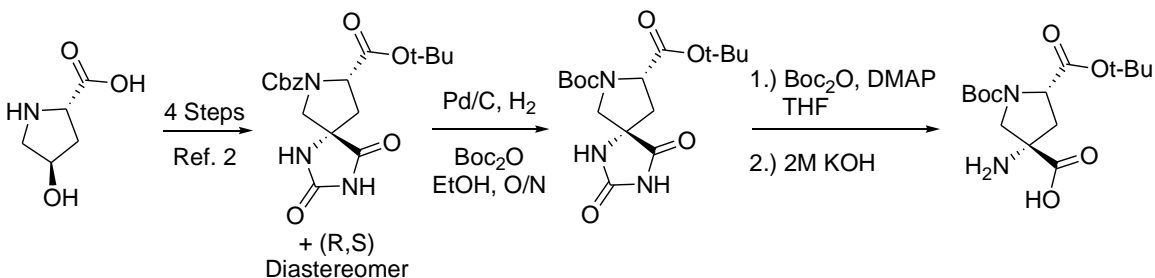


Figure 5.1. Synthesis of the Boc-protected amino acid *pro4* monomer.

be reserved for reactive side chain functionality to be removed at the end of the oligomer synthesis.

The synthesis of the Cbz protected hydantoin, compound **106**, from *trans*-4-hydroxyproline has been published² and routinely performed by every member of the Schafmeister lab on a multi-gram scale. Conversion of this material to the Boc protected species is straightforward and uses conventional protecting group chemistry and is outlined in Figure 5.1. The Cbz group of hydantoin **106** is removed under hydrogenolysis conditions with a catalytic amount of palladium in the presence of hydrogen. If this reaction is performed in the presence of di-*tert*-butyl dicarbonate a one-pot Cbz to Boc reaction is conveniently carried out to yield Boc-protected hydantoin **107** and its diastereomer. Separation of these diastereomeric *pro4* hydantoins is then carried out using the previously published conditions with similar recovered yields of each stereoisomer. The final step to the *pro4* amino acid, the hydrolysis of

the hydantoin **107**, is then carried out using the published procedure to produce the unfunctionalized Boc-protected amino acid **108** ready for reductive alkylation and incorporation into an oligomer.²

Solid-phase synthesis of functionalized pro4 oligomers. Conventional peptide synthesis is depicted in Figure **5.2** on the left-hand side of the Figure **5.2** and uses repetitive cycles to build up a polymer supported oligomeric peptide.⁷⁶ In the most common implementation, an activated residue (an amino acid with a more active leaving group) is added as a solution to acylate a resin-bound nucleophilic amine. Next, a temporary protecting group, usually Fmoc or Boc, is then removed to expose the next resin-bound nucleophile and then the process is repeated until the desired oligomer has been constructed. Finally, a reagent is added to cleave the oligomer from the solid support.

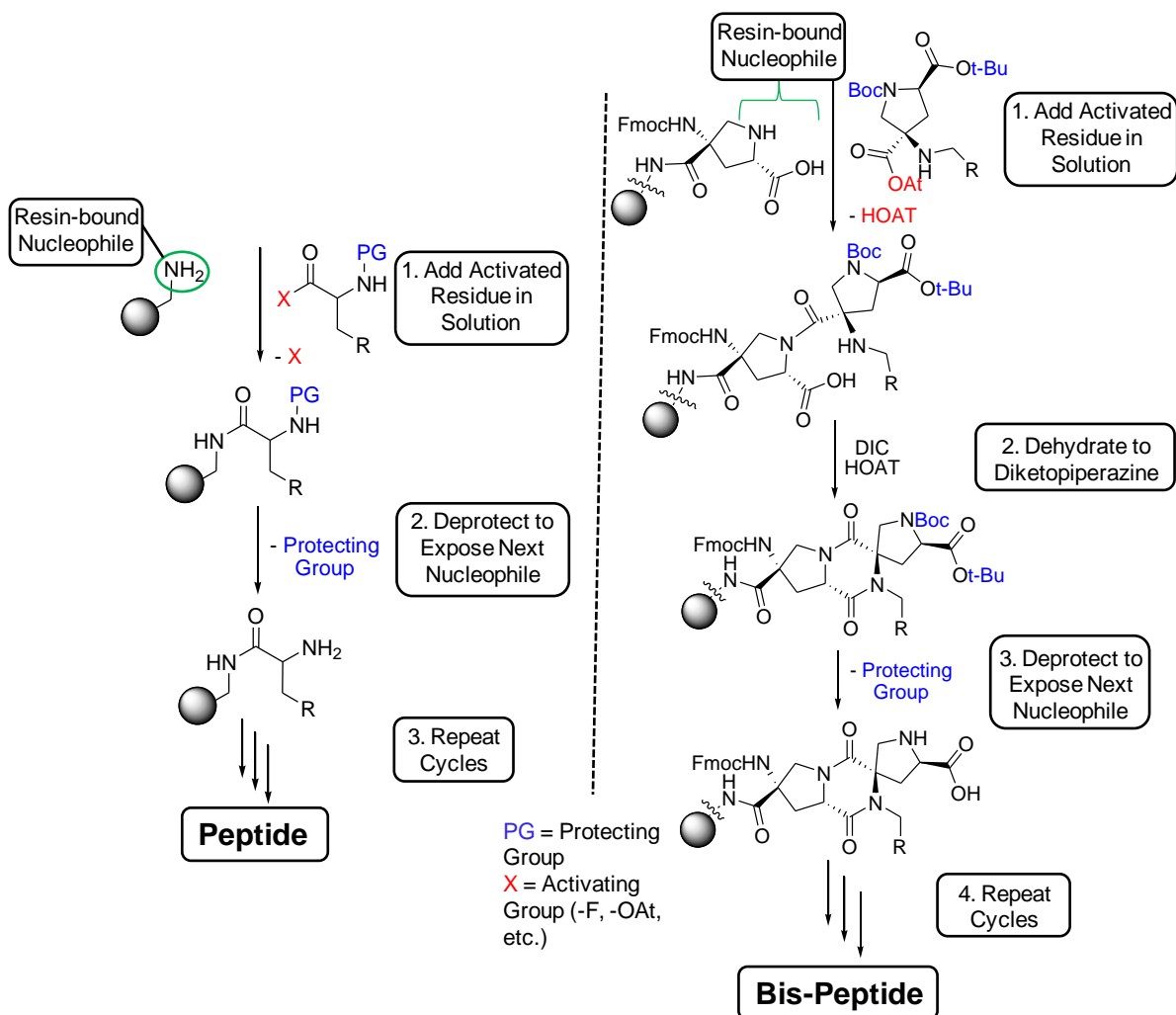


Figure 5.2. Comparison of the cycles of conventional peptide synthesis (left) and *bis*-peptide synthesis (right).

The assembly of *pro4* oligomers on solid-support follows a similar but modified procedure when compared to conventional peptide synthesis and is shown on the right hand side of Figure 5.2. The main differences are that in solid-phase *bis*-peptide synthesis the resin-bound nucleophile is now an amino acid (Chapters 2 and 3 have shown the value of amino acids as nucleophiles for the synthesis of hindered amino acids). The second difference is the inclusion of a supplemental, “dehydration” step. As shown in the Chapter 3, the initial acylation product of the amino-OAt ester and the amino acid nucleophile can produce variable amounts of both the single amide as well as the diketopiperazine product (see Figure 3.9 and Figure 5.2). Thus, after the initial reaction with the amino-OAt building block the resin is drained and thoroughly washed, followed by an additional aliquot of DIC in the presence of HOAT. This

converts any of the single amide products (either of the possible regioisomers) to the single, desired diketopiperazine. Next, simultaneous deprotection of both the Boc and *t*-butyl protecting groups is accomplished with 95% TFA in the presence of a silane scavenger, TIS. Similar to conventional peptide synthesis, we are now left with a resin-bound nucleophile to acylate with another incoming activated residue and the process is repeated until the desired oligomer is constructed.

In the first solid-phase synthesis we designed a cyclorelease step as the cleavage step. Cyclorelease strategies have been recognized in organic and peptide solid-phase synthesis as being able to generate clean product by using the chemoselectivity of the resin-bound compound.^{77,78} Here a deprotected amine on the penultimate residue would attack and displace the ester linkage to the resin, releasing the diketopiperazine-terminated product into solution. This requires that the linker would have a hydroxyl group to esterify. The other requirement would be that the linker must be stable to the acidic conditions which deprotect the monomer at each step. We developed two different implementations of this strategy that are further detailed below.

Although several possible linkers are commercially available, in the first generation we constructed the linker on the resin. This allowed us to use polyethylene-glycol (PEG) based resins⁷⁹ which would swell under a variety of solvent conditions since there was no commercially available system which satisfied all of the necessary criteria. Thus, more different types of chemistry could be employed on the resin including biological based assays since the polymer would swell in aqueous buffer. An amino-terminated PEG resin is available from Novabiochem⁸¹ at a very low cost since it is underivatized, and so this was the first support to be used to synthesize oligomers using solid-phase chemistry.

The synthesis is shown in Figure 5.3 begins with acylating the resin-bound primary amine with a protected serine derivative that has an Fmoc group on the α -amine and a trityl group on the β -hydroxy moiety. The Fmoc group was then removed and the amine was capped to give compound **109**. The amine is capped because the hydroxyl group is the linker of the system and the point of further expansion. Now, the hydroxyl group is exposed using 5% TFA to liberate the trityl protecting group and then esterified with any Fmoc-amino acid; for the first syntheses, a bromo-phenylalanine derivative **110** is used to serve as a mass spectrum handle since the isotopic abundance of bromine produces a characteristic pattern. The standard conditions of 2,4,6-mesitylene-1-sulfonyl-3-nitro-1,2,4-triazolide (MSNT) and methylimidazole (Melm) are used to form esters under mild conditions and so are commonly employed in peptide synthesis⁶³ and here give compound **111**. Next, the Fmoc group on the amino acid is removed

and the next *pro4* building block is brought in; this residue is the penultimate residue which will give the critical cyclorelease during the final step of the synthesis. This monomer, compound **75**, may be activated with the more conventional HATU procedure because the amine is still protected as the carbamate (as opposed to the sterically hindered secondary amine for which the “amino-OAT” activation protocol was developed for) to yield intermediate **112**. Next, the Boc and *t*-butyl groups were removed using TFA to expose the next resin-bound nucleophilic amino

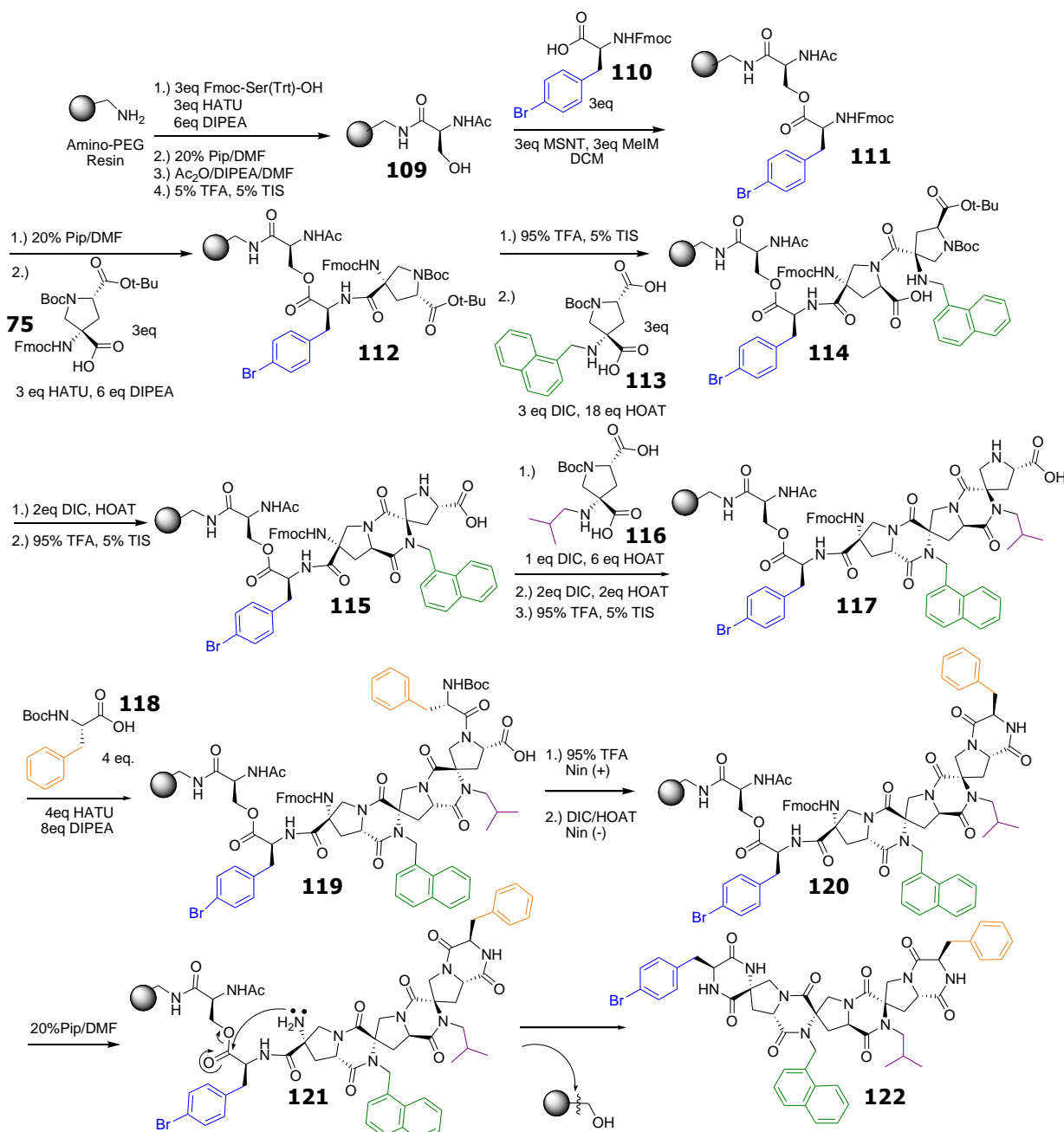


Figure 5.3. Solid phase synthesis of functionalized *pro4* oligomers using the serine-based linker system.

acid.

Now, the solid-phase parallels the solution-phase synthesis outlined in Chapter 3 using the previously determined methodology for activating and coupling sterically hindered amino acids. The next functionalized *pro4* monomer **113**, here with a naphthyl group, is brought in as the amino-OAt ester to give compound **114**, followed by a dehydration step to ensure all coupling product has formed the desired diketopiperazine. Again, a simultaneous deprotection is accomplished using TFA to expose the resin-bound nucleophilic amino acid of oligomer **115** and the system is ready for another coupling cycle. An additional *pro4* monomer **116**, here with an isobutyl group, was then brought in, subjected to the dehydration conditions, and then deprotected to give tetramer **117**. The final residue that was placed on the oligomer was a Boc protected amino acid, phenylalanine **118**, activated with HATU to give Boc-protected intermediate **119**. The Boc group was then removed and the diketopiperazine closed using the same conditions employed during the *pro4* assembly sequence to give oligomer **120**. This cyclization may be conveniently monitored using the ninhydrin test. Briefly, a primary amine, such as that exposed here upon Boc deprotection, produces a positive colorimetric response in the ninhydrin test. Once the diketopiperazine reaction is complete, usually an hour under the

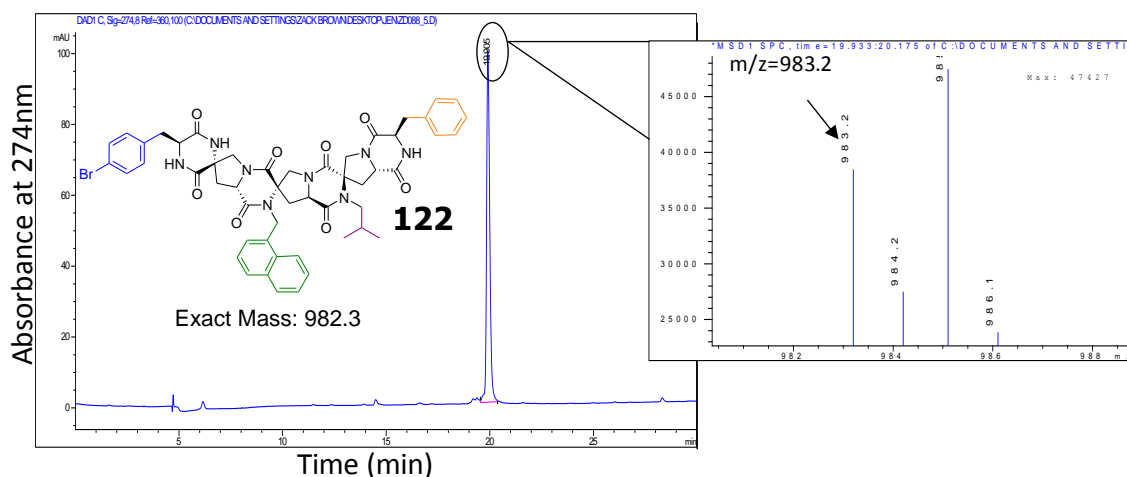


Figure 5.4. The purified LC-MS trace of oligomer **122** from the serine-based linker developed for solid-phase. The mass spectrum, shown as an inset, gives the expected mass of the product **122** + H⁺ and shows the distinctive isotopic abundance of bromine.

reaction conditions of excess dehydrating agent, the ninhydrin test then gave a negative result because the functional group is now a secondary amide as in compound **120**.

Deprotection of the first *pro4* monomer and concomitant cyclorelease of the oligomer from the resin was affected with 20% piperidine in DMF. Upon removal of the Fmoc group to give compound **121**, the exposed primary amine attacked the ester linkage to the resin, forming a diketopiperazine, and caused the material to be released into solution. One drawback of this procedure is that the desired product is contaminated with the fulvene byproduct of the Fmoc deprotection step. Nevertheless, the material was RP-purified to give a single peak, with the chromatogram and the mass spectrum shown in Figure **5.4**. The mass spectrum is shown as an inset and is consistent with the expected mass of oligomer **122** and gives the distinctive isotopic abundance of bromine.

Therefore, this new serine-based linker system is a competent means of producing *bis*-peptides via solid-phase. The linker was stable to the conditions employed during the synthesis and the cyclorelease of the final product proceeded smoothly. Further improvements could be made, but this was an exciting first step towards producing functionalized *bis*-peptides using the new methodology on solid-phase.

The exploratory solid-phase strategy using the designed serine-based linker was successful, and so other resins were explored to define the scope and find the system with the greatest utility. Initially, the PEG resin was employed to be able to use many different types of solvents on solid support, including more polar solvents such as water or methanol which would not be amenable to the traditional PS resins. However, we subsequently demonstrated that commercially available polystyrene resins with the HMBA linker were compatible with this new synthetic methodology. This hydroxyl based linker has excellent acid stability properties so it would be amenable to the repetitive TFA treatments.⁸¹

In our next solid-phase synthesis of a *bis*-peptide we made a few notable improvements. First, the initial *pro4* monomer **75** is directly attached to the hydroxyl linker, again using the MSNT/Melm protocol. This facilitated a more divergent synthesis by being able to functionalize that terminal position with any amino acid as the final step whereas it was the first step in the

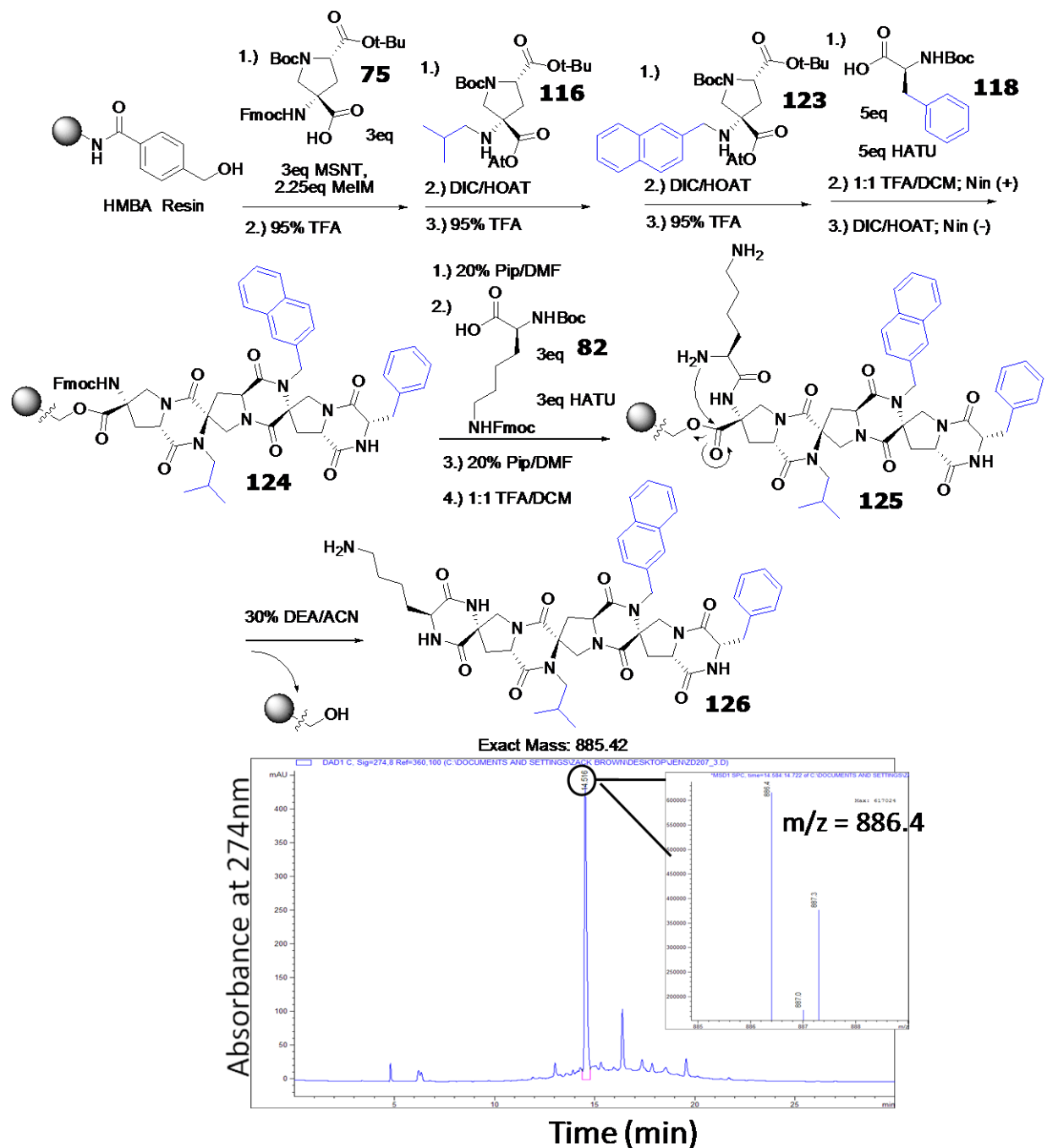


Figure 5.5. Solid phase synthesis and LC-MS trace of the crude cleavage product of oligomer **126** using the HMBA resin. Unlabeled peaks did not have identifiable masses.

synthesis for the serine-based linker system. (For example, in this synthesis compound **82** is the last residue added, whereas with the previous solid-phase synthesis it would have been the first residue.) This will become important as more applications of the functionalized oligomers are developed; suffice it to say though that diversity in synthesis, especially later in the synthetic endeavor, is always valuable. Also, the protecting group employed on this final residue (amino acid derivative **82**) was changed to a Boc group for synthetic ease (see below). This prevented the oligomer from being cleaved from the resin during the 20% piperidine deprotection and being contaminated with the Fmoc deprotection side product, dibenzofulvene as in the synthesis above. As can be seen in Figure 5.5, a similar synthesis to that undertaken for the serine-based linker system was used for this oligomer. Briefly, two subsequent functionalized *pro4* monomers **116** and **123** followed by Boc-phenylalanine **118** are coupled to the resin to produce the resin-bound tetramer **124**. The Fmoc group was then removed followed by acylation the Boc-protected lysine derivative **82**. Deprotection of both the side chain and α -amine of the lysine gave resin-bound intermediate **125**, followed by treatment with diethylamine (DEA) was able to cleave the oligomer from the resin to produce compound **126**. The crude chromatogram of the cleavage mixture is shown in Figure 5.5 and shows the purity that can be obtained when using a cyclorelease strategy. (See also Chapter 4 for an additional synthesis on the HMBA resin of the helix mimics that proceeds with excellent crude purity.)

Therefore, another successful solid-phase synthetic strategy was developed, this time using the HMBA resin. Notable improvements of this strategy include the use of an inexpensive and commercially available resin/linker combination, the synthetic versatility of placing the cleaving residue last and the purity of the final product. This methodology will allow more *bis*-peptides to be rapidly synthesized and tested for interesting properties and was a noteworthy improvement which facilitated the synthesis of the helix mimic *bis*-peptides in Chapter 4.

Synthesis of tail to tail oligomers. One of the overarching goals of the Schafmeister group is the design and synthesis of shape programmable, highly functionalized molecules.² Since the *pro4* amino acids are *bis*-amino acids (they have two orthogonal sets of amino acids mounted on a cyclic core) there exists the opportunity for even more architectural motifs by reversing the building blocks and connecting the prolinyl amino acid sides to each other. This is shown schematically in Figure 5.6 and highlights how the building block approach, coupled with rational design and judicious protecting group manipulation, can create different architectures for various applications.

A functionalized *pro4* amino acid is shown in the center of Figure 5.6 with the two amino acid cores highlighted. The quaternary amino acid half is referred to the “head” in the Schafmeister group because this is the conventional direction of oligomer building. The other

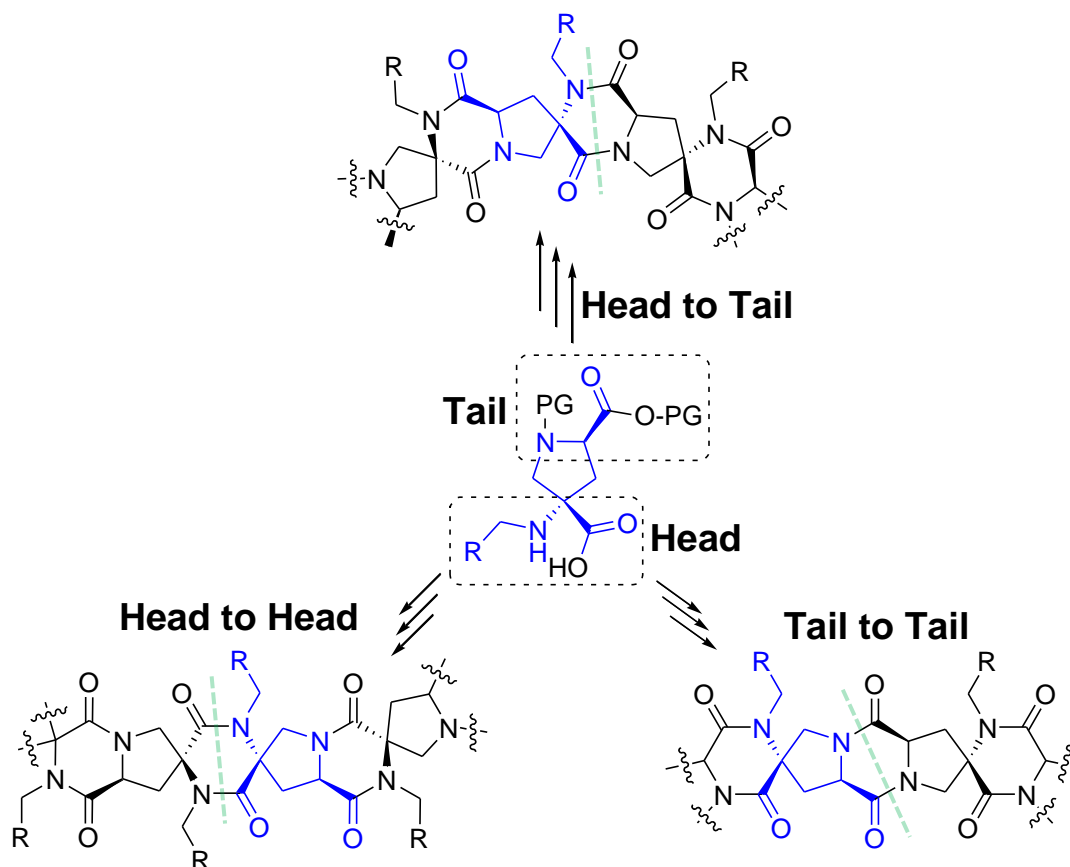


Figure 5.6. Schematic showing how a *pro4* monomer may be coupled in various ways to form different architectures.

side, the prolinyl amino acid, is referred to as the “tail” to distinguish it from the head as it is on the opposite side of oligomer elongation. As will be shown, by synthetic manipulation of the monomer each adjacent pair of *bis*-amino acids can be combined in three different ways. Two we have seen in Chapter 3, the “Head to Tail” of the functionalized oligomers (pentasubstituted diketopiperazines) and the “Head to Head” of both the symmetric and the asymmetric hexasubstituted diketopiperazines. Finally there is the “Tail to Tail” motif which forms a tetrasubstituted diketopiperazine and could align the functional groups directly at each other, an additional structure that may prove valuable in future applications.

This “Tail to Tail” motif is the least straightforward architecture to access from the current *pro4* monomer synthesis. In the final step of the monomer synthesis (see Figure 5.1), the “head” amino acid group is formed after the hydrolysis of the hydantoin while the “tail” (pyrrolidine

amino acid side) remains protected. Thus, synthetic manipulation of the “tail” requires more steps and some exploratory chemistry was required.

The first synthetic target for a “Tail to Tail” motif, compound **127**, is shown in Figure 5.7. Two functional groups for the oligomer, that of a carboxylic acid and a phenol, were chosen as representative proteogenic side chains. These two groups also had the synthetic challenge of being reactive groups so they would need to be protected through the course of the oligomer assembly. The *pro4* fragments necessary to construct this oligomer are also shown in Figure 5.7, with the left hand side “tail”, compound **128**, being protected with an Alloc group so that the carboxylic acid can be activated for coupling. The right hand side “tail”, compound **129**, can then

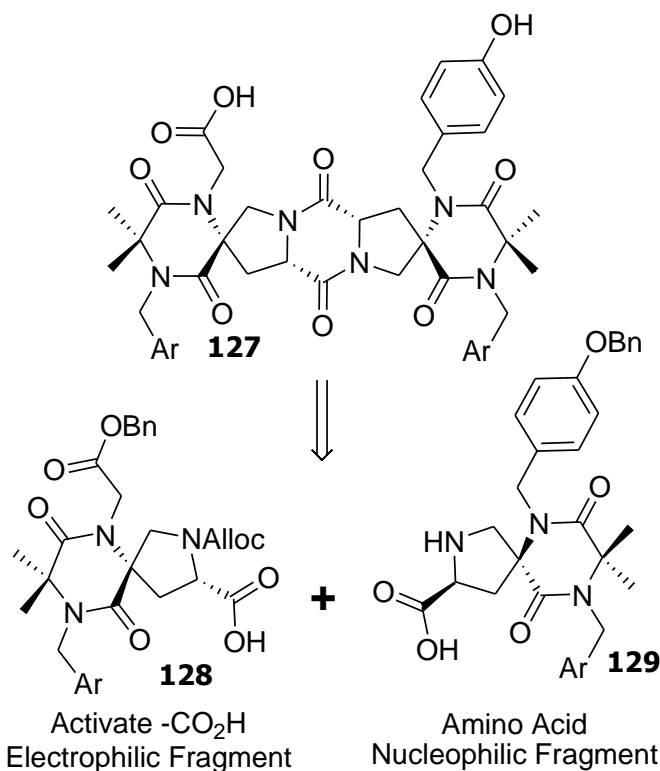


Figure 5.7. Retrosynthetic analysis of a “Tail to Tail” oligomer showing the two *pro4* fragments which need to be assembled. Ar = Aryl group (Naphthyl).

be used as the nucleophilic amino acid to couple with the electrophilic fragment. It should be said that for the purposes of this synthesis, either fragment could serve as the nucleophilic or electrophilic portion; the choices made here were purely based on synthetic convenience.

Starting from the Boc/*t*-butyl *pro4* amino acid **108**, the protected carboxylic acid was installed using glyoxylate **130** (the procedure is outlined in Chapter 3).⁴⁸ This functionalized *pro4* amino acid monomer **131** was then activated to form the amino-OAt ester using the 1:1:6 amino

acid/DIC/HOAt protocol and coupled to the Aib derivative compound **132**. After an overnight reaction at room temperature, an additional aliquot of DIC was added to convert any residual single amide product to the corresponding diketopiperazine, compound **133**. Here again we see another application of this new acyl-transfer coupling since these asymmetric hexasubstituted diketopiperazines are a significant synthetic challenge. Next the Boc and *t*-butyl groups were simultaneously removed by the addition of TFA. The pyrrolidine nitrogen was then reprotected, this time as the allyl carbamate group (Alloc) via allyl chloroformate to give fragment **128**. This completed the synthesis of the electrophilic fragment (the fragment which was going to be activated). The synthesis of the nucleophilic fragment, compound **129**, parallels the one just

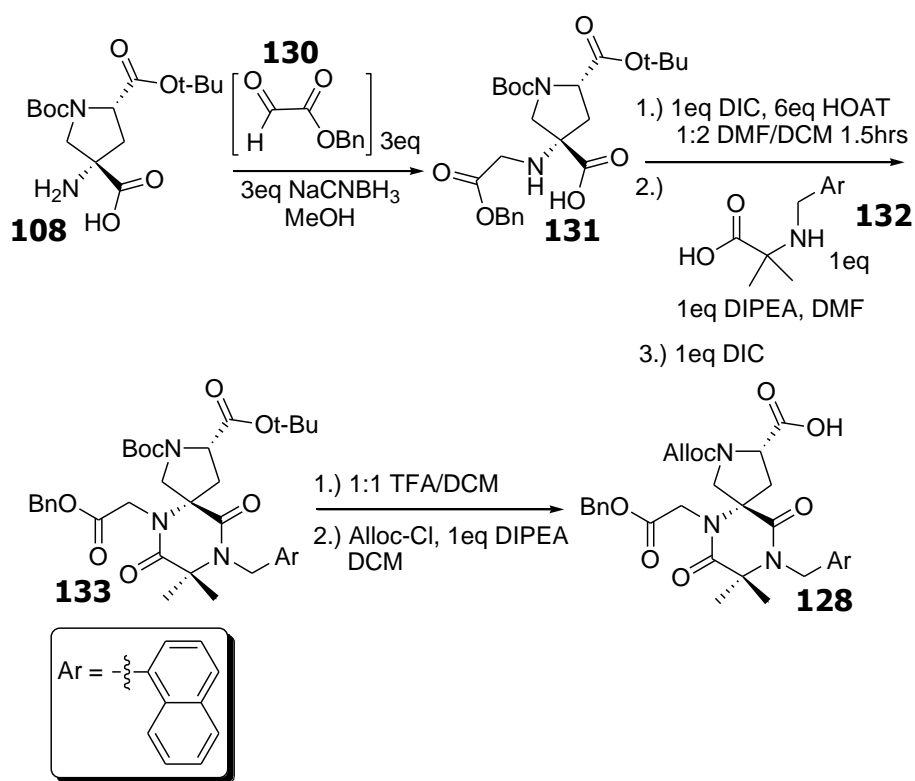


Figure 5.8. The synthesis of the electrophilic fragment for the “Tail to Tail” oligomer, compound **128**.

described but instead uses the *pro4* monomer with a benzyl protected phenol and terminates with the deprotection to the pyrrolidine amino acid to leave the prolinyl amino acid exposed.

Next the fragments **128** and **129** were joined to create the tetrasubstituted diketopiperazine between them; this chemistry is detailed in Figure 5.9. First the electrophilic fragment, compound **128**, was activated as the –OAt ester using the baseless DIC/HOAT strategy⁵⁰ in a DMF/DCM solvent mixture. Next the nucleophilic fragment, compound **129**, was

added with one equivalent of DIPEA. After 3 hours at room temperature, LC-MS characterization showed that the fragments had been coupled in a nearly quantitative yield to give protected intermediate **134**. Next the Alloc protecting group was removed using palladium(0) (in the form of palladium tetrakis(triphenylphosphine)) in the presence of the allyl scavenger borane dimethylamine.³⁵ At this stage the amino acid intermediate spontaneously cyclized to form diketopiperazine product **135**. This was a welcome result to not have to supply an exogenous activating agent to initiate full dehydration to achieve diketopiperazine **135**. Although not surprising giving the spontaneous nature of diketopiperazine formation with tertiary

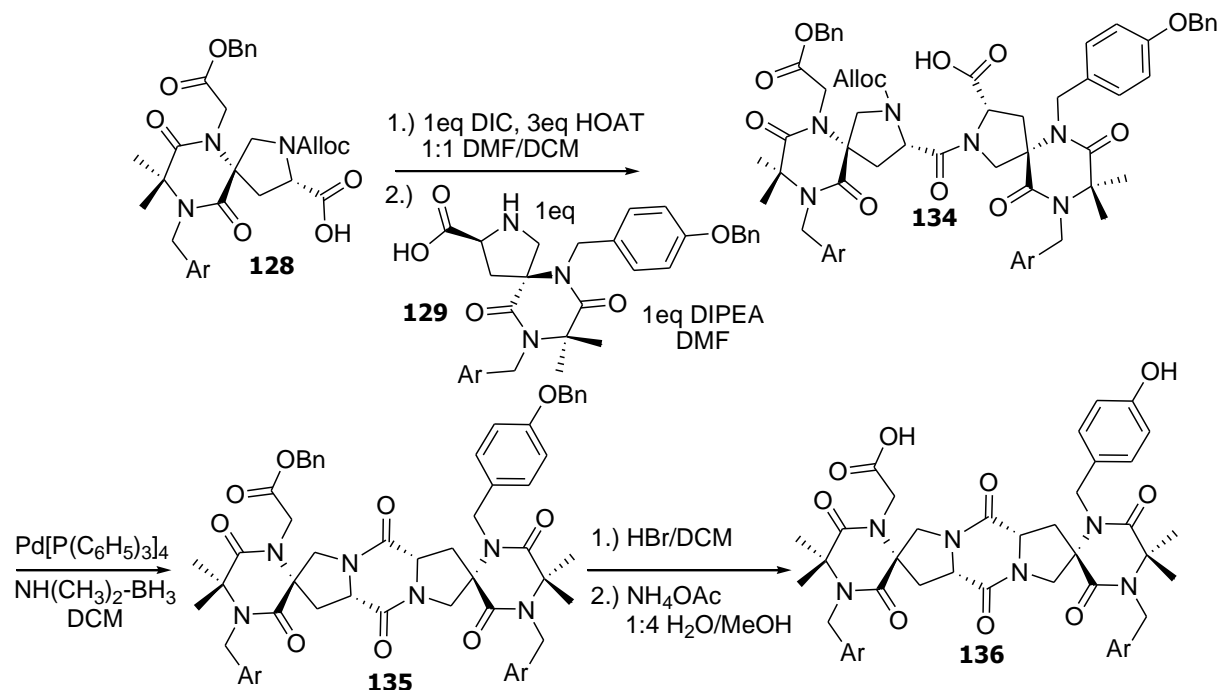


Figure 5.9. Synthesis of the “Tail to Tail” oligomer **136** by coupling of the “electrophilic” fragment **128** and the “nucleophilic” fragment **129**.

amides, it was still an open question as to how facile the closure would be for the diprolinyl system. Treatment of the fully protected oligomer with HBr in AcOH removed the benzyl ester, although it was found that these conditions also capped the phenolic oxygen with an acetate group. However, this acetate group was then easily removed by dissolving the material in a mixture of aqueous ammonium acetate and methanol with conventional heating overnight to generate the fully deprotected heterodimeric species, compound **136**.

Shown in Figure 5.10 is an Amber 94 minimized structure of compound **136**, the heterodimeric diketopiperazine. Here the fused cyclic core system of the pyrrolidine-diketopiperazine-rigidifies the molecule and points the phenol and the carboxylic acid toward the same face. This motif might be valuable in the synthesis of catalysts and other applications where the functional groups need to be aligned with each other.

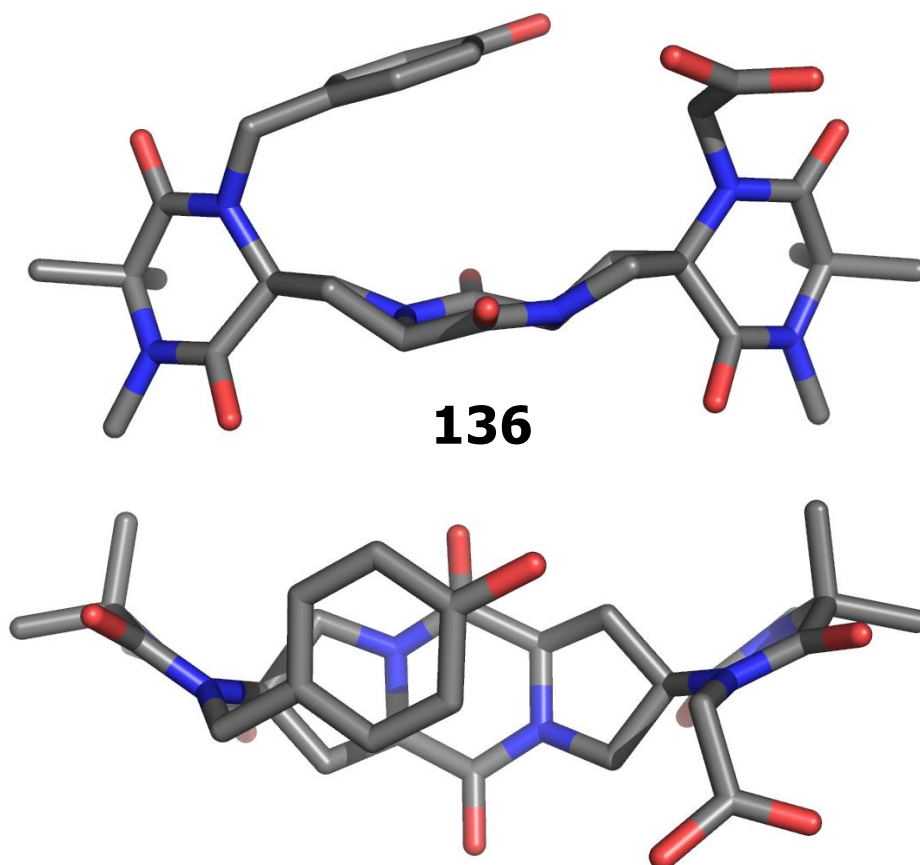


Figure 5.10. Amber 94 minimized structure of the “Tail to Tail” oligomer **136** showing the alignment of the functional groups. Hydrogens and naphthyl groups are omitted for clarity. Image created with PyMol.

A synthetic route towards the final coupling architecture was found to be straightforward and high-yielding. This strategy will be employed by future bis-peptide chemists during their construction of functional macromolecules.

5.3 Conclusion

This chapter has presented a few elaborations of the new *bis*-peptide assembly technique. For further synthetic versatility, the Boc-protected hydantoin was established as a more convenient protecting group for the *pro4* amino acid. Moving the solution-phase chemistry introduced in Chapter 3 to solid-phase allowed more compounds to be easily synthesized, and, coupled with a new cyclorelease strategy, produced clean material. This was critical to the synthesis of the set of helix-mimic bis-peptides presented in Chapter 4. Finally, a new coupling architecture was detailed, the “Tail to Tail” motif, which produced a tetrasubstituted diketopiperazine between the monomers and aligned the functional groups in a way that was not previously possible. These results will add to the already extensive toolbox of *bis*-peptide technology and will allow us to access more diverse *bis*-peptide structures.

5.4 Experimental Details

General Methods. Anhydrous Dichloromethane (DCM), anhydrous dimethylformamide (DMF), anhydrous Methanol (MeOH), HBr (33% in glacial AcOH) and redistilled Diisopropylethylamine (DIPEA) were obtained from Sigma-Aldrich and used without purification. Pd/C was obtained from Strem Chemicals. All amino acids were obtained from either Novabiochem or Bachem. HOAT was obtained from Genscript. All other reagents were obtained from Sigma-Aldrich and used without further purification.

HPLC-MS analysis was performed on a Hewlett-Packard Series 1200 with a Waters Xterra MS C18 column (3.5 μ m packing, 4.6 mm x 150mm) with a solvent system of H₂O/acetonitrile with 0.1% formic acid at a flow rate of 0.8mL/min. NMR experiments were performed on a Bruker Advance 500MHz NMR; NMR chemical shifts (δ) reported relative to DMSO-*d*₆ residual solvent peaks unless otherwise noted. When possible, rotamers were resolved by performing the analysis at 365K. Assignment of 2D NMR data was performed using Sparky 3, T. D. Goddard and D. G. Kneller, University of California, San Francisco.

RP-purification was performed on an ISCO (Teledyne, Inc.) automated flash chromatography system with a RediSep R_f-12gm RP column or on a Varian Prostar Prep HPLC with a Waters Xterra column (5 μ m packing, 19 mm x 100mm) with a solvent system of H₂O/acetonitrile with 0.1% formic acid at a flow rate of 18 mL/min. HRMS analysis was performed by Ohio State University Proteomics Research Facility (ToF/ES).

General Procedure for the Preparation of Functionalized Building Blocks. The functionalized *pro4* derivatives were prepared from the corresponding *pro4* amino acids using the method of reductive alkylation as described in Chapter 3. The building blocks were then reverse-phase purified and the desired fractions pooled and lyophilized and used in the activation procedure as described below.

Pro4(S,S)-Boc-Hydantoin (compound 107). Pro4(S,S)-Cbz-Hydantoin (compound 106) was synthesized as described previously.² The starting material (3.00gm, 7.7mmole), Boc₂O (3.4gm, 15.4mmole), and Pd/C (150mg) was dissolved in tetrahydrofuran (77mL, conc. 100mM) and added to a 250mL flask with stirring to which a hydrogen balloon was fitted. The vessel was placed under vacuum to remove dissolved gases and backfilled with hydrogen multiple times. The reaction was performed overnight at room temperature. The reaction mixture was filtered through Celite, concentrated *in vacuo* and obtained as a white solid (2.46gm, yield 90%). LCMS analysis (5-95% H₂O/ACN with 0.1% formic acid): t_r= 17.1min; calcd for Entry 107+Na⁺: 378.2; found: 377.9. The product was not characterized further and taken to the next reaction.

Pro4(S,S)-Boc-amino acid (108). Pro4(S,S)-Boc-Hydantoin (compound 107) (5.0gm, 14.1mmole), DMAP (dimethylaminopyridine, 86mg, 0.7mmole), Boc-anhydride (9.2gm, 42.3mmole) and THF (210mL) were added to a 500mL round bottom flask and allowed to stir for 1.5hrs. The reaction mixture was then concentrated *in vacuo*, and the oil was dissolved in 56mL of THF. 2M potassium hydroxide (56mL) was then added with vigorous stirring and the reaction was allowed to proceed for 30 minutes. The reaction mixture was then transferred to a 500mL separatory funnel and 200mL of diethyl ether was added. The aqueous layer was then transferred to a beaker and cooled to 0°C in an ice bath. 2M HCl was then added dropwise until pH~7. The product was then filtered through a Buchner funnel and dried under high vacuum at 50°C to yield a white solid (3.21gm, 69% yield). ¹H NMR (500 MHz, DMSO-*d*₆, 365K, δ= 4.24 (t, 1H, *J*=8.33Hz), 4.00 (d, 1H, *J*=11.3Hz), 3.61 (d, 1H, *J*=11.3Hz), 2.81 (dd, 1H, *J*=8.67,4.62Hz), 2.32 (dd, 1H, *J*=8.02,5.35Hz), 1.47 (s, 9H), 1.41 (s, 9H). ¹³C NMR (500 MHz, DMSO-*d*₆, 365K), δ 170.8, 158.6, 153.4, 82.1, 80.4, 60.8, 59.5, 53.4, 37.3, 28.4 (3C), 28.1 (3C).

General Procedure for Removal of Boc and *t*-Butyl Groups. The Boc and *t*-Butyl ester protecting groups were simultaneously cleaved from the resin bound oligomer by treatment with 95% trifluoroacetic acid (TFA) with 5% triisopropylsilane (TIS) used as a scavenger. The deprotection was allowed to proceed for one hour, washing the resin 5x with DCM, and then the

deprotection was repeated for an hour. The resin was then washed 5x with DCM, 5x with DMF, and neutralized with 5% DIPEA in DMF.

General Procedure for Removal of Fmoc Group. Fmoc deprotection was conducted by treatment of the resin with 20% piperidine in DMF for 5 minutes, washing the resin 5x with DMF, treatment with 20% piperidine in DMF for 15 minutes, and finally washing the resin 5x with DMF.

General Procedure for *Bis*-Amino Acid Activation and Coupling. The *bis*-amino acid to be activated (3eq relative to resin loading) was suspended in a 1:2 mixture of DMF:DCM (conc. of 50mM) followed by HOAT (6eq relative to amino acid). With stirring, the diisopropylcarbodiimide (DIC, 1eq relative to amino acid) was then added and the activation allowed to proceed for 1.5 hours at room temperature. The resin was then suspended in a minimal amount of DMF (~200 μ L), and DIPEA (2eq relative to resin loading) was added. The preactivated amino-OAt ester was then added in a single portion and allowed to react for the specified amount of time. The resin was then washed 3x with DCM and then 3x with DMF. The resin was then treated with an additional aliquot of DIC (5eq relative to resin loading) and HOAT (5eq relative to resin loading) in a 1:2 DCM:DMF mixture and allowed to react for 1 hour to convert any of the single amide product into the corresponding diketopiperazine.

Solid Phase Synthesis of Oligomer 122 (Using the Serine-Based Linker). 60mg of Amino-PEG resin (0.6mmole/gm resin loading, 36 μ mole) was charged to a 4mL solid phase reactor and agitated using a magnetic stir bar and thoroughly washed with DCM. Fmoc-(L)-Ser(OTrt)-OH, (108 μ mole, 62mg) and HATU (108 μ mole, 41mg) were combined in DMF (540 μ L, conc. of 200mM); DIPEA (216 μ mole, 38 μ L) was added and the reaction mixture allowed to sit for 10 minutes. The preactivated species was then added to the resin and allowed to react for one hour, followed by thorough washing of the resin with 5x DMF, and then 5x with DCM. The Fmoc group was removed using the "General Procedure for the Removal of the Fmoc Group" and the amine was capped using an excess of acetic anhydride (720 μ mole) in 1mL of DMF in the presence of DIPEA (216 μ mole, 38 μ L). The side chain trityl protecting group of the serine was then removed using 10x 1mL of 5% TFA in the presence of the silane scavenger 5% TIS to give compound **109**. The first residue Fmoc-BromoPhenylalanine-OH, compound **110**, (108 μ mole, 65mg), MSNT (1-(2-Mesitylenesulfonyl)-3-nitro-1H-1,2,4-triazole, 108 μ mole, 32mg) and *N*-methyl-imidazole (83 μ mole, 7 μ L) were dissolved in 0.7mL of DCM (anhydrous), added to the

resin, and allowed to react for 2 hours. The Fmoc group was then removed using the “General Procedure for Removal of Fmoc Groups”. The first *bis*-amino acid, compound **75** (108μmole, 60mg) was activated using HATU (108μmole, 41mg) were combined in DMF (540μL, conc. of 200mM); DIPEA (216μmole, 38μL) was added and the reaction mixture allowed to sit for 10 minutes. The preactivated species was then added to the resin and allowed to react for one hour, followed by thorough washing of the resin with 5x DMF, and then 5x with DCM followed by deprotection using the “General Procedure for Removal of Boc and *t*-Butyl Groups”.

The next *bis*-amino acid, naphthyl functionalized *bis*-amino acid **113** (108μmole, 51mg), was activated and coupled for 3 hours using the “General Procedure for Bis-Amino Acid Activation and Coupling” followed by deprotection using the “General Procedure for Removal of Boc and *t*-Butyl Groups”. The next *bis*-amino acid, isobutyl functionalized *bis*-amino acid **116** (108μmole, 42mg), was activated and coupled for 3 hours using the “General Procedure for Bis-Amino Acid Activation and Coupling” followed by deprotection using the “General Procedure for Removal of Boc and *t*-Butyl Groups”. Boc-(L)-Phe-OH, compound **118** (180μmole, 48mg) and HATU (180μmole, 69mg) were combined in DMF (0.9mL, conc. of 200mM); DIPEA (360μmole, 63μL) was added and the reaction mixture allowed to sit for 10 minutes. The preactivated species was then added to the resin and allowed to react for one hour, followed by thorough washing of the resin with 5x DMF, and then 5x with DCM. The Boc group was then removed with 1.5mL of 1:1 TFA in DCM for 20 minutes, followed by washing of the resin with 5x DCM and repeating the Boc deprotection treatment. The resin was then washed 5x with DCM, 5x with DMF, and neutralized with 5% DIPEA in DMF. A ninhydrin test was positive, which indicated the presence of a primary amine. The resin was then treated with an additional aliquot of DIC (5eq relative to resin loading) and HOAT (5eq relative to resin loading) in a 1:2 DCM:DMF mixture and allowed to react for 1hour. A subsequent ninhydrin test was negative, which indicated the diketopiperazine had been closed and the secondary amide had been formed.

The resin was then washed 5x with DCM and 5x with DMF. Removal of the Fmoc group using the “General Procedure for Removal of Fmoc Group” was initiated to give compound **121** followed by cleavage from the resin to give oligomeric *bis*-peptide **122**. The reaction was allowed to proceed overnight at room temperature. Finally, the material was RP-purified to give a single peak via LC-MS analysis with a mass consistent with the expected product (see Figure 5.4).

Solid Phase Synthesis of Oligomer 126 (Using the HMBA linker). 75mg of HMBA-AM resin (1.1mmole/gm resin loading, 83 μ mole) was charged to an 8mL solid phase reactor and agitated using a magnetic stir bar and thoroughly washed with DCM. The first bis-amino acid, compound **75**, (247 μ mole, 137mg), MSNT (1-(2-Mesitylenesulfonyl)-3-nitro-1H-1,2,4-triazole, 247 μ mole, 73mg) and *N*-methyl-imidazole (186 μ mole, 15 μ L) were dissolved in 1.2mL of DCM (anhydrous), added to the resin, and allowed to react for 2 hours. The *bis*-amino acid was then deprotected with 1.5mL of 95% TFA using the “General Procedure for Removal of Boc and *t*-Butyl Groups”.

The first *bis*-amino acid, isobutyl functionalized amino acid **116** (247 μ mole, 96mg), was activated and coupled for 3 hours using the “General Procedure for Bis-Amino Acid Activation and Coupling” followed by deprotection using the “General Procedure for Removal of Boc and *t*-Butyl Groups”. The next *bis*-amino acid, naphthyl functionalized amino acid **123** (247 μ mole, 117mg), was activated and coupled for 3 hours using the “General Procedure for Bis-Amino Acid Activation and Coupling” followed by deprotection using the “General Procedure for Removal of Boc and *t*-Butyl Groups”. Boc-(L)-Phe-OH, compound **118** (413 μ mole, 110mg) and HATU (413 μ mole, 158mg) were combined in DMF (2.1mL, conc. of 200mM); DIPEA (825 μ mole, 144 μ L) was added and the reaction mixture allowed to sit for 10 minutes. The preactivated species was then added to the resin and allowed to react for one hour, followed by thorough washing of the resin with 5x DMF, and then 5x with DCM. The Boc group was then removed with 1.5mL of 1:1 TFA in DCM for 20 minutes, followed by washing of the resin with 5x DCM and repeating the Boc deprotection treatment. The resin was then washed 5x with DCM, 5x with DMF, and neutralized with 5% DIPEA in DMF. A ninhydrin test was positive, which indicated the presence of a primary amine. The resin was then treated with an additional aliquot of DIC (5eq relative to resin loading) and HOAT (5eq relative to resin loading) in a 1:2 DCM:DMF mixture and allowed to react for 1hour. A subsequent ninhydrin test was negative, which indicated the diketopiperazine had been closed and the secondary amide had been formed. The resin was then washed 5x with DCM and 5x with DMF.

The Fmoc group was removed using the “General Procedure for Removal of Fmoc Group”. Boc-(L)-Lys(Fmoc)-OH, compound **82** (413 μ mole, 193mg) and HATU (413 μ mole, 157mg) were combined in DMF (2.1mL, conc. of 200mM); DIPEA (825 μ mole, 144 μ L) was added and the reaction mixture allowed to sit for 10 minutes. The preactivated species was then added to the resin and allowed to react for 1hour, followed by thorough washing of the resin with 5x DMF, and then 5x with DCM. The Fmoc group was then removed from the lysine side chain using the “General Procedure for Removal of Fmoc Group”. The Boc group was then removed

with 1.5mL of 1:1 TFA in DCM for 20 minutes, followed by washing of the resin with 5x DCM and repeating the Boc deprotection treatment to give resin-bound oligomer **125**. The oligomer was then cleaved from the resin with 10% DIPEA in DMF (total of 1.5mL of solution) overnight at room temperature. For LC-MS analysis, see Figure 5.5.

***N*-Naphthyl-Aib (compound 132)**. Amino-isobutyric acid (Aib, 1.5gm, 14.6mmole) was charged to a 250mL round bottom flask and 70mL (conc. of 200mmole) of anhydrous MeOH was added followed by 1-Naphthylaldehyde (2.4mL, 17.5mmole) and the reaction was allowed to stir for 45 min at 55°C. Next, NaCNBH₃ was added (1.4gm, 22mmole) and the reaction was stirred overnight with conventional heating at 55°C. The reaction mixture was then concentrated *in vacuo* and the viscous oily residue was suspended in minimal 1:1 H₂O/ACN and RP-Purified, and the desired fractions pooled and lypholized to yield compound (2.1gm, 58% yield). LC-MS analysis, (5-95% H₂O/ACN with 0.1% formic acid) compound **132**: t_r=9.6min., calced. for compound(**132**)+H⁺= 244.1; found: 244.2.

“Electrophilic Fragment” Compound 128. The synthesis of the electrophilic fragment for the “Tail to Tail” coupling began with the functionalized *pro4*(2*S*,4*S*) amino acid derivative whose synthesis was already described in Chapter 3. This functionalized *bis*-amino acid, compound **131**, (450mg, 940μmole) was activated with the “General Procedure for Bis-Amino Acid Activation and Coupling”. Meanwhile, *N*-Naphthyl-Aib (compound **132**, 274mg, 1.1mmole) was dissolved in DMF (5mL) and DIPEA was added (2.2mmole, 384μL). After the *pro4* derivative **131** had been activated for 1.5 hours, these two solutions were combined and allowed to react overnight at room temperature. An additional aliquot of DIC was then added and the reaction was allowed to proceed for another 3 hours to convert any remaining single amide product into the desired hexasubstituted diketopiperazine, compound **133**. The reaction mixture was concentrated *in vacuo* to remove most of the DCM and the residue was suspended in EtOAc followed by washing 3x with saturated NH₄Cl, 3x with NaHCO₃ and then brine. The crude product was then concentrated to yield a white solid (88% yield, 830μmole). LC-MS analysis, (5-100% H₂O/ACN with 0.1% formic acid) compound (**133**): t_r=29.3min., calced. for compound(**133**)+Na⁺= 708.3; found: 708.3. The fully protected compound **133** was then dissolved in 30mL of DCM followed by the addition of 30mL of TFA and the reaction was allowed to stir at room temperature for 4 hours. The reaction mixture was concentrated under reduced pressure, the residue resuspended win DCM and rotovapped to dryness 3 times to remove a majority of the TFA. Finally, the residue was suspended in a minimal amount of 1:1

H₂O/ACN and RP-purified; the desired fractions were pooled and lyophilized to yield amino acid **sc1**. (55% yield, 240mg) $t_r=16.8\text{min.}$, calced. for compound(**sc1**)+H⁺= 530.2; found: 530.2. The pyrrolidine nitrogen of amino acid intermediate **sc1** was then protected as the Alloc derivative. Amino acid **sc1** (210mg, 397 μmole) was suspended in DCM, one equivalent of DIPEA (397 μmole , 69 μL) was then added followed by one equivalent of allyl chloroformate (397 μmole , 42 μL). The reaction was allowed to proceed at room temperature overnight. The reaction was worked up by first removing most of the DCM under reduced pressure, suspending the residue in EtOAc and washing 3 times with saturated NH₄Cl and then brine. (93% yield, 226mg) $t_r=22.9\text{min.}$, calced. for compound(**128**)+H⁺= 614.2; found: 614.2. The material was not purified or characterized further and used directly in the next coupling reaction.

“Nucleophilic Fragment” Compound 129. The synthesis of the nucleophilic fragment for the “Tail to Tail” coupling parallels that of the electrophilic fragment **128** above and so will only be described briefly. The Benzyl-protected phenol functionalized *pro4(2S,4S)* amino acid **sc2** (330mg, 628 μmole) was activated with the “General Procedure for Bis-Amino Acid Activation and Coupling” and coupled with *N*-Naphthyl-Aib **132** (compound, 183mg, 753 μmole) in DMF (5mL) with DIPEA (1.5mmole, 262 μL). After work-up, Yield 86% (396mg of hexasubstituted diketopiperazine). LC-MS analysis, (5-100% H₂O/ACN with 0.1% formic acid) compound (**sc3**): $t_r=31.3\text{min.}$, calced. for compound(**sc3**)-Boc+H⁺= 634.4; found: 634.3. The fully protected compound was then deprotected as above with 1:1 TFA/DCM, followed by multiple resuspensions and concentrations to remove the majority of the TFA. The residue was suspended in a minimal amount of 1:1 H₂O/ACN and RP-purified; the desired fractions were pooled and lyophilized to yield amino acid. (51% yield, 159mg) $t_r=19.6\text{min.}$, calced. for compound(**sc4**)+H⁺= 578.3; found: 578.3.

“Tail to Tail” Coupling, Compound 136. Finally, the two fragments were coupled to produce the tetrasubstituted diketopiperazine **136**. First, the electrophilic portion **128** was activated using the baseless conditions DIC/HOAT. Briefly, electrophilic fragment **128** (120mg, 196 μmole) was suspended in 1:1 DCM/DMF (2mL total, conc. of 100mM) and 1 equivalent of DIC was added (31 μL , 196 μmole) and the activation was allowed to proceed for one hour. The nucleophilic fragment, compound **129**, (113mg, 196 μmole) along with one equivalent on DIPEA (34 μL , 196 μmole) was added to the activated residue and the reaction was allowed to proceed for 3 hours. LC-MS analysis, (5-100% H₂O/ACN with 0.1% formic acid) compound (**sc5**): $t_r=29.8\text{min.}$,

calced. for compound(**sc5**)+H⁺=1173.5; found: 1173.3. The Alloc deprotection was initiated directly in this vessel to the crude reaction mixture by the addition of tetrakis(triphenylphosphine)palladium(0) (0.2 equivalents, 45mg) and the allyl scavenger borane-dimethylamine (6 equivalents, 70mg) and the reaction was allowed to proceed for 2 hours at room temperature. LC-MS analysis revealed that spontaneous diketopiperazine closure has taken place in the alloc deprotection mixture: (5-100% H₂O/ACN with 0.1% formic acid) compound (**sc6**): t_r=29.1min., calced. for compound(**sc6**)+H⁺=1071.5; found: 1071.2. Benzyl deprotection was then initiated on the crude alloc deprotected material by the addition of 1:1 33% HBr/AcOH/DCM (20mL total) and the reaction was allowed to proceed for one hour. The crude reaction mixture was then concentrated under reduced pressure and resuspended in DCM several times to drive off most of the HBr. LC-MS analysis, (5-100% H₂O/ACN with 0.1% formic acid) compound (**sc7**): t_r=23.9min., calced. for Dimer of compound(**sc7**)+H⁺=1865.8; found: 1865.4. Under the highly acidic conditions of the benzyl deprotection (AcOH in the presence of HBr) the phenolic oxygen will be capped with an acetate group. This group is easily removed under mild conditions though. Compound **sc7** was suspended in 8mL of MeOH and 2mL of 0.8M NH₄OAc and the reaction was stirred overnight at 55°C using conventional heating. The reaction mixture was then concentrated under reduced pressure and RP-purified; the desired fractions were pooled and lyophilized to yield the Compound. Final Yield 23%, 40mg (after coupling and 3 deprotection steps). . LC-MS analysis, (5-95% H₂O/ACN with 0.1% formic acid) compound (**136**): t_r=23.9min., calced. for Dimer of compound(**136**)+H⁺=1781.8; found: 1781.3. See Appendix for NMR characterization.

Chapter 6

Asymmetric Macrocycles as Variable Size and Shape Molecular Receptors

In this chapter the solid-phase synthesis of a series of unfunctionalized *bis*-peptide macrocycles is presented. An exploration of their host-guest properties with an amphiphilic fluorescent dye illustrates that the building block approach to macrocycle construction can create different size hydrophobic cavities. These macrocycles, when combined with the methodology to functionalize bis-peptides, may yield powerful new designer macromolecules for molecular recognition or catalysis applications.

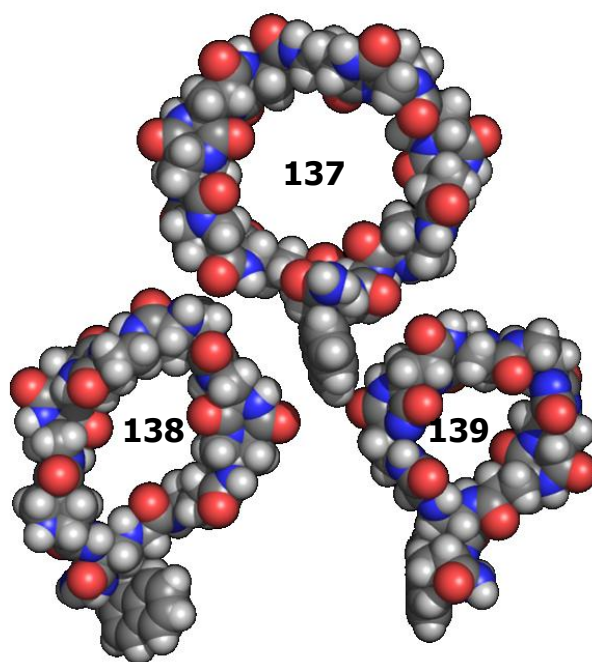


Figure 6.1. Space-filling representation of three macrocycles synthesized containing variable numbers of *bis*-amino acids. Compound **137** has a total of 8 pro4 building blocks, compound **138** has 6 building blocks and compound **139** has 4.

6.1 Introduction

Proteins have evolved complex shapes in order to carry out the immense number of complex tasks needed to sustain life. Perhaps most importantly in the aqueous environment of biology, is the ability to create a hydrophobic pocket to sequester substrates from solution and perform chemical reactions on them. With this encapsulation, the chemical environment can be very different from bulk solvent, and various reactions may be manipulated in ways not possible in an aqueous media.¹ Hydrophobic cavities can also provide substrate recognition and impart selectivity to the protein, allowing enzymes to select a certain substrate from the complex solution within a cell.

Host-guest chemistry is a rapidly evolving field which seeks to understand the principles of molecular recognition, for both synthetic, molecular design purposes as well as to elucidate the principles of noncovalent interactions which play such a large role in the world of biology.⁸² Binding phenomena are extremely solvent dependent, and many synthetic systems have been developed based on hydrogen-bonding between the host and the guest in an organic solvent. This presents a distinct challenge to work within an aqueous media where solvent will compete for hydrogen bonds.

Two examples of well-studied, organic macrocycles that may be synthesized in variable sizes are shown in Figure 6.2, the cyclodextrins and cucurbiturils. Beta-cyclodextrin (β -CD), compound **140**, is shown on the left, a cyclic oligosaccharide composed of seven α -D-glucopyranoside units. β -CD is a torus shaped macrocycle with a hydrophilic exterior, which

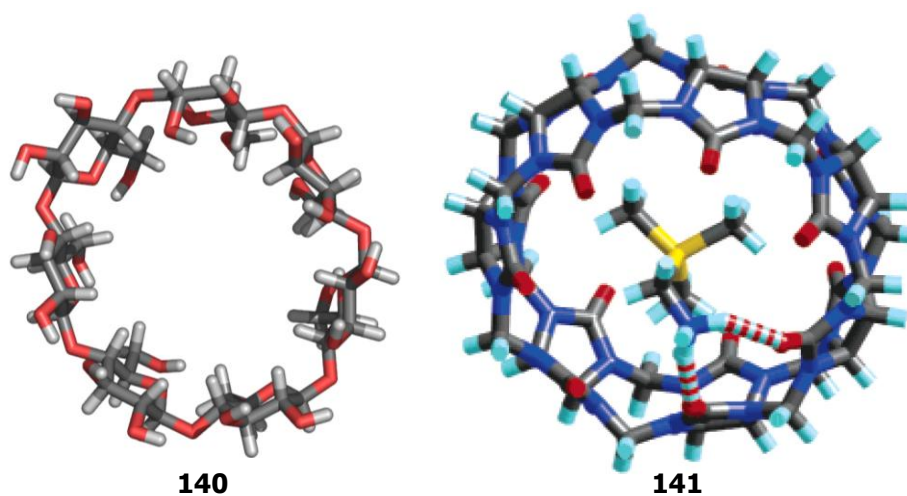


Figure 6.2. Two examples of variable size organic macrocycles from the literature. On the left is β -cyclodextrin, compound **140**, one of a series of cyclic oligosaccharide. On the right cucurbit[7]uril, compound **141**, with a bound guest, trimethylsilyl methylamine. Reproduced from ref. 38. Drawings are not to scale relative to each other.

imparts water solubility, and a hydrophobic interior to participate in host-guest chemistry.⁸³ An internal network of hydrogen bonds also imparts rigidity to the macrocycle. β -cyclodextrin is just one of a series of cyclic oligosaccharides, with the other common ones being α -cyclodextrin (composed of six α -D-glucopyranoside monomers) and γ -cyclodextrin (composed of eight α -D-glucopyranoside monomers). An example of the modular size of the cyclodextrins can be illustrated with their ability to complex a hydrophobic guest, ibuprofen, measuring their association constants by capillary electrophoresis: α -CD ($K_a=55 \text{ M}^{-1}$), β -CD ($K_a=2600 \text{ M}^{-1}$) and finally γ -CD ($K_a=59 \text{ M}^{-1}$).⁸³ Although many factors will contribute to molecular recognition, one of the most obvious is physical size of the hydrophobic cavity, and the ability to systematically alter that size is powerful. Another example of an organic macrocycle with a tunable size is compound **141** in Figure 6.2, a cucurbit[7]uril with a trimethylsilyl methylamine guest.⁸⁴ The cucurbiturils are a series of methylene-bridged glycouril units (the number in brackets represents the number of monomers), with the fused nature of the bicyclic system imparting significant structural rigidity.⁸⁵ An illustration of the inclusion properties of cucurbiturils is shown in Figure 6.2 on the right: the trimethylsilyl methylamine guest binds the cucurbit[7]uril **141** host with a K_a of 8.88×10^8 , but has no detectable binding to either the slightly smaller cucurbit[6]uril or slightly larger cucurbit[8]uril as determined by ^1H NMR.⁸⁴ This again highlights the influence of size in molecular recognition: similar chemical environments exist within the interiors of the respective series of either cyclodextrins or cucurbiturils, but the size of the macrocycle will significantly impact the binding affinities of the various guests.

The main drawback of these two families of macrocycles is the difficulty involved in adding arbitrary chemical functionality to them in a chemoselective and regioselective manner. This would allow a wider range of guests to be explored beyond those which have direct chemical complementarity to the macrocycle as well as extend their applicability to other supramolecular applications. Although much work on the selective modification of cyclodextrins exists, it is still a difficult task to specifically modify certain hydroxyl groups in the presence of all of the others.⁸⁶ The cucurbituril skeleton as well as the synthesis to achieve them also leaves little room for appending other chemical groups, and, to date, only aliphatic and aromatic groups have been placed on the macrocycles.⁸⁵

Our water-soluble, *bis*-peptide scaffolds are a promising platform for the construction of large, chiral macrocycles. The modular building block approach allows systematic variation of the size (through the number of monomers) and the shape (through the incorporation of different stereochemistry *bis*-amino acids) to tune the properties of the macrocycle for specific applications. Diverse chemical functionality may also be appended to the macrocycle in specific

places to impart differential recognition properties and assist in binding substrates through various interactions. Such macrocycles with rigid pockets may be able to sequester molecules from solution or be used as novel catalysts. Macrocyclic, hydrophobic architectures will be a significant milestone towards realizing the full potential of *bis*-peptide scaffolds as proteomimetic systems.

6.2 Results and Discussion

Solid-phase synthesis of the macrocycles. A total solid phase construction of the macrocycles, including the critical macrocyclization step, was developed. This allows variation of the constituent monomers (to control size and shape) as well as the addition of other functionality to the system. Although many different chemical routes could be implemented to affect the critical macrocyclization step, the derivatization of orthogonally protected amines proved to be high yielding and effective. With a number of orthogonal amine protecting groups commercially available,³⁵ selective unmasking and derivatization on solid phase is a robust method which allows construction of macrocycles. By converting one of the amines to an electrophilic site with an α -bromo acetyl group and using the other primary amine as a nucleophile to displace the halide, the on resin macrocyclization proceeded smoothly. Performing the cyclization step on the resin took advantage of the “pseudo-dilution” effect.⁸⁷ If attempting to close a macrocycle in solution, the reaction must be manipulated to favor intramolecular versus intermolecular attack, which could form dimers or even higher order oligomers. The conventional way to suppress the solution phase intermolecular attack is to use a high dilution of the material, usually in the low millimolar range. With the material anchored to the resin, it is physically unable to reach other molecules and therefore unable to do anything besides intramolecular attack. Also, after the cyclization step, the molecule must have the remaining protecting groups removed and the molecule rigidified by closing the diketopiperazines. Both of these steps are able to be performed on the resin, so that upon cleavage from the resin the completed molecule may be obtained.

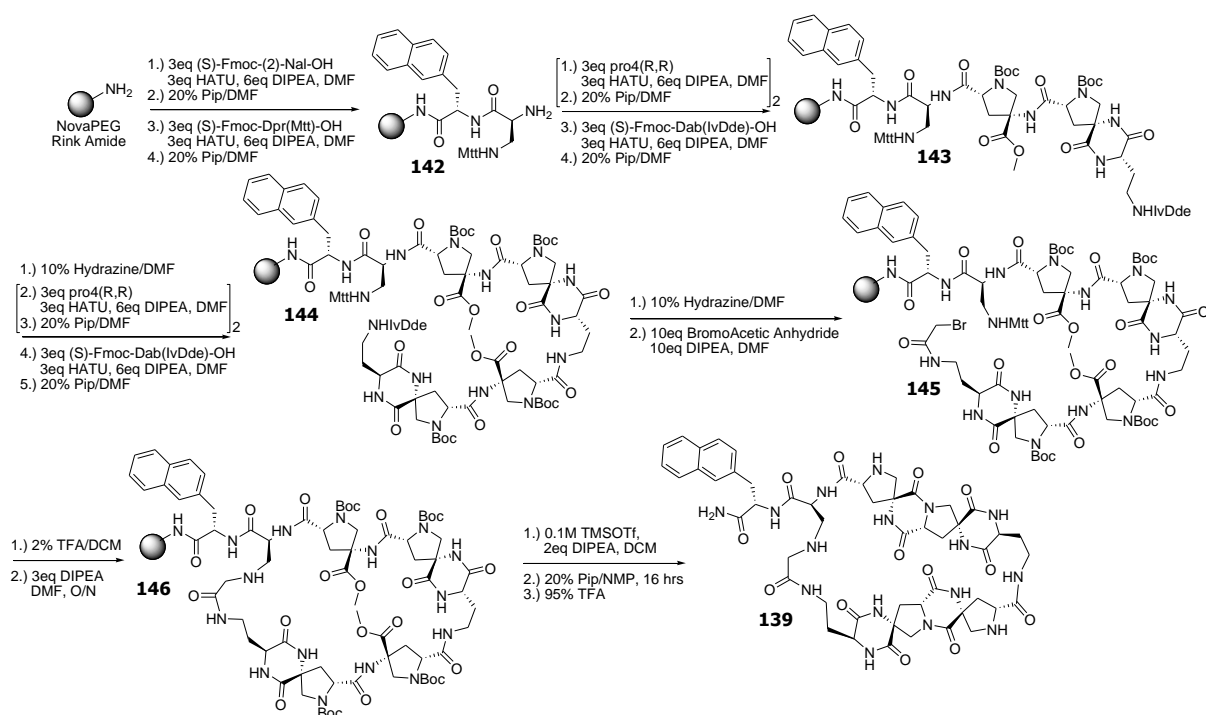


Figure 6.3. The solid phase synthetic scheme of the 2H2 macrocycle, compound **139**. Other size macrocycles (greater number of monomers) are synthesized in an analogous fashion by incorporating additional monomers.

A representative synthetic scheme for the smallest macrocycle (compound **139**, 2H2) is shown in Figure 6.3; other macrocycles were constructed in a similar fashion with only varying the number of monomers comprising each fragment. The solid phase construction begins with a polyethylene glycol (PEG) based resin⁷⁹ functionalized with a Rink Amide linker (cleavable with 95% trifluoroacetic acid). Linear Fmoc solid phase synthesis is used to install a chromophoric amino acid (here naphthylalanine) and then an orthogonal diaminopropionic acid (Dpr) residue (the amino side chain is protected with a weak acid cleavable methyl-trityl, Mtt, group) to give resin-bound intermediate **142**. Next, two *pro4*(2R,4R) monomers, followed by a diaminobutanoic acid (Dab) residue with the hydrazine cleavable dioxocyclohexylidene-based (IvDde) group on the amino side chain.³⁵ Upon deblocking the α -amino group with 20% piperidine, spontaneous diketopiperazine formation ensues by the primary amine attacking the previous *pro4*(2R,4R) monomer's methyl ester to give intermediate **143**. Linear chain extension then resumes after removal of the side chain amino protecting group, the IvDde group, with 10% hydrazine in DMF. The exposed primary amine is now used to construct the second *pro4* fragment of the macrocycle, with two *pro4*(2R,4R) monomers being followed by an additional Fmoc-Dab(IvDde)-

OH residue. Again, during the Fmoc removal of the Dab monomer, a diketopiperazine is formed with the previous *pro4* monomer in the same way as described above. Thus, the linear synthesis was completed with two orthogonal primary amines in compound **144**: one removed with weak acid (the Mtt group), and one removed with a basic nucleophile (the IvDde group). Macrocyclization was accomplished by first liberating the IvDde-protected amine with hydrazine, followed by converting it to an electrophile by the acylation with bromoacetic anhydride to install

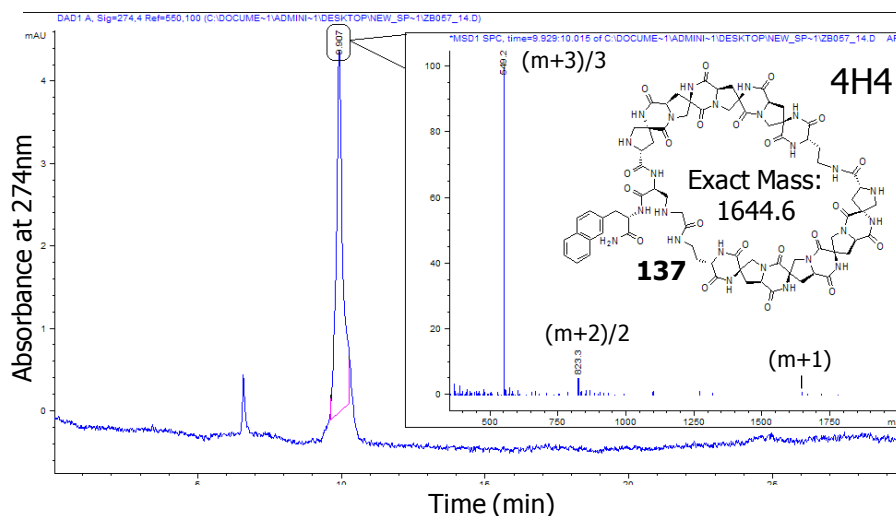


Figure 6.4. RP-HPLC chromatogram (0-50% H₂O/ACN with 0.1% formic acid) of the largest macrocycle synthesized, compound **137**, showing the major peak has a mass consistent with macrocycle **137** (calc. for compound **137** + H⁺ = 1645.6, found 1645.2).

an α -bromo acetate functionality to give protected electrophile **145**. Next, exposure of the second primary amine with 2% trifluoroacetic acid, and stirring the resin overnight with 3 equivalents of diisopropylethylamine gave quantitative macrocyclization as judged by LC-MS to give resin-bound macrocycle **146**. Quantitative cyclization was also monitored by the ninhydrin test: a negative test indicates all primary amines have been converted to secondary amines. On resin diketopiperazine closure between the monomers was accomplished by removal of the secondary amine Boc protecting groups using trimethylsilyl triflate (TMSOTf)⁸⁸ and subsequent stirring the resin overnight in 20% piperidine in DMF. Product release then resulted from exposure of the resin to 95% TFA with scavengers to give macrocycle **139**.

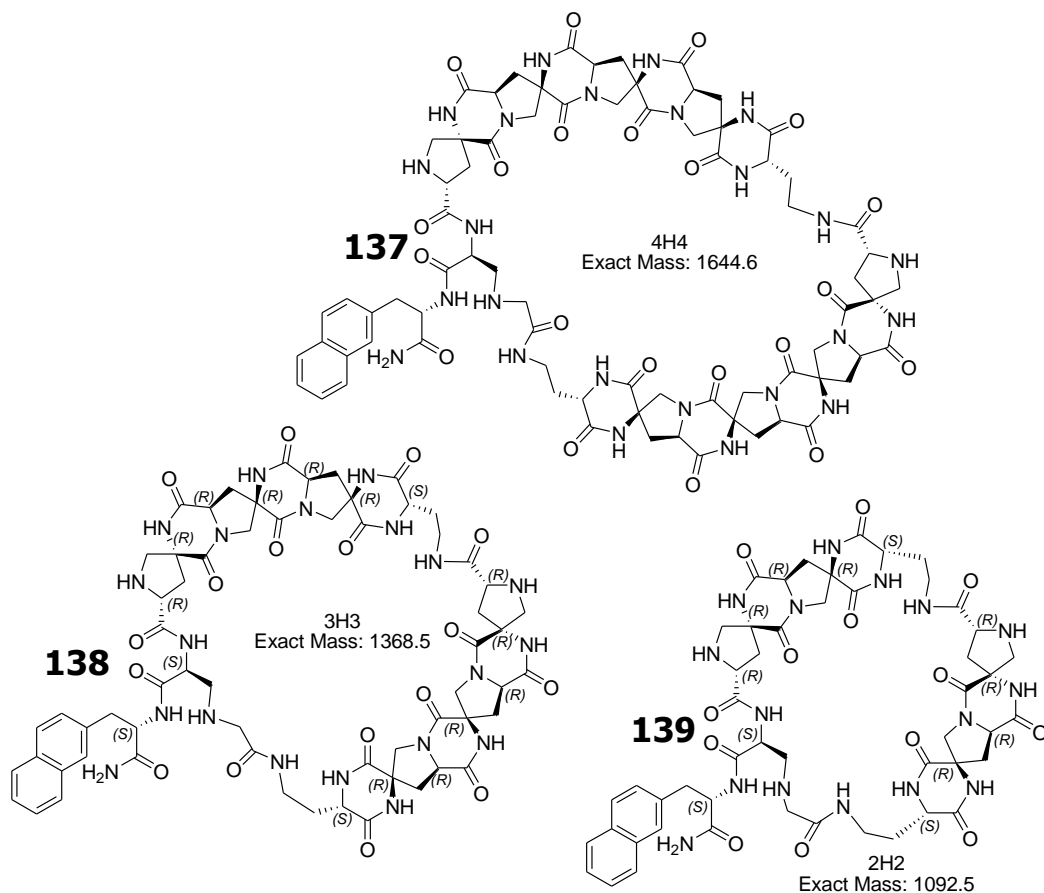


Figure 6.5. Examples of the variability of sizes of macrocycles already synthesized. The nomenclature xHy represents the number of building blocks of the first arm (x), the hinge designated by (H), and the number of building blocks of the second arm (y). For example, 4H4 means four monomers, an alkyl hinge, then an additional 4 monomers to give macrocycle **137**. All of the above structures were made using the same stereochemistry monomer: *pro4(2R,4R)*.

Three examples of macrocycles were synthesized using this methodology and their structures are shown in Figure 6.5, varying only the number of monomers in each fragment to create different size hydrophobic cavities within the macrocycle. All three macrocycles underwent on-resin cyclization and diketopiperazine closure smoothly, indicating this may be a general chemistry to synthesize a variety of distinct size and shape macrocycles by including other monomers. All three crude macrocycles were then purified by RP-HPLC. The HPLC chromatogram of the largest macrocycle synthesized (compound **137**), with the mass spectrum of the product as an inset, is shown in Figure 6.4.

It is unknown whether the cyclization step would proceed smoothly if the fragments were first rigidified via diketopiperazine closure; this awaits further mechanistic analysis. On the other hand, diketopiperazine closure seems to be more facile on the cyclized material, although

strict control reactions have not been performed yet. Interestingly, an unrigidified, but cyclized control was attempted of the largest macrocycle, the 4H4 (compound **137**) but not completely successful. After macrocyclization of the unrigidified intermediate, immediate cleavage from the resin was performed. Upon examination of the LC-MS trace, two of the internal diketopiperazines had been closed (data not shown). This indicates they must have undergone the intramolecular aminolysis during the resin cleavage step with trifluoroacetic acid, a reaction not previously seen in our group.

Molecular recognition of the macrocycles. To explore the molecular recognition capabilities of the macrocycles, the versatile fluorescent dye 8-anilino-naphthyl-sulfonic acid (ANS), compound **147**, was used. This dye is used to probe chemical environments in host-guest chemistry: in an aqueous environment, the fluorescence is quenched, but upon sequestration into a hydrophobic domain there is a dramatic increase in fluorescence. Aside from its use as a hydrophobic guest, ANS can also be used as a probe of protein folding.⁸⁹ An unfolded protein may have hydrophobic cavities that ANS may become sequestered in and subsequently fluoresce, while many proteins in their native states would not have such exposed hydrophobic pockets and so the fluorescence would be quenched. Here ANS is used to ascertain whether the macrocycles are both large enough to accommodate the dye as well as if

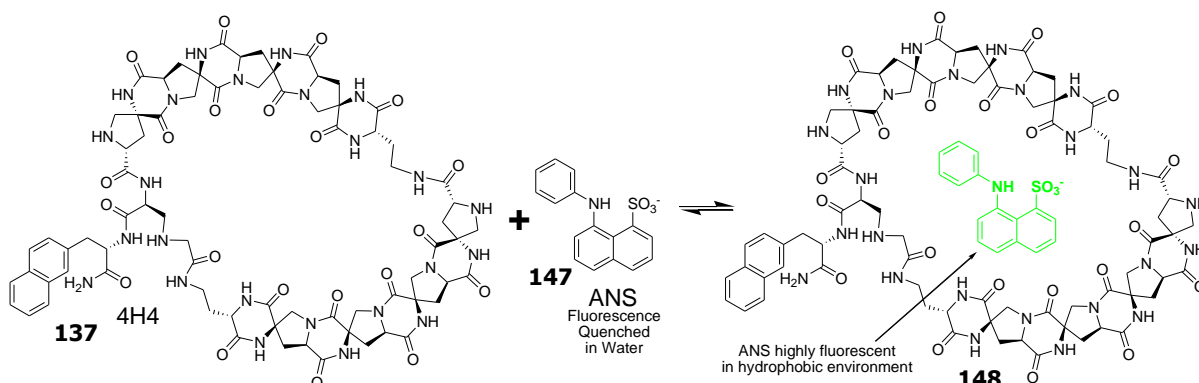


Figure 6.6. Schematic of how the amphiphilic dye ANS, compound **147**, becomes fluorescent upon its inclusion into a hydrophobic cavity when in an aqueous solvent.

a structured, hydrophobic environment is present and this is illustrated in Figure 6.6. Therefore, if the *bis*-peptide presents a large enough macrocycle to accommodate ANS then there will be a dramatic increase in the measured fluorescence.⁹⁰

A 1mM stock solution of ANS in 0.1M NaPO₄ was prepared and added to each of the macrocycles for a final concentration of 23μM ANS, while the final concentration of compound **137** was 60μM, compound **138** 370μM, and compound **139** 320μM. Emission fluorescence

spectra of each of the three solutions were then taken (excitation wavelength 365nm, recording emission from 400-700nm) and are shown in Figure 6.7 below.

Evident from the various spectra was the necessity of a large hydrophobic cavity to sequester the ANS dye from bulk solvent, initiating fluorescence. The smallest macrocycle, compound **139** (2H₂), shows only the background fluorescence of ANS, indicating no association between the host and guest. A small increase for the next macrocycle, compound **138** (3H₃), shows possible weak association between the macrocycle and dye, and was consistent with the hypothesis that compound **138** has a larger cavity than compound **139**. Compound **137** (4H₄) though, being the largest of the series of macrocycles, appeared to be large enough guest to accommodate the amphiphilic dye. Both a large increase in the fluorescence intensity as well as the expected hypsochromic shift of the spectrum indicated the largest macrocycle presents a hydrophobic cavity capable of complexing this organic molecule of modest size. Therefore, it has been shown that, consistent with the hypothesis of including greater numbers of building blocks within each fragment, larger hydrophobic cavities may be created for host-guest chemistry.

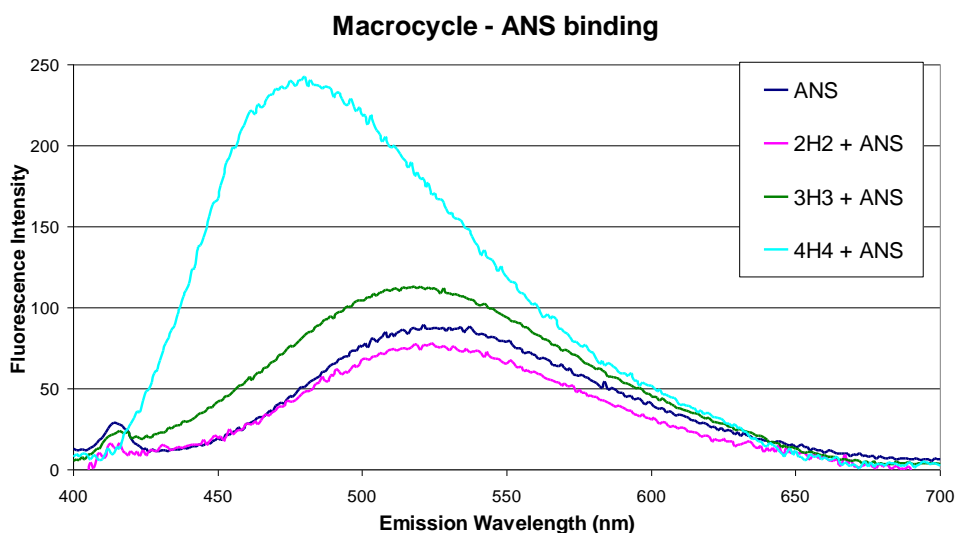


Figure 6.7. Fluorescence emission spectra of compound **137** –“4H₄” (60μM) and ANS (23μM), compound **138** –“3H₃” (370μM) and ANS (23μM), and compound **139** –“2H₂” (320μM) and ANS (23μM). All spectra recorded in 0.1M NaPO₄ buffer and are the average of at least three scans.

6.3 Conclusion

A modular, total solid-phase construction of a series of variable size macrocycles composed of *bis*-amino acids has been shown. The critical macrocyclization step, a halide displacement from an α -bromoacyl group by a primary amine, proceeded smoothly and quantitatively on the resin. The macrocycles were shown have differential binding properties toward the same amphiphilic dye, ANS, based on the size of the hydrophobic cavity. This design scheme provides a readily modifiable architecture which can be used to append other chemical functionalities for designed catalytic or molecular recognition purposes.

Variable shape macrocycles could be created by incorporating some of the other fourteen building blocks our research group has developed synthetic access to. Thus, inclusion of other *bis*-amino acids should allow synthetic access to a wide range of macromolecular scaffolds.

6.4 Experimental Details

General Methods. Trifluoromethanesulfonic acid trimethylsilylester (TMSOTf), hydrazine (45% aqueous solution), bromoacetic anhydride, *N*-methyl-pyrrolidinone, 8-anilino-naphthylsulfonic acid (ANS) were obtained from Sigma-Aldrich and used without purification. All Fmoc-amino acids, HATU and NovaPEG Rink Amide resin were obtained from Novabiochem or Acros Organics. Fluorescence emission spectra were obtained on a Cary Eclipse fluorescence spectrophotometer.

Solid Phase Synthesis of Macrocycles.

General Procedure for Residue Coupling. All coupling reactions employed a three-fold excess of the residue (180 μ mole), three-fold excess of HATU (180 μ mole), and six-fold excess of DIPEA (360 μ mole). In a typical reaction, the amino acid and HATU were dissolved in DMF (900 μ L, concentration of 200mM) and then DIPEA was added. The solution was allowed to stand at room temperature for 10 minutes to ensure complete activation before adding it to the resin. The coupling reactions were allowed to proceed for a minimum of 45 minutes, followed by a thorough washing of the resin with 3x DCM and 3x DMF. For all acylation reactions here, double couplings were employed.

General Procedure for Fmoc Removal. Except when noted, the terminal Fmoc group was removed using 1.5mL of 20% piperidine in DMF for 30 minutes. The resin was subsequently washed with 3x DMF and 3x DCM.

Synthesis of Bis-Peptide Macrocycles. PEG Rink Amide (100mg, resin loading 0.6mmole/gm, total of 60 μ moles of resin bound amines) was charged to a 10mL polypropylene solid phase reactor and the resin was swelled in 1mL of DCM for one hour.

The following amino acids were coupled for all macrocycles in this order using the general procedure for residue coupling followed by the general procedure for Fmoc removal: Fmoc-(S)-2-Naphthylalanine-OH, Fmoc-(S)-Diaminopropionic Acid-OH (side chain protecting group: methyl-trityl), *pro4(2R,4R)* monomer and finally another *pro4(2R,4R)* monomer.

For the 3H3 and 4H4 macrocycles, either one or two additional *pro4(2R,4R)* monomers were coupled using the general procedure followed by the Fmoc removal using the general procedure.

Next, for all macrocycles Fmoc-(S)-Diaminobutanoic acid-OH (side chain protecting group: IvDde) was coupled using the general procedure followed by Fmoc removal using 1.5mL of 20% piperidine in DMF. This deprotection reaction was allowed to proceed for 2 hours to close the diketopiperazine with the previous *pro4(2R,4R)* monomer. The resin was subsequently washed with 3x DMF and 3x DCM. The primary amine of the side chain of the diaminobutanoic acid residue was then exposed by suspending the resin in 1mL of 10% hydrazine in DMF for 1 minute and repeating this hydrazine treatment nine more times. The resin was then thoroughly washed with 5x DMF and 5x DCM. Two additional *pro4(2R,4R)* monomers were then coupled using the general procedure followed by the Fmoc removal using the general procedure.

For the 3H3 and 4H4 macrocycles, either one or two additional *pro4(2R,4R)* monomers were coupled using the general procedure followed by the Fmoc removal using the general procedure.

Next, for all macrocycles Fmoc-(S)-Diaminobutanoic acid-OH (side chain protecting group: IvDde) was coupled using the general procedure followed by Fmoc removal using 1.5mL of 20% piperidine in DMF. The deprotection reaction was allowed to proceed for 2 hours to close the diketopiperazine with the previous *pro4(2R,4R)* monomer. The resin was subsequently washed with 3x DMF and 3x DCM. The primary amine of the side chain of the diaminobutanoic acid residue was then exposed by suspending the resin in 1mL of 10% hydrazine in DMF for 1 minute and repeating the hydrazine treatment nine more times. The resin was then thoroughly washed with 5x DMF and 5x DCM.

To install the α -bromo acyl group on the exposed primary amine of the diaminobutanoic acid, bromoacetic anhydride (155mg, 600 μ mole) was dissolved in 1.5mL of DMF in a 15mL polypropylene tube and 209 μ mole of DIPEA was added. This solution was then immediately added to the resin and the reaction was allowed to proceed for 45 minutes followed by washing with 3x DMF and 3x DCM. The reaction was then repeated.

The methyl-trityl group of the diaminopropionic acid residue was then removed by suspending the resin in 1mL of 2% trifluoroacetic acid in DCM for 1 minute and repeating the TFA treatment nine more times. The resin was then thoroughly washed with 5x DCM and 5x DMF and then neutralized with 5% DIPEA in DMF.

All macrocycles were then cyclized by suspending the resin in 1mL of DMF with 31 μ L of DIPEA (180 μ mole) and then placing the reactor in a conventional oven at 55 $^{\circ}$ C overnight. The macrocyclization reaction may be monitored by the ninhydrin test: a negative test indicates a complete reaction by conversion of a primary amine (positive ninhydrin test) into a secondary amine (negative ninhydrin test).

The Boc protecting groups on the secondary amines of the *pro4* building blocks were then removed on resin using a published procedure. Trifluoromethanesulfonic acid trimethylsilylester (TMS triflate, 81 μ L, 450 μ mole) and DIPEA (108 μ L, 622 μ mole) were dissolved in 1.5mL of anhydrous DCM and the solution was allowed to react for 20 minutes. The resin was washed with 3x DCM and the TMS triflate deprotection was repeated followed by washing with 3x DCM and 3x DMF.

The diketopiperazines between the *pro4*(2R,4R) monomers were then closed by suspending the resin in 1.5mL of 20% piperidine in *N*-methyl-pyrrolidine and placing the reactor in an oven overnight.

With the solid phase assembly completed, the scaffold was then cleaved from the resin. Prior to cleavage, the resin was thoroughly washed with 5x DMF, 5x DCM, 3x MeOH and then dried overnight *in vacuo*. Cleavage was accomplished with 1.5mL of 95% trifluoroacetic acid, 2.5% triisopropylsilane and 2.5% H₂O for 5 hours at room temperature. The cleavage cocktail was then removed with a stream of nitrogen, the residue suspended in 1mL of 1:3 ACN/H₂O and purified by preparatory HPLC. The desired fractions were pooled and lyophilized (Figure 14, Chapter 3 of the text shows the LCMS characterization of the largest macrocycle, the 4H4).

Macrocycle	Calc. Mass (M+2H⁺)/2	Found Mass
2H2 (four total building blocks)	547.3	547.2
3H3 (six total building blocks)	685.3	685.0
4H4 (eight total building blocks)	823.3	823.3

Table 6.1. Calculated and found masses for the three macrocycles synthesized.

Fluorescence Binding of ANS and Macrocycles. Fluorescence emission spectra were recorded on a Cary Eclipse Fluorescence Spectrometer with the excitation and emission slits set to 5nm. Emission was monitored from 400-700nm with an excitation wavelength of 365nm. The scan rate was set to 600nm/min, and the data was averaged with a minimum of five scans. Samples were measured in a 1cm quartz cell (NSG Precision Cells, Inc.). Background scans of the macrocycle in 0.1M NaPO₄ (pH=7.1) without ANS were subtracted from all data sets.

A stock solution of 200mM ANS was prepared in 0.1M NaPO₄ (pH=7.1). The lyophilized macrocycles were dissolved in 500μL 0.1M NaPO₄ (pH=7.1). The concentration of each macrocycle solution was determined using a previously determined calibration curve for the naphthyl chromophore. An aliquot of the ANS stock solution was added, and the concentration was adjusted with 0.1M NaPO₄ (pH=7.1) to produce the following working concentrations of the solutions: ANS (23μM for all experiments), 2H2 (320μM), 3H3 (375μM) and 4H4 (60μM).

Appendix

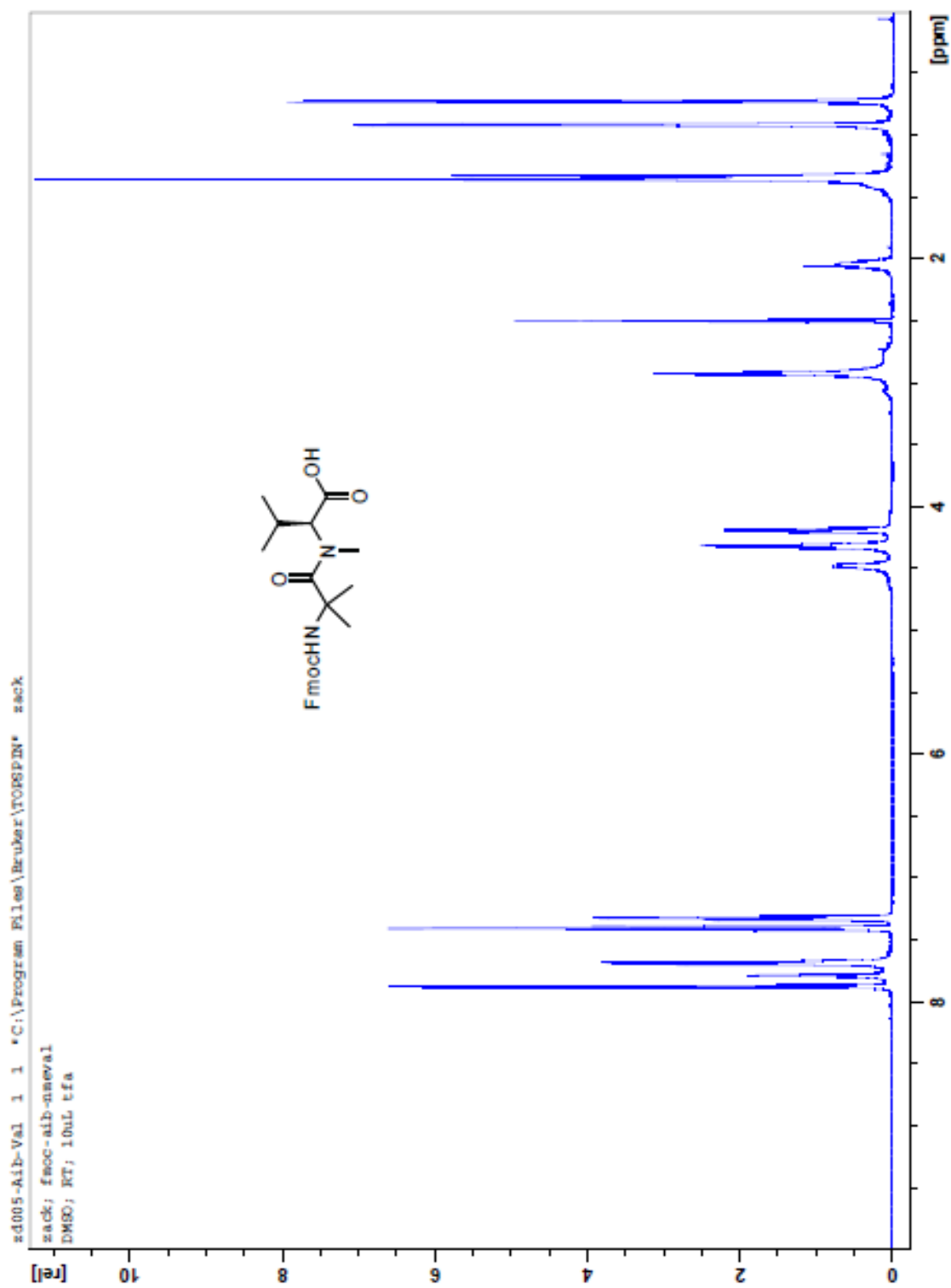


Figure A.1. ^1H NMR (25mM in $\text{DMSO-}d_6$) spectrum of dipeptide **9**, Fmoc-Aib-NMe-Val-OH.

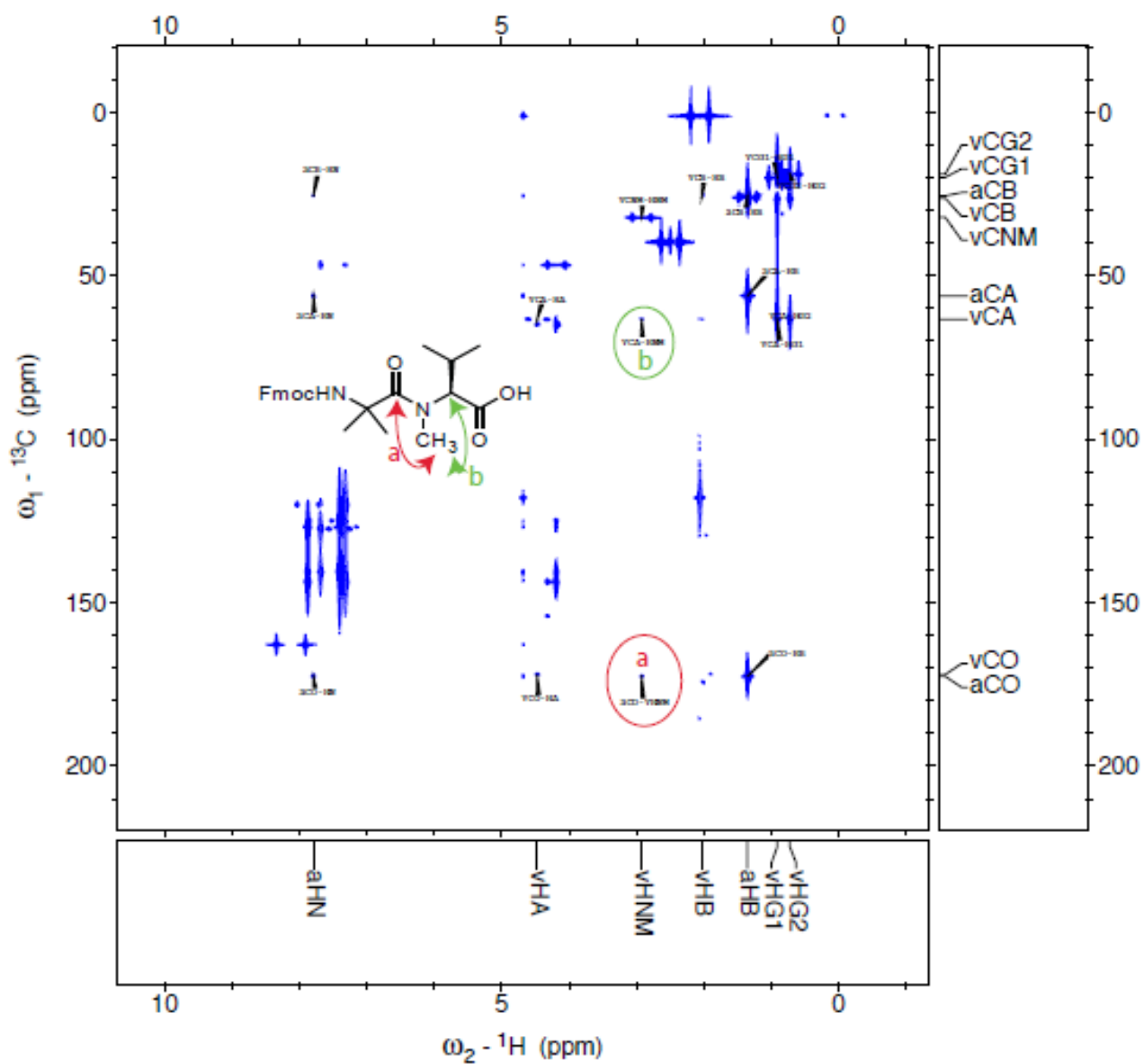


Figure **A.2**. HMBC NMR (25mM in DMSO- d_6) spectrum of dipeptide **9**, Fmoc-Aib-NMe-Val-OH. The correlations referenced in the text which provide evidence for the existence of the tertiary amide are highlighted.

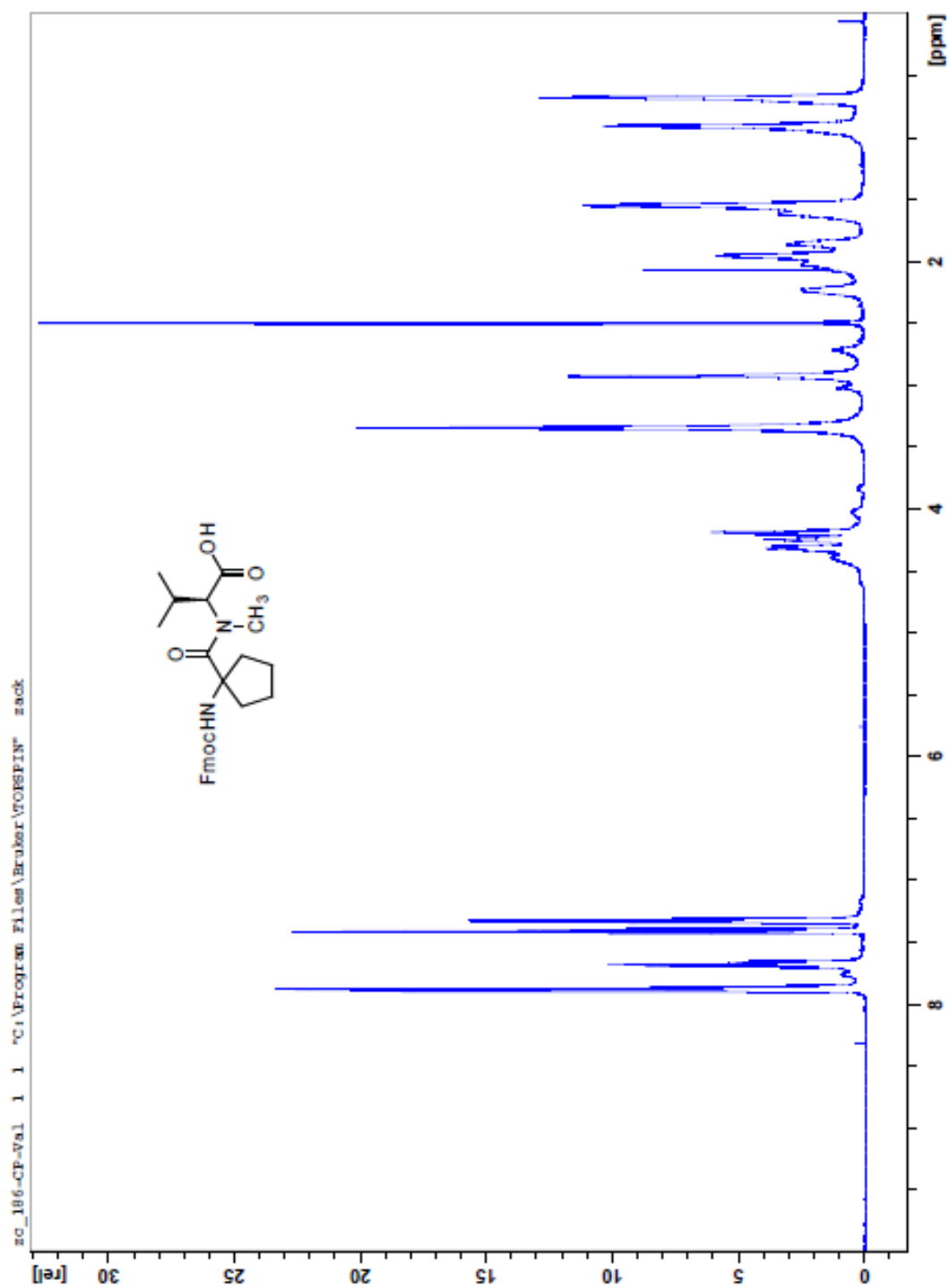


Figure A.3. ^1H NMR NMR (25mM in $\text{DMSO}-d_6$) spectrum of dipeptide **16**, Fmoc-Ac₅c-NMe-Val-OH.

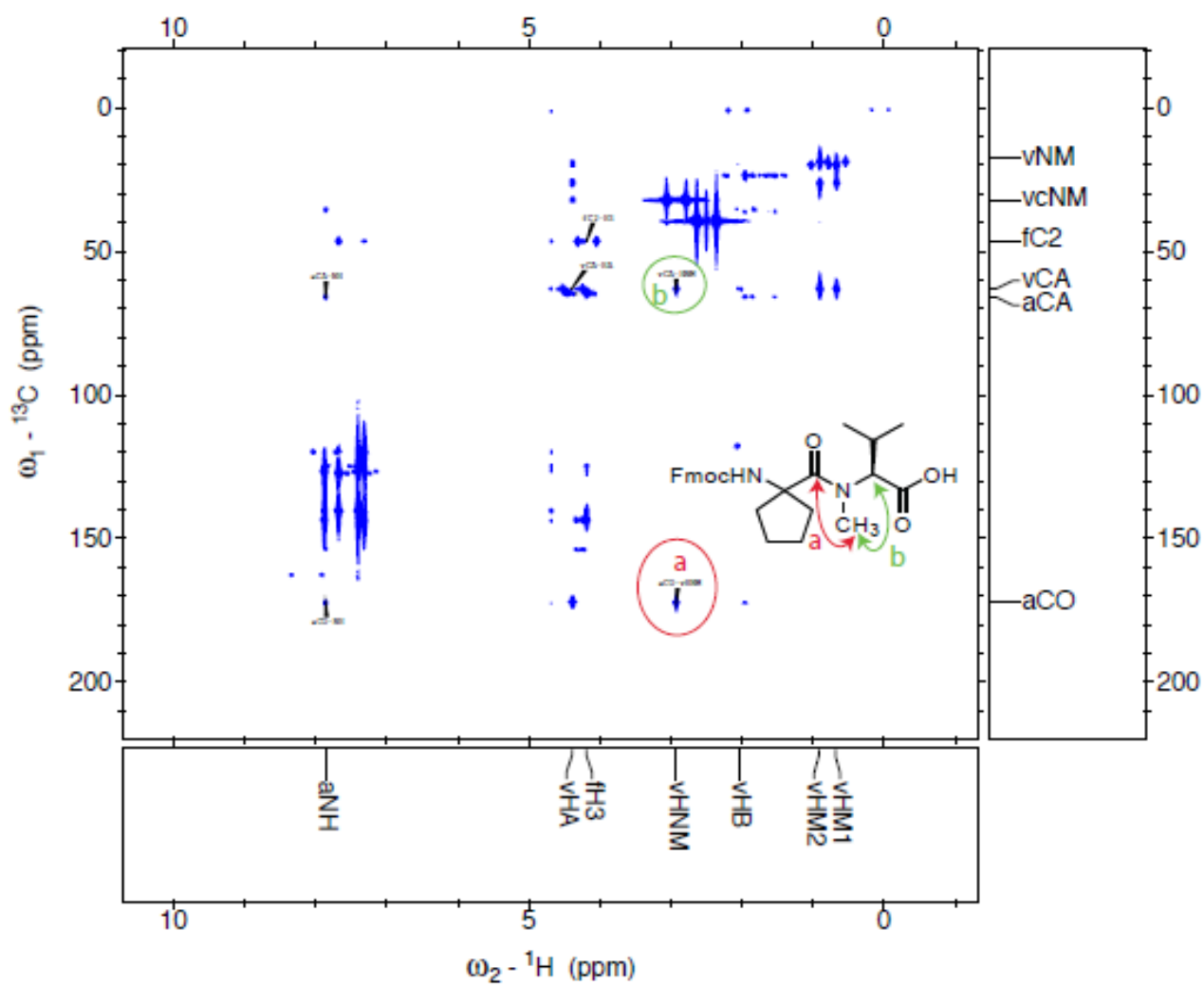


Figure A.4. HMBC NMR (25mM in DMSO-*d*₆) spectrum of dipeptide **16**, Fmoc-Ac₅c-NMe-Val-OH. The correlations referenced in the text which provide evidence for the existence of the tertiary amide are highlighted.

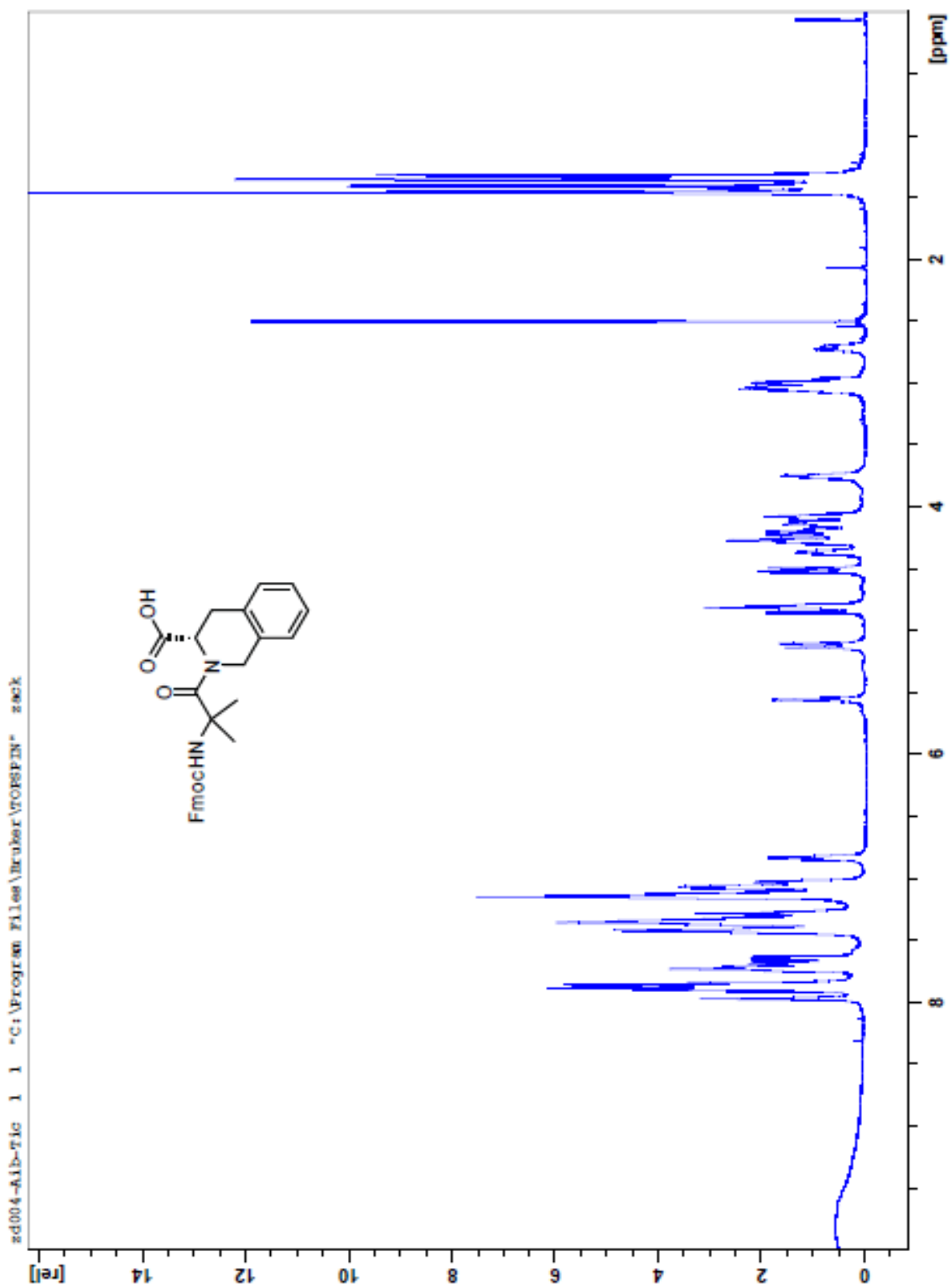


Figure A.5. ¹H NMR NMR (25mM in DMSO-d₆) spectrum of dipeptide **10**, Fmoc-Aib-Tic-OH.

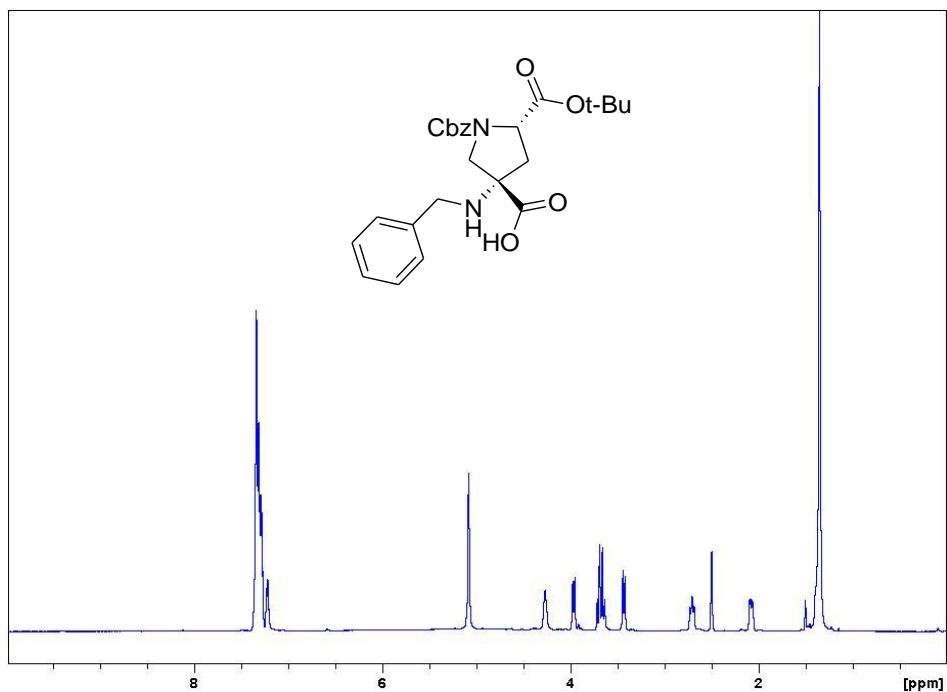


Figure A.6. ¹H NMR (500 MHz, DMSO-*d*₆, 365K) of Pro4(S,S)-benzyl functionalized (compound **36**, Table 3.1).

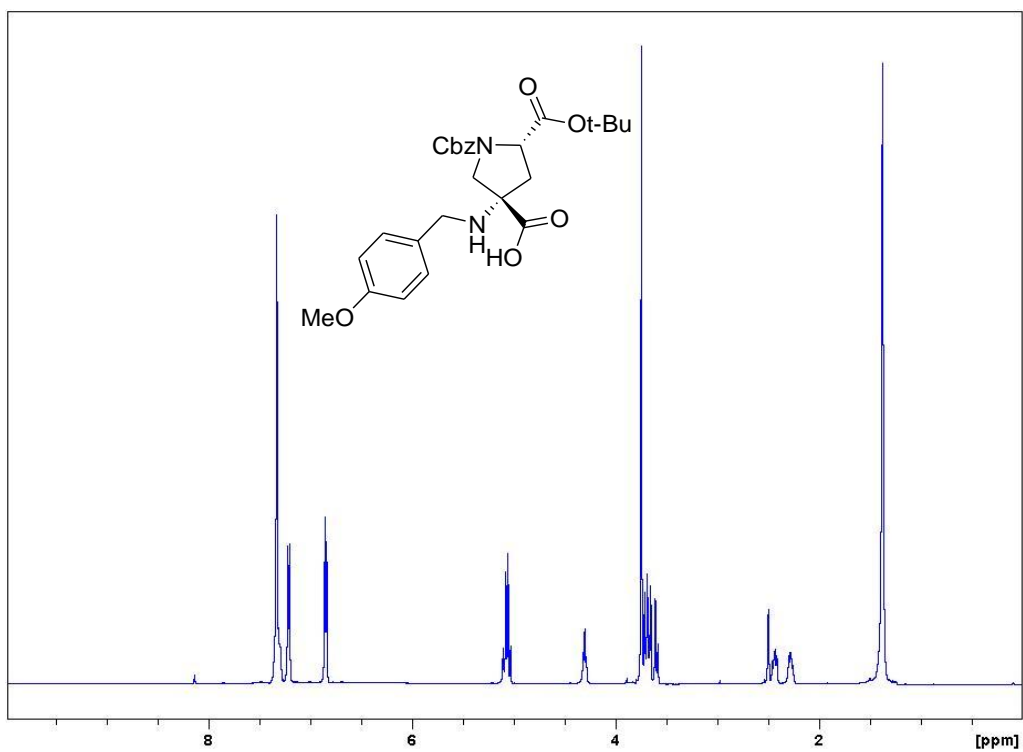


Figure A.7. ¹H NMR (500 MHz, DMSO-*d*₆, 365K) of Pro4(S,S)-anisole functionalized (compound **37**, Table 3.1).

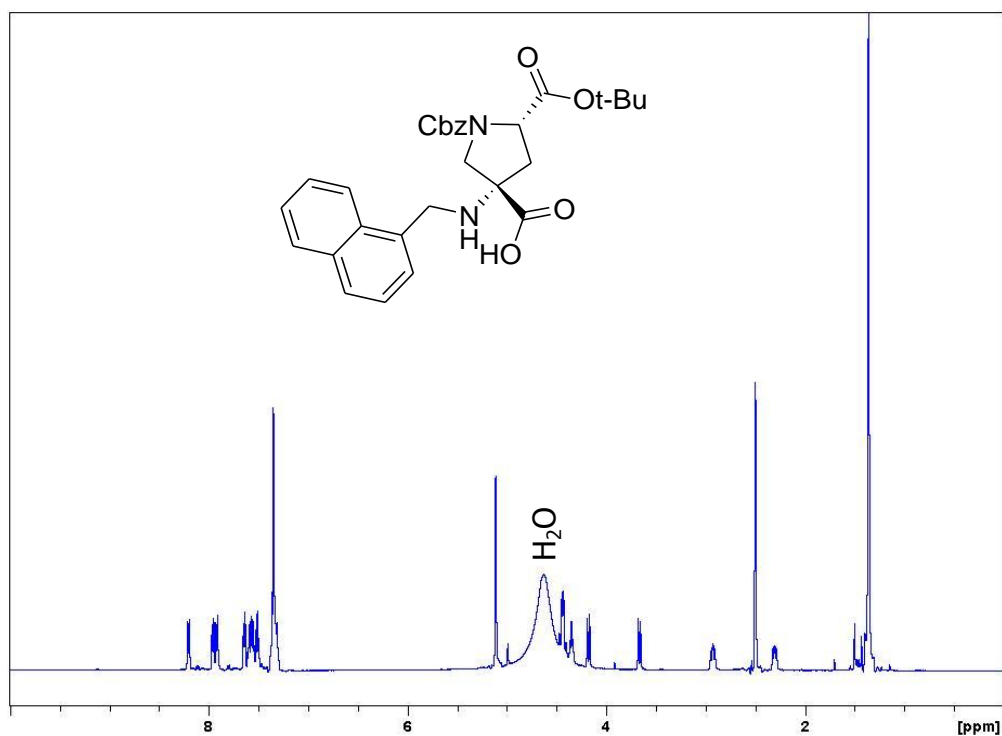


Figure **A.8.** ^1H NMR (500 MHz, $\text{DMSO-}d_6$, 365K) of Pro4(S,S)-naphthyl functionalized (compound **38**, Table 3.1).

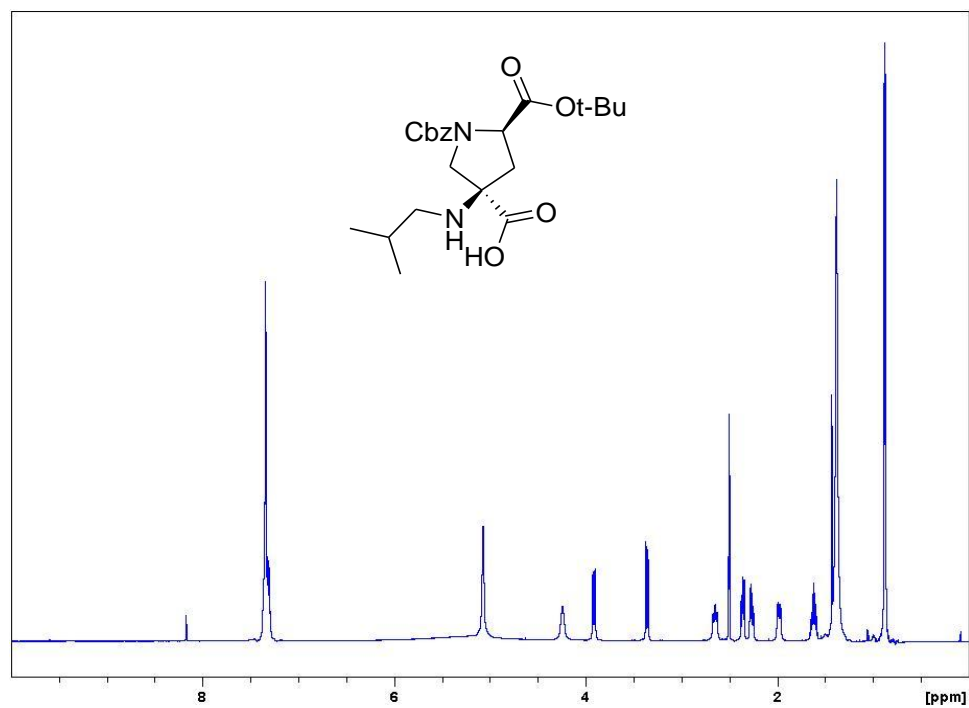


Figure **A.9.** ^1H NMR (500 MHz, $\text{DMSO-}d_6$, 365K) of Pro4(R,R)-isobutyl functionalized (compound **40**, Table 3.1).

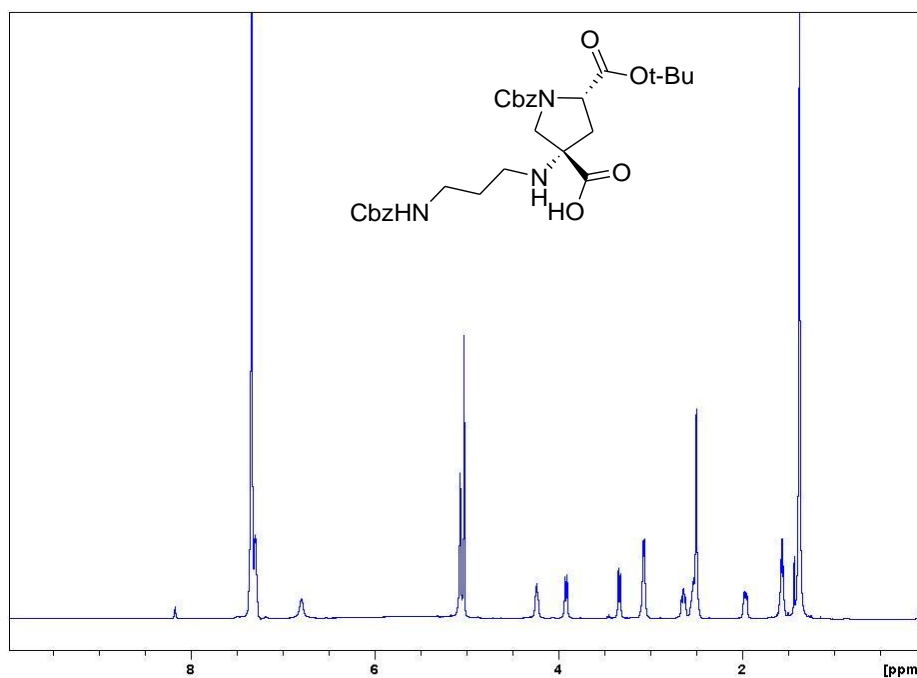


Figure A.10. ^1H NMR (500 MHz, $\text{DMSO-}d_6$, 365K) of Pro4(S,S)-Cbz-aminopropyl functionalized (compound **41**, Table 3.1).

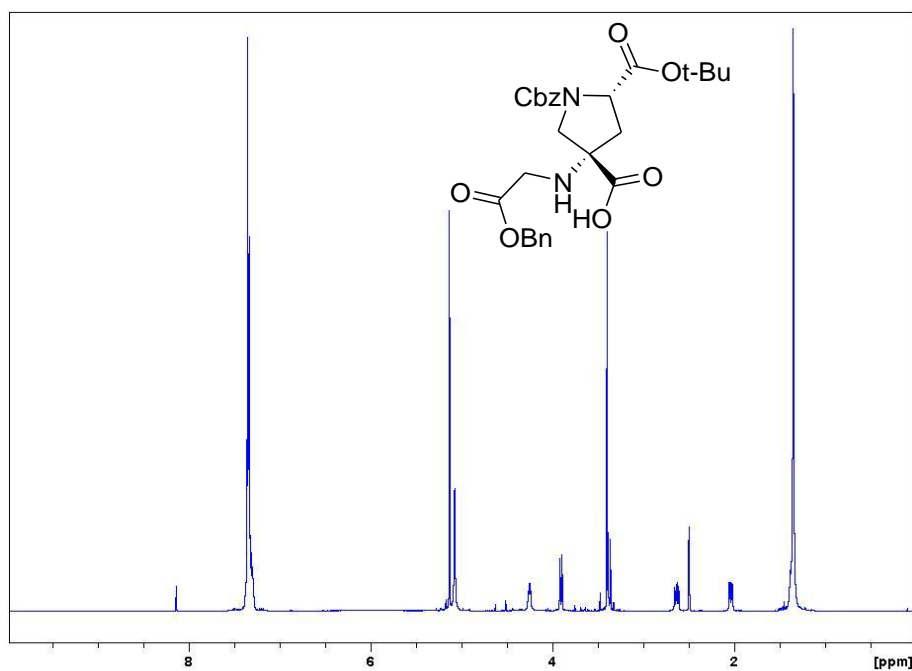


Figure A.11. ^1H NMR (500 MHz, $\text{DMSO-}d_6$, 365K) of Pro4(S,S)-benzyl carboxylate functionalized (compound **42**, Table 3.1).

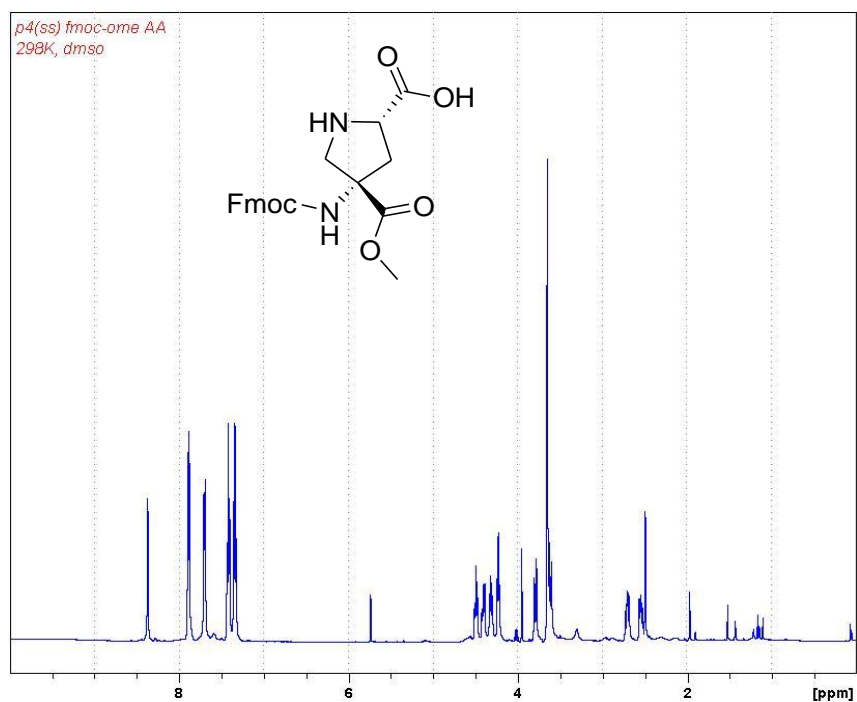


Figure A.12. ^1H NMR (500 MHz, DMSO- d_6 , 298K) of Pro4(S,S)-Fmoc,OMe (compound **66**).

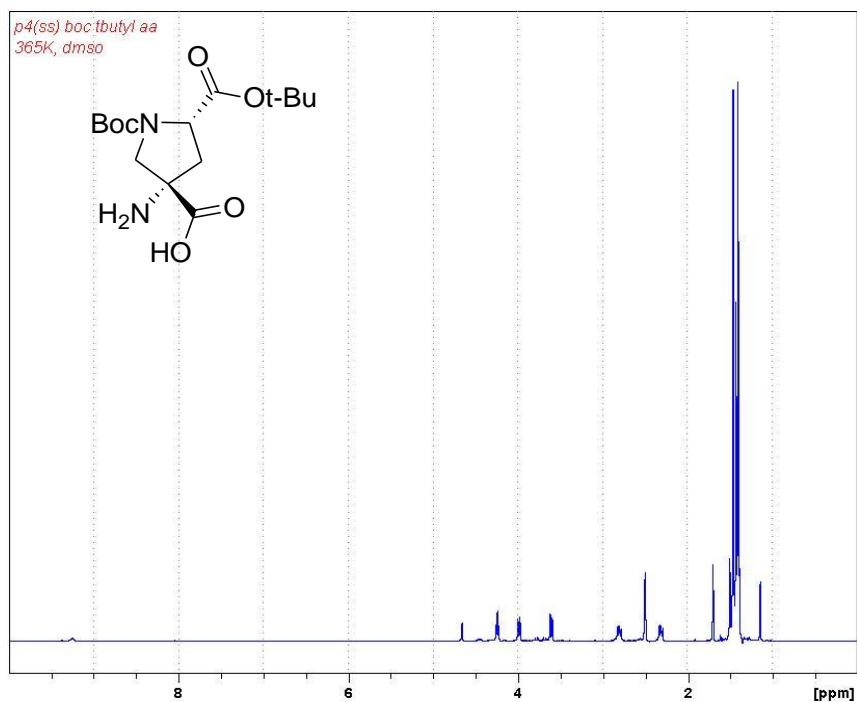


Figure A.13. ^1H NMR (500 MHz, DMSO- d_6 , 365K) of Pro4(S,S)-Boc-amino acid (compound **108**).

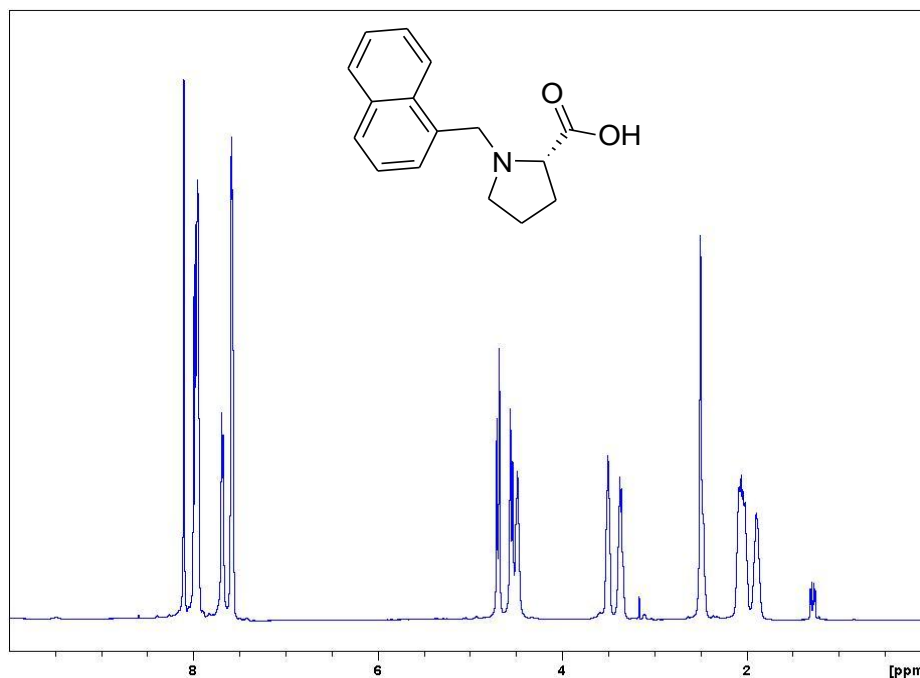
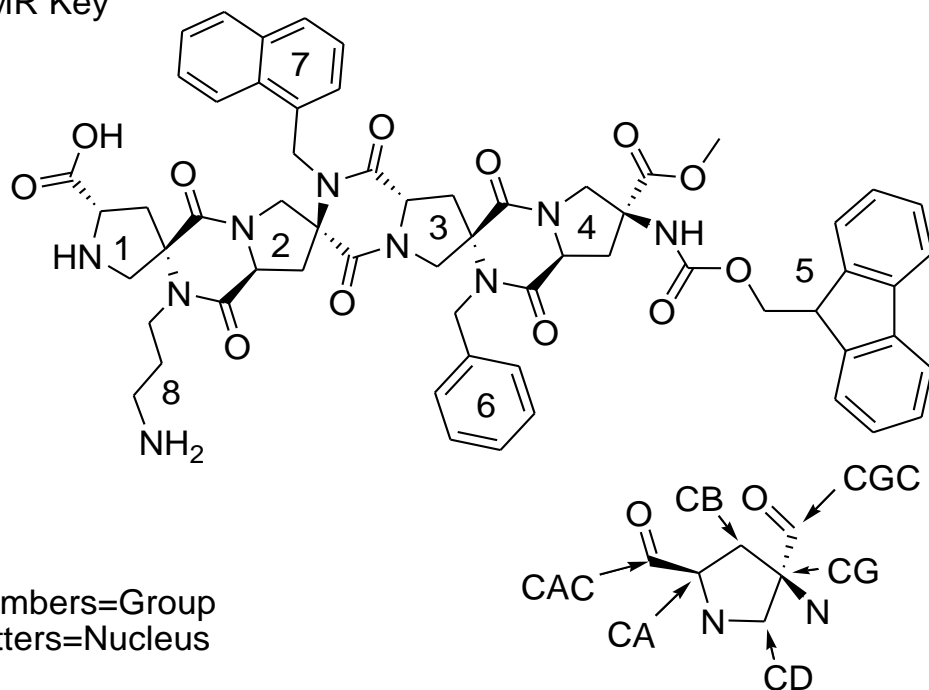


Figure A.14. ¹H NMR (500 MHz, DMSO-*d*₆, 298K) of *N*-(2-methylenaphthyl)-proline (compound 62).

Tetramer (Compound **69**)
NMR Key



Numbers=Group
Letters=Nucleus

Figure A.15. NMR key for the ^1H and ^{13}C assignments for tetramer **69**.

Group	Atom	Nuc	Shift	SDev	Assignments	Group	Atom	Nuc	Shift	SDev	Assignments
1	HA	1H	4.19	0.008	6	1	CA	13C	57.24	0.056	3
1	HB1	1H	2.28	0.012	7	1	CB	13C	36.28	0.039	2
1	HB2	1H	2.63	0.012	4	1	CD	13C	48.18	0.094	3
1	HD1	1H	3.74	0.001	3	1	CG	13C	68.34	0.004	3
1	HD2	1H	3.48	0.015	3	1	COA	13C	167.93	0.027	2
2	HA	1H	4.40	0.014	6	1	COG	13C	163.87	0.072	4
2	HB1	1H	2.58	0.003	2	2	CA	13C	55.66	0.014	3
2	HD1	1H	3.87	0.006	6	2	CB	13C	37.20	0.041	2
2	HD2	1H	3.58	0.003	2	2	CG	13C	66.58	0.046	4
3	HA	1H	4.61	0.01	6	2	COA	13C	166.58	0.046	3
3	HB1	1H	2.54	0.005	3	2	COG	13C	164.38	0.036	3
3	HB2	1H	2.81	0.01	4	3	CA	13C	55.73	0	2
3	HD1	1H	3.89	0.007	3	3	CB	13C	37.06	0	1
3	HD2	1H	3.60	0	1	3	CD	13C	49.85	0.102	2
4	HA	1H	4.76	0.008	5	3	CG	13C	66.41	0.036	5
4	HB1	1H	2.70	0.014	6	3	COA	13C	167.01	0.02	3
4	HD1	1H	4.00	0.005	8	3	COG	13C	164.68	0.012	2
4	HMe	1H	3.68	0.001	2	4	CA	13C	55.90	0.048	3
4	NH	1H	8.43	0.013	5	4	CB	13C	37.71	0.127	2
5	H1	1H	4.34	0.002	4	4	CD	13C	54.25	0.022	3
5	H2	1H	4.24	0.001	2	4	CG	13C	61.27	0.009	3
6	H2	1H	7.25	0.009	3	4	CMe	13C	52.52	0	1
6	HA1	1H	5.10	0.014	7	4	COA	13C	167.73	0.081	3
6	HA2	1H	4.63	0.019	6	4	COG	13C	172.00	0.041	3
7	H3	1H	7.71	0	1	5	C1	13C	65.56	0.042	2
7	H9	1H	8.05	0.01	4	5	C2	13C	46.50	0.029	4
7	HA1	1H	4.90	0.017	8	5	CO	13C	155.96	0	1
7	HA2	1H	5.33	0.013	8	6	C1	13C	137.90	0	1
8	HA1	1H	3.54	0.005	5	6	CA	13C	44.83	0.073	5
8	HA2	1H	3.24	0.013	7	7	C1	13C	132.52	0	1
8	HB1	1H	1.84	0.007	3	7	C9	13C	122.78	0.024	2
8	HB2	1H	1.71	0.037	4	7	CA	13C	43.61	0.099	4
8	HG	1H	2.79	0.009	2	8	CA	13C	39.54	0.062	4
8	NH	1H	7.76	0	1	8	CB	13C	26.82	0.044	5
						8	CG	13C	36.42	0	1

Table A.1. ^1H and ^{13}C assignments for tetramer **69**.

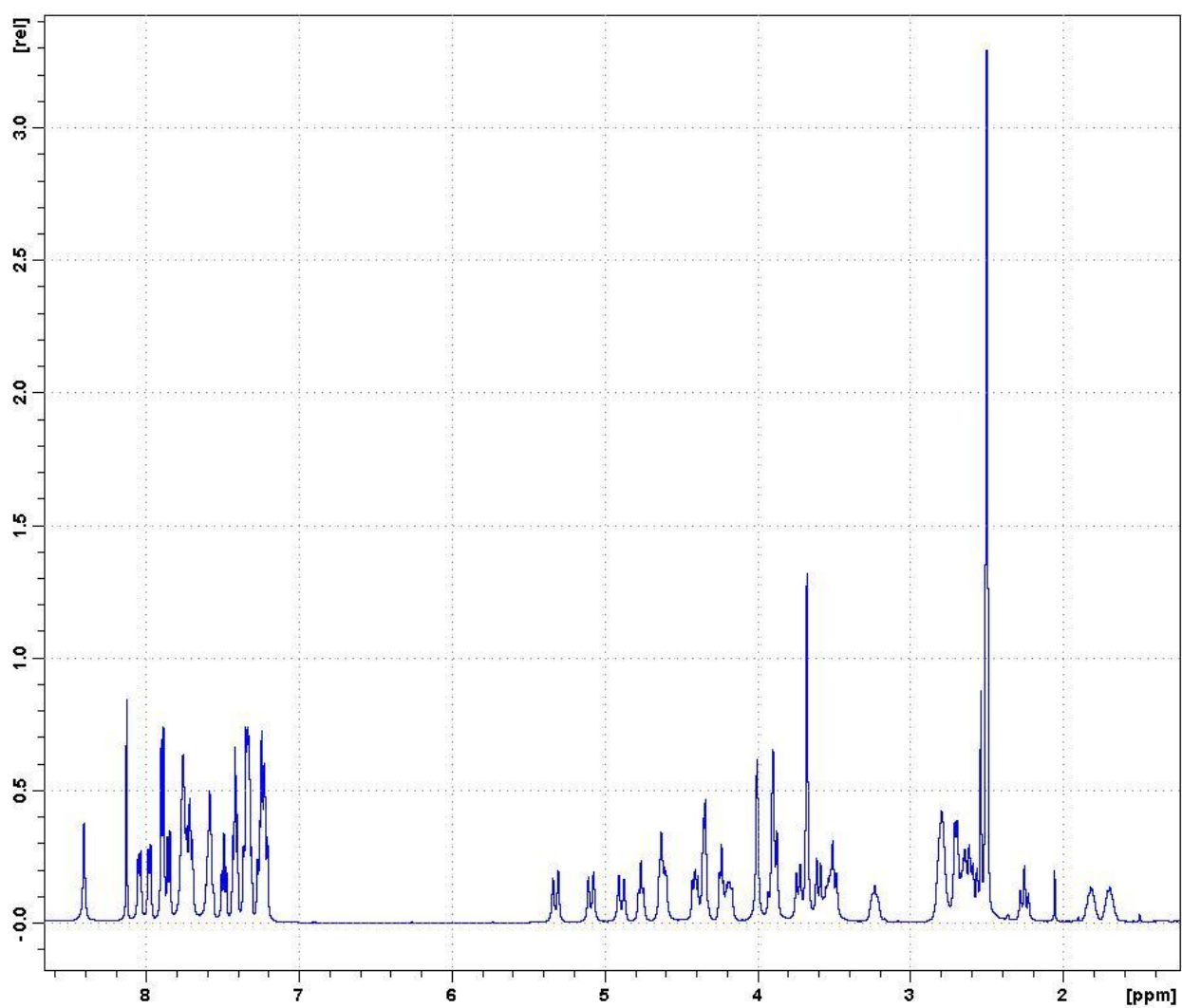
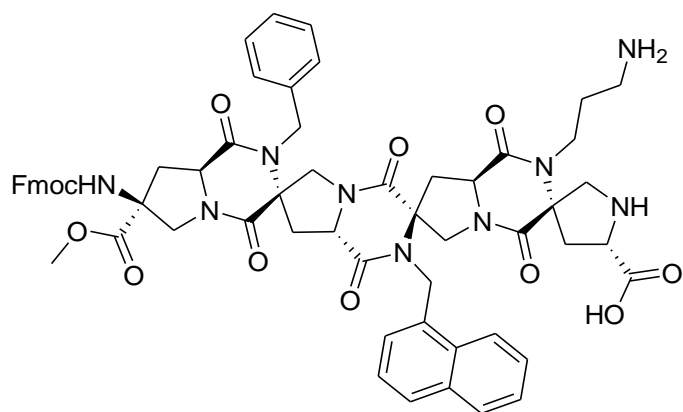


Figure A.16. Tetramer (**69**), ¹H: 10mM in DMSO

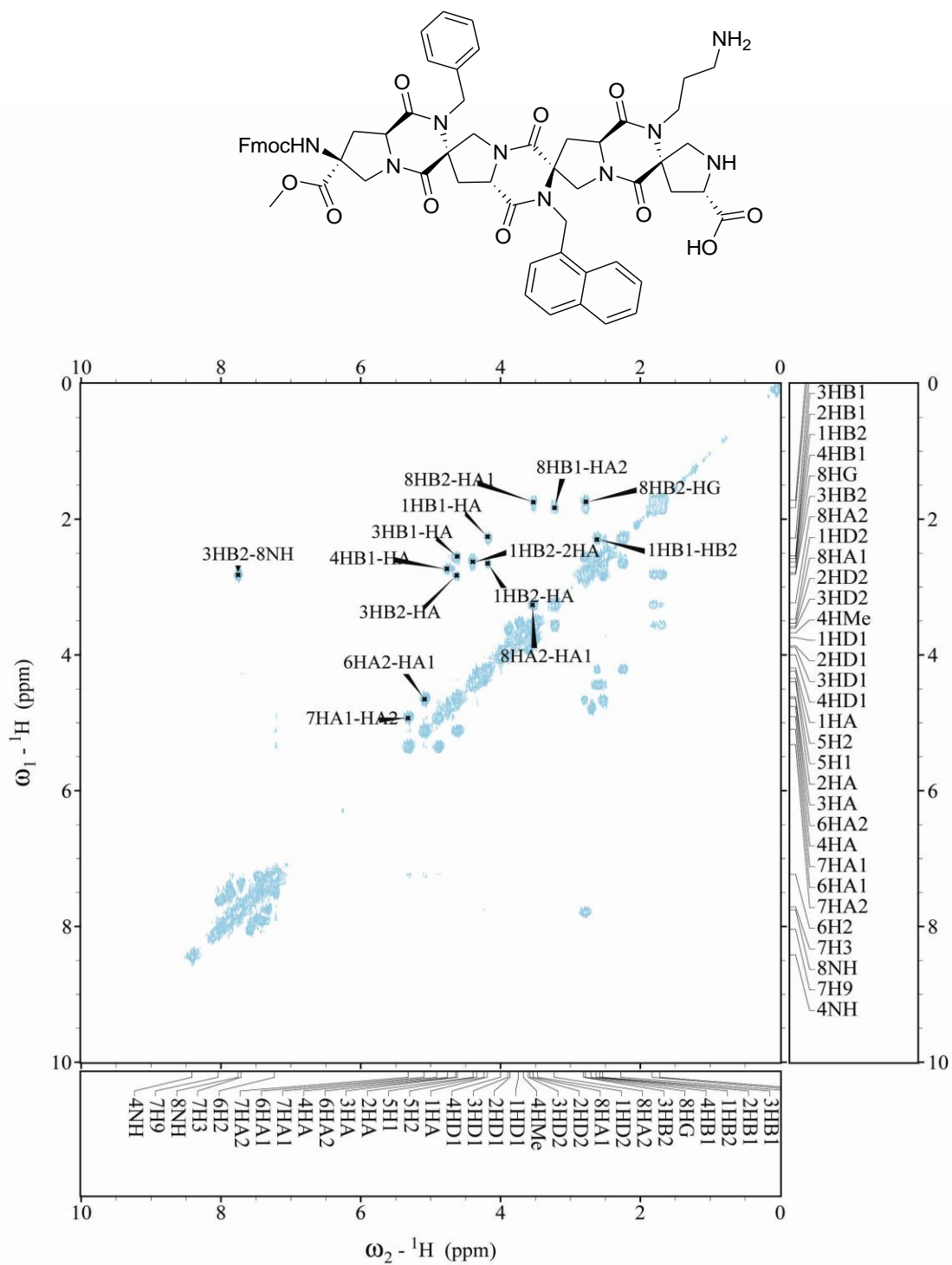


Figure A.17. Tetramer (69) COSY: 10mM in DMSO

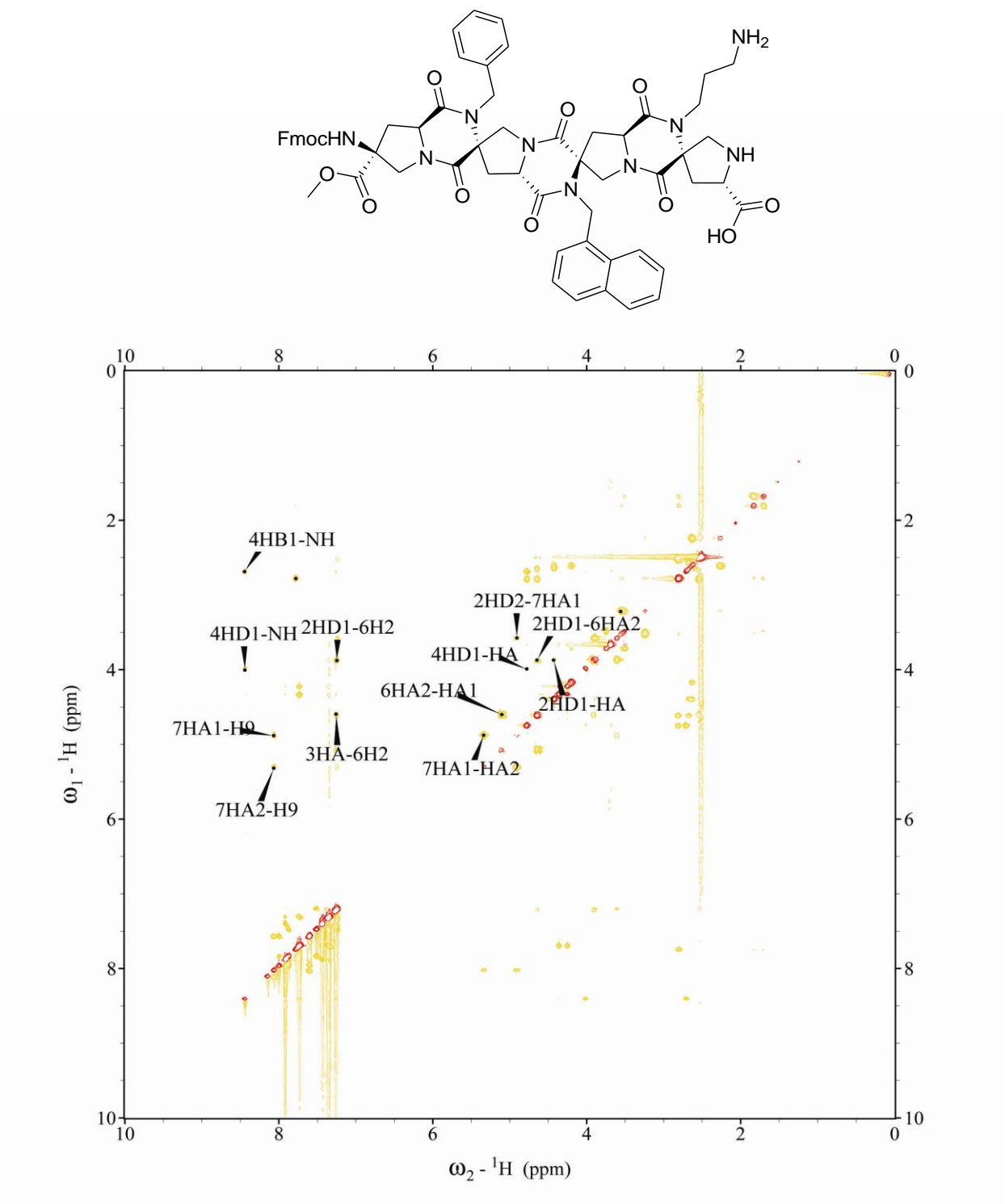


Figure A.18. Tetramer (**69**) ROESY: 10mM in DMSO

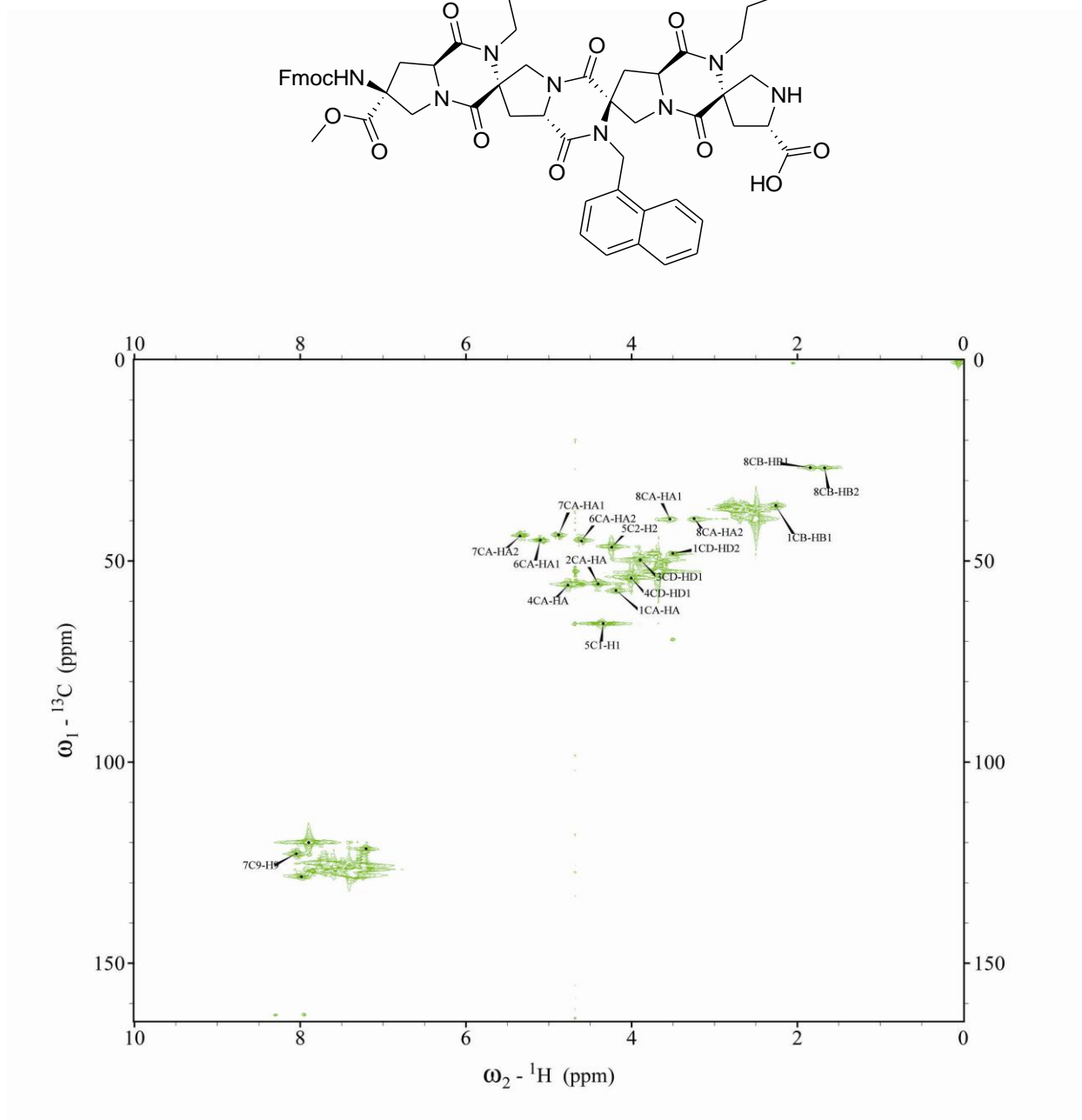


Figure A.19 Tetramer (69) HMQC: 10mM in DMSO

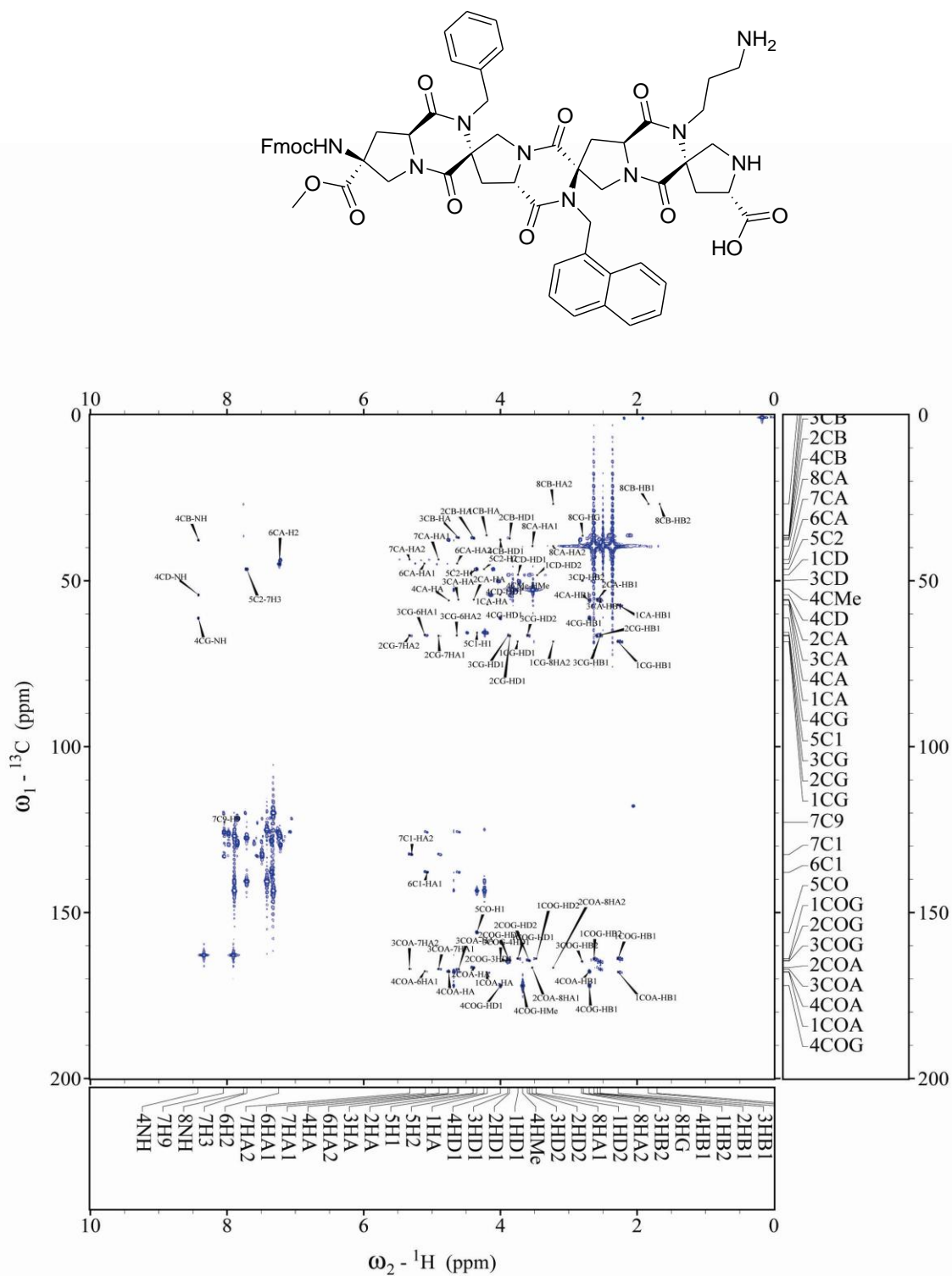


Figure A.20 Tetramer (69) HMBC: 10mM in DMSO

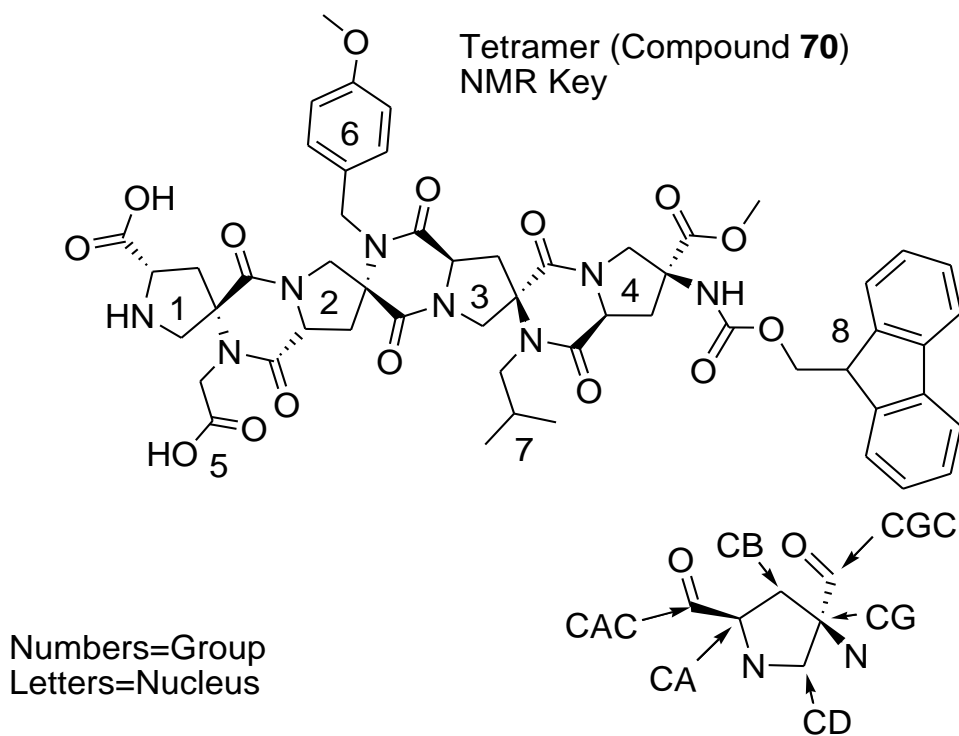


Figure A.21. NMR key for the ^1H and ^{13}C assignments for tetramer **70**.

Group	Atom	Nuc	Shift	SDev	Assignments	Group	Atom	Nuc	Shift	SDev	Assignments
1	HA	^1H	4.563	0.092	5	1	CA	^{13}C	59.323	0.002	2
1	HB1	^1H	2.739	0.02	4	1	CB	^{13}C	37.237	0	1
1	HB2	^1H	2.443	0.001	3	1	CG	^{13}C	67.373	0.009	3
1	HD1	^1H	3.576	0.011	3	1	COA	^{13}C	168.322	0	2
2	HA	^1H	4.362	0.008	6	1	COG	^{13}C	164.213	0	2
2	HB1	^1H	2.462	0.012	3	2	CA	^{13}C	59.065	5.137	3
2	HB2	^1H	2.696	0	1	2	CB	^{13}C	36.849	0	1
2	HD1	^1H	3.846	0	1	2	CG	^{13}C	66.358	0.032	3
3	HA	^1H	4.941	0.036	6	2	COA	^{13}C	166.047	0.009	3
3	HB1	^1H	2.819	0.078	4	3	CA	^{13}C	58.205	0.329	2
3	HB2	^1H	2.656	0.021	5	3	CB	^{13}C	34.865	0.406	4
4	HB1	^1H	2.706	0.029	5	3	CG	^{13}C	65.402	0.007	3
4	HD1	^1H	3.92	0.001	4	3	COA	^{13}C	167.93	0	1
4	HD2	^1H	3.884	0.001	2	4	CB	^{13}C	37.482	0.315	4
4	HM	^1H	3.644	0	2	4	CD	^{13}C	53.805	0	1
4	NH	^1H	8.25	0.007	5	4	CG	^{13}C	61.351	0.001	3
5	HA1	^1H	4.232	0.001	3	4	CM	^{13}C	52.62	0	1
5	HA2	^1H	4.18	0	2	4	COA	^{13}C	168.369	0.01	3
6	H2	^1H	7.253	0.24	6	4	COG	^{13}C	171.678	0.021	5
6	H3	^1H	6.901	0.025	6	5	CO	^{13}C	170.038	0.029	2
6	HA1	^1H	4.917	0.02	7	6	C1	^{13}C	129.474	0.064	3
6	HA2	^1H	4.378	0.039	5	6	C2	^{13}C	126.918	0.67	4
6	HM	^1H	3.751	0.03	4	6	C3	^{13}C	114.022	0.396	3
7	HA1	^1H	3.212	0.026	7	6	C4	^{13}C	158.013	0.012	3
7	HA2	^1H	3.472	0.035	9	6	CA	^{13}C	44.501	0.018	3
7	HB	^1H	1.693	0.039	11	6	CM	^{13}C	55.191	0.461	2
7	HG1	^1H	0.851	0.024	5	7	CA	^{13}C	48.324	0.241	7
7	HG2	^1H	0.787	0.016	6	7	CB	^{13}C	28.27	0.522	6
						7	CG1	^{13}C	20.13	0.269	2
						7	CG2	^{13}C	19.758	0.052	4

Table A.2. ^1H and ^{13}C assignments for tetramer **70**.

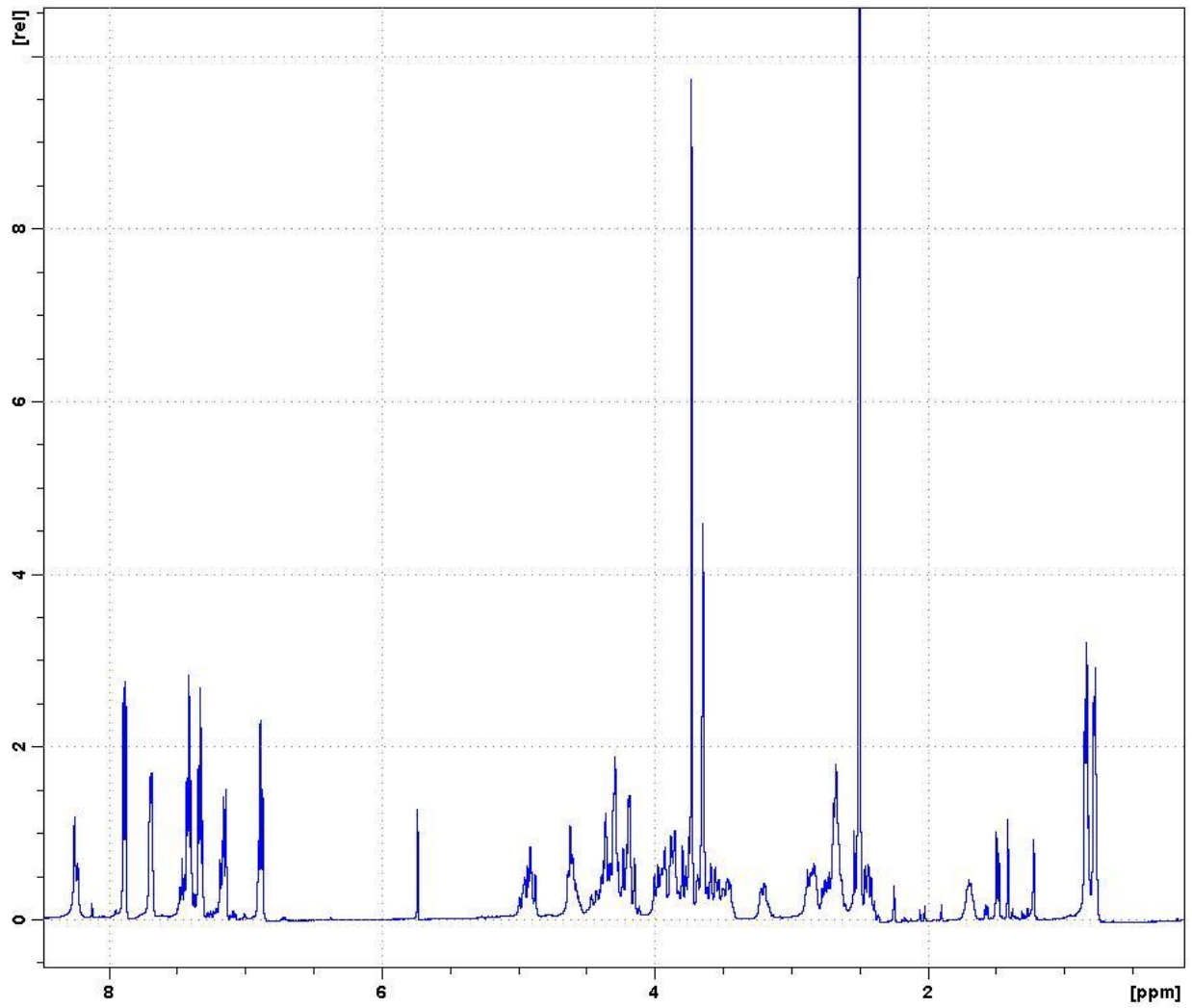
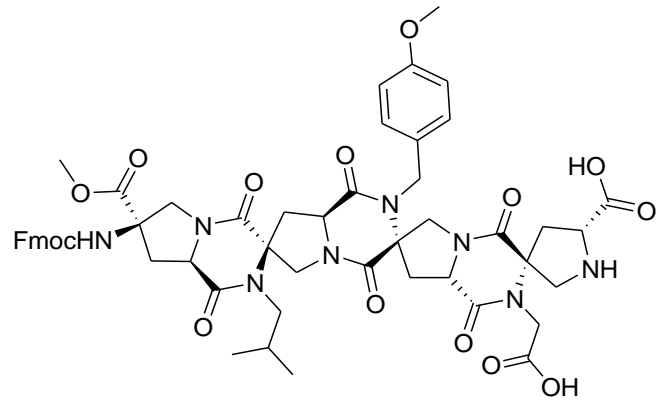


Figure A.22 Tetramer (70) ¹H: 10mM in DMSO

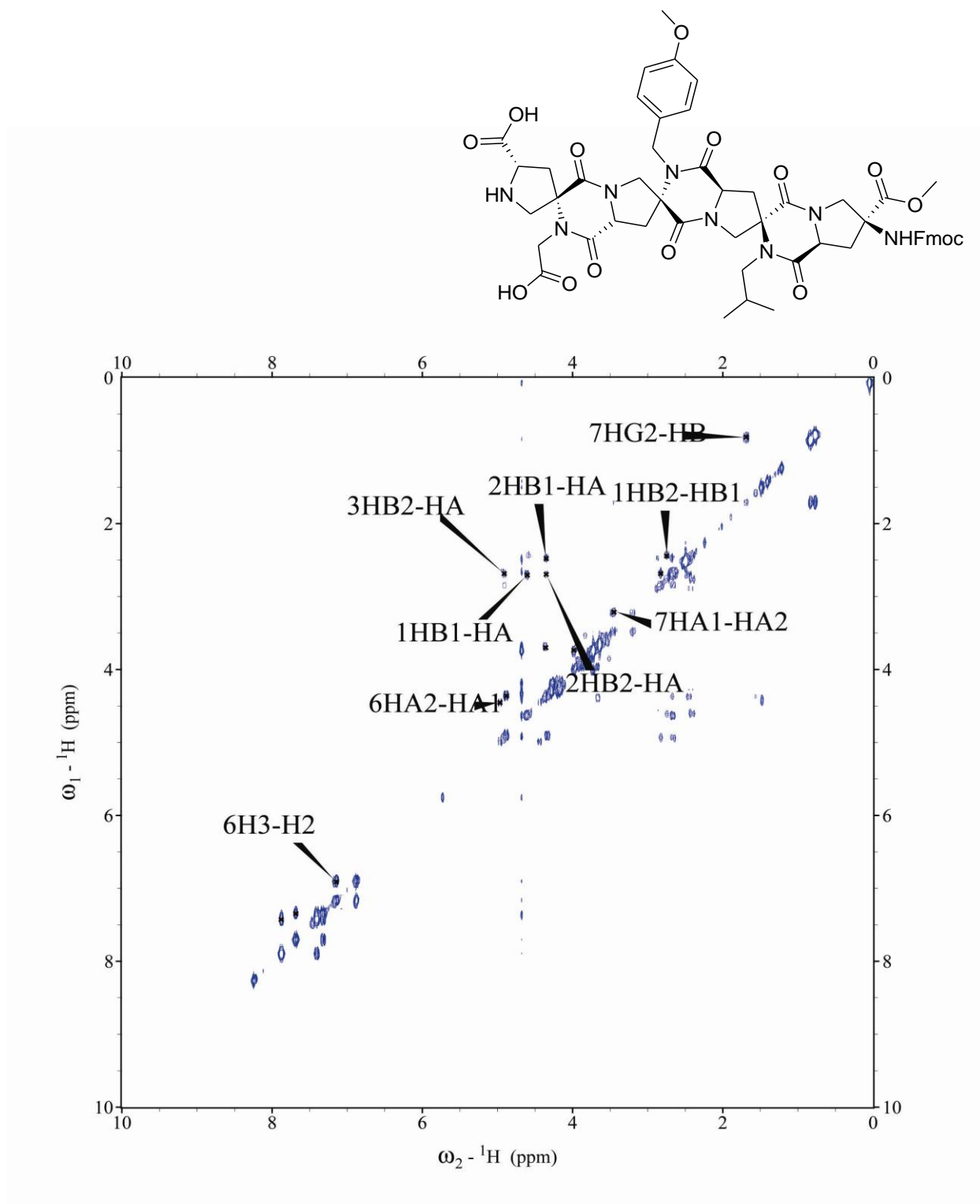


Figure A.23 Tetramer (70) COSY: 10mM in DMSO

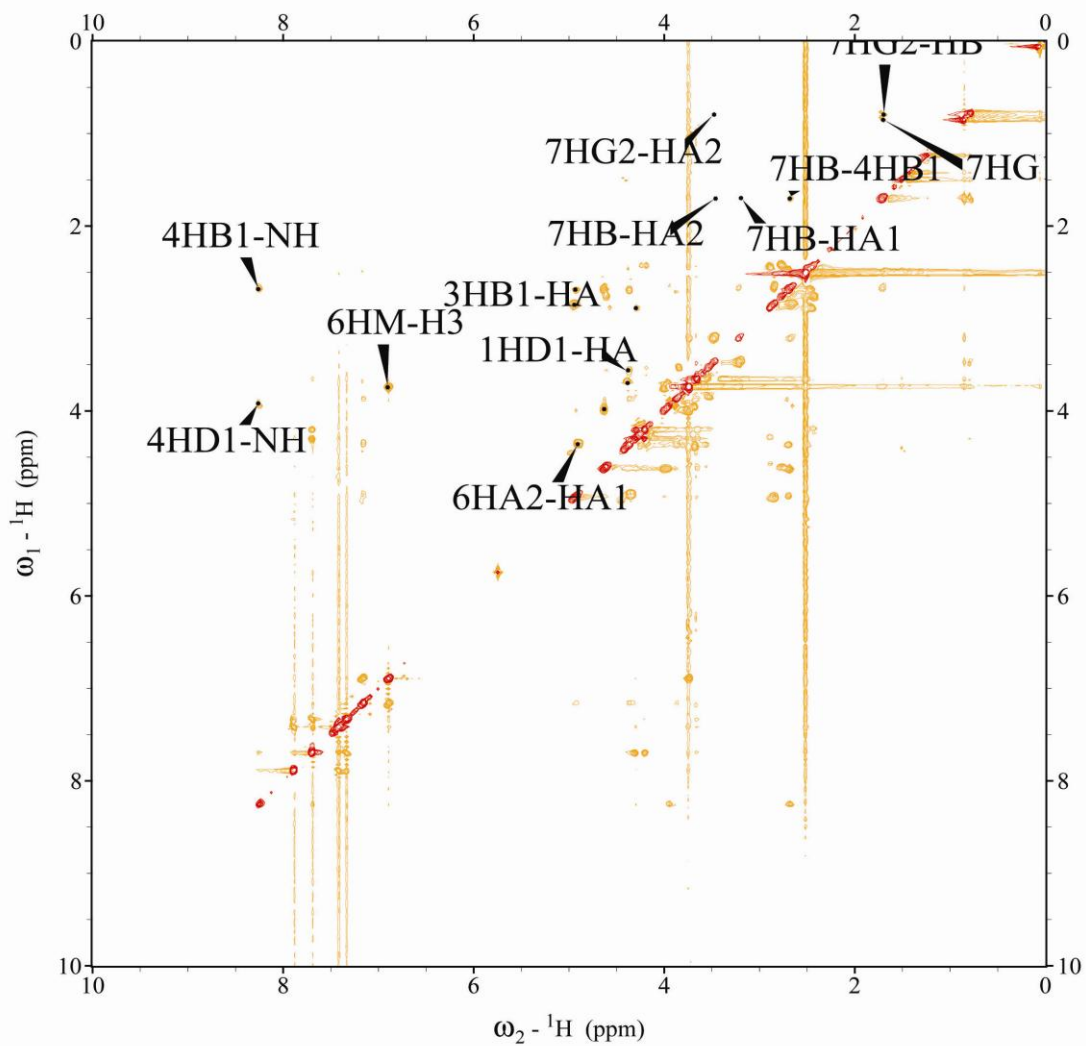
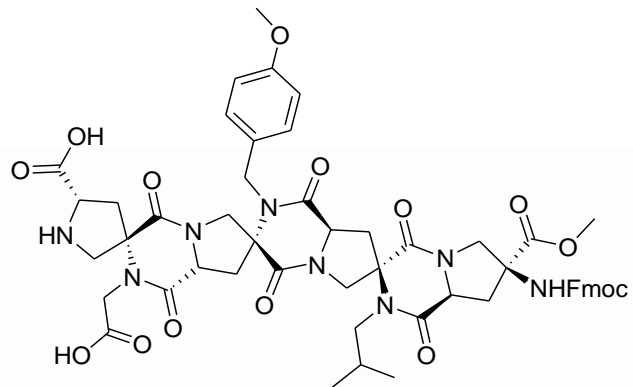


Figure A.24 Tetramer (70) ROESY: 10mM in DMSO

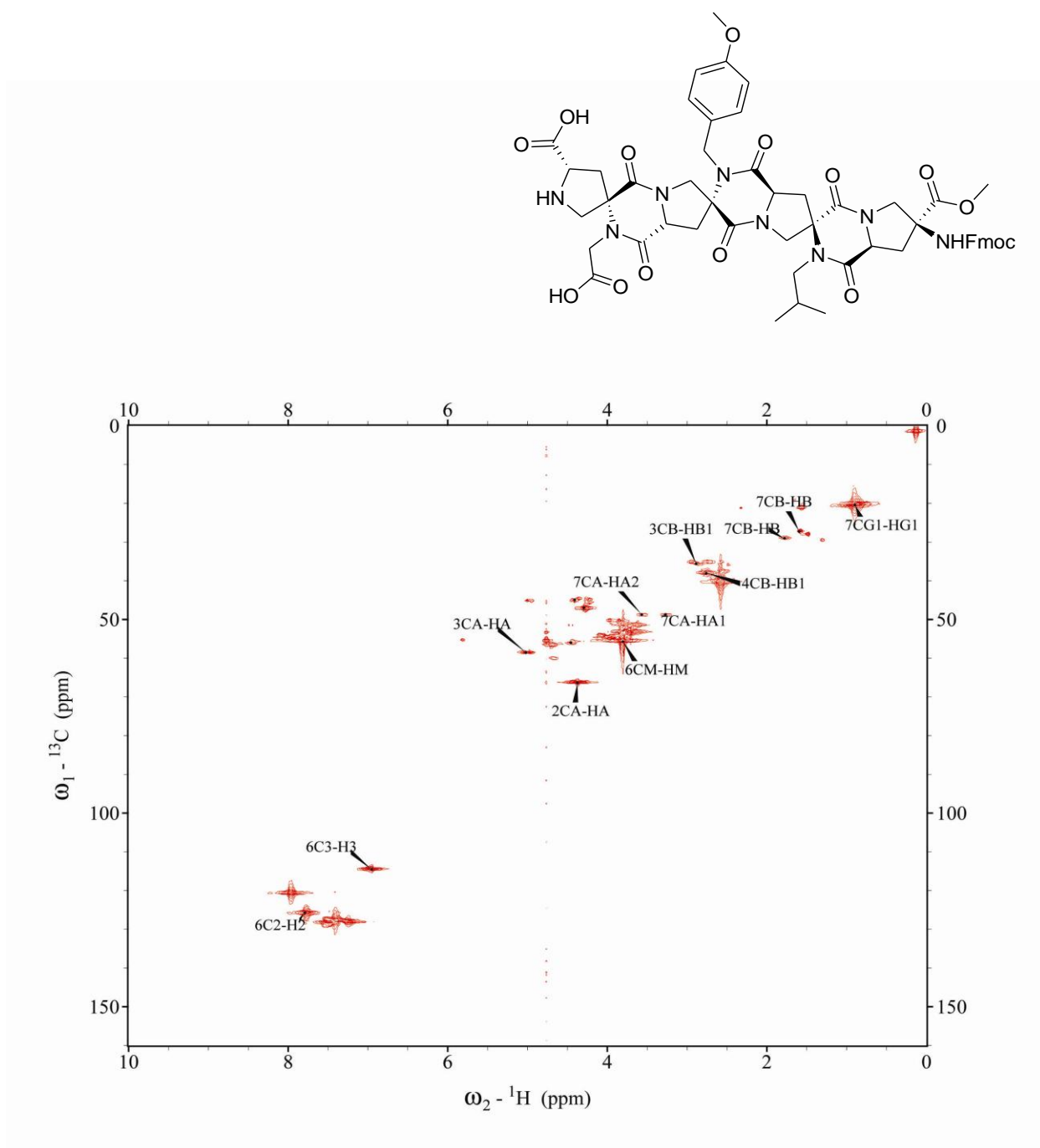


Figure A.25 Tetramer (70) HMQC: 10mM in DMSO

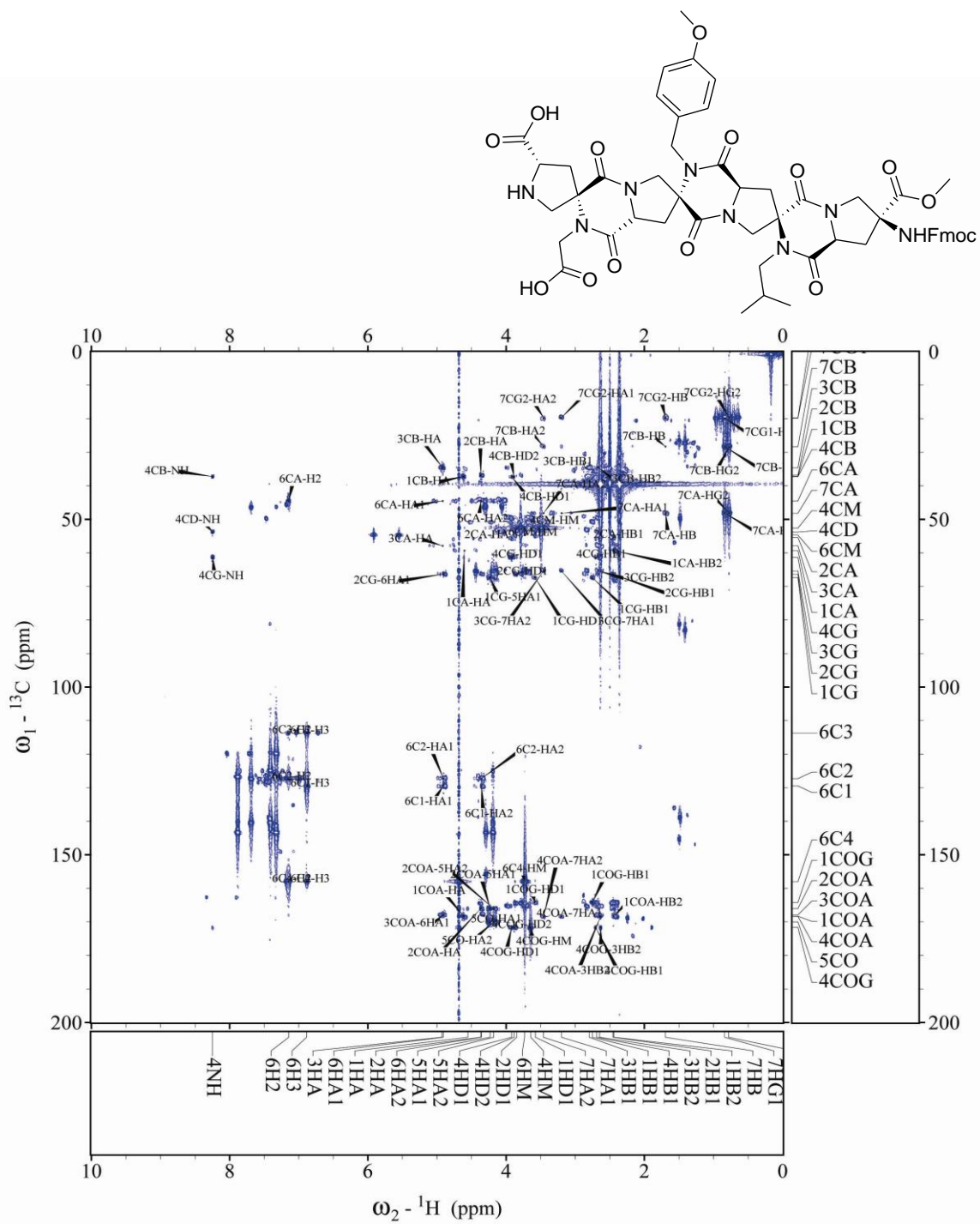


Figure A.26 Tetramer (70) HMBC: 10mM in DMSO

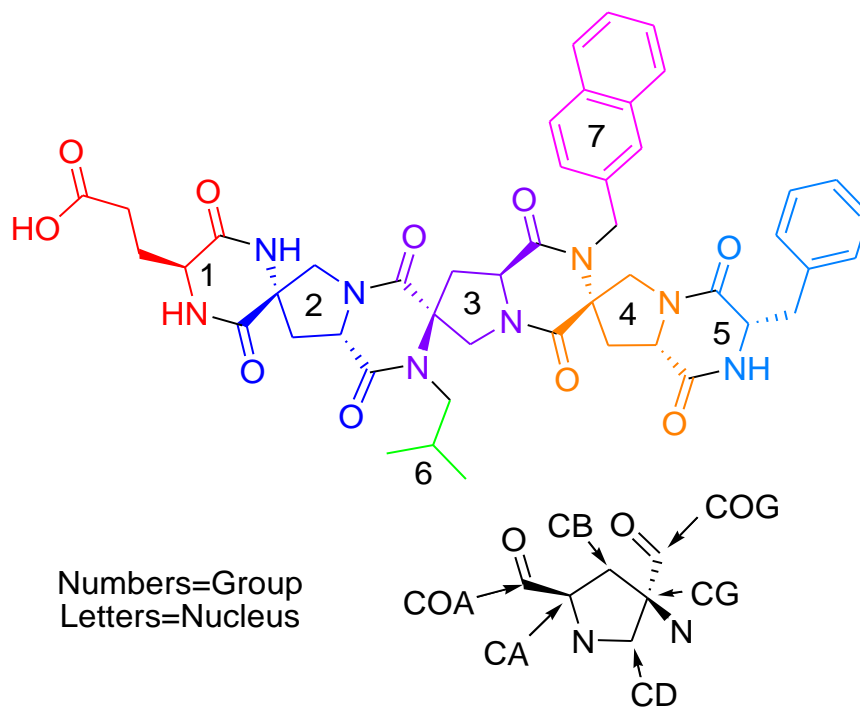


Figure A.27. NMR key for the ^1H and ^{13}C assignments for helix mimic **103**.

Group	Atom	Nucleus	Shift	StanDev	Assignments	Group	Atom	Nucleus	Shift	StanDev	Assignments
1	CA	^{13}C	53.173	0.005	4	1	HA	^1H	4.077	0.001	3
1	COO	^{13}C	173.564	0.027	3	1	HB1	^1H	2.251	0.004	3
2	CA	^{13}C	57.659	0.072	4	1	HB2	^1H	1.94	0.006	5
2	CAC	^{13}C	168.323	0.013	3	1	HG	^1H	2.329	0.002	2
2	CB	^{13}C	41.356	0.033	4	1	NH	^1H	8.502	0.006	3
2	CD	^{13}C	55.196	0.094	3	2	HA	^1H	4.726	0.003	7
2	CG	^{13}C	59.746	0.057	5	2	HB1	^1H	2.221	0.002	8
2	CGC	^{13}C	168.98	0.039	5	2	HB2	^1H	2.735	0.002	7
3	CA	^{13}C	55.756	0	1	2	HD1	^1H	3.661	0.002	7
3	CAC	^{13}C	167.394	0.059	4	2	HD2	^1H	3.879	0.008	7
3	CB	^{13}C	37.044	0	2	2	NH	^1H	8.453	0.002	3
3	CG	^{13}C	66.024	0.015	4	3	HA	^1H	4.535	0.005	8
4	CB	^{13}C	37.956	0	1	3	HB1	^1H	2.475	0.012	6
4	CG	^{13}C	66.694	0.055	4	3	HB2	^1H	2.65	0.011	3
5	C1	^{13}C	137.009	0	2	3	HD1	^1H	4.132	0.002	3
5	CA	^{13}C	56.383	0	1	4	HA	^1H	4.175	0.003	4
5	CB	^{13}C	35.347	0.076	3	4	HB1	^1H	2.018	0.004	6
5	CO	^{13}C	164.269	0.057	2	4	HB2	^1H	2.569	0.009	4
6	CA	^{13}C	48.449	0.117	5	4	HD1	^1H	3.77	0.006	4
6	CB	^{13}C	28.337	0.023	2	5	HA	^1H	4.418	0.003	5
6	CG1	^{13}C	19.903	0	1	5	HB	^1H	3.043	0.001	5
6	CG2	^{13}C	19.919	0.056	4	5	NH	^1H	8.207	0.004	4
7	C1	^{13}C	135.366	0	2	6	HA1	^1H	3.496	0.005	8
7	C2	^{13}C	124.53	0.217	3	6	HA2	^1H	3.084	0.004	9
7	CA	^{13}C	45.472	0.089	3	6	HB	^1H	1.732	0.013	5
						6	HG1	^1H	0.869	0.009	4
						6	HG2	^1H	0.815	0.013	3
						7	H2	^1H	7.576	0.003	4
						7	HA1	^1H	4.942	0.005	6
						7	HA2	^1H	3.985	0.004	9

Table A.3. ^1H and ^{13}C assignments for helix mimic **103**.

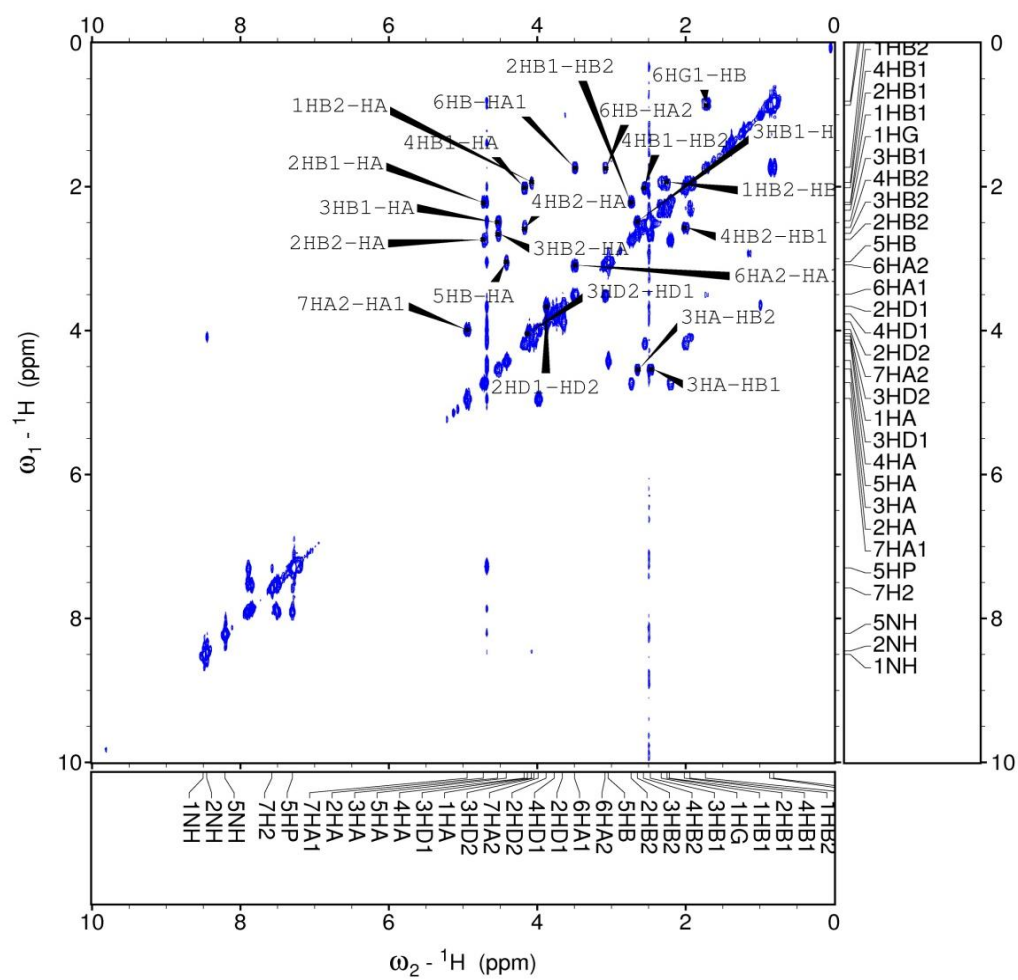
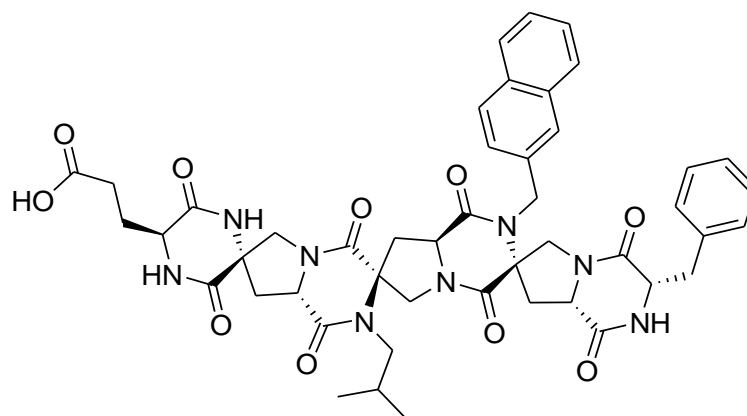


Figure A.28. Helix Mimic 103 COSY: 8mM in DMSO

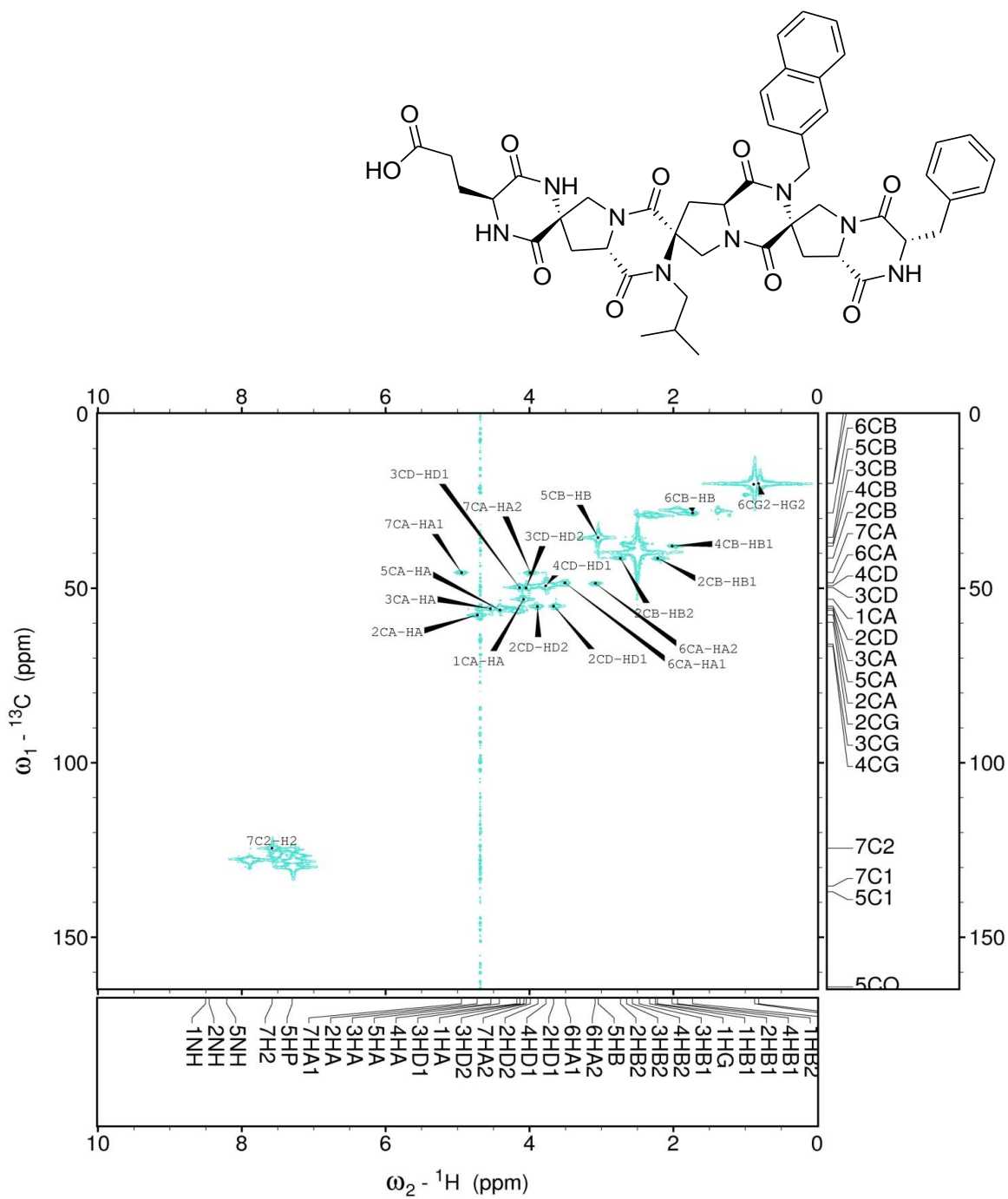


Figure A.29 Helix Mimic 103 HMQC: 8mM in DMSO

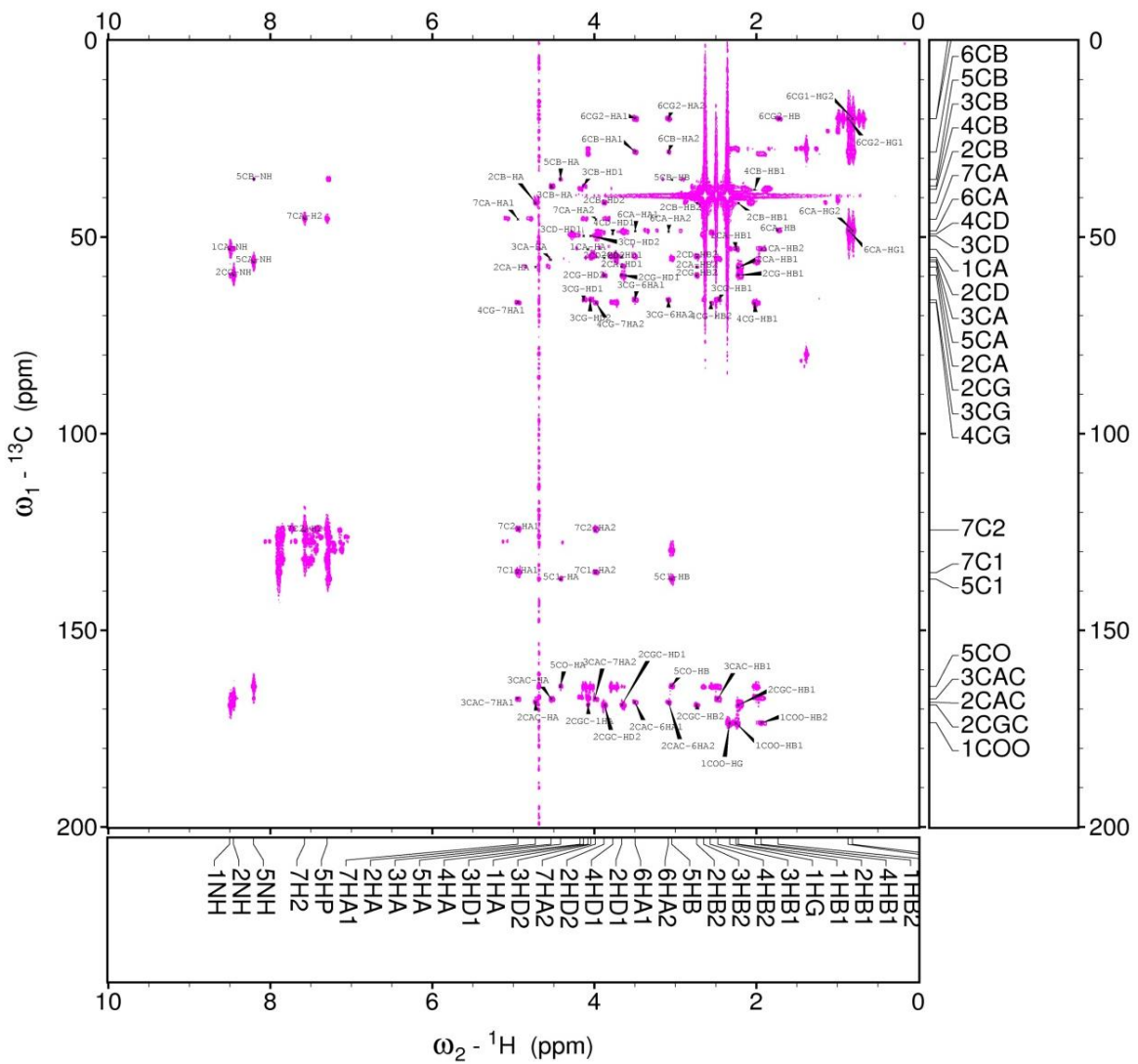
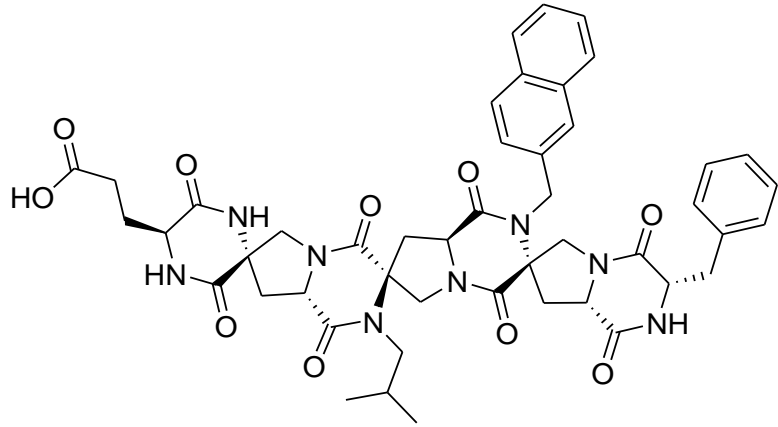


Figure A.30 Helix Mimic 103 HMBC: 8mM in DMSO

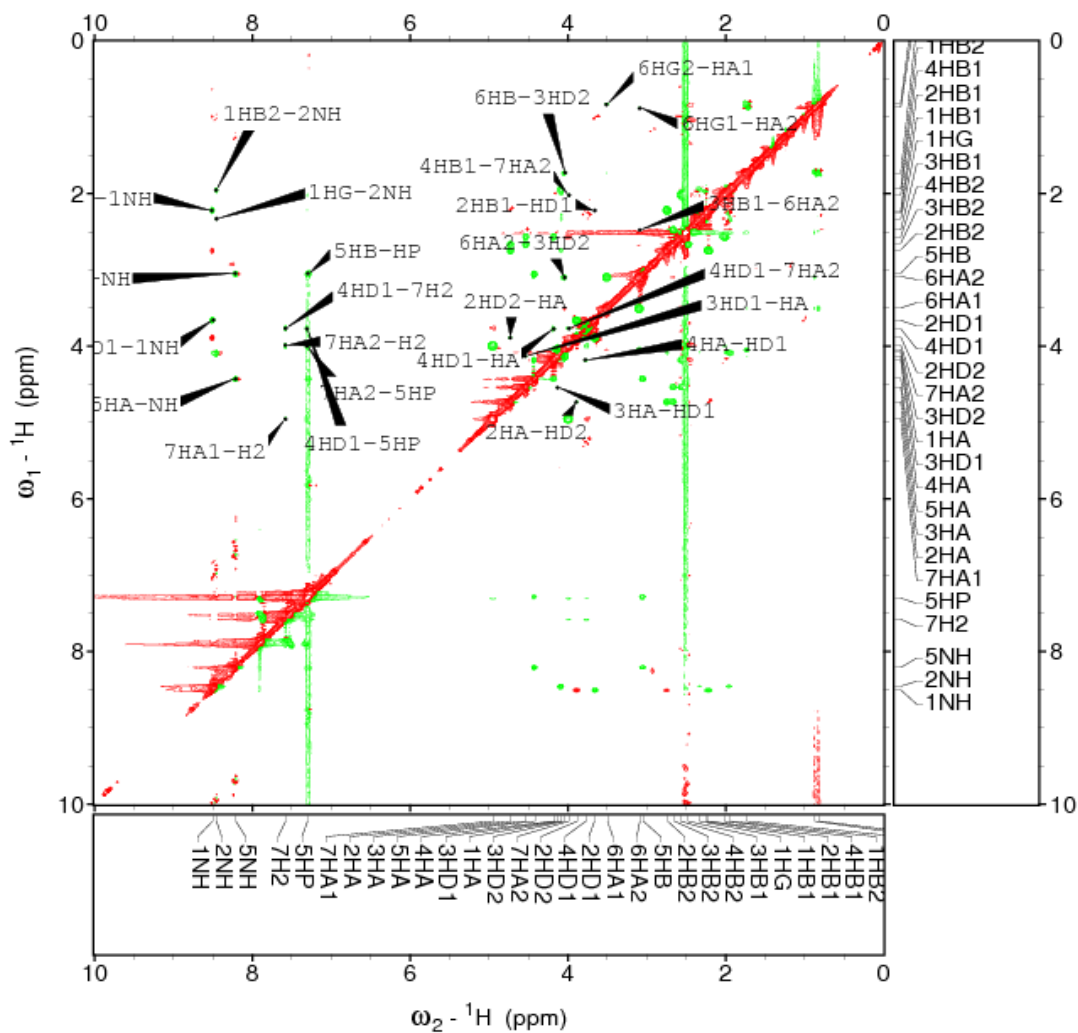
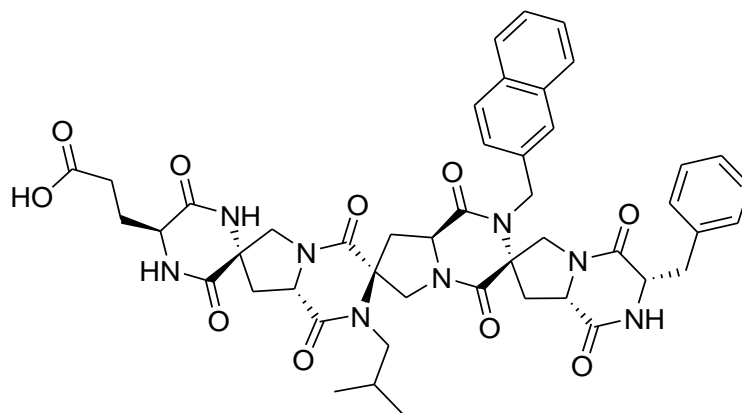


Figure A.31 Helix Mimic 103 ROESY: 8mM in DMSO

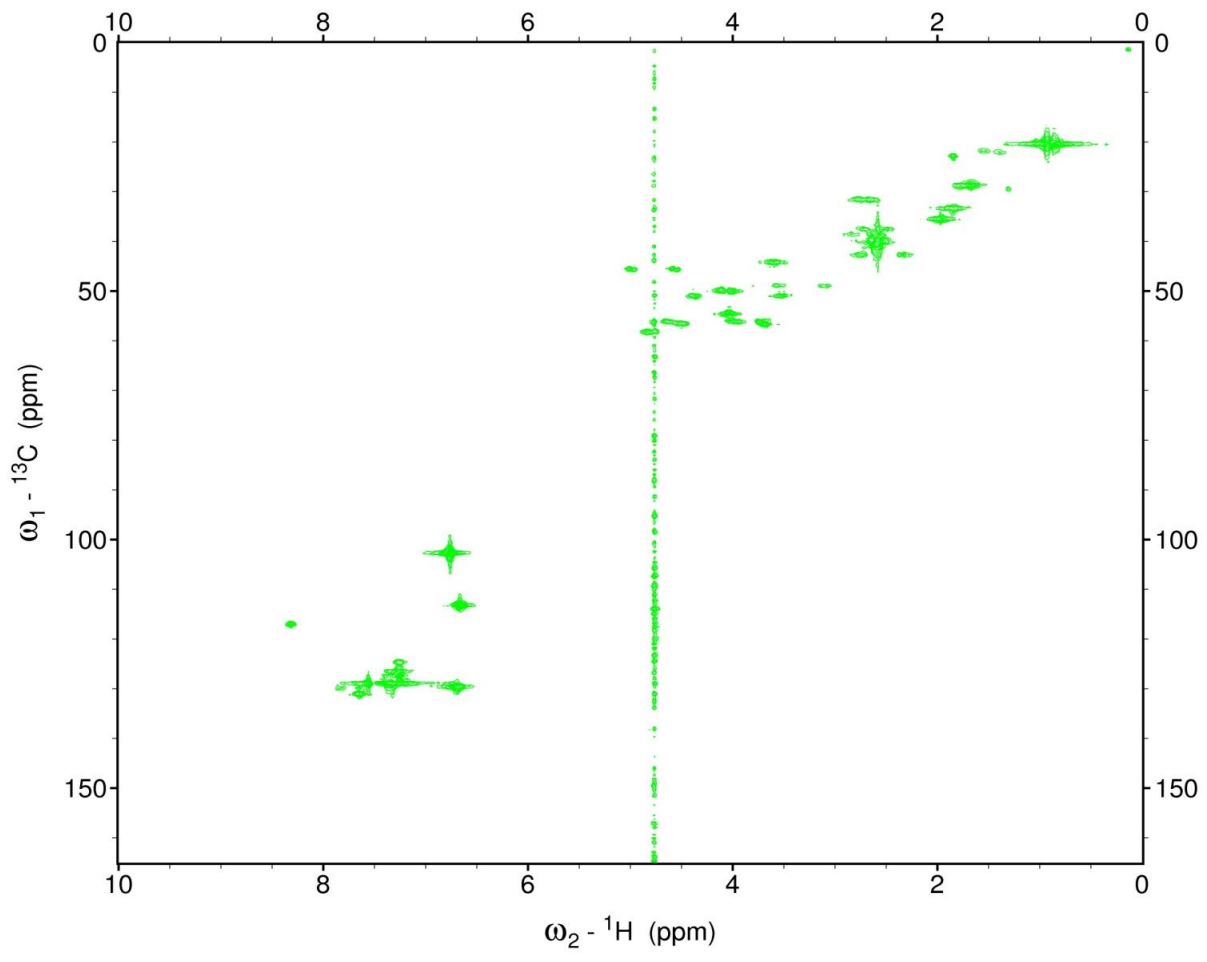
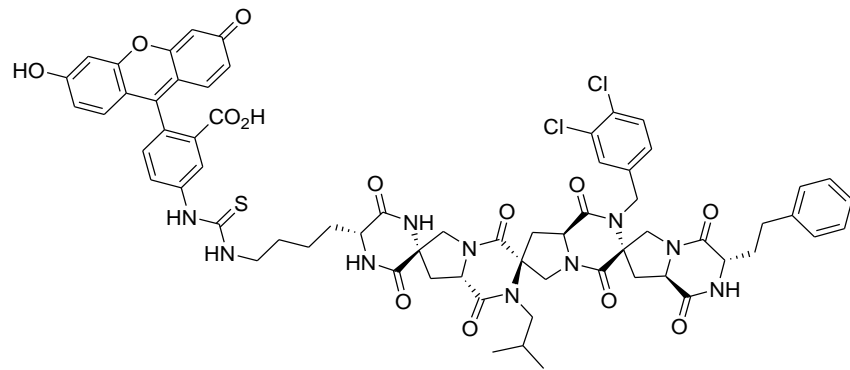


Figure A.32 Helix Mimic **84** HMQC: 8mM in DMSO

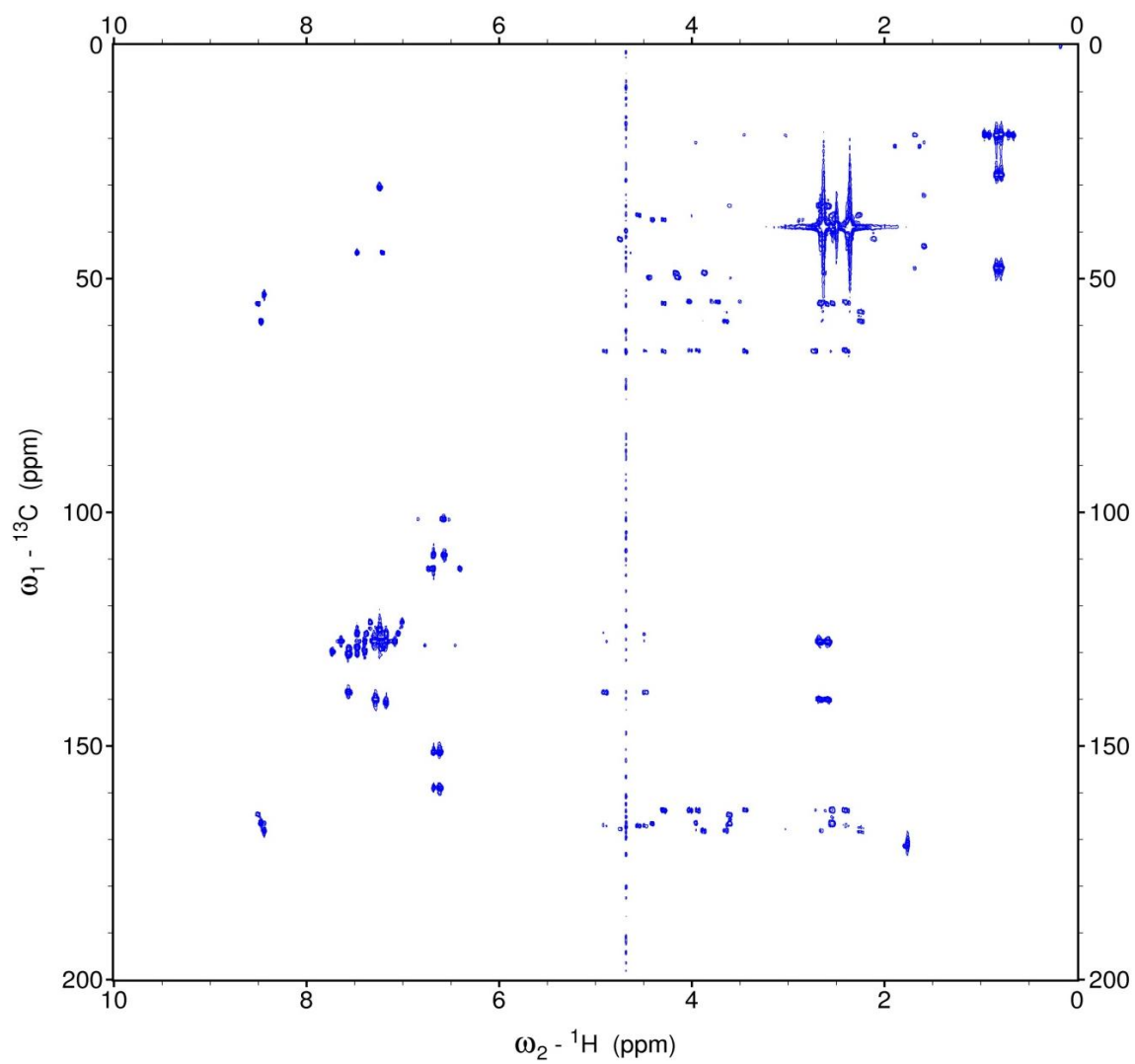
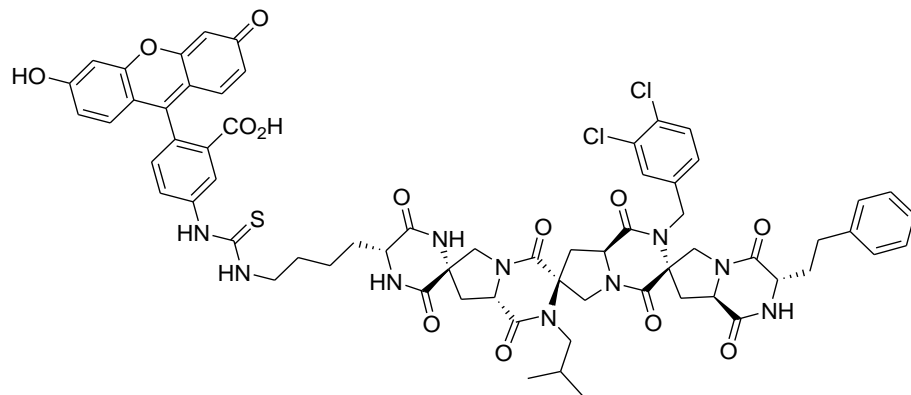


Figure A.33 Helix Mimic 84 HMQC: 8mM in DMSO

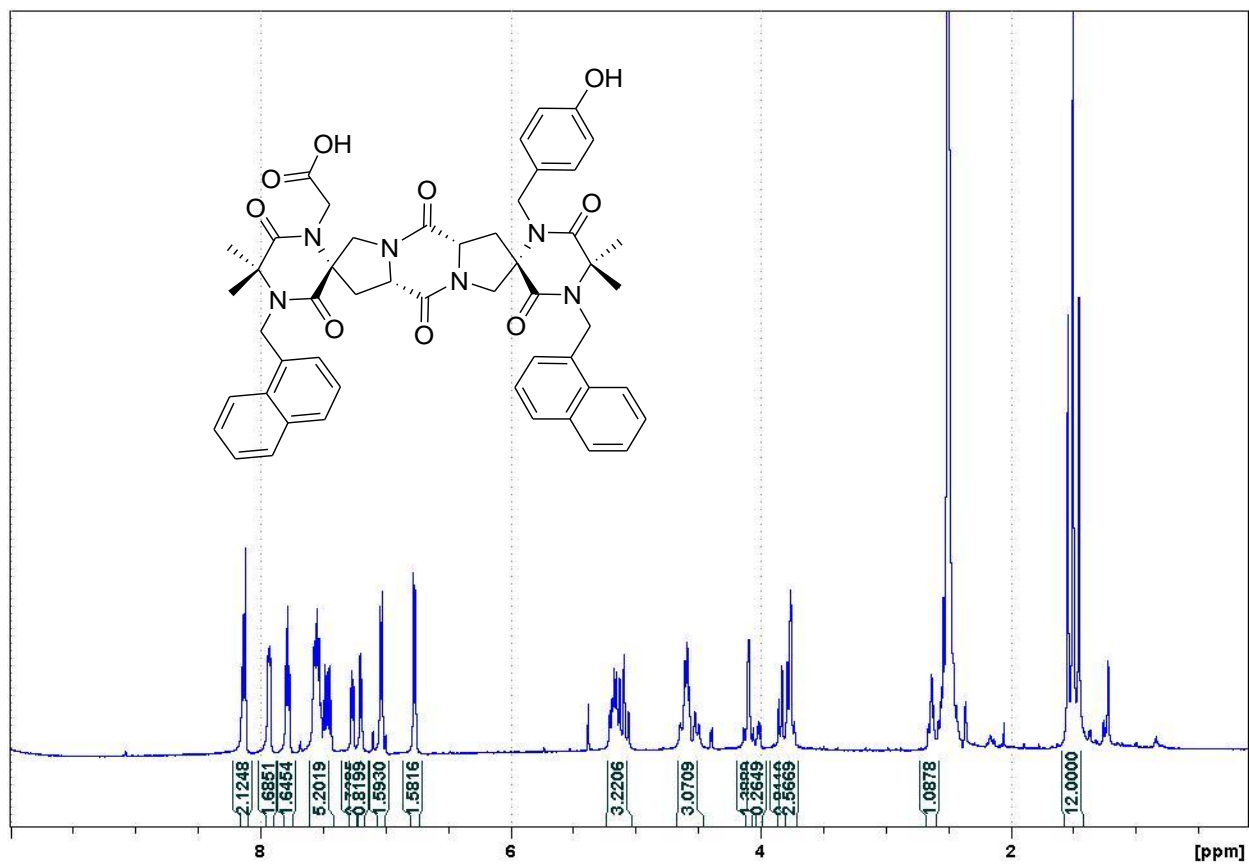


Figure A.34 Tail to Tail Oligomer 136 ^1H : 10mM in DMSO

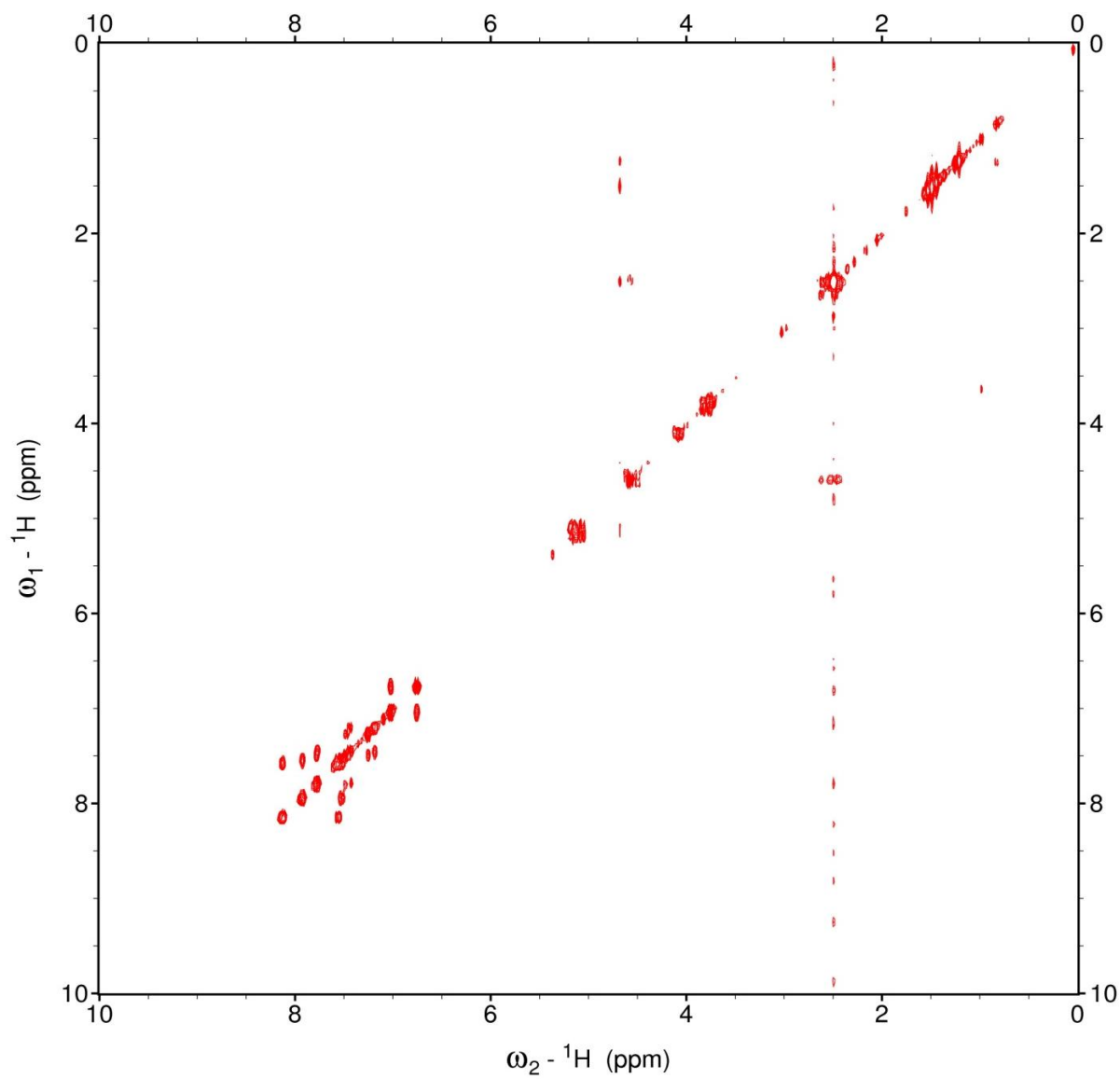
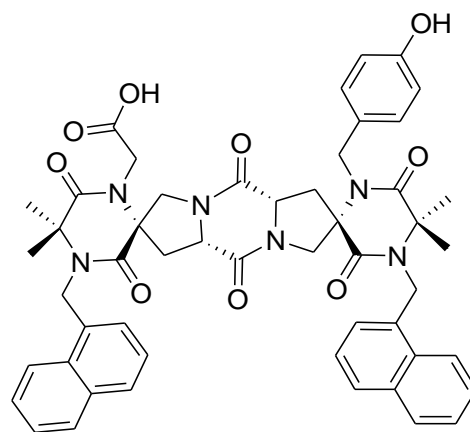


Figure A.35 Tail to Tail Oligomer 136 COSY:10mM in DMSO

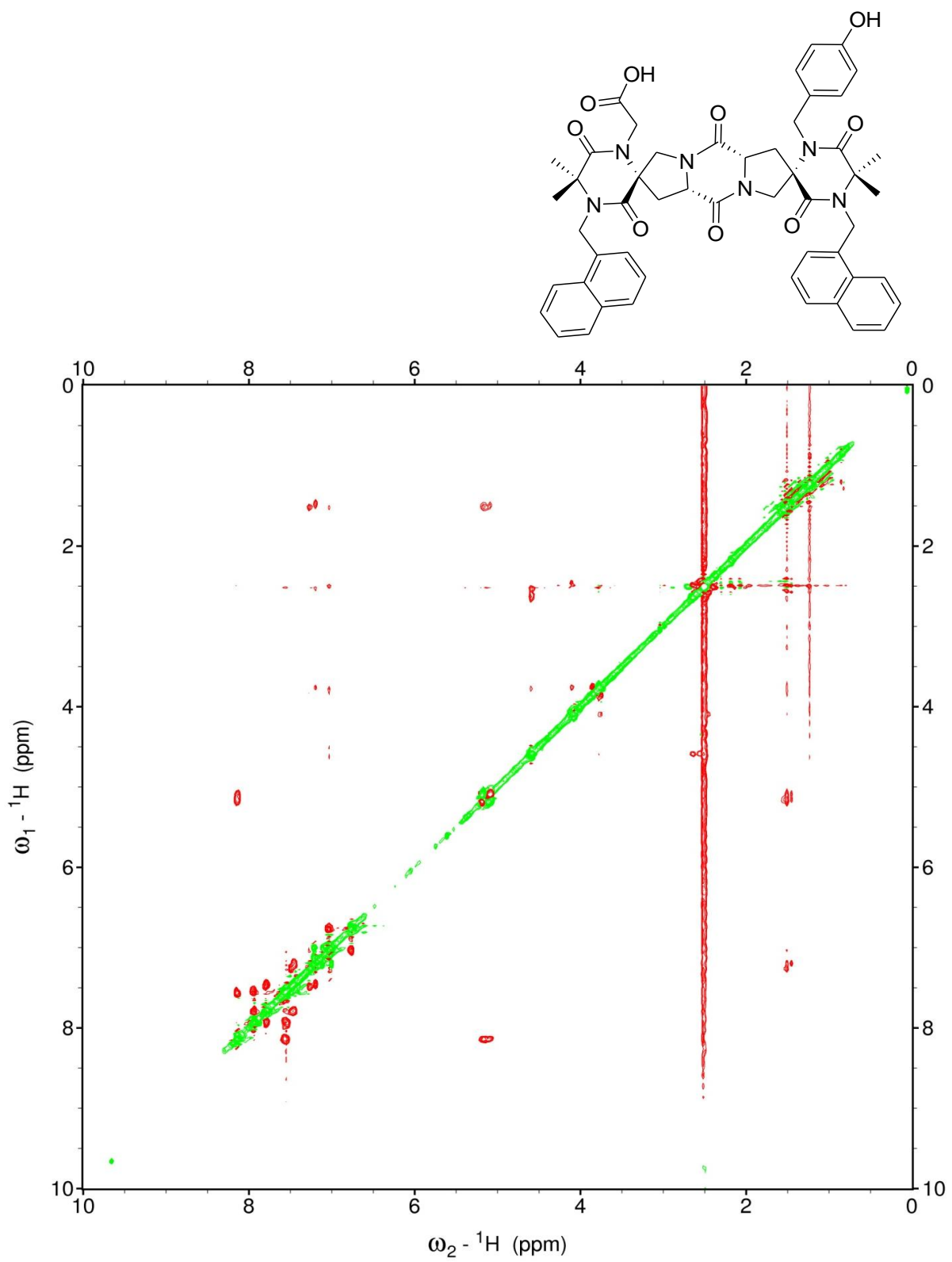


Figure A.36 Tail to Tail Oligomer 136 ROESY:10mM in DMSO

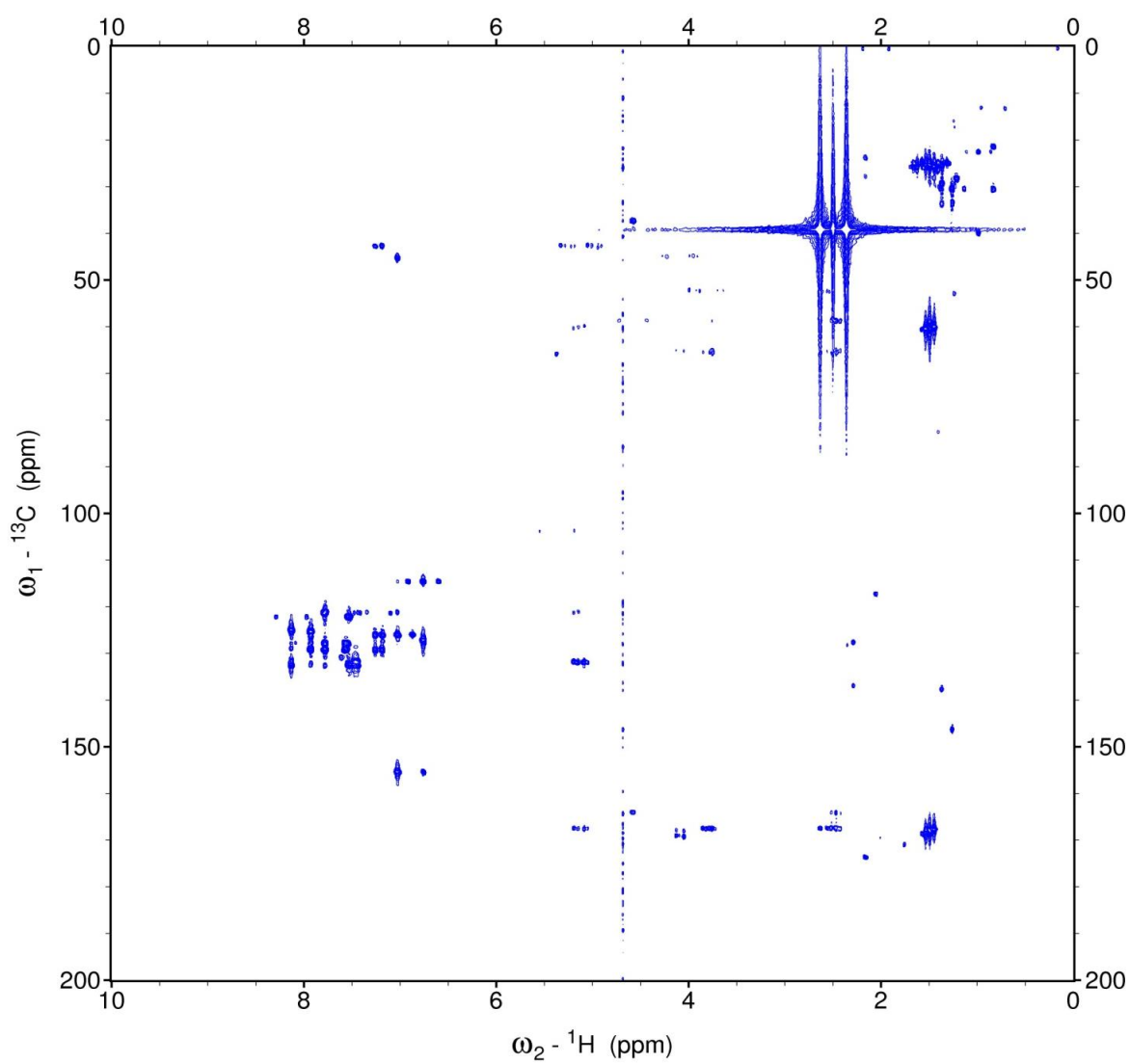
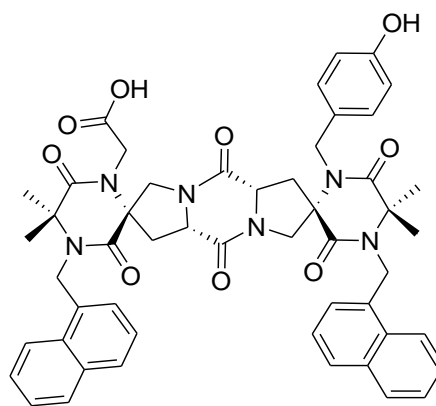


Figure A.37 Tail to Tail Oligomer 136 HMBC:10mM in DMSO

Bibliography

- 1.) Creighton, T. *Proteins Structures and Molecular Properties*; W.H. Freeman: New York, **1993**.
- 2.) Schafmeister, C.E.; Brown, Z.Z.; Gupta, S. Shape-Programmable Macromolecules. *Acc. Chem. Res.* **2008**, 41, 1387-1398.
- 3.) Cheng, R.; Gellman, S.; DeGrado, W. beta-Peptides: From Structure to Function. *Chem. Rev.* **2001**, 101, 3219-3232
- 4.) Verdine, G.L.; Walensky, L.D. The Challenge of Drugging Undruggable Targets in Cancer: Lessons Learned from Targeting BCL-2 Family Members. *Clin. Cancer Res.* **2007**, 13, (24), 7264-7270.
- 5.) The PyMOL Molecular Graphics System, Version 0.98, Schrödinger, LLC.
- 6.) Kussie, P.H., Gorina, S., Marechal, V., Elenbaas, B., Moreau, J., Levine, A.J., Pavletich, N.P. Structure of the MDM2 oncoprotein bound to the p53 tumor suppressor transactivation domain. *Science* **1996**, 275, 948-953.
- 7.) Murray, J.K., Gellman, S.H. Targeting protein-protein interactions: Lessons from p53/MDM2 *J. of Peptide Science* **2007**, 88, (5), 657-686.
- 8.) Vassiley, L.T. p53 Activation by Small Molecules: Application in Oncology. *J. Med. Chem.* **2005**, 48, (14), 4491-4499.
- 9.) Vega, S., Kang, L.W., Velazquez-Campoy, A., Kiso, Y., Amzel, L.M., Freire, E. A structural and thermodynamic escape mechanism from a drug resistant mutation of the HIV-1 protease. *Proteins* **2004**, 55, 594-602.
- 10.) Zhang, X., Houk, K.N. Why Enzymes Are Proficient Catalysts: Beyond the Pauling Paradigm. *Acc. Chem. Res.* **2005**, 38, (5), 379-385.
- 11.) Brown, Z.Z., Schafmeister, C.E. Exploiting an Inherent Neighboring Group Effect of α -Amino Acids To Synthesize Extremely Hindered Dipeptides. *J. Am. Chem. Soc.* **2008**, 130, (44), 14382-14383.
- 12.) Brown, Z.Z., Schafmeister, C.E. Synthesis of Hexa- and Penta-Substituted Diketopiperazines from Sterically Hindered Amino Acids. *Org. Lett.*, **2010**, 12 (7), 1436-1439.
- 13.) Dill, K.A., Ozkan, S., Shell, M., Weikl, T. The Protein Folding Problem. *Ann Rev Biophysics*, **2008**, 37, 289-316.
- 14.) Hill, D., Mio, M., Prince, R., Hughes, T., Moore, J. A Field Guide to Foldamers. *Chem. Rev.* **2001**, 101, 3893-4012.
- 15.) Delnoye, D. A. P.; Sijbesma, R. P.; Vekemans, J.; Meijer, E. W. π -Conjugated Oligomers and Polymers with a Self-Assembled Ladder-like Structure. *J. Am. Chem. Soc.* **1996**, 118, 8717-8718.
- 16.) Kajtar, M., Bruckner, V. The optical rotatory dispersion of γ -linked oligo- and polypeptides of glutamic acid. *Tetrahedron Lett.* **1966**, 7, 4813-4818.
- 17.) Zuckermann, R., Kerr, J., Kent, S., Moos, W. Efficient method for the preparation of peptoids [oligo(N-substituted glycines)] by submonomer solid-phase synthesis. *J. Am. Chem. Soc.* **1992**, 114, (26), 10646-10647.

- 18.) Orner, B.P., Ernst, J., Hamilton, A.D. Towards Proteomimetics: Terphenyl Derivatives as Structural and Functional Mimics of Extended Regions of an α -Helix. *J. Am. Chem. Soc.* **2001**, 123, 5382-5383
- 19.) Gellman, S.H. Foldamers: A Manifesto. *Acc. Chem. Res.* **1998**, 31, (4), 173-180.
- 20.) Davis, J.M., Tsou, L.K., Hamilton, A.D. Synthetic Non-Peptide Mimetics of α -Helices. *Chem Soc. Rev.* **2007**, 36, 326-334.
- 21.) Horne, W.S., Gellman, S.H. Foldamers with Heterogeneous Backbones. *Acc. Chem. Res.* **2008**, 41, (10), 1399-1408.
- 22.) Patgiri, A., Jochim, A. L., Arora, P. S. A Hydrogen Bond Surrogate Approach for Stabilization of Short Peptide Sequences in Alpha-Helical Conformation. *Acc. Chem. Res.* **2008**, 41, 1289-1300.
- 23.) Schafmeister, C.E., Po, J., Verdine, G.L. An All-Hydrocarbon Cross-Linking System for Enhancing the Helicity and Metabolic Stability of Peptides. *J. Am. Chem. Soc.* **2000**, 122, (24), 5891-5892.
- 24.) Watching Peptide Drugs Grow Up. *Chemical and Engineering News.* **2005**, 83, (11), 17-24.
- 25.) Greenberg M.L., Cammack N. Resistance to enfuvirtide, the first HIV fusion inhibitor. *J Antimicrob. Chemother.* **2004**, 54, (2), 333-340.
- 26.) Albericio, F. Developments in Peptide and Amide Synthesis. *Curr. Opin. Chem. Biol.* **2004**, 8, 211–221.
- 27.) Humphrey, J. M., Chamberlin, A. R. Chemical Synthesis of Natural Product Peptides: Coupling Methods for the Incorporation of Noncoded Amino Acids into Peptides. *Chem. Rev.* **1997**, 97, 2243–2266.
- 28.) Adessi, A., Soto, C. Converting a Peptide into a Drug: Strategies to Improve Stability and Bioavailability. *Curr. Med. Chem.*, **2002**, 9, 963-978.
- 29.) Chatterjee, J., Gilon, C., Hoffman, A., Kessler, H. N-Methylation of Peptides: A New Perspective in Medicinal Chemistry. *Acc. Chem. Res.* **2008**, 41, (10), 1331-1342.
- 30.) Pritchard, D.I. Sourcing a chemical succession for cyclosporin from parasites and human pathogens. *Drug Discov. Today* **2005**, 10, (10), 688-691.
- 31.) Wenschuh, H., Beyermann, M., Haber, H., Seydel, J., Krause, E., Bienert, M., Carpino, L., El-Faham, A., Albericio, A. Stepwise Automated Solid Phase Synthesis of Naturally Occurring Peptaibols Using Fmoc Amino Acid Fluorides. *J. Org. Chem.*, **1995**, 60, (2), 405–410.
- 32.) Moretto, V.; Valle, G.; Crisma, M.; Bonora, G. M.; Toniolo, C. Monomer Units for the β -bend Ribbon Structure: MeAib Peptides. *Int. J. Biol. Macromol.* **1992**, 14, 178–184.
- 33.) Fischer, E., Fourneau, E., *Ber. Them. GM.*, **1901**, 34, 2868.
- 34.) For a recent review, see: Montalbetti, C., Falque, V. Amide Bond Formation and Peptide Coupling *Tetrahedron* **2005**, 61, 10827–10852.
- 35.) Isidro-Llobet, A., Alvarez, M., Albericio, F. Amino-Acid Protecting Groups *Chem. Rev.*, **2009**, 109, (6), 2455–2504.
- 36.) Han, S., Kim, Y. Recent development of peptide coupling reagents in organic synthesis. *Tetrahedron* **2002**, 60, (11), 2447-2467.
- 37.) Wenger, R. Total Syntheses of 'Cyclosporin A' and 'Cyclosporin H', Two Fungal Metabolites

- Isolated from the Species *Tolypocladium Inflaturn1* GAMS. *Helv. Chim. Acta* **1984**, 67, (2), 502-525.
- 38.) Carpino, L. A., Ionescu, D., El-Faham, A., Henklein, P., Wenschuh, H., Bienert, M., Beyermann, M. Protected amino acid chlorides vs protected amino acid fluorides: Reactivity comparisons. *Tetrahedron Lett.* **1998**, 39, 241–244.
- 39.) Carpino, L. A., Beyermann, M., Wenschuh, H., Bienert, M. Peptide Synthesis via Amino Acid Halides. *Acc. Chem. Res.* **1996**, 29, 268-274.
- 40.) Wenschuh, H.; Beyermann, M.; Winter, R.; Bienert, M.; Ionescu, D.; Carpino, L. Fmoc Amino Acid Fluorides in Peptide Synthesis-Extension of the Method to Extremely Hindered Amino Acids. *Tetrahedron Lett.* **1996**, 37, 5483-5486.
- 41.) Freet, E., Coste, J., Pantaloni, A., Dufour, M., Joiun, P. PyBOP and PyBroP: Two Reagents for the Difficult Coupling of the α,α -dialkyl Amino Acid, Aib. *Tetrahedron* **1991**, 47, 259-270.
- 42.) Kaduk, C.; Wenschuh, H.; Beyermann, M.; Forner, K.; Carpino, L.; Bienert, M. Synthesis of Fmoc-amino acid fluorides via DAST, an alternative fluorinating agent. *Lett. Pept. Sci.* **1996**, 2, 285–288.
- 43.) Schwarz, J.S. Preparation of acyclic isoimides and their rearrangement rates to imides. *J. Org. Chem.* **1972**, 37, (18), 2906-2908.
- 44.) Dawson, P. E., Muir, T. W., Clark-Lewis, I., Kent, S. B. H. Synthesis of Proteins by Native Chemical Ligation. *Science* **1994**, 266, 776–779.
- 45.) Coin, I., Dolling, R., Krause, E., Bienert, M., Beyermann, M., Sferdean, C., Carpino, L. Depsipeptide Methodology for Solid-Phase Peptide Synthesis: Circumventing Side Reactions and Development of an Automated Technique via Depsidipeptide Units. *J. Org. Chem.* **2006**, 71, 6171–6177.
- 46.) Salvatore, R., Yoon, C., Jung, K. Synthesis of Secondary Amines. *Tetrahedron* **2001**, 57, 7785-7811.
- 47.) Szardenings, A.; Burkoth, T.; Look, G.; Campbell, D. A Reductive Alkylation Procedure Applicable to Both Solution- and Solid-Phase Syntheses of Secondary Amines. *J. Org. Chem.* **1996**, 61, 6720-6722.
- 48.) Bishop, J.E., O'Connell, J., Rapoport, H. The Reaction of Thioimides with Phosphorous Ylides. *J. Org. Chem.* **1991**, 56, 5079-5091.
- 49.) Tullberg, M.; Grotli, M.; Luthman, K. Synthesis of Functionalized, Unsymmetrical 1,3,4,6-Tetrasubstituted 2,5-Diketopiperazines. *J. Org. Chem.* **2007**, 72, 195-199.
- 50.) Carpino, L., El-Faham, A. The Diisopropylcarbodiimide/ 1-Hydroxy-7-azabenzotriazole System: Segment Coupling and Stepwise Peptide Assembly. *Tetrahedron* **1999**, 55, 6813-6830.
- 51.) MOE; 2009.05 ed.; Chemical Computing Group Inc.: 1010 Sherbrooke Street West, Suite 910, Montreal, Canada H3A 2R7, 2002.
- 52.) Cornell W.D., Cieplak P., Bayly C.I., Gould I.R., Merz K.M. Jr, Ferguson D.M., Spellmeyer D.C., Fox T., Caldwell J.W., Kollman P.A. A Second Generation Force Field for the Simulation of Proteins, Nucleic Acids, and Organic Molecules. *J. Am. Chem. Soc.* **1995**, 117, 5179–5197.
- 53.) Jones, S., Thornton, J.M. Principles of Protein-Protein Interactions. *Proc. Nat. Acad. Sci.* **1996**, 93, 13-20.

- 54.) Arkin, M., Wells, J.A. Small-molecule Inhibitors of Protein–Protein Interactions: Progressing Towards the Dream. *Nature Rev. Drug Disc.* **2004**, 3, 301-317.
- 55.) Shangary, S., Wang, S. Small-Molecule Inhibitors of the MDM2-p53 Protein-Protein Interaction to Reactivate p53 Function: A Novel Approach for Cancer Therapy. *Annu. Rev. Pharmacol. Toxicol.* **2009**, 49:223–241.
- 56.) Vousden, K., Lane, D. p53 in health and disease. *Nat. Rev. Mol. Cell Bio.* **2007**, 8, 275-283.
- 57.) Gudkov, A., Komarova, E. Prospective therapeutic applications of p53 Inhibitors. *Biochem. And Biophys. Res. Comm.* **2005**, 331, 726-736.
- 58.) Komarov, P., Komarova, E., Kondratov, R., Christov, K., Coon, J., Chernov, M., Gudkov, A. A Chemical Inhibitor of p53 that Protects Mice from the Side Effects of Cancer Therapy. *Science* **1999**, 285, 1733-1737.
- 59.) Nader, F., Bradford, G. Small Molecule Inhibitors of p53/mdm2 Interaction. *Curr. Topics in Med. Chem.* **2005**, 5, 159-165.
- 60.) Fasan, R., Dias, R., Moehle, K., Zerbe, O., Vrijbloed, J., Obrecht, D., Robinson, J. Using a β -Hairpin To Mimic an α -Helix: Cyclic Peptidomimetic Inhibitors of the p53–HDM2 Protein–Protein Interaction *Angew. Chem. Int. Ed.* **2004**, 43, 2109–2112.
- 61.) Kritzer, J. A., Zutshi, R., Cheah, M., Ran, F. A., Webman, R., Wongjirad, T. M., Schepartz, A. Miniature Protein Inhibitors of the p53–hDM2 Interaction. *Chem. Bio. Chem.* **2006**, 7, 29-31.
- 62.) García-Echeverría, C., Chène, P., Blommers, M., Furet, P. Discovery of Potent Antagonists of the Interaction between Human Double Minute 2 and Tumor Suppressor p53. *J. of Med. Chem.* **2000**, 43, 3205-3208.
- 63.) Menge, B., Nimtz, M., Frank, R. An Efficient Method for Anchoring Fmoc-amino Acids to Hydroxyl-functionalised Solid Supports. *Tetrahedron Lett.* **1990**, 31, 1701-1704.
- 64.) Zondlo, S., Lee, A., Zondlo, N. Determinants of Specificity of MDM2 for the Activation Domains of p53 and p65: Proline27 Disrupts the MDM2-Binding Motif of p53. *Biochemistry* **2006**, 45, 11945-11957.
- 65.) Jameson, D.M., Sawyer, W.H. Fluorescence Anisotropy Applied to Biomolecular Interactions. *Methods in Enzymol.* **1995**, 246, 283-300.
- 66.) Jameson, D.M., Seifried, S.E. Quantification of Protein-Protein Using Fluorescence Polarization. *Methods* **1999**, 19, 222-233.
- 67.) Bernal F., Tyler A.F., Korsmeyer S.J., Walensky L.D., Verdine G.L. Reactivation of the p53 tumor suppressor pathway by a stapled p53 peptide. *J. Am. Chem. Soc.* **2007**, 129, 2456-2457.
- 68.) Harker, E., Daniels, D., Guarracino, D., Schepartz, A. α -Peptides with Improved Affinity for hDM2 and hDMX. *Bioorg. and Med. Chem.* **2009**, 17, 2038-2046.
- 69.) Pettersen EF, Goddard TD, Huang CC, Couch GS, Greenblatt DM, Meng EC, Ferrin TE. UCSF Chimera--a Visualization System for Exploratory Research and Analysis. *J. Comput. Chem.* **2004**, 25, 1605-1612.

- 70.) Czarna, A., Popowicz, G., Pecak, A., Wplf, S., Dubin, G., Holak, T. High Affinity Interaction of the p53 Peptide-Analogue with Human Mdm2 and Mdmx. *Cell Cycle* **2009**, 8, 1176-1184.
- 71.) Reed, D., Shen, Y., Shelat, A., Arnold, A., Ferreira, A., Zhu, F., Mills, N., Smithson, D., Regni, C., Bashford, D., Cicero, S., Schulman, B., Jochemsen, A.G., Guy, K., and Dyer, M.A. Identification and characterization of the first small-molecule inhibitor of MDMX *J. Bio. Chem.*, **2010**, 285, 10786-10796.
- 72.) Danovi, D., Meulmeester, E., Pasini, D., Migliorini, D., Capra, M., Frenk, R., de Graaf, P., Francoz, S., Gasparini, P., Gobbi, A., Helin, K., Pelicci, P.G., Jochemsen, A.G., and Marine, J.-C. Amplification of Mdmx (or Mdm4) directly contributes to tumor formation by inhibiting p53 tumor suppressor activity. *Molecular and Cellular Biology* **2004**, 24, 5835-5843.
- 73.) Zheng, T., Wang, J., Song, X., Meng, X., Pan, S., Jiang, H., Liu, L. Nutlin-3 cooperates with doxorubicin to induce apoptosis of human hepatocellular carcinoma cells through p53 or p73 signaling pathways. *J. Cancer Res. Clin. Oncol.* **2009**, 136, 1597-1604.
- 74.) Arzumanyan, A. *Personal Communication*.
- 75.) Graphpad Prism version 5.02 for Windows, GraphPad Software, San Diego California USA, www.graphpad.com
- 76.) Pennington, M., Dunn, B. *Peptide Synthesis Protocols*. Humana Press: New Jersey, **1994**.
- 77.) For examples of cyclorelease strategies, see: A.) Beebe, X.; Schore, N.E.; Kurth, M.J. Polymer-supported Synthesis of 2,5-disubstituted Tetrahydrofurans. *J. Am. Chem. Soc.* **1992**, 114, 10061-10062; B.) Nicolaou, K.C.; Pastor, J.; Winssinger, N.; Murphy, F. Solid Phase Synthesis of Macrocycles by an Intramolecular Ketophosphonate Reaction: Synthesis of a (dl)-Muscone Library. *J. Am. Chem. Soc.* **1998**, 120, 5132-5133. C.) Liu, H.; Wan, S.; Floreancig, P.E. Oxidative cyclorelease from soluble polymeric supports. *J. Org. Chem.* **2005**, 70, 3814-3818.
- 78.) For a review, see: Phoon, C. W.; Sim, M. M. The Scope and Future of Traceless Synthesis in Organic Chemistry. *Current Organic Chemistry* **2002**, 6, 937-964.
- 79.) Garca-Martin, F., Quintanar-Audelo, M., Garca-Ramos, Y., Cruz, L., Gravel, C., Furic, R., Ct, S., Tulla-Puche, J., Albericio, F. ChemMatrix, a Poly(ethylene glycol)-Based Support for the Solid-Phase Synthesis of Complex Peptides. *J. Comb. Chem.* **2006**, 8, (2), 213-220.
- 80.) Novabiochem, EMD4Biosciences, www.emdchemicals.com
- 81.) Sheppard, R., Williams, B. Acid-labile resin linkage agents for use in solid phase peptide synthesis. *Int. J. Pep. Prot. Res.* **1982**, 20, 451-454.
- 82.) Anslyn, E., Dougherty, D. *Modern Physical Organic Chemistry*; University Science Books: New Jersey, **2006**.
- 83.) Szejtli, J. Introduction and General Overview of Cyclodextrin Chemistry. *Chem. Rev.* **1998**, 98, 1743-1754.
- 84.) Liu, S., Ruspic, C., Mukhopadhyay, P., Chakrabarti, S., Zavalij, P., Isaacs, L. The Cucurbit[n]uril Family: Prime Components for Self-Sorting Systems. *J. Am. Chem. Soc.* **2005**, 127, 15959-15967.

- 85.) Lee, J., Samal, S., Selvapalam, N., Kim, H., Kim, K. Cucurbituril Homologues and Derivatives: New Opportunities in Supramolecular Chemistry. *Acc. Chem. Res.* **2003**, 36, 621-630.
- 86.) Khan, A., Forgo, P., Stine, K., D'Souza, V. Methods for Selective Modifications of Cyclodextrins. *Chem. Rev.* **1998**, 98, 1977-1996.
- 87.) Malesevic, M., Strijowski, U., Bachle, D., Sewald, N. An Improved Method for the Solution Cyclization of Peptides Under Pseudo-Dilution Conditions. *J. Biotech.* **2004**, 112, 73-77.
- 88.) Lejeune, V., Martinez, J., Cavelier, F. Towards a Selective Boc Deprotection on Acid Cleavable Wang Resin. *Tet. Lett.* **2003**, 44, 4757-4759.
- 89.) Semisotnov G., Rodionova N., Razgulyaev O., Uversky V., Gripas' A., Gilmanshin R. Study of the Molten Globule Intermediate State in Protein Folding by a Hydrophobic Fluorescent Probe. *Biopolymers* **1991**, 31, 119-128.
- 90.) Bodine, K., Gin, D., Gin, M. Synthesis of Readily Modifiable Cyclodextrin Analogues via Cyclodimerization of an Alkynyl-Azido Trisaccharide. *J. Am. Chem. Soc.* **2004**, 126, 1638-1639.